Postglacial relative sea-level reconstruction and environmental record from isolation Basins in NW Iceland

Tucker, Owen E.

Postglacial Relative Sea-level Reconstruction and Environmental Record from isolation Basins in NW Iceland

By Mr Owen E. Tucker

For M.S.c by Research

6th October 2005

Supervisors Dr J. Lloyd & Dr M. Bentley

Department of Geography
University of Durham
Science Site
South Road
DH1 3LE

Contents page

List of figures

48. List of Appendix

List of plates

Front cover: A view north from the middle Djúpavik site, Vestfirðir, NW Iceland

Glossary

BSi	Biogenic silica
DIc	Diatom isolation contact
DIC	Dissolved inorganic carbon
DOC	Dissolved organic carbon
DSi	Concentration of dissolved silica
LGM	Last glacial maximum
LOI	Loss-on-ignition analysis
NADW	North Atlantic deep water
OD	National datum
THC	Thermohaline circulation
RSL	Relative sea-level
a.s.l	height above mean sea-level

Abstract

Isolation basin methodology was successfully applied to a number of coastal basins in NW Iceland. Basin isolation was traced using a combination of bio-lithostratigraphy (diatoms) and other geo-chemical proxies (biogenic silica, loss-on-ignition, and sodium). Limited data was available to develop an event chronology which was based primarily the Saksunarvatn Ash, identified in many of the lake cores. 6 sea-level index points were identified from a staircase of isolation basins between 1m and 75m a.s.l. and used to reconstruct the first preliminary relative sea-level curve for northwest Iceland.

The marine limit was tightly constrained around ca. 75m a.s.l. by the different litho-biostratigraphy of two basins The reconstruction of changes in relative sea-level suggest that relative sea-level fell from ca. 75m a.s.l at 12.8 cal. Ka BP to below 22.7m a.s.l sometime after 9.2 ^{14}C Ka BP (ca. 10.3 cal. Ka BP). This relative sea-level fall corresponds to an actual isostatic land uplift of ca. 100.4m at a rate of 4cm yr^{-1}.

The majority of basins investigated had evidence of isolation occurring before the onset of organic accumulation within the basin. This characteristic of isolation basins stratigraphy in Iceland was more pronounced in those basins that isolated earlier implying that climate may have been an influence. I speculate that a cold harsh climate, indicated by diatoms and low lake and catchment bio-productivity at the time of isolation, caused a time-lag between full hydrological and sedimentological isolation and the onset of organic deposition within the basin. It may prove difficult to radiocarbon date isolation contacts that are particularly organic-poor and alternative methods like tephrochronology may be additionally required in order to produce future Icelandic RSL data with a tight chronological control.

Attempts to produce a record of environmental and climatic change from NW Iceland met with mixed success. High levels of background tephra prevented a climate signal being recorded by biogenic silica analysis. The Saksunarvatn Ash was well distributed across Vesfirðir facilitating correlation with other marine and terrestrial sites around the North Atlantic of palaeoenvironmental importance. Were the Saksunarvatn Ash was found deposited in clastic-rich, fresh water gyttja, it has been suggested that those areas were still experiencing cool temperatures during the early Pre-Boreal. Diatom, Loss-on-ignition and pH analysis clearly show the Pre-Boreal warming from ca. 10.1 cal. Ka. BP.

Acknowledgements

The fieldwork costs were supported by a grant from the Department of Geography, University of Durham. I would to give special thanks to Jerry Lloyd and Mike Bentley for the advice and guidance through out the year and to Anthony Newton for analysing all the tephra deposits. I am also very grateful to Peter Abbott, Katherine Alexander, Lindsay Fletcher, Robert Holdway, Duncan Mackay and Ben Ripley for help with fieldwork. Finally, I would like to thank Frank Davies and Amanda Hayton for their assistance in the laboratory.

Declaration

I hereby declare that this thesis is solely the work of myself. Where other sources and information has been used they have been clearly referenced to the appropriate person.

CHAPTER 1

INTRODUCTION AND STUDY AIMS

1.1 Introduction

This thesis present results for a relative sea-level (RSL) reconstruction from the south coast of Vestfirðir, NW Iceland. RSL curves can provide information about the size of former LGM ice sheet, the timing of deglaciation, and the pattern of post-glacial isostatic uplift. Isolation basin stratigraphy is perhaps the most accurate and reliable method to record past changes in sea-level.

Research of this kind has proved very successful in reconstructing the deglacial history of Fennoscandianavia (e.g. Snyder et al., 2000; Corner et al., 2001), Greenland (e.g. Bennike 1995 & 2000; Long et al., 2003;) and Scotland (e.g. Shennan et al., 1994). This technique benefits from strong biostratigraphical and altitudinal control. Unlike other Scandinavian areas, the application of isolation basin stratigraphy in Iceland has been limited to the Skagi peninsula (Rundgren et al., 1997). However, some interpretations of regressions and transgressions of sea-level in the Skagi record can be compromised on biostratigrahical grounds and the record is hampered by poor diatom preservation, especially in the apparent "marine" periods of deposition.

RSL research in Iceland has relied heavily upon the interpretation of morphological features related to sea-level e.g. raised beaches (e.g. Einarsson 1968; Hjort et al., 1985; Ingólfsson et al., 1995). These features can be difficult to date accurately and the reliability of interpretations often questioned. Thus, the record of RSL change in Iceland has suffered from spare data that is ill-defined spatially, as well as and temporarily. The principal aim of this study is to apply the isolation basin technique in Iceland to improve the reliability of RSL reconstructions and to investigate any variability in isolation basin litho-biopstratigraphy from sites along the south and northeast Vestfirðir coast.

Iceland's lack of long biostratigraphical records (with the exception of the record from the Skagi peninsula (Björck et al., 1992; Rundgren et al., 1997; and Rundgren 1995)) has hampered attempts to reconstruct terrestrial environmental changes since the LGM. Eiríksson et al., (2000) reconstructed the palaeoceanographic regime around Iceland during the LGM and through the Holocene. Recently, Andrews et al., (2002b) discussed Holocene changes in sediment characteristics for core sites off the east coast of Vestfirðir. To evaluate this research and to contribute to the understanding of environmental change for northwest Iceland, this study presents evidence of environmental changes in NW Iceland during the Pre-Boreal and early-middle Holocene.

The pattern of LGM glaciation in Iceland is a matter of debate. It is unclear whether a single continuous ice sheet resided over the whole of Iceland reaching out as far as the shelf-break, or whether an independent ice-cap rested over Vestfirðir. The examination

of regional RSL curves would help to end this debate. Furthermore, it has been recently recognised that the thermohaline circulation (THC) can have severe impacts on the climate of the North Atlantic Region. Iceland, the most north-westerly territory of Europe and still covered in part by permanent ice caps, is located in the Greenland-Norwegian Sea, which is known to be an area critical for the formation of North Atlantic Deep Water (NADW) which drives the THC. It is not known at present what impact the former Icelandic ice sheet/s had on the THC at the climax to the last glaciation. An improved understanding of the dimensions of the former Icelandic ice sheet from better RSL records may help to determine the impact that wastage of the Icelandic ice sheet may have had on the North Atlantic THC.

1.2 Study aims and objectives

1.2.1 Relative sea-level reconstruction for southern Vestfirðir

Aim (1)

It is the intention of this investigation to sample and report the stratigraphy of a series of isolation basins on Vestfirðir's south coast in order to attempt to reconstruct RSL changes since the LGM. A chronology will be constructed with the aid of numerous tephra deposits.

Until recently, there has been an almost exclusive dependence on morphological and stratigraphical evidence from terrestrial sites to describe changes in relative sea-level (RSL). Interpretations of these features may be unreliable and there has been difficulty in dating. Recently, there has been some advances concerning the position of the LGM ice-front (Andrews et al., 2002; Andrews & Helgadóttir 2002) although, the stratigraphy of many end moraines is often too poorly known to disprove a readvance (Ingólfsson 1991). Early studies into the deglaciation of Iceland lack any robust temporal control and chronologies rely far too heavily on long distance analogies with NW Europe (Maizel & Caseldine 1991). Interpretations of local and regional deglaciation patterns for much of Iceland rest on relatively few radiocarbon dates and with limited dated lacustrine sediments it is not surprising that changes in RSL since the Weichselian maximum are poorly defined for all areas of Iceland.

Thoroddsen (1905-06) was a "monoglacialist" and proposed that during the Weichselian glaciation a single, large ice sheet rested upon the entire island. Since then it has been assumed that maximum glaciation occurred around 18Ka BP and based on offshore continental shelf morphological features the Icelandic ice sheet extended to the shelf break (Ingólfsson 1991). The "Vatnajökull-centric view" believes in a single and

continuous glaciation of Iceland during the LGM, generating a pattern of Holocene isostatic adjustment that results in a sequence of raised shorelines inferred to tilt more-or-less uniformly to the north and west (Hansom & Briggs 1991). Discrepancies in the altitude of the marine limit around Iceland resulted in the formulation of an alternative hypothesis. Some believe that the northwest peninsula, otherwise known as Vestfirðir, may have been glaciated by a separate ice cap during the LGM (e.g. Sigurvinsson 1983; Einarsson 1968, 1978). If so, Vestfirðir will have had an independent history of deglaciation and subsequent isostatic recovery, forming a regionally distinctive sequence of morphological and stratigraphical features related to sea-level (Hansom & Briggs 1991). Hence, Andrews & Helgadöttir (2003) explain that there are two main questions that are yet to be fully answered in Iceland; was there a separate ice cap across Vestfirðir, or did it join with the main Iceland ice cap? What was the extent of glaciation during the LGM at ~22 cal. Ka BP?

Multiple RSL studies based on isolation basin stratigraphy allow past sea-levels to be accurately fixed in time and space with comparatively small altitudinal errors. Marine-fresh transitions can be traced by analysing microfossils and other geochemical proxies and radiocarbon dating of the point of final isolation provides a sea-level index point (SLIP). Combining a series of SLIP's from a "staircase" of basins at different altitudes allows the reconstruction of regional RSL.

The following broad questions will be addressed in this thesis:

1. What are the characteristics of Icelandic isolation basin stratigraphy and is it suitable for RSL reconstructions in Iceland?
2. What is the pattern of RSL change for the south coast of Vestfirðir and how does it compare with other RSL records around Iceland?
3. Can any broad agreements or disagreements be made with other RSL data in that region.

1.2.2 Early-middle Holocene palaeo-environmental reconstruction from northeast Vestfirðir

Aim (2)

The second main objective of this thesis is to investigate the environmental record preserved in isolation basins from a range of proxies. The results from a multi-proxy (diatom microfossil and concentration, biogenic silica, loss-on-ignition, pH and particle size analysis) study reconstructing an early-middle Holocene environmental record from northeast Vestfirðir are presented. Changes in this biogeochemical record can then be

used to assess possible climate changes. The record from the isolation basins investigated can then be compared with published studies recording climate change in the climate and environment of Iceland and the North Atlantic in general. A chronology of these events will be produced using tephra layers preserved in the basin sediments.

There is an ongoing debate concerning the style and extent of glaciation during the late Weichselian in Iceland. It remains to be resolved whether Iceland was (i) glaciated by one all encompassing ice sheet centred over the Grimsvötn caldera and extending over the entire area of Iceland to the shelf break; or (ii) glaciated by one major ice sheet that resided over the mainland extending offshore but maybe not as far as in scenario (i) with a second, much smaller ice cap that formed over Vestfirðir, the prominent large peninsula in the northwest (Ingólfsson & Norðdahl 2001). By examining at the post-glacial evolution of a lake system in northeast Vestfirðir it may be possible to reconstruct a history of post-glacial events in Vestfirðir and to assess the synchronicity of potential events with other evidence from around the rest of Iceland.

Detailed analysis of ice core data from the summit of the Greenland ice sheet have demonstrated the relative stability in climate during the Holocene when compared to the larger climatic shifts that took place during the late Weichselian (Alley et al., 1997). Anderson (2000) however, explained that there is often much more variability contained in late-glacial and Holocene diatom and other fossil records, than is apparent from ice cores. Nevertheless, changes in diatom populations coupled with other proxies has enabled deglacial histories to be reconstructed for all of the formerly glaciated regions in the Northern Hemisphere (e.g. Snyder et al., 2000; Grönlund & Kauppila 2002; and Perren et al., 2003). Alley et al., (1997) reported the occurrence of a significant climate oscillation approximately half the amplitude of the Younger Dryas ca. 8.2Ka BP (Figure 1).

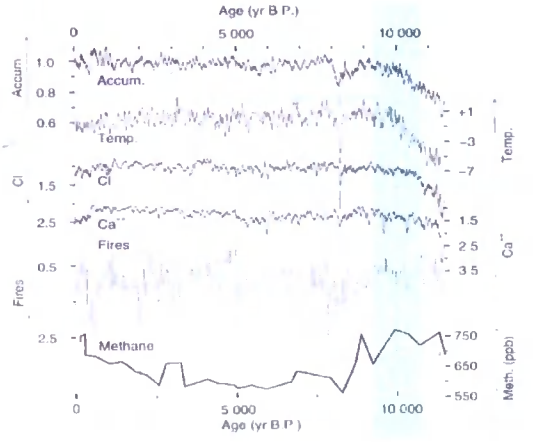

Figure 1 Multi-proxy changes recorded in the GRIP ice core during the "8.2" Ka BP climate event (Alley et al., 1997).

This event was characterised by cold, dry, dusty and low methane conditions and had a similar marine and terrestrial pattern to that of the Younger Dryas, suggesting a role for the THC (Alley et al., 1997). High resolution sampling of isolation basin sediments should identify any evidence for this climate event (which has been observed throughout the North Atlantic region) from northeast Vestfirðir coast. I will also investigate the environmental history of lakes to try and identify a signature of other early-mid-Holocene climate events including the climatic optimum and the Neoglacial.

There is evidence from ice and marine core records of a number of climatic cycles during the last glaciation and into the Holocene. Dansgaard-Oeschegner cycles occur on millennial timescales and result in progressive cooling. Bundles of Dansgaard-Oeschegner cycles make up longer-term cycles of climatic cooling called Bond Cycles. Bond cycles end with the massive discharge of icebergs that have deposited ice-rafted debris in distinct layers across the North Atlantic (Bond et al., 1992). Dahl-Jensen et al., (1998) reports evidence of the Holocene's "Climatic Optimum" between 8-4 cal. Yr BP, the Neoglacial at ca. 4 cal. Yr BP and the Medieval warm and Little ice age during the last few hundred years, from Greenland ice core date. Clearly, there are a number of climatic phenomenon that may be identified for NW Iceland from lacustrine sediments and this project will endeavour to do so.

The interpretation of results will be discussed in the context of previous research into late Weichselian and early Holocene environmental and climate change (e.g. Björck et al., 1992; Rundgren 1995; Eiríksson et al., 2000; and Andrews et al., 2002b). There is also a need to produce long biostratigraphical records for Iceland to help understand terrestrial environmental changes since the LGM. More importantly the reporting of a tephrachronology for Vestfirðir will assist correlation with both marine and terrestrial environmental records and facilitate tighter control for any RSL record that may be constructed in the future.

The following broad questions will be addressed in this thesis:

1. What changes can be observed in the multi-proxy environmental record?
2. Are there any tephra layers? And can a chronology for the above events be constructed?
3. How has the climate for northeast Vestfirðir changed during the early-middle Holocene?
4. How do other known climate records for northern Iceland correlate with the new record reconstructed in this study?

5. Do lakes from NW Iceland record large scale regional climate events of the early to middle Holocene (e.g. the 8.2 Ka BP event, the Climatic Optimum, and the Neoglacial)?

CHAPTER 2

BACKGROUND

2.1 Introduction

In this section follows a broad background of relevant research in order to inform and to place this investigation into a wider context. Attempts have not been made to provide an encyclopaedia of facts regarding "diatoms" or their role as an environmental indicator, nor have I attempted to provide a complete documentary of all research over the past few decades into the deglacial history of Iceland. In both circumstances I have presented core themes and key discoveries to facilitate clear understanding of the objectives and content of this thesis. Biogenic silica is a relatively new environmental proxy and there are many concerns about its accuracy and practicability. A brief discussion of the theory behind this method and current debates concludes this chapter.

Iceland lies in the middle of the North Atlantic Ocean in a position that is highly sensitive to north-south oscillations of the oceanic and atmospheric fronts (Figure 2). Ruddiman & McIntrye (1981) showed that these fronts have migrated south on numerous occasions since the LGM in response to changing climate conditions and fluctuations in Northern Hemisphere ice sheets. High-resolution records from Iceland are therefore well positioned to record shifts in climate in the northern Atlantic region. It is believed that melt-water released from the wastage of the Icelandic ice sheet may have had a critical impact on the formation of deep-water in the Greenland-Iceland-Norwegian sea, at the end of the Weichselian glaciation.

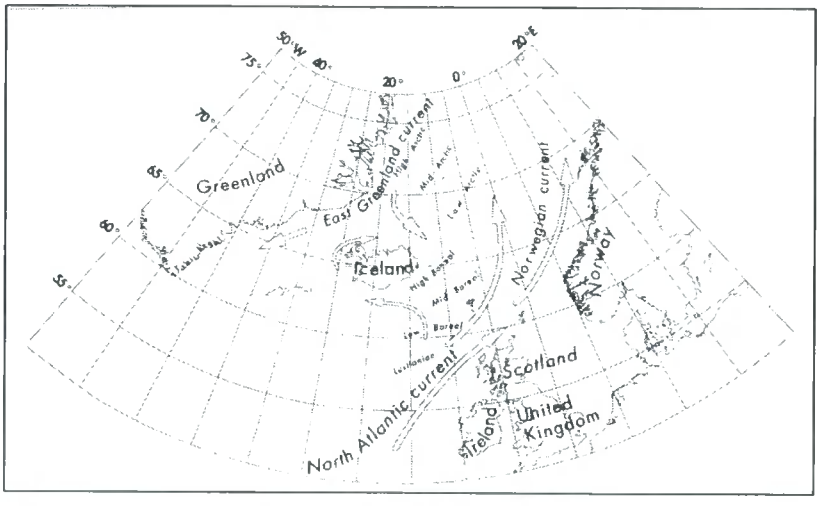

Figure 2 Ocean circulation patterns around Iceland (Source: Eiríksson et al., 1997)

The deglacial pattern of Iceland is poorly defined and it is still unknown whether a separate ice cap occupied Vestfirðir during the LGM. Relative sea-level research is highly dependent on morphological and stratigraphical evidence with loose chronological control (Maizel & Caseldine 1991). The following review is not an attempt to

comprehensively list all research to date but hopes to provide insights into the known features of Iceland's deglaciation and draw attention to current debates.

Thoroddsen (1882) was the first to view Iceland as a formerly deglaciated landmass, despite the presence of large ice caps that persist to the present day. Since then much of the early work was conducted by Thórarinsson (e.g. 1937) and Einarsson (e.g. 1961). The pattern of RSL relies heavily on morphological evidence such as raised shorelines and buried marine deposits that can be difficult to date accurately. Hence, the current deglacial chronology is based on relatively few radiocarbon dates of marine molluscs found in deglacial sequences in coastal areas and a very limited number of radiocarbon dated lacustrine sediments (Ingólfsson & Norðdahl 1994). Where moraine sequences and stratigraphic relations have been used to infer changes in climate, it has had to be assumed that glaciers tend to respond at a similar time to a given climate change, regardless of local environmental conditions or the internal dynamics of the glacier system (Maizel & Caseldine 1991). Where dateable material has been unavailable stratigraphical and morphological correlations rely upon the apparent parallelism between the timing of events with northwest Europe (Ingólfsson & Norðdahl 1994).

Iceland does and has experienced heavy volcanism (Figure 13 & 14) and layers of deposited tephra can prove extremely useful as stratigraphical markers and aid chronology. However, tephra is rarely found in inorganic sub-soils and the potential for tephrochronology during the late Weichselian and early Holocene is limited by the almost uninterrupted glaciation of Iceland (Ingólfsson & Norðdahl 1994). Nevertheless, since Thoroddsen (1905-06) first suggested the "Concept of maximum deglaciation" there has been a debate concerning whether *refugia* existed in certain locations, especially on high coastal mountains and the tips of peripheral peninsulas. If *refugia* were present during the Late Weichselian, the Skógar tephra, which has been correlated with the Vedda Ash (ca. 10.6 ^{14}C Ka BP) in Norway (Norðdahl & Haflidasson 1992) and has been observed in sediments of Late Weichselian age, may prove invaluable in fixing the chronology for Late Weichselian deglacial events.

2.2 Relative sea-level history of Iceland

The age of the marine limit around Iceland is a matter of debate. The marine limit is highest in southern Iceland at ca. 110 m a.s.l, ca. 60-80m a.s.l in western Iceland, and between 40-50m a.s.l elsewhere (Ingólfsson et al., 1995). However, Hansom & Briggs (1991) reported marine limits of ca. 70m a.s.l on the east coast of the neck of land joining Vestfirðir to the mainland; John (1974) observed raised marine terraces at ca. 135m a.s.l on Vestfirðir's west coast; Einarsson (1959) suggested a marine limit at ca. 35m a.s.l in Eyjafjörður, northern Iceland; and Hjort et al., (1985) mapped raised

shorelines at just 26m a.s.l in Hornstrandir on the north coast (Figure 17). Ingólfsson (1991) believes that the timing of the marine limit is most likely not synchronous around the island and there are two possible reasons for variations in altitude: (1) Differential down-warping of Iceland caused by differential glacial load during the Weichselian and therefore subsequent differential isostatic rebound; and (2) metachronous age of the marine limit due to regionally different deglaciation patterns.

Hansom & Briggs (1991) produced a preliminary RSL curve for the east coast of the neck of land between Vestfirðir and the mainland. Shells in glacio-marine clay, 1m a.s.l at Asmundarnes were radiocarbon dated to 9930 BP. The shell rich beach comprising remains of *Nucella Sp.* at ca. 4m a.s.l was dated to ca. 4000 BP by John (1974). The "Nucella" beach was found at numerous other sites including Hvítahlid, Asgardsgrund and Smáhamrar (Hansom & Briggs 1991). The latter site also contained excellent raised shoreline features with an unbroken series of ca. 30 beach ridges from sea-level to ca. 70m a.s.l. However, a peat dated in a swale at ~40m a.s.l gave an anonymously young age of 8875+/-50 BP (Hansom & Briggs 1991). At Hvítahlid, a 3m deep section cut into silts that lacked diatoms but contained abundant marine dinoflagellates, where intercalated with two layers of fresh water peat. These sediments were interpreted as representing a regression-transgression-regression of sea level and each peat layer was dated to 8830+/-60 BP and 6910+/-100 BP at 8.5m and 6m a.s.l respectively (Hansom & Briggs 1991).

Rundgren et al., (1997) produced the first isolation basin derived RSL record for Iceland using a combination of morphostratigraphy and biostratigraphy from isolation basin sedimentary sequences on the Skagi peninsula of northern Iceland (Figure 3). They suggest that sea-level fell ~45m between 11.3-9.1 ^{14}C Ka BP corresponding to a total isostatic rebound of ~77m. Two minor transgressions punctuate the record during late Younger Dryas and early Pre-Boreal and were probably caused by the expansion of local ice caps and readvances of the main inland Icelandic ice sheet (Rundgren et al., 1997). RSL falls below present before ca. 9 ^{14}C Ka BP.

Results from the Skagi RSL curve are based on the microfossil analyses of five coastal lakes at varying altitudes between 47m and 13m a.s.l and one open section at 1.5m a.s.l. The local marine limit is assumed to be around 65m a.s.l although the basal sediments from the highest lake (Torfadalsvatn ca. 47m a.s.l) do not contain any marine sediment. Rundgren et al., (1997) argue that this provides a limiting date on isolation, occurring before 11.3 ^{14}C Ka BP. The presence of small amounts of brackish taxa half way up the core in an unusual deposit of blue-grey clay, also containing low pollen counts, is presented as showing that the lake was close to and possibly even connected to sea level at 10.1 ^{14}C Ka BP.

Figure 3 RSL curve from Skagi peninsula, northern Iceland (Rundgren et al., 1997).

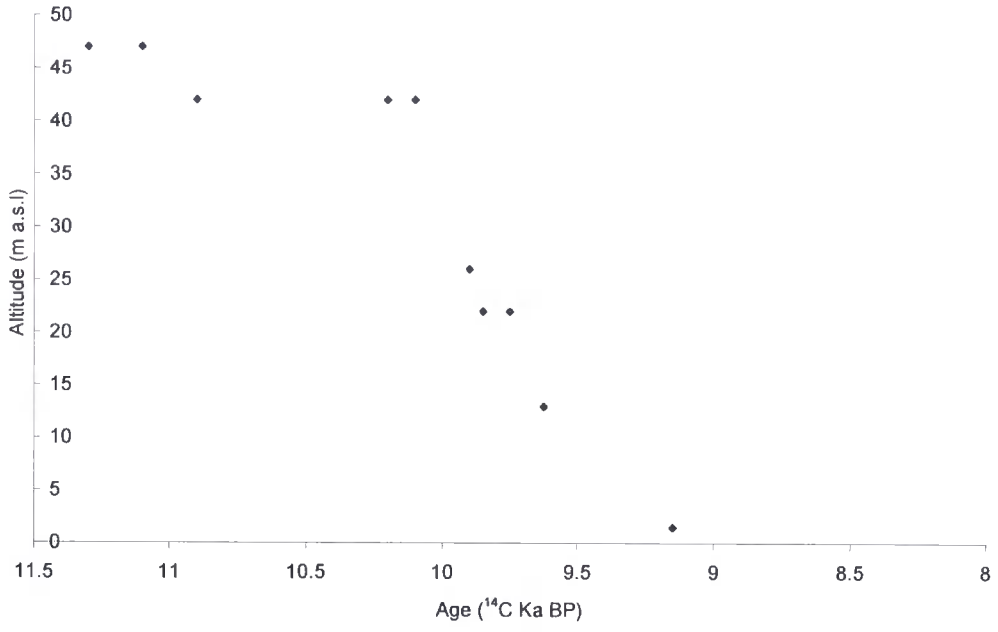

A transgression-regression sequence at ~10-10.2 ^{14}C Ka BP for Lake Hraunsvatn (~42m a.s.l) is based on the occurrence of just a small proportion of brackish taxa above a barren zone containing no diatom fossils. The evidence for this interpretation is the weakest for all the basins. Lake Geitakarlsvatn (~26m a.s.l) has increasing proportions of brackish taxa to the base and again this has been interpreted as representing close proximity to sea level. A limiting date of ca. 9.9 ^{14}C Ka BP was obtained from this lake. The basal sediments from Lake Kollusákurvatn (~22m a.s.l) were void of diatoms with the sediments above containing a good isolation sequence. An increase in marine diatoms towards the top of this core is interpreted as a return to marine conditions before a final regression. Lake Neðstavatn (~13m a.s.l) contained an excellent isolation sequence dated to ca. 9.6 ^{14}C Ka BP. The record is fixed at the bottom by an open section containing a totally fresh assemblage of diatoms and dated to 9.2-9.1 ^{14}C Ka BP i.e. RSL fell below present at approximately 9 ^{14}C Ka BP.

The microfossil data for three lakes (Lakes Torfadalsvatn, Hraunsvatn, and Kollusakurvatn) used in this study are far from conclusive and tentative conclusions at best should be made. There are problems generated by large errors with the radiocarbon dates, although attempts were made to tighten the chronology using a combination of tephrachronology, pollen biostratigraphy, and spatial relationships with morphological features. Despite these difficulties the RSL record from the Skagi peninsula still represents the best RSL data to date for the entire island. The Skagi RSL record is consistent with the early deglaciation and rapid isostatic uplift generally believed to have occurred in Iceland after the LGM. There is however, a failure to

mention whether sediment cores were successfully "bottom out" onto impenetrable substrate and if not conclusions derived from the bio-stratigraphy of some of the basal sediments may be unreliable.

2.3 Deglacial history of Iceland

Norðdahl (1979 & 1981) suggested a three-phased Weichselian glaciation for northern Iceland. During the LGM the Icelandic ice sheet extended off the coast and across the small island of Grímsey, where exposed bedrock is embroided with glacial striae. Following this there was a period of repeated glacier retreat and readvance with the formation of ice-dammed lakes. Finally, full recession of the ice sheet occurred followed by a brief readvance. The following review of Iceland's history of deglaciation comes from Ingólfsson & Norðdahl (1994):

The Weichselian maximum in Iceland is inadequately defined in both time and space because the ice margins were offshore. Before 13 cal. Ka BP there was still extensive offshore glaciation and it is believe that retreat was initiated during this period being driven by either climate amelioration or alternatively by a rise in global sea-level. Between 13-12 cal. Ka BP a massive transgression in NE Iceland occurred and was probably accompanied by a glacier readvance ~12.7 cal. Ka BP (Pétursson 1991). By 12.3 cal. Ka BP the ice margin was inland of present coastline, at least in western and northeastern Iceland (Ingólfsson 1991; and Norðdahl 1991). RSL higher than during Holocene marine limit (ML). The Allerød interstadial (ca.12-11cal. Ka BP) was terminated by glacier readvance ~11.8 cal. Ka BP in western Iceland reaching a position seaward of the present coastline (Norðdahl 1991). RSL higher than present. There were however many ice-free areas on coastal peninsulas and elevated coastal mountains, especially in northern Iceland. Glaciers probably terminated close to present coastline (Norðdahl 1991).

During the Younger Dryas chronozone ca. (11-10 cal. Ka BP) a second readvance culminating in ~10.6 cal. Ka BP occurred in western and central northern Iceland, and the continuous ice sheet reached to or beyond the present coastline. Glaciers also extended over the Reykjávik area during this period (Hjartarsson 1989; Ingólfsson et al., 1995). The first high-resolution terrestrial biostratigraphical record indicates arctic tundra conditions on the outer coast in central northern Iceland at 10.4 cal. Ka BP (Björck et al., 1992). Deglaciation of coastal lowlands commenced ca. 10.3 cal. Ka BP. RSL was high. Post-glacial marine limit around Iceland dates 10.3-9.7 cal. Ka BP (Ingólfsson 1991; and Norðdahl 1991). During the early Pre-boreal (9.8-9.6Ka cal. BP) glacier readvance and/or ice marginal still-stands were recorded in southwest, central northern and central southern Iceland (Hjartarson & Ingólfsson 1988; Ingólfsson 1991;

and Norðdahl 1991). After 9.6 cal. Ka BP there was rapid deglaciation with RSL falling below present at 9.4 cal. Ka BP in southwestern Iceland (Thors & Helgadöttir 1991). Pollen record from central northern Iceland indicates transition from a cold climate by 10.4 cal. Ka BP to interglacial sub-polar maritime climate, characterised by birch-juniper heath land by ca. 9.2 cal. Ka BP (Björck et al., 1992).

Jennings et al., (2000) reconstructed environmental conditions for Iceland's southwestern shelf between 12.7-9.4 ^{14}C Ka BP. Melt water increased during the Allerød indicating glacier retreat on land. During the Younger Dryas melt water diminished and cold conditions were in place by 11.14 ^{14}C Ka BP. Retreat of the ice margin began sometime between 10.3-9.94 ^{14}C Ka BP and onset of post-glacial deposition occurred by 9.94 ^{14}C Ka BP. Similar oceanographic conditions to the present day were established by 9.7 ^{14}C Ka BP.

Thors & Helgadöttir (1991) identified a rapid regression in the early Holocene from ca. 65m to -30m a.s.l. followed by transgression to present. This was based on radiocarbon dated marine shells (ca. 9030+/-1280 ^{14}C yrs. BP) and a submerged freshwater peat in Faxaflói that was discovered by dredging activities in 1968.

There is increasing evidence that the Weichselian glacial history of southwestern Iceland was characterised by a fluctuating local glacier over the Reykjanes peninsula, rather than the central ice cap which covered most of Iceland (Eiríksson et al., 1997). Stratigraphical evidence from the three sections at Surdanes indicates that the glacier did not extend to the present coastline at ca. 28Ka BP and the area was essentially ice-free. There was no sediments of late Weichselian age and therefore, it was assumed that ice had overridden this area at that time. Ice disappeared from the coastal areas by the Bølling chronozone and evidence from the Fossvogur beds suggests that Surdanes was ice-free by the Allerød-Younger Dryas transition. A readvance was indicated during the Younger Dryas, which culminated with influxes of relatively warm water.

Late glacial and Holocene marine sediments have been dated and studied around northern Iceland (e.g. Andrews et al 2002; Eiríksson et al., 2002) and southwestern Iceland (e.g. Jennings et al., 2000) and have indicated rapid deglaciation of the shelf during the Bølling-Allerød interval, ca. 11-13Ka BP (Andrews et al., 2002). There is also evidence for cold conditions existing in Iceland during the Younger Dryas chronozone (e.g. Andrews & Helgadöttir 2003; Jennings et al., 2000; and Rundgren et al., 1997). However, the deglacial history of Vestfirðir is somewhat different to the rest of Iceland and this may be a consequence of it being potentially an independent area of ice loading. Ingólfsson et al., (1995) showed Vestfirðir as a separate ice centre where a broad U-shaped ice divide draining primarily into Ísafjardardjúp, a large fjord system in

the northwest. Andrews et al (2002a) explains that the limited glaciation during the late Weichselian across Vestfirðir is supported by low marine limits from Hornstrandir (Hjort et al., 1985); the Strandir coast (Norðdahl 1991); and around Húnaflói (Rundgren et al., 1997). Recent research into modelling of the former Icelandic ice sheet have not been consistent, with Webb et al., (1999) suggesting a single cohesive ice sheet centred over central Iceland and extending to the shelf break, whereas Stokes & Clark (2001) favour a smaller independent ice mass over Vestfirðir.

Andrews et al., (2002) reconstructed a sediment history from Djúpáll, off the northwest coast of Vestfirðir. The evidence suggests that the LGM ice marginal position (Figure 4) of the ice stream in Ísafjardardjúp, only extended to the mouth of the fjord complex (Andrews & Helgadöttir 2003). On the eastern coast of Vestfirðir, Andrews & Helgadöttir (2003) discovered that the former Icelandic ice sheet extended out to the shelf break and must have been formed by ice streams draining the west central highlands. Here, glacially deposited diamictons are overlain by post-glacial mud with intermittent ice rafted debris (IRD) that was more abundant during the Younger Dryas chronozone (Andrews & Helgadöttir 2003). A radiocarbon date was obtained from foraminifera and indicated that the Húnaflói shelf was deglaciated by ca. 13Ka cal. BP (Andrews & Helgadöttir 2003). The lack of any thick deglacial sediments suggests that this deglaciation was very rapid (Andrews & Helgadöttir 2003).

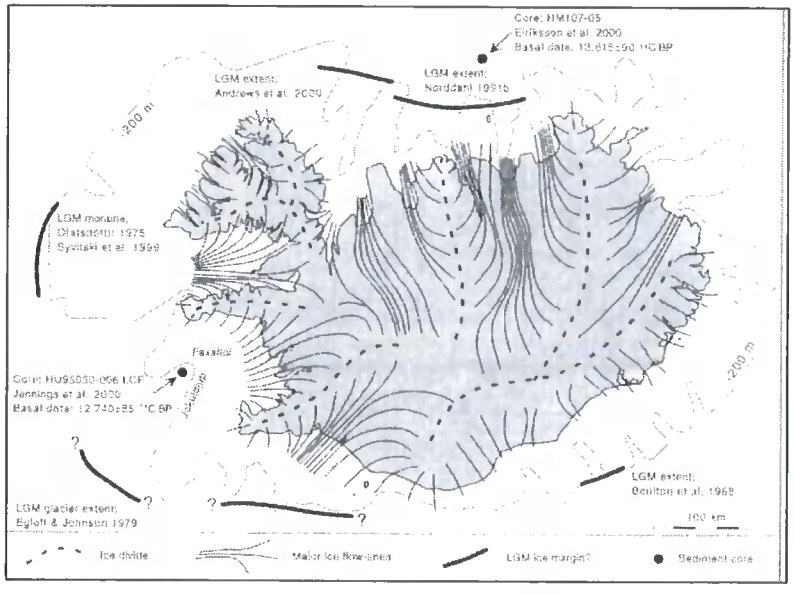

Figure 4 The known LGM ice positions for Iceland (Source: Norðdahl & Ingólfsson 2001)

In summary, it is generally assumed that coalescing ice streams from central ice centres extended beyond the present coastline during the Weichselian maximum around 18Ka BP (Oxygen isotope stage 2) (Eiríksson et al., 1997). During the Bølling chronozone,

high shorelines and marine deposits within the current coastline represent major shrinkage of the main ice caps at that time (Ingólfsson 1987; 1988). Two readvances have been documented for the west and southwestern Iceland and have been correlated with the Older Dryas and Younger Dryas chronozones (Eiríksson et al., 1997). The well radiocarbon dated Fossvogur beds in Reykjarvík show marine deposition during the Allerød (Geirsdóttir & Eiríksson 1994; Sveinbjörnsdóttir et al., 1993). Geirsdóttir & Eiríksson (1994) suggested glaciomarine deposition at the margin of an expanding tidewater glacier at the Allerød-Younger Dryas transition, followed by continued transgression and increased distance from the ice-marginal process (Eiríksson et al., 1997). Rundgren et al., (1997) showed that these two readvances resulted in two minor transgressions of sea-level in northern Iceland.

2.4 Current debates

The size and extent of the former LGM ice sheet is a matter of debate between a relatively restricted glaciation e.g. Hjort et al., (1985) or extensive glaciation (e.g. Andrews & Helgadöttir 2003). Thoroddsen (1905-06) was a "monoglacialist" and proposed (based on observations of glacial striae on all Icelandic peninsulas) that a single ice sheet occupied Iceland during the Weichselian and extended offshore. It was assumed that the LGM volume and extent occurred around 18Ka BP and from Icelandic shelf features it was inferred that the ice sheet extended to the shelf-break (Ingólfsson 1991). Einarsson (1961, 1967, 1978, and 1991) put forward a morphological synthesis for the deglaciation of Iceland based on a broad summary of earlier work (Ingólfsson 1991). This model included two stadials and two interstadials and recognised a relatively limited Younger Dryas glaciation and implied that the marine limit around Iceland formed before the Younger Dryas (Ingólfsson et al., 1995). Since then a series of studies with improved radiocarbon chronologies have criticised the timing and pattern of this model in favour of a more heavily glaciated Younger Dryas and more numerous glacier readvances during deglaciation (e.g. Ingólfsson et al., 1995; Ingólfsson 1991; Norðdahl 1991). The new deglaciation concept of Ingólfsson (1991) and Norðdahl (1991) has resulted in the review of past research and chronologies have been revised to fit (e.g. Ingólfsson et al., 1995).

There is an increasing body of evidence opposing the "Vatnajökull-centric" view whereby "isostatic adjustment during the late Weichselian and early Holocene was controlled largely by the wastage of the Vatnajökull ice sheet, and resulted in a sequence of raised shorelines inferred to tilt more-or-less uniformly to the north and west" (Hansom & Briggs 1991). Despite evidence of declining raised shoreline altitudes towards the coast (e.g. Einarsson 1963; Ingólfsson 1991) Rundgren et al., (1997) found it difficult to identify any trend in a series of raised shorelines on the Skagi peninsula. Hansom & Briggs (1991)

suggest an alternative hypothesis from the models of Einarsson (e.g. 1961, 1967, 1978, and 1991), Ingólfsson (1991), and Norðdahl (1991). It is possible that the prominent northwest peninsula of Vestfirðir held an independent ice cap during the Weichselian glaciation of Iceland and therefore experienced an essentially independent history of deglaciation, resulting in a regionally distinctive sequence of features related to sea-level change (Hansom & Briggs 1991).

The presents/absence of *refugia* on Iceland is key to the debate on the lateral extent of the former Icelandic ice sheet during the late Weichselian. Lindroth (1931) developed this idea in Iceland, although Hoppe (1968 & 1982) has dismissed many of the potential sites as having been previously overridden by late Weichselian ice. Buckland & Dugmore (1991) believe that despite Iceland existing for more than 15million years as an island; it lacks endemic species due to the frequency and severity of past glaciations. Buckland & Dugmore (1991) suggest that low powers of dispersal and affiliations of most biota with northwest Europe, couple with the prevailing westerly flow of ocean and atmospheric circulation, contradicts the hypothesis for the arrival of plankton from an aerial source. They conclude that the most likely origin of colonisers was from ice rafts and in-flood debris from a rapidly decaying Fennoscandinavian ice sheet during the early Holocene (Buckland & Dugmore 1991). Biostratigraphical analysis of Lake Torfadalsvatn, on the Skagi peninsula, by Rundgren (1995) shows evidence for shrubs and dwarf shrubs in northern Iceland by ca. 10.9 ^{14}C BP. Rundgren (1995) suggests that the spread of plants to Iceland may have occurred earlier than previously thought, although the possibility that they survived in mountain *refugia* during the last glaciation can not be ruled out. As well as providing a minimum date for deglaciation, analysis of sediments from lakes on Vestfirðir's northeast coast may shed light on the presents of possible *refugia* in the area.

2.5 Diatom applications in RSL research and palaeoenvironmental reconstruction

Diatoms are microscopic unicellular algae, which normally live in wet, naturally illuminated environments as plankton, or attached to a substrate (Palmer & Abbot 1986). Diatoms are particularly sensitive to their environment and can help us to understand past changes. It is assumed that a living diatom assemblage is faithfully recorded in the sedimentary record (Flower 1993) and all efforts should be undertaken at the site to minimise the adverse effects of processes that may have encouraged non-replication of the diatom population.

Diatom microfossil analysis is widely used for the reconstruction of past environments (e.g. Snyder et al., 2000; and Wolf 2003) and has proved especially effective in tracing

the isolation from the sea of coastal lakes (e.g. Shennan et al., 1994; 1996; Corner et al., 1998; 2001; and Long et al., 1999; 2002; 2003). Fossil diatom assemblages have also been used for palaeo-reconstructions of pH (e.g. Renberg & Hellberg 1982; Charles 1985; and Weckström et al., 1997); Nutrient levels (Hall & Smol 1993); Dissolved organic content (e.g. Pienitz & Smol 1993); and water temperature (Birks 1995; Korhola et al., 1995).

The linkages between diatom populations and climate change are yet to be resolved fully. Many authors have discussed the possible direct and indirect influence that climate may or may not have on a diatom community (Figure 5 & 6). Causal relationships between diatom communities and their environment are difficult to explain given the many environmental variables that diatoms may respond to (e.g. Light availability, duration of the growing season, nutrient availability, turbulence, lake exposure, habitat types and availability, lake stratification and temperature).

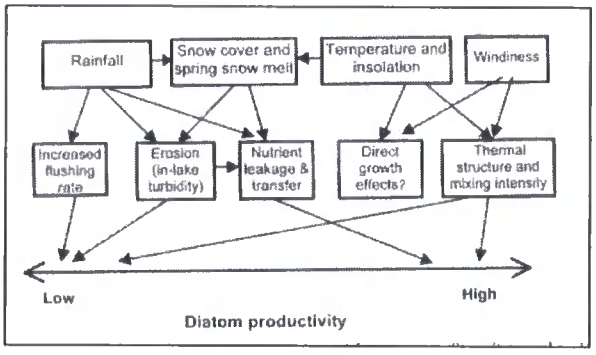

Figure 5 Indirect influence of climate on diatom productivity (Source: Anderson 2000).

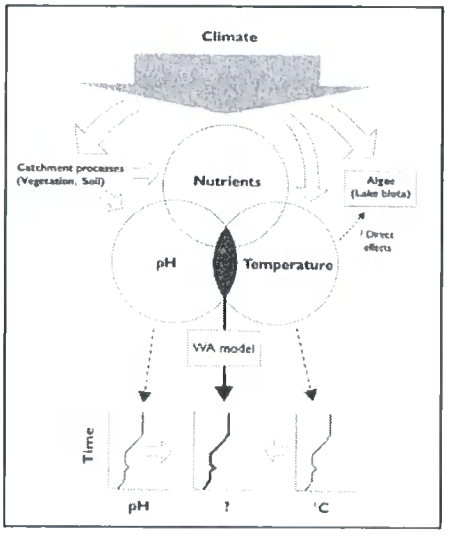

Figure 6 The influence of climates on pH, nutrients, and temperature of aquatic habitats (Anderson 2000).

Diatoms are found in a wide range of aquatic habitats and their dissolution-resistant silica walls have resulted in massive sedimentary accumulations (Graham & Wilcox eds. 2000). Each diatom secretes a rigid external structure known as a frustrule composed of amorphose opaline silica with organic coatings. This frustrule may be considered as one of two common types; Pennate or centric and is highly decorated with a variety of ornamentation's reflecting taxonomic diversity (Graham & Wilcox eds. 2000) allowing identification between different species to be possible. The abundant preservation of diatoms from a variety of environments (Figure 11a) and the possibility to distinguish between taxa has made diatoms ideal for palaeo-RSL studies as well as reconstructions of past environments.

Habitat Type	Description
Planktonic	"Free" floating in open waters
Epiphyton	Living attached to plants
Epilithon	Living attached to hard surfaces e.g. rocks
Epipsammon	Living on sand grains
Epipelon	Living on sediments
Aerophilic	Living in drier zones e.g. on moss on rocks within the spray zones of rivers and lakes, on snow and ice, soil and even in caves with sufficient light.

Figure 7 Diatom habitat type (Source: Moser et al., 1996)

A dominant population can be effectively replaced in a single season during a "bloom" (singular depositional events wherein large numbers of uni-specific communities may be deposited) and therefore diatoms show evidence for changing environmental conditions (Palmer & Abbot 1986). Hurley et al., (1985) believes that the nutrient supply to the euphotic zone is an important factor regulating phytoplankton growth. According to them "blooms" occur as a result of lake overturn which transfers nutrient rich bottom waters to the photic zone (Hurley et al., 1985). It was believed that periodic blooms of certain taxa would contribute an inappropriate bias to the microfossil content of sediments, although this is now considered not to be the case due to the continuous mixing of sediments by the process of bioturbation. Therefore, sediment composition may be considered analogous to the moving average although, there appears little benefit from sampling at very fine intervals (Palmer & Abbot 1986). Blooms in diatom production that occur over longer time periods i.e. hundreds of years, are a product of interglacial conditions where increased limnological activity is generated by fertilisation of the lake waters by nutrients released from the catchment and transported by meltwater to the basin (Qui et al., 1993)

Seawater may transport free-floating *planktonic* diatoms to coastal site of deposition. Planktonic diatoms tend to be circular in outline and are thus *centrics*. Their movement to a site of deposition rather than growth in a specific location reflecting local conditions mean that these types are often considered "contaminants" for palaeo-environmental reconstruction. However, for the simple matter of identifying sediments of marine origin

they are sufficient. Abbot and Palmer (1986) suggest it is often unwise to make palaeoenvironmental interpretations upon the basis of fluctuations in the frequency of a single taxa within an assemblage given that diatom populations and associated assemblages are often diverse (perhaps >30 taxa).

2.5.1 Diatoms and RSL research

RSL research has greatly benefited from the application of diatoms as recorders of environmental changes. Diatoms may be found in three zones near the seashore outlined in Figure 7.

Coastal Zone	Reference to tide nomenclature	Description
Subtidal zone	< lowest high tide	Simple communities.
Intertidal zone	Between extreme tides	Greatest variation in environmental conditions. e.g. Wave energy, depth, area and composition of exposed substrate, salinity, nutrient supply & illumination. High variability.
Supratidal zone	> Highest high tide	Harsh environment.

Figure 8 (source: Palmer & Abbot 1986)

Hustedt (1937-39) realised that diatoms have a very strong relationship to certain environmental variables including salinity and in 1957 introduced the Polyhalobian Classification System. The Polyhalobian system organises different taxa into five broad classifications depending on the salinity tolerance of each taxa:

- Polyhalobous (Prefer salinity >30‰) - *Marine* and *brackish* environments.
- Mesohalobous (Prefer salinity 30-0.2‰) - *Marine* and *brackish* environments.
- Oligohalobous-halophilous (Prefer slightly saline water) - *Brackish* and *freshwater.*
- Oligohalobous-Indifferent (Prefer *freshwater*, tolerate slightly saline water)
- Halophobous (Exclusively freshwater <0.2‰) - *Freshwater* environment.

2.5.1.1 Isolation Basins

Coastal lakes that occupy natural rock depressions and that have a history of connection and disconnection to the sea by relative sea level changes are known as isolation basins (Long et al. 1999) (Figures 8 & 9). A combination of lithological and biostratigraphy preserved in these basins can record the isolation and connection history of a lake from the sea (Shennan et al., 1994). The isolation of a coastal lake is controlled by the altitude of the threshold and if this can be related to a reference tide level and radiocarbon dated can provide very accurate information about the position of sea-level

at a given time and a given place. The analysis of a "staircase" of isolation basins allows reconstruction of changes in RSL for that area. The amount of isostatic rebound can be estimated from RSL curves therefore, providing a means to make direct estimations of the amount of former ice loading (e.g. Shennan et al., 2000). RSL curves provide a record of isostatic recovery mediated by eustatic sea-level changes thus allows the pattern of and rate of deglaciation to be elucidated and evaluated.

2.5.1.2 Definition of an Isolation Contact

The isolation contact is the horizon within the sediments that represents the time of lake isolation from the sea (Kjemperud 1986). Kjemperud (1986) proposed four isolation contacts of which three are relevant to this study (Figure 10). The diatom isolation contact (DIC) is the horizon that was the sediment-water interface at the time when the water in the photic zone of the isolation basin became fresh (Kjemperud 1986). Its importance is implicit in the fact that it represents the final isolation. When there was a total stop of marine incursions into the isolation basin the hydrological isolation contact formed (Kjemperud 1986). The sedimentological isolation contact, is the horizon where sediment characteristics change from a predominantly allochthonous minerogenic sediment to an autochthonous freshwater organic deposit (Long et al. 1999). Finally, the sediment/freshwater contact is defined by the sediment surface at the time when there is no longer any residual sea water persisting in the basin (Kjemperud 1986).

2.5.1.3 Isolation basin stratigraphy

It is common to interpret the stratigraphy of such basins with respect to three main "genetic facies units identified primarily on lithological character which reflects, in turn, major differences in depositional environment" (Corner et al. 1999 P.149). Diatom microfossils are used to establish the depositional environment of each facies unit because they are considered to respond ecologically to changes in salinity and other hydrographic parameters when a basin isolates from the sea due to postglacial shore displacement (Stabell 1985). Typical isolation basin stratigraphy includes a basal marine sediment unit upon which brackish and finally freshwater lake sediments have been deposited in turn (e.g.; Snyder et al., 1997; Corner & Haugane 1993; & Foged 1977). A more detailed description follows:

a) Marine Facies Unit I

A grey minerogenic clay-silt often found to contain isolated fish bone fragments and shells (Corner et al. 1999). Diatoms are typically exclusively polyhalobous and mesohalobous (Kjemperud 1981; Snyder et al., 1997; & Corner et al., 1999). This unit is

interpreted as having formed within a marine environment up and until the basin was isolated by a regression in RSL (Corner et al., 1999). Unfortunately, marine sediments are often sparsely populated by diatom microfossils (e.g. Rundgren et al., 1997), with a bias towards poorly preserved valves of more robust polyhalobous/mesohalobous varieties (Snyder et al., 2000), thus making sediments of a marine origin harder to identify.

b) Transitional Facies Unit II

Typically, a dark olive-grey to very dark-brown or black muddy gyttja (Corner et al., 1999). Unit II may have sub-mm thick fine jet-black laminations. This unit contains a greater organic content than Unit I (Snyder et al., 1997) and has a more varied diatom assemblage (Kjemperud 1981) with a tendency from marine to freshwater up the unit. The transitional unit describes a brackish depositional environment where as saline bottom waters become increasingly anoxic due to a lack of replenishment or an increase in seasonal variability in oxygen content the diatom flora gradually changes from marine to freshwater (Corner et al., 1999). It is currently thought that the fine black laminae were formed under a meromictic lake stratification that persisted for some time after isolation (Snyder et al., 1997; Snyder et al., 2000).

Snyder et al., (2000) studied the postglacial climate and vegetation history of Lake Yarnyshnoe-3, in the central-north area of the Kola Peninsula. Analysis of the diatom microfossils from this lake clearly shows that alkaliphilous taxa dominate the isolation from the sea. As has been observed previously, immediately above this unit *Fragilaria spp.* dominate, which is typical of early postglacial diatom assemblages (e.g. Kjemperud 1981; Stabell 1985; and Shennan et al., 1994). Early Holocene diatom assemblages dominated by benthic taxa, particularly *Fragilaria*, reflect changes in water chemistry and suggest an unproductive, alkaline, and immature lake system (Bradshaw et al., 2000). Abrupt changes in diatom taxa reflect rapid change during the early history of the lake including: The removal of salts from the lake and surrounding catchment; changes in flow characteristics; and changes in vegetation and climate at the beginning of the Holocene (Snyder et al. 2000).

c) Lacustrine Facies III

Unit III is often an olive-brown muddy gyttja or silty-gyttja mud with high organic content and often containing abundant *turfa humosa* (e.g. Corner & Haugane 1993; and Snyder et al. 1997). Oligohalobous-indifferent and oligohalobous-halophilous diatoms dominate. This unit is interpreted as having formed under freshwater lake conditions and the

thickness of the gyttja is partly dependant on the time elapsed since isolation (Corner et al., 1999).

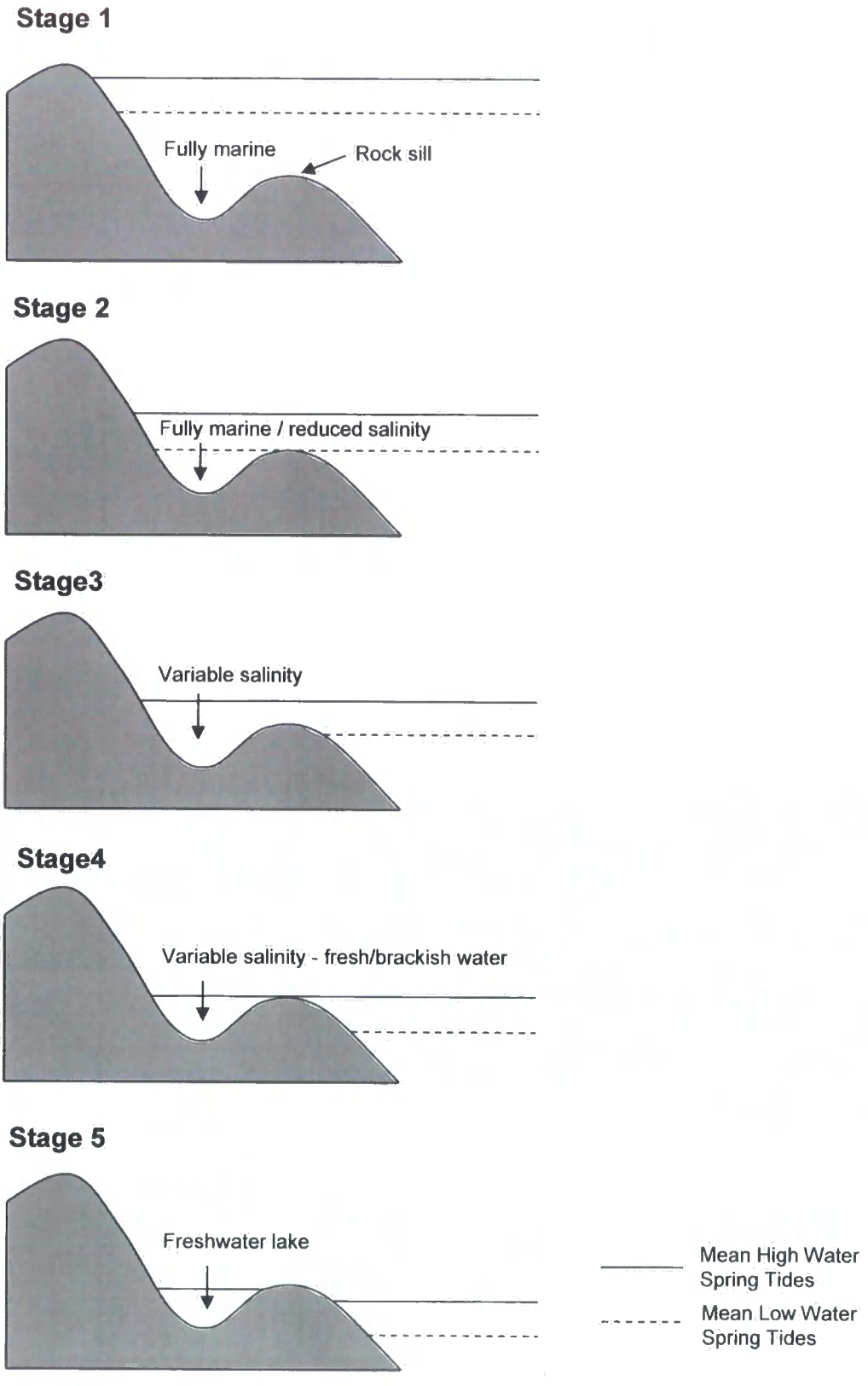

Figure 9 Schematic representation of an isolation basin during a RSL fall (Source: adapted Kjemperund 1981)

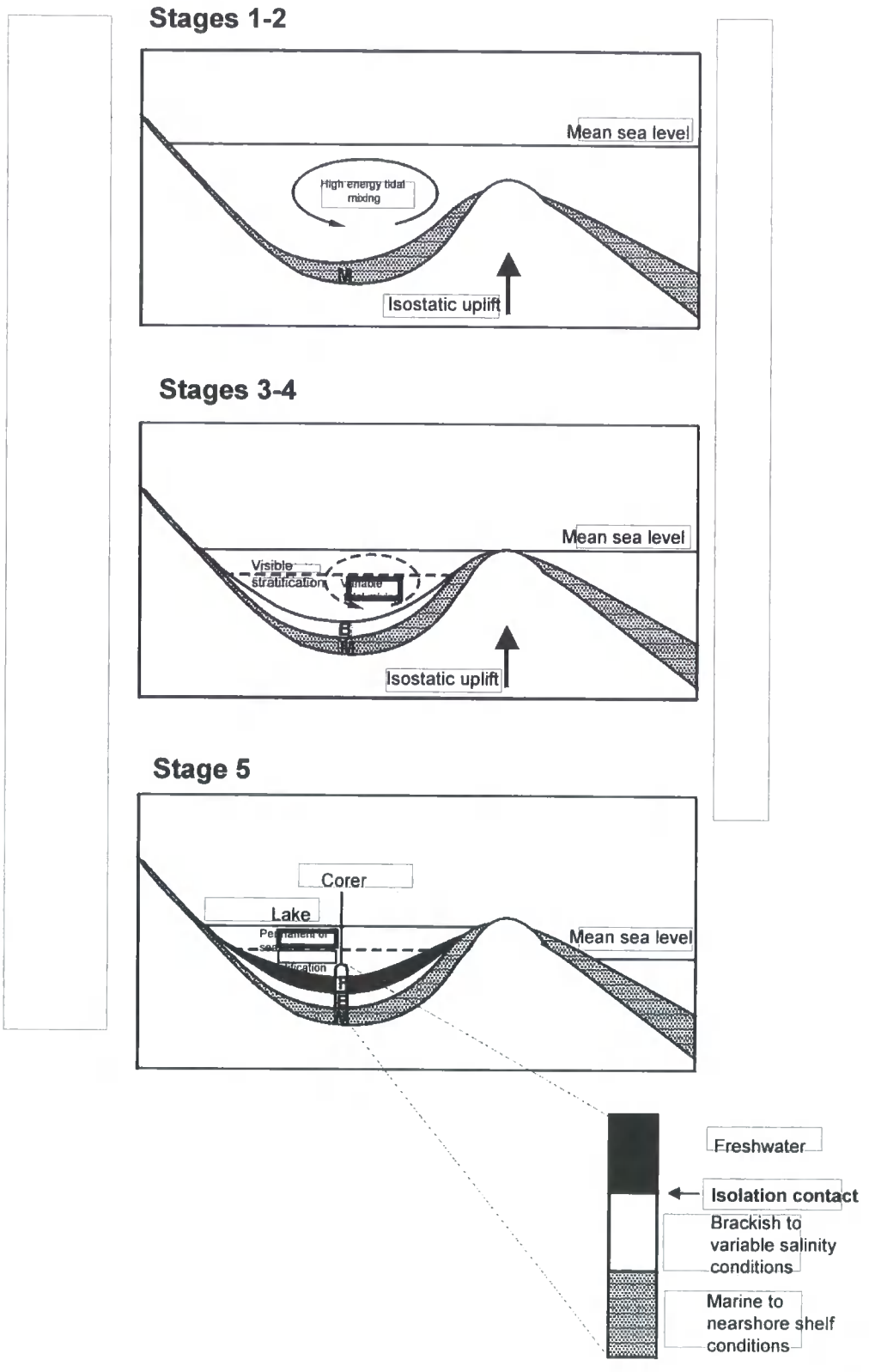

Figure 10 Schematic representation of the hydrological conditions in an isolation basin during an RSL fall (Source Mackay 2004 adapted from Kjemperund 1981)

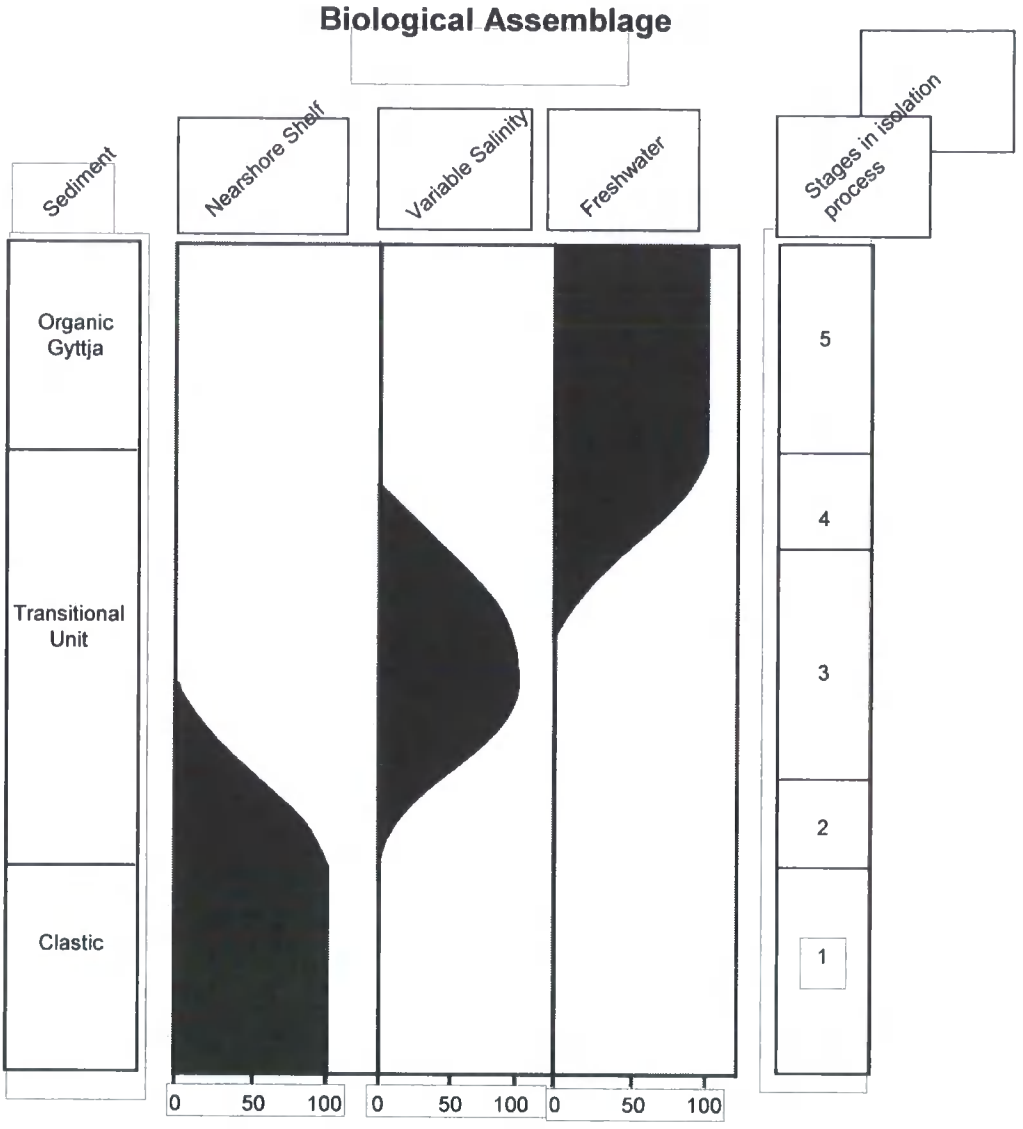

Figure 11 A conceptual model of the biological assemblage change during a RSL fall. The left column presents typical sediment types deposited during an isolation process. The right column relates to stages of the isolation process in figure 8 and 9 (Source Laidler 2003)

2.5.2 Diatoms and reconstructing past environments

Diatoms offer considerable potential for the reconstruction of past environments. During the Holocene since they respond rapidly to changes in climate and other environmental factors. For over a century ecologists, diatomists, bio-geographers and limnologist's alike have been generating a wealth of information on diatoms that now resides at our disposal. These studies identified that many taxa have narrow ecological tolerances and optima and are therefore potentially sensitive indicators of environmental changes (Moser et al., 1996).

An implicit assumption in all palaeoecological research is that the thanatocoenoses (i.e.death assemblage) are representative of the parent community (Moser et al., 1996). An understanding of the preservation potential of individual taxa allows an evaluation of a diatom assemblage with regards to this concept. Qualitative inferences can be made about the environment of a diatom population from the wealth of information accumulated on controlling variables such as: trophic status, habitat type (Figure 5 & 6), preservation potential, and oxygen requirement. However, in order to delineate clearly between environmental parameters in order to identify those that are primary controllers of change within diatom communities' multivariate statistics are required. Transfer functions based on conical correspondence analysis (CCA), de-trended conical correspondence analysis (DCCA), and weighted averaging (WA) regression and calibration have been developed from extensive regional data sets have been developed to established cause an effect relationships. The following list of environmental variables have been investigated: pH (e.g. Weckström et al., 1997; Birks et al., 1990); Salinity (Fritz et al., 1991); Nutrient levels (Hall & Smol 1993); Dissolved inorganic (DIC) and organic carbon (DOC) (Pienitz & Smol 1993); Hydrological conditions (Bradbury 1987); Light (Patrick 1977); Temperature (Pienitz et al., 1995); and Turbidity (Dean et al., 1984).

2.5.2.1 Diatoms and pH

It has long been recognised from the early work of Hustedt (1937-39) that diatoms have a strong relationship with pH. Nygaard (1956) was the first to introduce a quantitative aspect to the earlier workings of Hustedt, where diatoms were only classified into groups based on a range of pH tolerance from within which that taxa could be expected to be found (see Figure 11b). Nygaard (1955) developed three indices based upon the relative proportions of acid and alkaline taxa and attributed greater statistical "significance" to acidobiontic and alkalibiontic diatoms arguing that they were stronger ecological indicators than their acidophilous and alkaliphilous counterparts (Battarbee 1986).

Category	Description
Acidobiontic	Optimum distribution at pH <5.5
Acidophilic	Widest distribution at pH <7
Indifferent (circumneutral)	Greatest distribution around pH 7
Alkaliphilic	Widest distribution at pH <7
Alkalibiontic	Occurs only at pH >7

Figure 12 (source: Hustedt 1937-1939)

However, the Nygaard (1956) indices had three major limitations: (1) By definition an index provides relative values of a "parameter" around the integer 1 and does not actually measure lake water pH; (2) When using weighted averaging it is increasingly critical to accurately know the pH range of individual taxa so that taxa may be placed in the correct category (Battarbee 1986); (3) Renberg (1976) suggested that exclusion of circumneutral (oligohalobous-indifferent) taxa from the indices could lead to large fluctuations in the index unrelated to any real change in nature (Battarbee 1986).

Renberg & Hellberg (1982) modified Nygaards indices acting on earlier criticisms and incorporating circumneutral taxa into the calculations. They also provided a simple equation for conversion from Index to actual reconstructed pH. By doing this they removed one of the major problems of the Nygaard (1956) indices but nevertheless, the accuracy of their modifications is still highly dependent on the initial classifications of diatom taxa into Hustedts (1937-39) categories. Charles (1982) showed that their reconstruction of pH using Renberg & Hellberg (1982) equation are statistically correlated with actual pH to r^2 0.93. Using Index B and weighted averaging to reconstruct pH has proved especially useful where modern diatom assemblage data is absent and data used for taxa pH classification has been collated from literature sources (Battarbee 1986).

Over the past two decades the potential of fossil diatom assemblages to allow lake baseline pH conditions to be estimated and to illustrate late Holocene acidification has been realised (e.g. Renberg & Hellberg 1982; Stevenson et al., 1989; Birks et al., 1990; and Weckström et al., 1997). However, given that the sediment record obtained for the purposes of this study only covers the early-middle Holocene period in NW Iceland, the pH reconstruction will predate any anthroprogenically or naturally forced late Holocene lake acidification.

2.5.2.2 Diatoms and climate

It has proved difficult to establish any direct link between changes in climate and changes in diatom community composition or abundance. Nevertheless, aquatic scientists have not been deterred from attempting to develop diatom based transfer functions in an attempt to reconstruct air or lake water temperature (e.g. Weckström et al., 1997b). Anderson (2000) is critical of the early attempts to reconstruct temperature

from fossil diatom assemblages claiming that diatom-temperature models based on weighted averaging regression and calibration are weaker than those developed for salinity, pH and phosphorus. The strength of transfer functions developed for other parameters over those developed for temperature suggest that they are of greater importance for explaining the composition of observed diatom communities. Flower (1993) has showed through a series of laboratory studies, where all things being equal and with the removal of natural competition, diatoms respond with faster growth rates to increasing temperatures, although this has never been successfully demonstrated in a contemporary study.

Numerous studies have identified more than one parameter has having a statistically significant influence over a diatom population (e.g. Pienitz & Smol 1993). Moreover, this pattern is complicated further by the high levels of correlation that these variables have with each other. With the obvious diversity of influential variables on diatom communities it has become clear that even if temperature can never be identified as a controlling factor, the influence of climate on the processes that do is so strong that indirect effects can never be ruled out and some degree of cause and effect relationship must be present.

Probably the most direct influence that climate has upon diatom populations in Arctic, sub-Arctic and high mountainous regions is the seasonal development of an ice-pan. Smol (1983) developed an "Ice Pan Model" to describe the effects on the diatom community in such locations of seasonal ice cover. Sub-arctic lakes are dominated by low air temperatures and surfaces freeze over for a large proportion of the year limiting light availability for in-lake photosynthesis and thus, reducing the growing season and the productivity of lake fauna and flora (Perren et al., 2003). Douglas and Smol (1999) believe that in response to climate warming the duration of permanent ice-cover of sub-arctic and Arctic lakes as well as the thickness of the seasonal ice will be reduced and the Ice Pan Model describes the likely response of the diatom community to a reduction in the size and duration of the winter ice-pan. The Ice Pan Model may go some way to describing the effects of Holocene climate amelioration post-LGM in Iceland on freshwater lake diatom communities.

A reduction in the size of the ice-pan would promote an increase in the diversity of habitats by increasing the amount of photosynthetic active light into the euphotic zone for plankton growth, and allowing the littoral zone to be colonised by, mosses and thus epiphytic species (Perren et al., 2003). Furthermore, with a longer growing season diatom communities can establish themselves and reproduce for greater duration of the year increasing productivity and complexity (Perren et al., 2003). As the seasonal ice-pan shrinks in size deeper water becomes available for colonisation as the "moat"

increases between the ice-pan edge and the lake shoreline (Perren et al., 2003). Lotter & Bigler (2000) claim that with an increase in temperature a shift from small shallow water taxa to larger epiphytic bethic and planktonic species should be apparent. Therefore, after deglaciation and as Iceland began to warm due to the ameliorating affects of the Holocene the thickness and coverage of the seasonal ice pan would decrease. This would result in the opening up of deeper waters for habitation by diatoms and an overall longer growing season.

2.5.2.3 Diatoms and nutrient cycles

Diatoms are mainly influenced by the nutrient cycles of phosphorous and silica. The growth of diatoms is strongly dependent on the presence of dissolved silica (DSi) using the silica as a building material for their skeletal structures. Phosphorous is the key "growth" nutrient for diatoms and eutrophication of aquatic environments can be caused by phosphorous nutrient enrichment brought on my excessive inputs into the lake system (Schelske et al., 1983). The phosphorous and silica cycles are intimately linked through the growth and decay patterns of diatom communities.

Diatom communities can be sensitive to small changes in phosphorous, especially in phosphorous-limited systems (Conley et al., 1993). An increase in the supply of phosphorous and other important nutrients such as nitrogen may cause an increase in the productivity of diatoms and even a change from small benthic varieties to larger more nutrient demanding taxa. As diatom populations expand in numbers and size the demand on silica from the surrounding lake waters increases. As silica is extracted by an enlarged diatom community there is a reduction in the water column DSi reservoir through modification of the biogeochemical cycle of silica (Conley et al., 1993).

However, this expansion of the diatom population in response to a rise in nutrient flux into the lake can only be initiated if there is sufficient capacity of extra silica dissolved already in the lake waters. Hence, the levels of DSi in any lake system can be considered as important a regulator on diatom growth as the availability of nutrients. An increase in diatom productivity has the net effect of lowering the concentration of silica within the lake as silica is buried with successive death assemblages and removed from the cycle (Conley et al., 1993).

Barker et al., (2000) considered the possibility that thick tephra deposits may have adverse effects on the cycling of phosphorous creating "an impermeable barrier over the lake's sediment preventing the regeneration of nutrients such as phosphorous" (Telford et al., in press). The Saksunarvatn Ash was found in deposits >7cm thick in one of the study sites in this investigation and Iceland is known for its abundant tephras and

frequent volcanism (Figure 13). It is quite possible that phosphorous cycling in Icelandic lakes have been prohibited on numerous occasions throughout the Late Weichselian and Holocene.

2.6 Biogenic silica

Silica is present in lake and lagoonal environments in organic (or biogenic) (e.g. diatoms, phytoliths, radiolarians, siligoflagellates and sponge spicules) and inorganic forms (e.g. tephra, sand, silt and authigenic alumosilicates) (Conley 1998). BSi allows the amount of siliceous microfossil abundance in sediments to be quantified and it is believed that diatoms constitute the principal component (Conley 1998). Therefore, BSi has been extensively used as a proxy to measure diatom production and to reconstruct diatom productivity (Lisitsyn 1971). BSi analysis has been used to identify trends in late Holocene lake eutrophication (e.g. Schelske & Stoermer 1993; Conley 1988; Newberry & Schelske 1986; and Schelske et al; 1983). More recent applications have been as a proxy for diatom palaeo-productivity (e.g. Conley 1998; and Qiu et al; 1993). There have also been attempts to extract from lacustrine sediments a silica-isotopic signal with mixed success (e.g. Hu & Shemesh 2003; Rosqvist 1999; Colman 1995; Juillet Leclerc & Labeyrie 1987).

There are numerous techniques for the chemical determination of BSi: Direct x-ray diffraction after heated conversion of opal cristobalite (Ellis & Moore 1973); Direct x-ray diffraction of amorphous opal (Eisma & Van der Goost 1971); Direct infrared-spectroscopy of amorphous silica (Chester & Elderfield 1968); Elemented normative partitioning of bulk sediment chemistry (Leven 1977; Brewster 1983); Differential wet-alkaline extraction (Eggimann et al., 1980; DeMaster 1979); Microfossil counts (Pokeras 1986); and Biovolume (e.g. Conley 1988).

All methods have inherent systematic problems or are analytically cumbersome (Mortlock & Froelich 1989). Nevertheless, the wet chemical digestion technique has become the most popular amongst scientists because of its relative simplistically and due to problems with other methods. The wet chemical digestion technique is based on the principal that a weak base more readily dissolves the poorly crystalline silica of microfossils before more ordered mineral phases (Conley 1988). Flower (1993) believes that BSi results from the wet chemical digestion method may be unreliable due to readsorption back on to undissolved sediment, although these criticisms have been largely explained by Conley (1998) as experimental errors. Flower's (1993) suggestion that more than one method should be used to measure BSi to allow calibration is more constructive and may lead to more significant results. Conley (1998) makes some useful comments for the analysis of BSi using this technique and these have been

incorporated into the methodology used here. Typical errors for this technique are around +/- 10% (Conley 1988).

Conley (1998) believes that sampling the digestion solution at just one final time interval will result in an overestimation of BSi from sediments with low concentrations. Since organic and inorganic amorphous silica dissolve into solution at different rates sampling at multiple time intervals will allow a greater evaluation of the efficiency of the digest as well as an insight into the types of silica present. Examining the slope of dissolution with time provides information on the success of the digestion procedure and will highlight possible contamination by non-amorphous silica (Conley 1998). For low concentration BSi samples there tends to be changes in the gradient of the slope of BSi concentration extracted with time (Figure 12). The percentage of BSi in the sample can be estimated by extrapolation of the initial gradient (stage one) back to the x-axis. For samples with high BSi concentration a linear increase or significant slope change is often not found and a mean of the digestion sampling points should be taken (Conley 1998). The time-dependent technique determines whether the digestion has run to completion and any large increases in BSi extracted with time may reflect the presence of more silicified aquatic organisms (e.g. Sponge spicule (Conley & Schelske 1993)) or that a stronger solution is required in order to digest all the siliceous components (Eggiman et al., 1980).

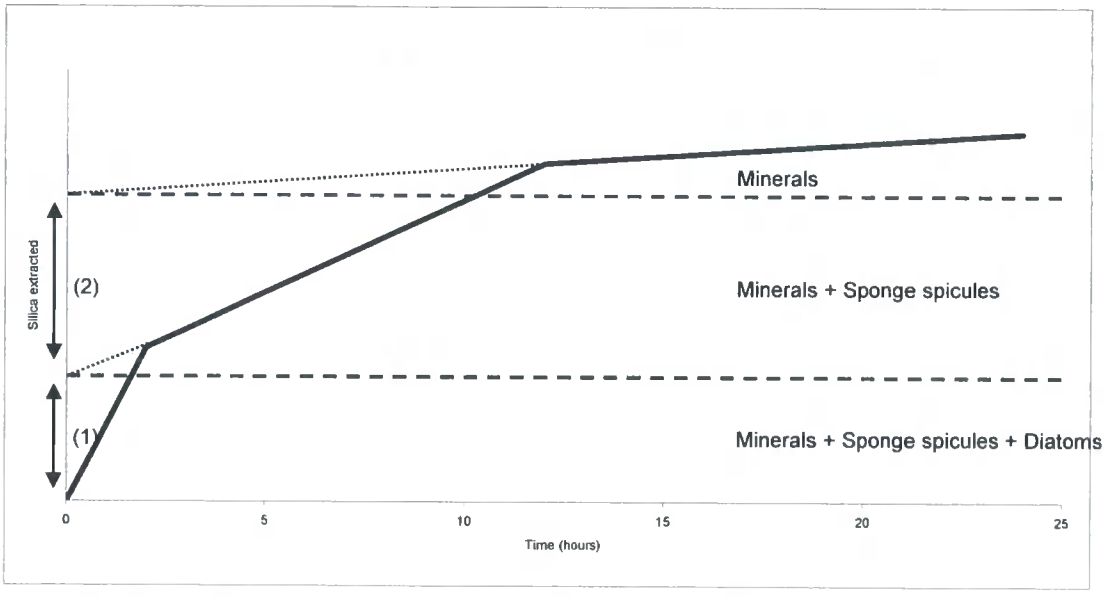

Figure 13 Hypothetical increase in the extraction of biogenic silica with time (Source: Adapted from Conley 1998).

It is assumed for the purpose of palaeo-environmental reconstructions that lake sediments faithfully record the characteristics of the overlying water mass and surrounding catchment. More lightly silicified diatoms may be naturally redissolved after death and thus a proportion of BSi is constantly recycled. Hence, all BSi values should be considered as potential underestimations until this problem is resolved. Sponge spicules are not thought to represent a major problem in sub-Arctic lake environments. Nevertheless, Conley & Schelske (1993) have shown than the more heavily silicified sponge spicules with relatively less surface area may take up to 8-12 hours to fully dissolve compared to 1.5-3.5 hours for diatoms (Mortlock & Froelich 1989). The biogeochemical cycle of silica in aquatic lake systems is closely linked to that of the phosphorous cycle, although Newberry (1986) clearly showed that BSi does not always reflect the trophic history of lakes. Nature also poses another problem for the determination of silica. Mean silica content of an assemblage will vary with species composition (Conley 1988). Therefore, any change in the diatom composition will reflect the correlation between diatom abundance and BSi (Conley 1988). One solution to this would be to measure diatom biovolume, which attempts to estimate taxa size into the abundance calculations.

Biogenic silica does not provide absolute accuracy because of natural and laboratory problems but also because there are no clear certified BSi standards (Conley 1998). There is a great deal of variability in results and it is important to optimise the technique for specific sediments (Conley 1998). It is yet to be quantified how much BSi is recycled into the system after deposition and this is expected to be site specific. Furthermore, Peinerud (2000) reported evidence of gradual dissolution of diatoms with depth after burial. Peinerud (2000) also explained that where concentrations of aluminium increased the solubility and dissolution rate of BSi decreased. It is believed that BSi concentration in sediments generally reflects siliceous microfossil abundance (Conley 1988) although there are concerns about whether methods used to reconstruct BSi are actually determining microfossil silica or other amorphous forms (Robbins et al., 1975).

2.7 Tephra deposits in Iceland and tephrochronology

Iceland's past volcanism provides invaluable assistance for the dating of climate events and correlating between sites that maybe thousands km's apart. Thorarinsson (1944) pioneered the use of tephra deposits as a correlating tool and dating medium. Tephra deposits are derived from volcanic eruptions and are often widely distributed and deposited in a variety of environments. "Tephras are an allochthonous input into a catchment-lake system with a known age and/or known source, and has the advantage of being geochemically and physically distinct from other sediments" (Boygle 1999). Tephras tend to be well dated and therefore provide the potential to calibrate late

Weichselian and Holocene chronologies for Iceland (Haflidason et al., 2000). Tephras have proved especially useful during the late Weichselian and early Holocene period where radiocarbon dating was limited by the low organic content of sediments (Haflidason et al., 2000). Grönvold et al., (1995) recently discovered evidence of the Vedde Ash and the Saksunarvatn Ash in the GRIP ice core from Greenland. Figure 15 provides a composite tephrochronology for the whole of Iceland.

There are four well-defined volcanic zones in Iceland with approximately 32 volcanic systems (Haflidason et al., 2000) (Figure 14). Each system is petrographically and geochemically distinguishable from each other (Jakobsson 1979). Individual tephras represent isochrons that can be used to correlate between marine and terrestrial sequences, thus circumventing spatial and temporal problems with radiocarbon dating from changes in the ocean reservoir effect (Andrews et al., 2002b). There have been ~20 eruptions per century during historical time and marine sediments have indicated that there was considerably less volcanism during glacials and periods of severe climate conditions, than during warmer periods (Haflidason et al., 2000). Sejrup et al., (1989) associated this periodic increase in explosive volcanism during interglacial periods to glacio-isostatic processes following deglaciation of Iceland.

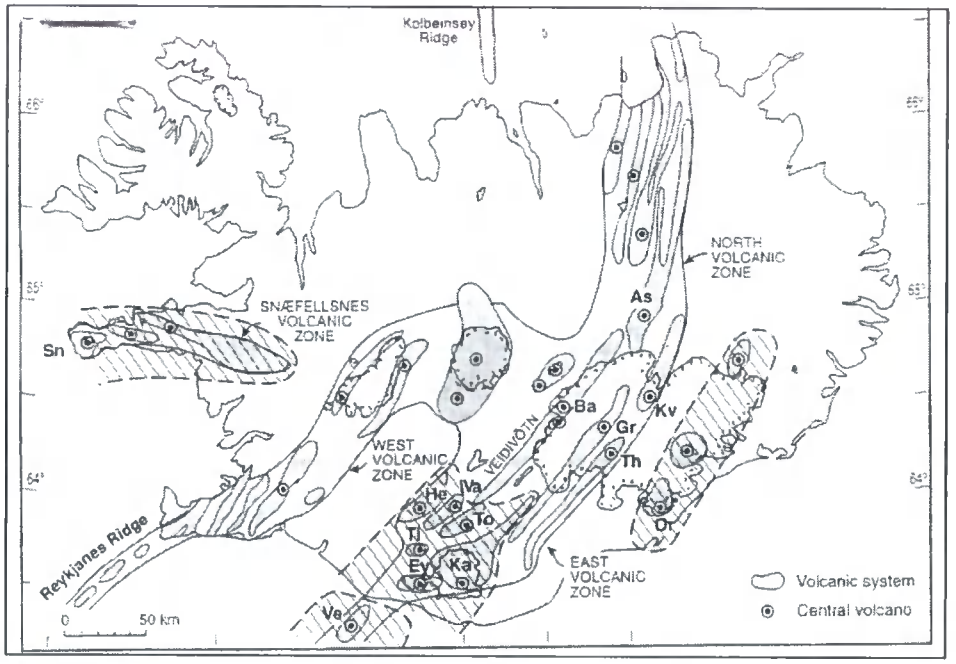

Figure 14 Volcanic zones of Iceland (Source: Haflidason et al., 2000).

The Vedde Ash (ca. 10.3 14C Ka BP) (Mangerud et al., 1986) has been observed throughout the North Atlantic region and corresponds to the Younger Dryas chronozone. This tephra was first identified in countries other than Iceland and it has now been shown to correlate with the Skógar tephra in northern Iceland (Norðdahl & Haflidason 1992). The most prominent stratigraphic tephra marker for Icelandic event stratigraphies

during the Pre-boreal is the basaltic Saksunarvatn Ash (ca. 8.9 ^{14}C Ka BP). This widespread tephra is thought to have originated from the Grímsvötn caldera complex, beneath Vatnajökull, southeast Iceland. The Saksunarvatn Ash has also been observed in Seltjörn peats, near Reykjavík (Ingólfsson et al., 1995), and off the north coast of Iceland (Andrews et al., 2002c; Eiríksson et al., 2002) where it forms a regional sub-bottom reflector and represents an invaluable regional isochron (Andrews et al., 2002c)

It is assumed for the purpose of palaeoenvironmental research than tephras are deposited in an essentially instantaneous "blanket-like" event (Boygle 1999) despite an awareness that patterns of sediment accumulation in lakes are variable due to: (1) Sediment focusing (Edwards & Whittington 1993); (2) Slumping and turbidity currents (Bennett 1986); and (3) Bioturbation or small scale bottom profile variations (Downing & Rath 1988). Boygle (1999) suggests that there is the potential to confuse between primary and secondary tephra deposits and goes on to list four aspects of stratigraphy to identify *in situ* tephras:

1. Sharp lower contact to the tephra deposit.
2. Stratigraphical position in relation to other tephras should remain the same over a wider area.
3. Over the local area, the apparent colour, grain size and geochemical change within the deposit should be constant.
4. The sample should be homogenous and relative amounts of "contaminants" from other volcanic processes should also remain constant between sites.

Boygle (1999) believes that the assumption of instantaneous "blanket" deposition can not be justified. This is based upon the detailed study of variations in a number of tephras between multiple sites from a relatively stable catchment in northern Iceland. In order to construct regional tephrochronologies, multiple cores from numerous sites are required (Boygle 1999). It is claimed that tephra can be highly mobile immediately after eruption, but also during reworking of sediments by in-lake processes (Boygle 1999).

The development of Iceland's terrestrial environment is poorly understood being hampered by a lack of long biological records extending beyond the early Holocene, with the exception of the Skagi peninsula (Rundgren et al., 1997; Rundgren 1995; and Björck et al., 1992). Weichselian environmental history is therefore contained mostly in minerogenic sediments in which tephras are rarely found (Haflidason et al., 2000). The use of tephrochronology during the late glacial period is also limited by the almost complete ice coverage of Iceland until ca. 9.7 ^{14}C Ka BP (Ingólfsson 1991) and poor peat formation on coastal lowlands (Eiríksson et al., 2002b). Nevertheless, there is

evidence for significant tephra deposits during the late glacial (e.g. Borrobol and Vedde Ash) which have contributed to improving the chronology of events during this period.

Rapid peat formation and high frequencies of distinctive tephras have supported radiocarbon-based chronologies for Holocene climate events in Iceland. Tephrochronology is more limited during the late Weichselian and early Holocene but the presence of two significant tephras has allowed correlation between the marine and the terrestrial environment as well as broadly bracketing climate events. Tephra deposits are numerous and provide an invaluable means for correlation and dating Icelandic sediments.

Figure 15 Tephrochronology of Iceland 2-12 ^{14}C Ka BP (Source: Hafliðason et al., 2000)

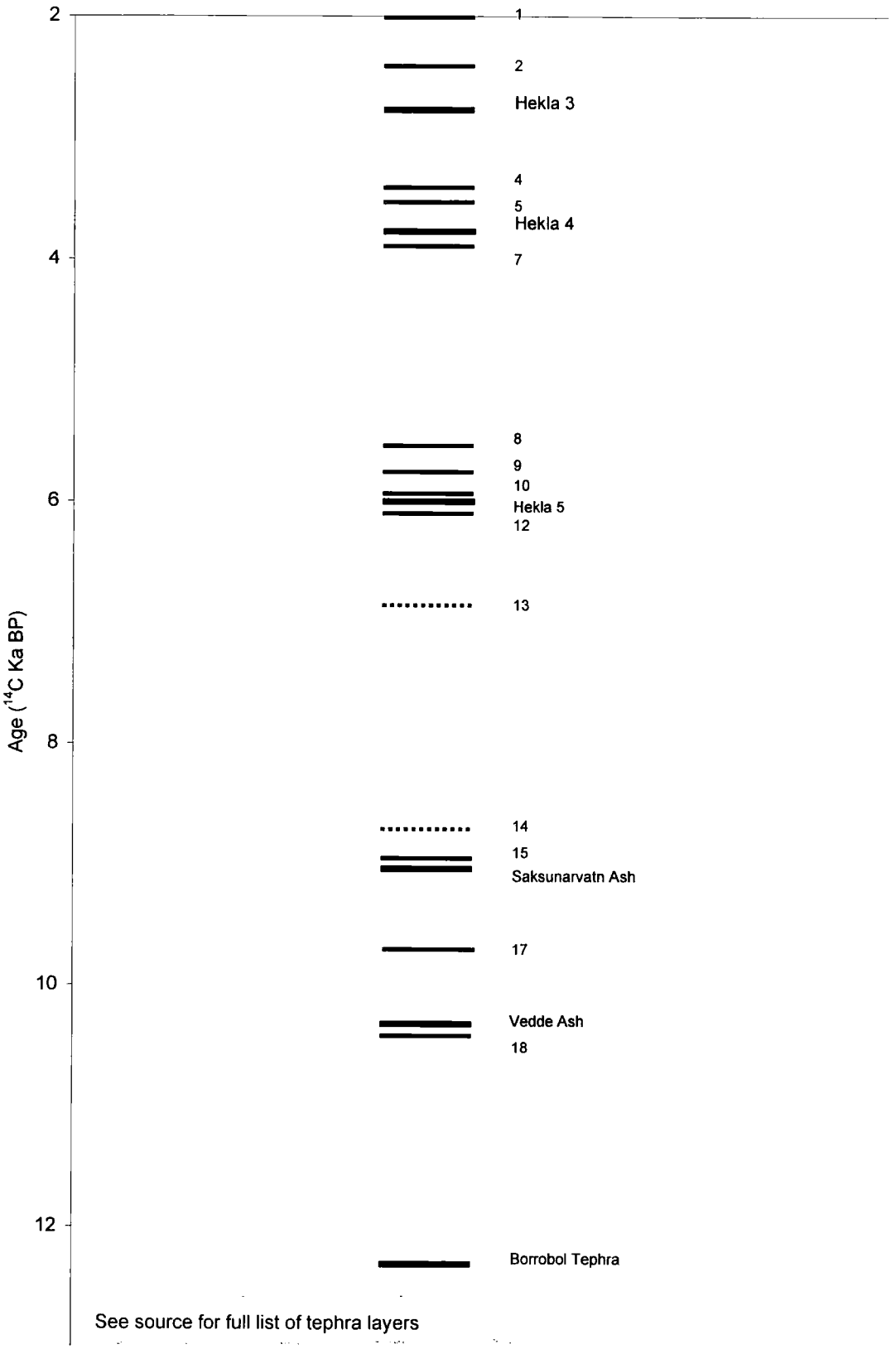

CHAPTER 3

GEOGRAPHICAL LOCATION AND SITE DESCRIPTIONS

3.1 Geographical location

Iceland is a prominent island in the northern Atlantic Ocean located between 64.5-66.5°N and 14-24°W. Iceland is situated within the supposed range of rapid marine and polar front migrations during Termination 1 (Ruddiman & McIntyre 1981). At present the Icelandic climate is controlled by shifts in the front between temperate and cold polar air. The sensitive position of Iceland in relation to these fronts means that high resolution records of Icelandic palaeoclimate may shed light on the climate history of the North Atlantic (Ingolfsson 1991).

Iceland is located in the middle of the Norwegian-Greenland Sea and therefore experiences a strong maritime influence (Seigert 2001). Today the surface oceanographic circulation around Iceland is dominated by the warm and saline Irminger Current (IC) which branches off from the North Atlantic Current further south (Figure 2). The IC forms a clockwise gyre around Iceland flowing towards the present day position of the Polar Front, where it meets the East Icelandic Current (EIC). The EIC is partly derived from the south flowing East Greenland Current and partly from the anti-clockwise gyre of the Icelandic sea. This flow is characterised by a cold, seasonally variable low-salinity tongue of surface water, which occasionally extends as far south as the north Icelandic shelf (Eiríksson et al., 2000).

Vestfirðir is the name of the large peninsula (ca. 104km^2) jutting out from Iceland towards Greenland (Figure 15 & 17). The peninsula is connected to the mainland by a narrow neck of land ca. 10km wide (Hansom & Briggs 1991). The Glama-Dranga plateaux, both of which occupy substantial areas at about 600-900m a.s.l (Hansom & Briggs 1991), dominate the north of the peninsula. There are currently four major icecaps on Iceland totalling some 11 000km^2 with Vatnajökull the largest (8000km^2) centred over the Grímsvötn volcanic caldera (Seigert 2000). Vestfirðir is mostly ice-free with the small Drángerjökull ice cap located in the north, a remnant of the former, much larger ice cap that once covered this area. All the study sites can be found on the south and northeast coasts of Vestfirðir (Figure 16).

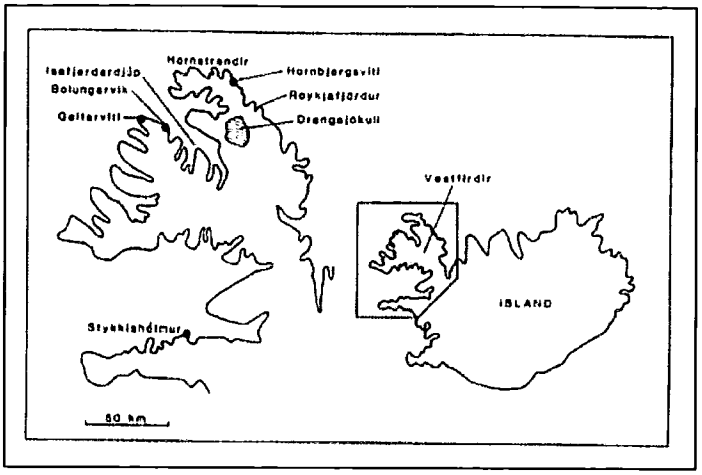

Figure 16 Location of Vestfirðir in Iceland (Source: Hjort et al., 1985)

The current climate of Iceland is internationally classed as "temperate" but with strong maritime modifications. Stötter et al., (1999) provides a more detailed appraisal of the climate type of northern Iceland describing it as "sub-polar maritime, as diurnal temperature variations are smaller than the annual amplitude." There are no metereological stations on Vestfirðir but its climate can be assessed from stations to the south at Stykkishólmur on the Snæfellsnes peninsula of Western Iceland and to the east from a station based at Akureyri (central north Iceland). Mean temperature at Stykkishólmur is 3.2°C and Akureyri 3.6°C respectively. Temperature highs occur in July (>10°C) and lows in January (-2.1°C to -1.2°C) (Stötter et al., 1999). Iceland experiences a long winter with the majority of months having mean temperatures below freezing. Winters are longer and colder in the interior than the coast where the climate is strongly mediated by the ocean.

Mean annual precipitation is approximately 700mm at Stykkishólmur (Stötter et al., 1999). The annual precipitation pattern of Iceland shows an early summer minimum (May) and a maximum in early winter (October) (Stötter et al., 1999). Ingólfsson & Norðdahl (1985) reported meteorological data from two stations from the Hornstrandir area (northern tip of Vestfirðir), although failed to state the length of the records and how they were measured. They claim from this data that in this low Arctic zone annual mean temperatures are +3.8-3.1°C, with monthly highs in August of +8.2-9.6°C, and lows in February of -0.8- -1.1°C, with an annual mean precipitation of 1265-1373mm. The maximum tidal range near Reykjavík is 3.8m. Present tidal information for our study location, important for levelling has been estimated from a small island (Flatley) off the south Vestfirðir coast: The modern day tidal range at Flatey is 4.1m.

Figure 17 Map of Reykholár and central south Vestfirðir

Figure 18 Coring location and site information for south coast Vestfirðir

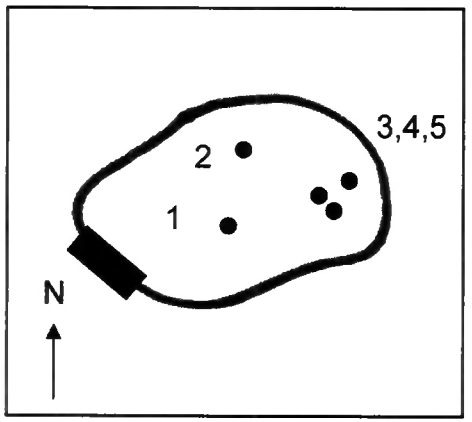

1) Mavatn (Sill 3.1m a.s.l)

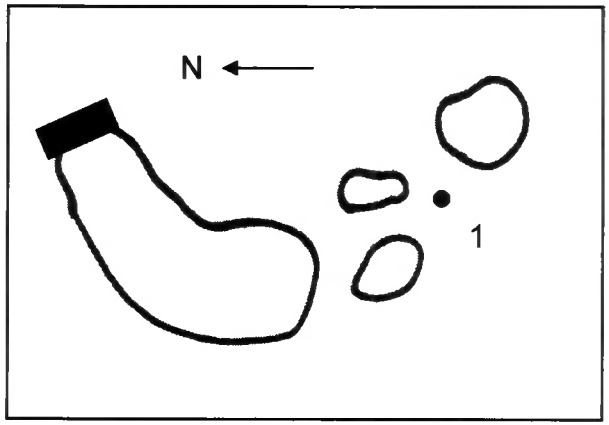

2) Hafrafellvatn (Sill 24.7m a.s.l)

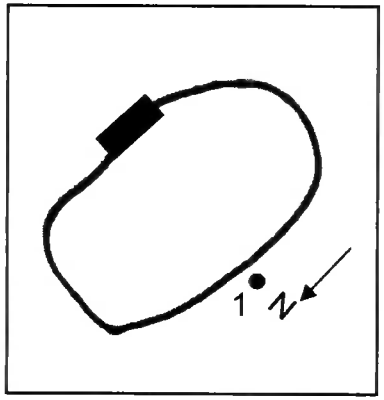

3) Hrishólsvatn
(Sill 40.1m a.s.l)4)

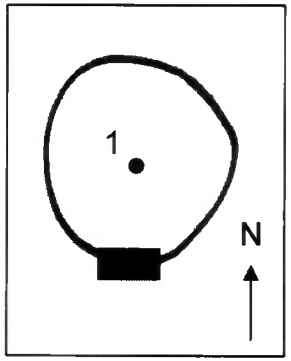

4) Hrishóls Bog 1
(Sill 79.1m a.s.l)

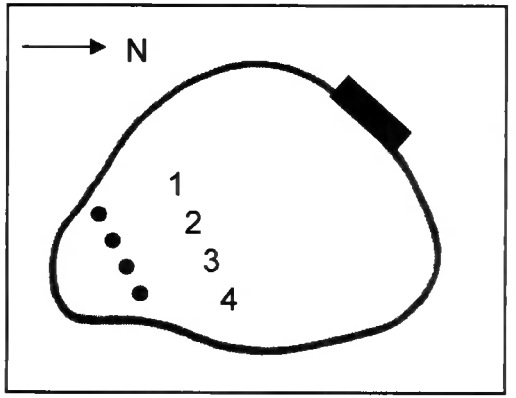

5) Berufjardenvatn (Sill 51.1m a.s.l)

Please note that diagrams are not drawn to scale

● Core location ▬ Sill

3.2 Site descriptions for the south coast of Vestfirðir (Reykhólar area)

Mavatn

Minimum threshold altitude: 1m +/- 1.3m above mean sea level (a.s.l)

Is a small circular lake ~300m x 100m and is located just to the south of Reykhólar on a flat area of exposed lowland extending out from the base of the Reykjanesfjall highlands to the north. A second lake drains into Mavatn via a drainage channel from the east and appears to have been extensively modified by human activity most likely for irrigation purposes. An outlet stream drains from Mavatn to the sea in the south. A small stream exiting the south bank of this small lake and draining to the sea indicates the location of the sill. Mavatn was cored using a livingstone corer in the middle of the lake and also in deeper water on the its eastern side (Figure 17 and Plate 1).

Plate 1 Reykhólar coastal flats.

Hafrafellvatn

Minimum threshold altitude: 22.7m +/- 1.3m a.s.l

Hafrafellvatn is located a few Km to the east of Reykhólar on a thin headland between two fjords. The present day site consists of a series of smaller lakes occupying the basin of a larger lake now partially filled with marsh. The site has highland to the north and south with the coastal road looping around to the west on a ridge of gravel that may possibly be an old marine terrace. The sill was located in the northeast of the lake forming a narrow exit to the sea, all other directions being blocked by clean bedrock. Sample core was taken from the present day marsh occupying the centre of the site (Figure 17 and Plate 2).

Plate 2 Hafrafellvatn

Hrishólsvatn

Minimum threshold altitude: 38m +/- 1.3m a.s.l

This site is located in the northeast inland corner of Berufjördur between Hrishólsháls and Hafrafell highlands. The coastal road passes along the west bank along the same gravel ridge reported at Hafrafellvatn. The site consists of a large infilling lake and back marsh, the latter of which was cored using the Russian sampler. Topography dictates that the lake must drain to the east but the large flat area of land made locating the sill difficult (Figure 17).

Berufjardenvatn

Minimum threshold altitude: 47m +/- 1.3m a.s.l

Berufjardenvatn is situated on an area of lowland linking Berufjördur with Poskafjördur to the northeast of the Reykjanesfjall highlands. This large site has a diameter of ~500m and an altitude of 51.1m a.s.l. Water depths were consistently around 1m and there was a small area of marsh towards the northern edge. In the northwest corner following contours down to the sea a small outlet stream highlighted the location of the sill. This site was cored systematically using Russian and Livingstone samplers from an inflatable boat along a transect across the southeast corner of the basin. Sample core was taken in the middle of the transect (Figure 17 and Plate 3).

Plate 3 Berufjardenvatn

Hrishóls Bogs 1,2, and 3

Minimum threshold altitudes: 75m, 100m, and 90m a.s.l +/- 1.3m

Three small sites were cored high on in the Hrishólsháls (Figure 16). At each site the lake had been in filled and a low marsh occupies the present day basin. All three basins are located in relatively high relief and had well defined rock sills. It appears from field observations that all three basins are linked by the same fluvial network forming a small staircase of basins (Figure 17)

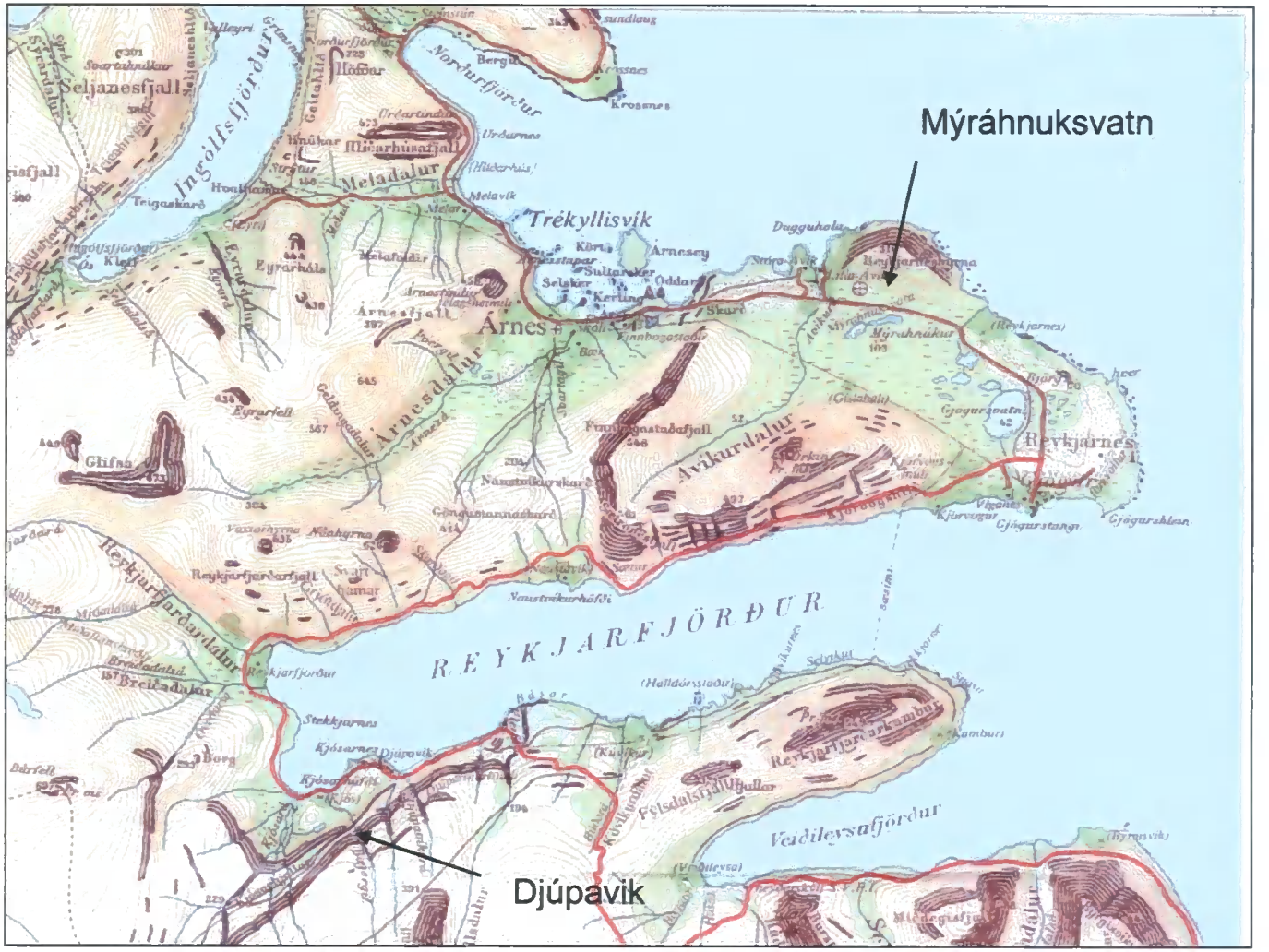

Figure 19 Map of northeast coast of Vestfirðir around Reykjarfjördur

3.3 Site descriptions for the Northeast coast of Vestfirðir

Mýrahnúksvatn

Minimum threshold altitude: 57m +/- 1.3m a.s.l

This site is found on the central flat plain of the Rekjarnes peninsula between Reykjarfjördur and Nordurfjördur systems. Mýrahnúksvatn is an elongated lake at 61.1m a.s.l and is ~100m long with an east-west long axis. The lake occupies the majority of the basin with only a small catchment limited by the very flat local relief. To the south the Avikurdalur highland may provide some seasonal melt-water through the lake system. The catchment is treeless grassland with isolated marsh in depressions and some intermittent exposed clean bedrock. A glacially moulder bedrock feature adjacent to the lake running parallel has a spot height of 103m OD. This site was cored from an inflatable boat using a Livingstone corer systematically along a transect across the short axis of the lake approximately a third of the way back from the sill (Figure 18). Water depths were consistently around 1m (Figure 18 and Plate 4).

Plate 4 Mýrahnúksvatn

Djúpavik

Minimum threshold altitude:14m +/- 1.3m a.s.l

This site is located in the southern inland corner of Reykjarfjördur and is the lowest lake of a staircase of three. A large stream was flowing through the upper lake and it was not cored. The middle lake and marsh was sampled (DJ1-03-03) but has not been included in this study. The lowest site has been completely in filled and is currently occupied by a shallow marsh. The site is surrounded by an amphi-theatre of bedrock ridges providing excellent steep sided relief. The well-defined narrow bedrock sill was located in the northern corner of the in filled lake. (Figure 18 and Plate 5).

Plate 5 Djúpavik

Figure 20 Coring location and site information for northeast coast Vestfirðir

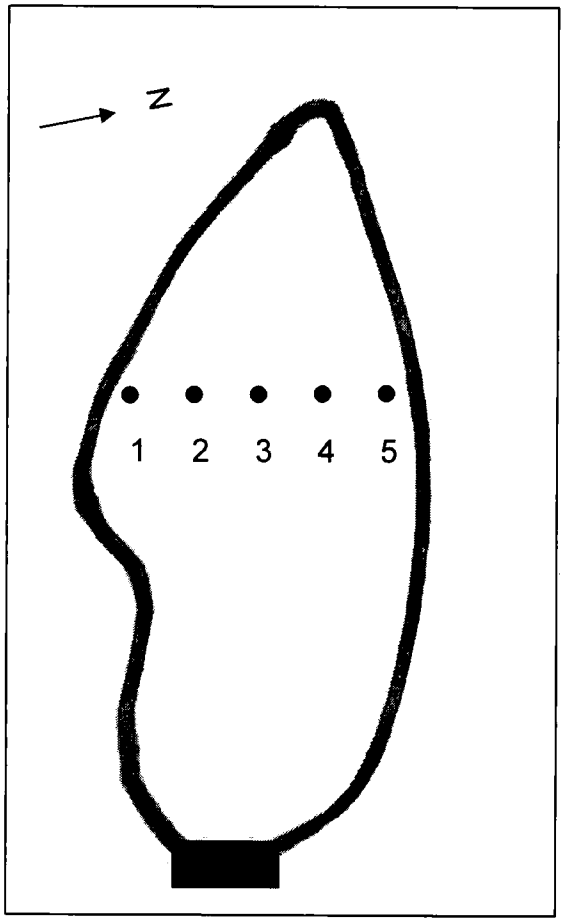

1) Djúpavik (Sill 16.1m a.s.l)

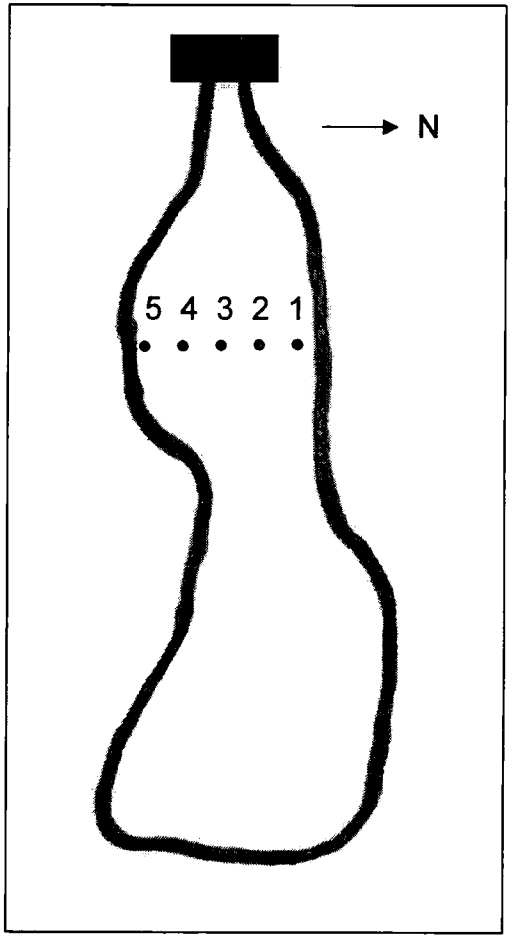

2) Mýrahnúksvatn (Sill 60.1m a.s.l)

Please note that diagrams are not drawn to scale

● Core location ▬ Sill

CHAPTER 4

METHODOLOGY

4.1 Introduction

Analysis was carried out on three Livingstone cores taken from Hafrafellvatn, Mýrahnúkkur and Mavatn sites, as well as a series of six overlapping Russian cores from the lower lake at Djúpavik. All cores were sampled for diatom microfossil, diatom abundance, biogenic silica, loss-on-ignition, and particle size analysis. Mavatn and Hafrafellvatn were also sampled for sodium concentration analysis.

4.2 Field methods

Sites were initially assessed on the merits of where sediments were most likely to have remained undisturbed i.e. away from the sill, inflow/outflow streams or other impacts on the lake system. Given the greater difficulty in coring from an inflatable boat, were marshes were could be found in suitable locations they were preferably cored. However, on a few occasions both lake and marsh were sampled and all efforts were made to obtain the best and most repeatable stratigraphy from any given site.

Sites were cored along transects and systematic intervals. Sample cores were collected using Russian or Livingstone corers depending on the stiffness of the sediments. In circumstances were the stratigraphy was particularly stiff a Gouge corer was used for sampling. Sediments were classified in the field according to Troels-Smith (1955) and carefully labelled and packaged.

When working from an inflatable boat all aspects of safety were strictly adhered to and no risks were taken.

Sites were surveyed using an EDM electronic apparatus into temporary benchmarks, which were subsequently related to a reference tide level.

4.3 Diatom microfossil analysis

Standard techniques for the preparation and mounting of slides for diatom analysis followed Palmer and Abbott (1986). Samples were chemically digested using 25ml of 20% hydrogen peroxide in a water bath at 85-100°C overnight. The oxidation and removal of organic matter is important because organic constituents of the sample may interfere with the visualisation of fine features on diatoms when viewed under a light microscope. When the supernatant becomes clear this is an indication that the digestion is complete, although for samples that contain a large proportion of minerogenic matter discolouration may still be present. Samples were allowed to cool before being centrifuged for 4 minutes at 4000rpm and the supernatant carefully decanted. 20-25ml

of distilled water was added to suspend diatoms in solution and a specific number of drops pipetted onto cover-slips and dried on a hotplate. Each sample was permanently mounted on glass slides using Naphrax as a mounting medium (which has a refractive index greater than silica i.e. R.I. 1.74).

Diatoms were identified and counted using a Nikon Light microscope at 1000x magnification with oil immersion. Apart from a few samples where diatom concentrations were very low, minimum counts of 300-500 valves per slide along continuous traverses was made. Traverses included equal proportions of "slide centre" and "slide edges" to eliminate error from the thermal sorting of diatoms that may occur when cover-slips are drying. In shallow, alkaline lakes massive blooms of *Fragilaria* taxa are common and may obscure fluctuations in more interesting or ecologically important taxa (Battarbee 1986). Therefore, it is necessary to make larger counts for samples containing high proportions of *Fragilaria* diatom species. Diatoms were identified using a variety of taxonomic references (Brun (1965); Denys (1991); Foged (1977, 1973, 1972, and 1964); Grönlund & Kauppila (2002); Hartley (1996); Hustedt (1930-66) and Smith (1950) and categorised according to the Halobian System which is based on diatom tolerance to salinity (Hustedt 1957; 1959). In general, nomenclature is consistent with Hartley (1996).

Summary diagrams were produced using TILIA (Grimm 1991) at >5% and >2% total diatom valves (TDV) depending on assemblage diversity i.e. a >5% TDV cut off point was used instead of >2% TDV were too many taxa were statistically significant at the lower value causing the summary diagram to be too complex and making interpretation more difficult. CONISS (Grimm 1987) cluster analysis was applied across all cores to identify ecological zones. Care was taken at all stages in the preparation of diatom slides as to not lose or damage valves, although Battarbee (1986) has show that rapid centrifuging or vigorous stirring can break fragile diatom valves.

4.4 Diatom abundance analysis

Diatom abundance analysis is a technique used to estimate the concentration of diatoms per unit weight of sediment. The most common method for this analysis is by using microsphere markers (Benninghoff 1962), but other methods have also been developed and proved useful, such as the Aliquot technique and Evaporation in a tray (Battarbee 1973b). Unfortunately, microspheres must be stored in a solution containing Mercuric chloride, a substance banned under University health and safety rules. Thus, an alternative approach to analysing diatom abundance had to be adopted.

The first stage of this method follows the standard procedure for diatom analysis as outlined above, with the added concern that it is essential to know the accurate weight of all samples at the beginning. Moreover, samples should be made up to a standard volume of 40ml after being centrifuged and decanted. Using accurate automatic GENEX pipettes 1ml of distilled water and 0.1ml of sample from the 40ml solution volume was pipetted on a cover slip and this was left to air-dry to reduce the effects of convection sorting of diatoms when dried over heat. Slides were then mounted in the conventional manner.

Every diatom individual fully or partially in optical view was counted at 10 equal intervals across a continuous traverse through the centre of a slide. As in diatom analysis 1000x magnification with oil immersion was used. Counts were multiplied to provide an estimated value for the number of individual diatom valves per cover-slip. Diatom counts were then adjusted to give values per gram sediment sample, after taking into account the percentage weight loss to the sediment sample from oxidation of organic matter, inferred from loss-on-ignition analysis. Only whole diatoms or those fragments that shared a common identifiable piece were included in the counts. By only counting fragments with common parts of the frustule ensures that counting duplication is minimised. It is therefore expected that this method will most likely underestimate the actual diatom abundance of each sample given the high fragmentation and numbers of unidentifiable pieces witnessed in some samples.

4.5 Biogenic silica analysis

Two different procedures have been used, both of which are variations of the wet alkaline digestion technique which is widely adopted (Conley 1998). The first procedure for the determination of biogenic silica follows Dobbie (1988), after Eggimann et al., (1980) and involves a single 4 hour chemical digestion using 2M $NaCO_3$ at 90-100°C. The second method first described by DeMaster (1979) and developed by Conley & Schelske (2001) involves the same chemical digestion but differs from the first method in that a series of sub-samples of the digestion solution are extracted at time-intervals. Samples from both methods were analysed in an ICP Mass Spectrometer and the results adjusted for aluminium derived silica by subtracting two times the measured aluminium from the measured biogenic silica. Biogenic silica was then expressed as a percentage of the total dry sample.

Glass and any aluminium containing apparatus should never be used in the preparation of samples for the analysis of biogenic silica. This rule also applies to the preparation of the chemical agent for digestion. Furthermore, silica is a weakly charged ion and

therefore may combine with contaminants in water supply if very pure water is not used throughout the process of extraction (Conley & Schelske 1993).

Cores were sampled for 0.2-0.5g of sediment using a cleaned stainless steel spatula at 4cm intervals. Samples were oven dried overnight at 100-110°C before being dry weighed and re-hydrated with a few drops of de-ionised water. Once re-hydrated 15 ml of 2M $NaCO_3$ was added and the samples were placed in a water bath at 90-100°C for a further 4 hours. Ideally, samples should be shaken at a low rpm when digesting but if this is not possible the samples should be regularly stirred (Conley & Schelske 2001). It is advisable that conical centrifuge tubes are not used during this procedure since they concentrate sediment in the bottom and prevent the digesting agent from acting on the entire sample (Conley % Schelske 2001).

Once removed, samples were allowed to cool before being stirred thoroughly with a plastic spatula. Samples were filtered (with washings) into 100ml plastic volumetric flasks using size 50 filter paper and made up to standard volume with de-ionised water. The solution was well shaken and transferred into clean labelled tubes (cleaned with de-ionised water and some of the sample) ready to be analysed by a PerkinElmer SCIEX ICP Mass Spectrometer ELAN DRC PL05.

The second methodology follows the procedure as outlined above until the samples are placed into the water bath. After 2 hours 1ml of the sample solution is accurately and carefully removed using an automatic GENEX pipette and quenched in 9ml of 0.02M HCL in a plastic 50ml volumetric flask. Samples were made up to standard 50ml volume ready for analysis by ICP. Further samples were taken at 3hrs, 4hrs, 5hrs, 6.5hrs and overnight.

4.6 Loss-on-ignition (LOI)

Loss-on-ignition is a technique used to measure the percentage organic content of sediments. According to Heiri et al., (2001) autochthonous algal remains generally constitute the majority of the organic carbon found in lacustrine sediments, although it is expected that material washed in from the surrounding catchment will also contribute to the total. Cores were sampled for 0.4-0.6g of sediment at 4cm intervals. It is good practice to try and keep all the samples roughly the same size. To ensure results are reproducible one should clearly state the temperature and duration of the ignition but also indicate an estimate of the sample size. This is important because, although each sample undergoes the same process, each sample does not relate to its neighbor directly since it is impossible to keep samples the same size given that an unknown proportion of water will be lost after drying. Standard practice dictates that all crucibles

are weighed empty first. Samples are then placed in an individual crucible and dried overnight in an oven at 100°C. The crucible and dried sample are then re-weighed before being ignited in a furnace at 550°C for 4 hours.

Optimum temperatures and duration of ignition vary depending on the nature of the sediment but it is widely considered that 4 hours at 550°C is a reasonable exposure time for "mixed sediment" (Heiri et al., 2001). At these parameters the initial rapid burning of organic material is largely completed and any weight loss due to the positioning of the crucibles in the furnace is kept to a minimum (Heiri et al., 2001). After four hours, samples are cooled in a desiccator and then re-weighed. The percentage of the sample that was organic material can be determined from the following equation:

% Organic content = dry weight-ignited weight/dry weight-weight of crucible (1)

One issue in the analysis of LOI in this project stems from the amount of sediment used per sample. Unfortunately, a smaller volume of sediment was collected from the lower Djúpavik site using a Russian sampler rather than the wider diameter Livingstone corer. The thinner core, plus the need to retain enough material for the analysis of other proxies limits the amount of sediment that could be used for the analysis of organic content. Smaller samples encourage the loss of structural water from clays and metal oxides, as well as inorganic carbon and volatile salts in temperatures as low as 500°C and this may lead to a slight overestimation of LOI results (Heiri et al., 2001). However, it is known that for smaller sediment samples the rate of weight lost is more rapid (Heiri et al., 2001) and so it is most likely, given the small amounts of sediment used in this study, that all the organic material per sample was burned off within the four hour ignition.

4.7 Particle size analysis

For particle size analysis, ~0.5g of sediment was sampled at 4cm intervals. Following Palmer and Abbott (1986) the organic component of the sample was digested in 20% hydrogen peroxide in a water bath at 85-100°C overnight. Samples were made up to constant volume with distilled water and centrifuged twice at 4000rpm for 4 minutes. The supernatant was then carefully decanted off and the sample made up to 25ml with distilled water with 2ml of Sodium hexametaphosphate added to each sample at the end in order to inhibit particle flocculation. Each sample was analysed by a Coulter Granulometer LS 230 Series. Results are divided into sand (>63μm), silt (3.9-63μm) and clay (>3.9μm) fractions and illustrated on area plots.

4.8 Environmental reconstruction of pH

It is known from numerous studies in many different locations that diatoms have a strong relationship to pH (Weckström et al., 1997; Stevenson et al., 1989; Charles 1985; and Hustedt 1937-39). However, the simple linear regressions that are often used for reconstructions are inappropriate given the multiple factors that influence the pH of lake waters. The most appropriate way to reconstruct pH would be to applied multivariate statistics to a large set of lakes within an area across natural environmental gradients. By doing this it is possible to make inferences about the variables that influence diatom populations from an area and to construct transfer functions, which can then be applied to the fossil record. However, surface sediment samples from a variety of lakes in our study area were not available and so an alternative method for reconstructing pH must be followed. pH will be reconstructed using Index B (Nygaard 1956) and converted into actual pH following Renberg & Hellberg (1982).

4.8.1 pH from Index B

Diatoms were classified for pH reconstruction following the boundaries outlined by Hustedt (1937-39) listed in Figure 12 earlier and repeated for convenience below.

Category	Description
Acidobiontic	Optimum distribution at pH <5.5
Acidophilic	Widest distribution at pH <7
Indifferent (circumneutral)	Greatest distribution around pH 7
Alkaliphilic	Widest distribution at pH <7
Alkalibiontic	Occurs only at pH >7

Figure 12 (source: Hustedt 1937-1939)

Using the percentages of individual taxa from each sample it is possible to calculate the relative numbers of "alkaline" and "acidic" units using Nygaard's (1956) Index B. Diatoms that favour more strongly alkaline waters or very acidic conditions are given a greater weighting in the calculation of the index.

$$\text{Index B} = \frac{\%\text{indifferent}+5(\%\text{acidophilic})+40(\%\text{acidobiontic})}{\%\text{indifferent}+3.5(\%\text{alkaliphilic})+108(\%\text{alkalibiontic})} \quad (2)$$

Renberg & Hellberg (1982) redefined the equation to reduce the bias of sensitivity towards alkaline taxa and added a conversion to the index allowing actual pH to be estimated (See below). They also addressed one of the major criticisms of the index and incorporated circumneutral taxa into the equation. It is believed that by doing so they have provided a more inclusive and accurate method to reconstruct pH. It has been shown by Charles (1982) that reconstruction's using Index B correlates well with actual pH measurements.

$pH = 6.4 - 0.85_{logindexB}$ (+/- 0.3 pH units) (3)

4.9 Sodium concentration analysis

Acid soluble total concentrations of sodium were determined using the following procedure described by Seppä et al., (2000). Samples were taken at 4cm intervals from Hafrafellvatn and Mavatn cores and dried in an oven at 100°C overnight. Samples were allowed to cool and then ground into a homogenous mass before c. 0.2g was carefully weighed out. Samples were then washed with 10ml de-ionised water into 100ml volumetric flasks and 10ml of standard HNO_3 added. A spatula of anti-bumping granules (what these made off?) was also added to the flask before heating for 30 minutes at 120°C on a specially designed flask hot-plate with condenser. Complete dissolution was ensured by increasing the temperature to 130°C and heating for a further 10 minutes. Finally, 3ml of de-ionised water was added to the solution and it was filtered through size 50 filter paper before dilution to 50ml. Samples were then analysed for sodium using a Varian SpectrAA 220FS Atomic Absorption Spectrometer.

4.10 Tephrochronology

All tephra deposits were either sampled directly in the field or from retrieved sample cores. The chemical analysis of these tephra layers was conducted by Dr. A. Newton, School of Geoscience, University of Edinburgh (see Acknowledgement).

4.11 Levelling of sills

The levelling of sills was done using an EDM electronic surveyor. Where the sill was difficult to identify transects were done using Sokisha levelling equipment to identify the shallowest point in the confining bedrock. Threshold altitudes were worked out and distributed by Bentley (pers. comm.). Raw values were then converted by the author of this study into values relative to mean sea-level using Icelandic tide tables. All altitudes thus are meters above mean sea level and denoted in this investigation as "a.s.l."

CHAPTER 5

RESULTS

5.1 Introduction

This Results Chapter is in two parts. Part One includes details of isolation basins and is organised by site and then by proxy. Part Two examines the data and evidence for past environmental changes during the early and middle Holocene period in Vestfirðir. All figures are included at the end of each section, respectively with diatom photographs on Plates 6 & 7 towards the back.

5.2 Evidence for the determination of isolation of basins from the sea

5.2.1 Mavatn

Minimum threshold altitude 1m +/- 1.3m a.s.l

Please refer to Figures 21 and 22 for lithology and Figure 19 for geographical location.

Diatom analysis

Eight samples were analysed for diatom microfossils across this 30cm long core. Figure 26 provides summary information at 2% TDV. This analysis revealed a transition from predominantly marine/brackish to freshwater taxa up through the core. Basal silty-clay is separated from a freshwater gyttja by a layer of course gravel 2cm thick. Below this layer polyhalobous, mesohalobous and some oligohalobous-halophilous diatoms dominate. Above the layer of course gravel the diatom assemblage consists exclusively of oligohalobous-indifferent taxa. Diatom preservation in the basal 15cm of this core was poor and it was only possible to make low valve counts i.e 100-150 valves.

Bio-stratigraphical Zone A (98-90cm)

The diatom assemblage in this zone was almost entirely composed of *Thallasiosira eccentrica*, a planktonic polyhalobous diatom. At this stage of the basins isolation it experiences considerable connection to the sea during the tidal cycle. *Thallassiosira eccentrica* is a diatom species that is often found in shallow littoral environments (Zong pers. Comm.). The volume of course minerogenic material present in the core supports this interpretation of depositional environment. It is unlikely that dissolution processes were the reason for poor diatom preservation in the basal 15cm. Many of the diatoms observed at this level were fractured and broken and the most likely explanation for poor preservation is low productivity due to the sites exposed, Atlantic facing location. Other polyhalobous taxa identified in this zone were only observed in small in low numbers.

Bio-stratigraphical Zone B (90-80cm)

Zone B is more diverse than Zone A with species representing all of Hustedt's (1937-39) classifications. *Thallasiosira eccentrica* is still abundant in this zone, which also includes the first observations of mesohalobous taxa (e.g. *Rhopalodia rupestris* and *Tabularia fasiculata*). Mesohalobous diatoms occur in shallow coastal and brackish water indicating that the basin had now begun its transitional phase. Oligohalobous-indifferent taxa (especially *Fragilaria spp.*) constitute a greater proportion of the assemblage. The assemblage diversity reflects hydrological changes experienced by the basin during isolation.

Bio-stratigraphical Zone C (80-78cm)

Between 78-80cm a coarse gravely layer was observed across the core separating the basal clastic unit from the well-humified lake gyttja above. It was not possible to sample this gravel layer for diatom analysis.

Bio-stratigraphical Zone D (78-63cm)

This upper zone is dominated by benthic oligohalobous-indifferent and oligohalobous-halophilous taxa, especially varieties of *Fragilaria*. *Tabellaria flocculosa* and *Rhopalodia gibba* also make significant contributions to the total assemblage as do *Cocconeis placentula var. euglypta*, *Navicula rhynocephala*, *Staurosirella elliptica*, *Synedra ulna var bicepts*. Polyhalobous taxa are absent from this sedimentary unit and the assemblage has been interpreted as representing a fully "fresh" lake environment. *Fragilaria virescens* are abundant between 70-78cmat the base of Zone C becoming less important towards the top as diversity increases with greater numbers of larger benthic diatoms. Oligohalobous-halophilous taxa *Diatoma spp.* appear towards the very top of the core. These taxa are most often found in freshwater environments but can tolerate slightly saline conditions. The presence of these taxa so high in the core reflect the basins continued close proximity to the sea.

Diatom isolation contact

According to the diatom data from Mavatn, the basin began to isolate between 85-90cm where mesohalobous taxa were first observed and isolation was completed by 77cm depth. When in the field, attempts were made to core two basins that were still connected to the sea. Unfortunately, we were unable to penetrate a course gravely layer that was encountered immediately beneath the surface. This observation provides a modern day analogue for the coarse gravel layer identified in the Mavatn sediment sequence. Furthermore, above this layer diatoms are identified as being all fresh with

only a short period of mesohalobous taxa beneath the gravel layer. Hence, the isolation of Mavatn basin, according to the diatom data occurs immediately above this gravel layer at 78cm. This interpretation is clearly supported by the least squares cluster analysis.

Loss-on-ignition analysis

Please see Figure 27. Mavatn is a small lake system located on an exposed shelf within close proximity to present sea-level. Its exposed setting may have some impact upon productivity within the lake and its small catchment. Basal sediment LOI results from 95cm up and until 75cm remain constant around 4% organic content suggesting a stable environment of similar conditions. Shortly after 75cm the percentage of organic material within the sediment increases in a single stepwise fashion from 4% to 8% before gently continuing to rise to approximately 13% organic material within the sample. A course gravel lag found in the core at 78-80cm was expected to produce the lowest measurement if it had been sampled.

Particle size analysis

Mavatn was sampled at 4cm intervals for particle size analysis and results are illustrated in Figure 27. The three different grain sizes; clay, silt and sand have been plotted separately to identify trends. A greater proportion of the basal sediment is clay (>20%) decreasing to 10% after 75cm. Between 75cm and the base silt content has a slight decreasing trend from 45-30% before increasing rapidly above 75cm and stabilising at ~60% of the total sediment around 65cm. The sand fraction appears to "mirror" that of silt and has an increasing trend between 90cm and 75cm peaking at >60%. Above 75cm the sand fraction dramatically decreases before stabilising at ~30% at and above 70cm.

Biogenic silica analysis

The tracing of an isolation sequence has never been attempted using % Biogenic silica (%BSi) and so the results from this analysis will be particularly interesting. 17 samples were analysed down the Mavatn core at 2cm intervals and the results shown in Figure 27. From 95cm to 77cm in the basal clay and gravel the %BSi remained constant at between 1.7 and 4 %BSi. Immediately above the unsampled gravel layer, between 78-80cm a broad peak in %BSi occurs with a maximum value of 53%Bsi. BSi values remain high for the following 5cm before returning to values just below 10%Bsi towards the top of the core.

Sodium concentration analysis

Sodium concentration was chemically measured across Mavatn (Ma03-06) in order to support other proxies attempting to locate the isolation contact. The chemical determination of sodium concentration for Mavatn can be viewed in Figures 27. 10 samples were analysed at 4cm intervals and values range from 5000-11 000mg/g, being consistent with analysis from other sites.

Sodium concentration for Mavatn is dominated by a single pronounced step between 83cm and 81cm where sodium concentration falls from 8661mg/g to 6688mg/g respectively. Above this level there is only a slight decrease in sodium concentration and below 83cm there is only a slight increase in sodium concentration. This single step change represents 33% of the difference from the highest and lowest recorded values of sodium concentration of the Mavatn record and occurs immediately below a 1-2cm thick gravel layer.

Determination of the isolation contact

Diatom analysis was the main method for identifying the conformable transition from a marine to a lacustrine environment, which is also supported by all other proxies. However, lithological boundaries do not always correspond to changes observed in the bio-stratigraphy. It was not possible to sample a gravel layer between 78cm and 80cm and distinct changes occur in the characteristics of the sediment above and below this lithological boundary. Below the layer the diatom microfossil assemblage is dominated by polyhalobous and mesohalobous diatom taxa. The sediments have poor organic content and high clay content. Below 80cm sodium concentration is high and BSi low as would be expected in a marine environment.

The diatom microfossil analysis supported by all other proxies highlight a distinct change in the sedimentation environmental representing the final isolation of the basin immediately above the gravel deposit. Clay and sand content are the first proxies to show change, decreasing and increasing from 90cm upwards respectively. Sodium concentration indicates a distinct step to lower values just before the gravel layer at 83cm, which is followed by a large peak in the BSi at 76cm (Figure 27). LOI is the final proxy to show any response to changing lake conditions beginning to increase from 75cm onwards. It was expected that biogeochemical proxies would respond before LOI as they would pick up direct changes in lake water chemistry rather than the lake flora and catchment productivity measured by LOI. Particle size analysis picks up changes in sediment types and source location as marine waters began to shallow and become increasingly littoral. If the results of sodium concentration are to be believed then the

cessation of full marine conditions occurred at 80cm. However, it was not until 76cm and 75cm that BSi and LOI indicate any changes.

All chemical and physical proxies analysed from this site feature a break in the record due to the inability to sample the gravel layer (ca. 78-80cm). However, when in the field it was noticed that attempts to core basins that were still connected to the sea were hampered by a course gravely lag immediately below the sediment surface. This modern analogue may provide some answers to the isolation of Mavatn. Hence, after taking into account all the relevant data, it appears that the isolation of this basin should be considered at the top of the gravel layer at 78cm depth.

5.2.2 Hafrafellvatn

Threshold altitude 22.7mx +/- 1.3m a.s.l

Please refer to Figures 21 & 22 for lithology and Figure 19 for geographical location.

Diatom analysis

15 samples were taken across this 80cm core at 4cm intervals for diatom analysis (Figure 28. Across the transition a higher resolution of sampling was undertaken at 2cm intervals. A complex isolation pattern was recorded with two significant oscillations between freshwater and brackish/marine taxa during the one isolation sequence. Diatoms are well preserved throughout most of the core apart from the basal 15cm. Diatom analysis revealed a relatively long (c.30cm) biostratigraphical isolation sequence following a I-IIv (variant transitional unit)-III pattern. This isolation sequence is unique with regard to the other basins in this study because of its length (Plate 8).

Plate 8 Hafrafellvatn sample core

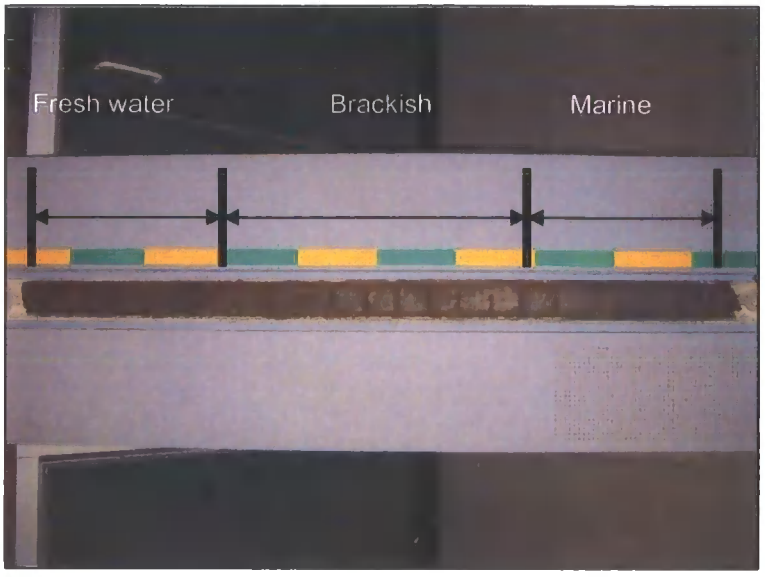

Bio-stratigraphical Zone A (436-434

At the very base of the blue-grey clayey silt the preservation of diatoms was poor and counts of 150-200 valves were made. Nevertheless, this unit is dominated by numerous polyhalobous and mesohalobous taxa and has therefore been interpreted as having a marine origin. The planktonic polyhalobous *Thallassiosira eccentrica* was the most abundant, although it was often found fragmented. Other polyhalobous taxa include *Tabularia sp.*, *Nitzschia socialis*, and *Odontella aurita*. Mesohalobous taxa contributed approximately 20% to this zones TDVs, especially *Navicula digitaradiata* and *Nitzschia sigma*. Low amounts of oligohalobous-indifferent and oligohalobous-halophilous taxa are most likely to be a consequence of catchment in-washing.

Bio-stratigraphical Zone B (434-403cm)

Zone B represents the long transitional period of this isolation sequence. Productivity and preservation are better than the basal sediments and counts in excess of 300 valves were possible. As is typical of transitional litho-facies the diatom population is the most diverse with 34 different taxa present at >2% TDV and representing all of Hustedt (1937-39) groups. The transitional zone is highly complex with polyhalobous taxa still present towards the base and again, along with significant contributions of mesohalobous taxa, at two points (414cm and 422cm) further up the zone (Figure 28).

Between 434cm and 423cm the diatom population of this zone is similar to the basal marine assemblage with the one exception that the proportion of polyhalobous taxa has decreased in favour of oligohalobous-indifferent diatoms. There are no taxa from any classification above 10% TDV illustrating the diversity of the diatom community.

From 423cm to 418cm and between 418cm and 410cm a similar change occurs. The proportions of mesohalobous taxa (i.e. *Nitzschia constricta*, *Niztschia sigma*, and *Scolipleura tumida*) increase to account for more than 60% of the assemblage and a coincident reduction in the proportions of oligohalobous-indifferent taxa occurs at the same time. The polyhalobous taxa *Navicula Hudsonis* is also present in these two events.

It is possible that this "seesaw" pattern reflects two separate inudations of the basin by seawater. However, this is not supported by the homogenous lithological unit, which shows no evidence of a sudden influx of marine sediment at these two instances. Further, since mesohalobous and oligohalobous-halophilous taxa can co-exist these changes in assemblage composition most likely represent hydrological upheavals during basin isolation. Inbetween the first and second mesohalobous "highs" and after the second "high" the diatom assemblages are dominated by the oligohalobous-indifferent taxa.

Bio-stratigraphical Zone C (403-365cm)

This upper zone is composed almost entirely by fresh water diatoms with small amounts of mesohalobous taxa towards the base. Many of the oligohalobous-indifferent taxa that are presence are similar to those that were beginning to appear towards the base of Zone B (before the two in-washing events were recorded in the bio-stratigraphical record). Larger fresh water benthic diatoms have replaced the smaller benthic *Fragilaria* forms and the assemblage has stabilised with reduced diversity. *Cymbella caesipitosa* and *Epithemia sorex var gracilis* are the dominant species but are replaced by *Amphipleura pellucida* and *Cocconeis placentula var euglypta* towards the very top of the core.

Diatom isolation contact

Diatom analysis from Hafrafellvatn has identified a stratigraphically long and eventful isolation sequence not seen elsewhere within this study. Isolation began at 414cm and the cessation of all marine influence occurred at 403cm (Figure 28). Given what we know about the deglaciation pattern of Iceland and subsequent expected rates of change in RSL, it is most unlikely that the ~30cm transition is a product of a slow

isostatic uplift rate coupled with a large tidal range. Given the deep water depths (indicated by the thick sediment sequence) during isolation meromictic stratification (described elsewhere by Snyder et al., 1997; O'Sullivan 1983; and Dickman 1979) may have been a problem at this site. However, laminations that are often found associated with such hydrological regimes were not observed and the majority of taxa were benthic living in shallower water depths.

Loss-on-ignition analysis

Hafrafellvatn was sampled at 4cm intervals for LOI analysis and the results illustrated in Figure 27. LOI results from Hafrafellvatn are consistent with the pattern of changing organic content observed elsewhere for isolation basins (e.g. Snyder et al., 1997; and Bennike 1995). Between the base at 440cm and 414cm there are no changes in organic content of the sediment samples remaining constant at ~4%. From 414cm until 350cm there is a constant increase in the proportion of the sediment that is organic peaking at just over 35%.

Particle size analysis

Hafrafellvatn was sampled at 4cm intervals for particle size analysis and results plotted in Figure 29. The main lithological boundary is clearly shown by the clay fraction with a step change beginning at 400cm. Here the proportion of clay in the sediment decreases from >20% to ~10%. The silt and sand fractions almost perfectly "mirror" each other suggesting that any process that results in an increase in sand also has the effect of reducing the flux of silt into the lake system. Hence, the silt and sand sediment fractions are coupled and as one increases, one decreases. The principal component of the sediment throughout the core until 372cm is silt, which increases gently from 50-70%. After 370cm the silt fraction falls suddenly to 25% being replaced by sand, which then constitutes 50-70% of the sediment in the core. At 430cm and 394cm there are sharp increases in sand by 15-20% coinciding with sharp decreases in silt by the same magnitude. There is also a slight decrease in the amount of clay in the core at both peaks. Both peaks do not correspond to any significant changes in diatom fauna and thus makes me believe that the source of the increase in sand must have been terrestrial. Each peak may also represent sediment reworking or changes in sediment movement within the lake.

Biogenic silica analysis

Hafrafellvatn was sampled at 4cm intervals for %BSi and results can in seen in Figure 29. The record of %BSi for this core demonstrates considerable variability although a slight increasing trend can be observed. The record is dominated by a large peak at 394cm indicating ~20%BSi in that sample. Values of %BSi below this peak tend to be between 2 and 8%BSi and above this peak values tend to be between 5-10%.

Sodium concentration analysis

Sodium concentration was chemically measured across Hafrafellvatn (Ha03-01) in order to support other proxies attempting to locate the isolation contact. Sodium concentration for Hafrafellvatn has been illustrated in Figures 29. 12 samples were taken across Hafrafellvatn at 8cm intervals and values range from 5000-10000mg.g. Up through the core from Hafrafellvatn there is a general decreasing trend from a peak of 10204mg.g at 430cm to a minimum of 5125mg.g at 374cm. The weak correlation of this decreasing "up core" trend is consistent with the variability observed in the sodium concentration record. However, the correlation coefficient may have been improved had a greater number of samples been analysed across the core.

Determination of the isolation contact

Above 403cm there is no longer any record of polyhalobous diatoms within the microfossil record (Figure 28). The majority of mesohalobous taxa have also disappeared by 404cm, although there are small occurrences of mesohalobous *Ctenophora pulchella*, *Navicula digitaradiata* and *Nitzschia sigma* at 398cm. Single cm intervals are insufficient to differentiate between samples given sediment bioturbation and mixing that commonly occur at the bottom of lakes. The diatom isolation contact is defined as the location in the sediment profile where there is no longer any marine influence apparent in the core. Taking the isolation contact to be at this point, the microfossil data suggests a depth of 403cm.

An isolation contact for Hafrafellvatn at this depth is also strongly supported by all of the other proxies. LOI begins to increase at 414cm from low percentages of the marine phase (3-5% LOI) but the sediment still contains less than 10% organic material until after 400cm where it climbs gradually to 35% at the very top of the core (Figure 29). Likewise, BSi analysis shows a slightly increasing trend from the base upward but more importantly a large peak at 394cm. It is possible that this peak represents the "bloom" in diatoms that can occur in a recently emerged coastal lake. Sodium concentration analysis for Hafrafellvatn is less clear than the other proxies applied. Despite showing a

falling trend up the core there is no obvious indication of the final isolation. Sëppa et al., (1999) demonstrated a strong post-isolation secondary peak representing sodium in washing from the surrounding catchment. There is evidence of a secondary peak in sodium concentration at 398cm, although the resolution is insufficient to define this further. It is unusual that the amount of clay in the core decreases around the isolation of the basin. One would expect an increase in clay with decreases in both silt and sand as the energy levels within the basin diminish. However, at the same time, although the proportions of silt do decrease, the amount of sand increases. In conclusion, there is a wealth of data from multiple proxies that have allowed the isolation contact to be well defined. Final isolation of Hafrafellvatn occurred at 405cm, based primarily on microfossil analysis, but also supported by LOI, BSi, sodium concentration and particle size analysis.

5.2.3 Hrishólsvatn

Minimum threshold altitude 38m +/- 1.3m a.s.l

Please refer to Figures 21 & 22 for lithology and Figure 19 for geographical location.

Diatom analysis

Valve counts over 300 valves were made providing a good representation of the entire assemblage. Figure 30 shows the summary diagram for this core at >2% TDV. The base of the core is characterised by oligohalobous-indifferent taxa with some mesohalobous taxa decreasing up through the core. Polyhalobous taxa were completely absent. A full isolation sequence has not been observed, but there is clear evidence of a brackish depositional environment towards the core base.

Bio-stratigraphical Zone A (437-431cm)

The basal zone has a diverse assemblage with a large contribution of oligohalobous-indifferent taxa including: *Gyrosigma acuminatum*, *Fragilaria vaucheriae*, *and Synedra parasitica var subconstricta*. More importantly within this zone is the notable presence of mesohalobous taxa at 2-5% TDV. These include: *Ctenophora pulchella*, *Navicula digitaradiata*, *Nitzschia sigma*, *Rhopalodia rupestris*, and *Tryblionella levidensis var salina* (Figure 30). Mesohalobous taxa represent 20% TDV of Zone A. Zone A has been interpreted as a brackish transitional zone where the basin has some connection to the sea during the tidal cycle. The lack of any polyhalobous signal indicates that the base of this core has been deposited during the latter stages of the isolation process. There is also a significant proportion of oligohalobous-halophilous taxa (e.g. *Amphora*

ovalis var libyca) in this zone. These diatoms are present in all zones of this core suggesting continuous close proximity to the sea.

Bio-stratigraphical Zone B (above 431-429cm)

This zone is also dominated by oligohalobous-indifferent taxa but with small contributions of oligohalobous-halophilous taxa and the complete absence of mesohalobous diatoms. This zone is composed of >40% *Fragilaria pinnata* (a species commonly found immediately post isolation in isolation basins (e.g. Shennan et al., 1995) and >10% *Fragilaria construens*.

Diatom isolation contact

Diatom evidence from this lake reveals an incomplete sequence, where the full marine phase is missing. Nevertheless, there is evidence of a brackish transitional phase for approximately 10cm from a number of identified mesohalobous and olighalobous-halophilous taxa.

In addition, the mesohalobous taxa present have also been found in other isolation basins within the same study area where the isolation from the sea has been easier to identify. Finally, the disappearance of mesohalobous diatoms in zone B coincides with a bloom in *Fragilaria spp.* (Figure 30) which, is a common feature of isolation basins observed within this study (Mavatn, Berufjardenvatn, and Mýrahnúksvatn), elsewhere in Iceland (Rundgren et al., 1997); and further afield (Stabell 1985; Corner & Haugane 1993; and Long et al., 2003).

Despite not being able to record a full isolation sequence there is still strong evidence of a change in lake salinity conditions at the base of this core. The point of isolation is when mesohalobous taxa drop off/disappear from the record and essentially that part of the isolation sequence has been faithfully recorded i.e 431cm. Thus it is possible to infer the position of sea-level from this data and a basal date would be limiting of the time of lake isolation.

5.2.4 Berufjardenvatn

Minimum threshold altitude: 49m +/-1.3m a.s.l

Please refer to Figures 21-22 for lithology and Figure 19 for site location.

Diatom analysis

A total of 6 samples were analysed for diatom microfossils across the basal 60cm of this core and a summary of results can be viewed in Figure 31 at 2% TDV. The overlying sediments have previously been analysed for diatoms by K. Alexander (Unpublished BA thesis 2004) and were found to be entirely fresh. The basal 25cm of this core were almost completely void of diatom microfossils. Berufjardenvatn has been divided into three zones following the typical litho-bostratigraphical isolation pattern.

Bio-stratigraphical Zone A (418-406cm)

These clastic basal sediments are dominated by polyhalobous and mesohalobous taxa and have been interpreted as having a marine origin. Polyhalobous taxa *Cocconeis costata* is abundant at >20% TDV in both samples analysed in this zone with *Rhabdonema minutun* constituting >15% of the assemblage towards the top (Figure 31). In this zone there are also significant contributions to the assemblage from mesohalobous taxa including *Nitzschia sigma*, *Cocconeis scutellum* and *Tabularia fasiculata*. These taxa increase in proportion from 20-30% TDV up the zone. Oligohalobous-indifferent taxa provide ~25% of the assemblage, but from numerous low frequency counts. Only *Fragilaria pinnata* is present in any noticeable fashion constituting ~15% TDV of the assemblage at 418cm.

Bio-stratigraphical Zone B (400-406cm)

Zone B is the transitional phase of the isolation of this basin. Polyhalobous and mesohalobous taxa diminish within this zone and are replaced primarily by oligohalobous-indifferent diatom varieties, but also by some oligohalobous-halophilous and halophobous taxa (Figure 31). Zone B has no fewer than 41 different taxa represented at >2% TDV with only 5 taxa (*Amphipleura pellucida*, *Fragilaria construens*, *Fragilaria pinnata*, *Navicula subtillisima*, and *Staurosirella pinnata*) constituting more than 5% TDV to the assemblage each. Only *Cocconeis costata* is present from the polyhalobous classification and in only a very small number. Mesohalobous taxa *Cocconeis scutellum*, *Ctenophora pulchella*, *Navicula digitaradiata*, *Niztschia sigma*, *Rhopalodia gibba var parrallela*, and *Tabularia fasiculata* are all still present, but again all in low quantities. The proportions of *Fragilaria pinnata* more than double within Zone

B from ~25% TDV at 404cm to ~60% TDV at 401cm. At the lithological boundary between clayey-silt and gyttja at 401cm salt tolerant oligohalobou-halophilous taxa, especially *Amphora ovalis var libyca,* were observed.

Bio-stratigraphical Zone C (400-390cm)

Lithologically, Zone C is still located within the clayey-gyttja that contained Zone B, although there are increasing amounts of organic material (Figure 31 & 32). The diatom flora is exclusively oligohalobous-indifferent being dominated by *Fragilaria spp.*, especially *Fragilaria pinnata* which constitutes almost 90% TDV of the assemblage at 398cm (see Figure 31). This zone has been interpreted as a fresh diatom assemblage and appears typical of a lake that has recently isolated. Bradshaw et al., (1994) claimed that post-isolation *Fragilaria spp.* blooms are a product of changes in lake water chemistry, but also can be indicative of early-postglacial lake environments due to there increased competitiveness over more demanding diatom taxa (Grönlund & Kauppila 2002). The Saksunarvatn Ash is found above the section of core analysed for diatom microfossils implying a date of isolation pre-9.2 ^{14}C Ka BP.

Diatom isolation contact

This basin has presented a well-formed i-ii-iii isolation sequence that occurred during the early post-glacial period in Iceland. According to the diatom data the final isolation of this basin from marine incursion took place at 400cm (Figure 31). The transition from marine conditions to fresh occurred over a period of just 8cm of sedimentation. The high diversity of diatom species, the lack of planktonic diatom forms and the presence of mainly small, benthic taxa suggest low productivity and cold environment conditions shortly after isolation. This interpretation is supported by the location of the isolation contact within the basal clastic sediments. However, the bloom in *Fragilaria spp.* may also be interpreted as having been a result of rapid changes in lake water chemistry.

Loss-on-ignition analysis

20 samples were taken for loss-on-ignition (LOI) analysis across the two lowermost Russian cores between 360cm and 450cm. Results can be seen in Figure 32. LOI analysis for Berufjardenvatn is consistent with the results from Mavatn. From 446cm to 404cm LOI remains constant with values between 1% and 3.5% organic content. Between 404cm and 400cm LOI double from 3.5% to 6.8% representing the one major step change in the record. Thereafter, LOI exhibits some slight oscillations but remains constant between 6.3% and 9% with maybe a very slight increasing trend.

Determination of the isolation contact

Due to time constraints Berufjardenvatn was only sampled for diatom and LOI analysis and so the determination of the isolation contact lacks the data from, BSi, particle size and sodium concentration. Diatom microfossil analysis has identified that there is no longer any marine or brackish influence recorded by the fossil assemblages above 400cm (Figure 31). This observation correlated exceptionally well with the LOI data, which indicates a distinct step change in LOI between 404cm and 400cm depth (Figure 32). Despite the low organic content of this lake system this change in the LOI record has been interpreted as the isolation contact of the basin and represents increased lake flora productivity as well as an increase in the flux of organic material derived from the catchment being deposited. In conclusion, the isolation contact for Berufjardenvatn occurs at 400cm as indicated by both diatom microfossil and LOI analysis.

5.2.5 Hrishóls Bogs (1,2 and 3)

Threshold altitudes: 75m +/- 1.3m, 100m +/- 1.3m, and 90m +/- 1.3m a.s.l

Please refer to Figures 21 & 22 for lithology and Figure 19 for geographical location.

Figures 33 and 34 provide summary information of diatom analysis at 2% TDV for Hrishóls Bogs 1 and 2. Sample core from Hrishóls Bog 1 contained a greeny-brown gyttja with some minerogenic material above a dark blue-grey clayey-silt with increasing amounts of sand and gravel to base. The Saksunarvatn Ash was present in the core between 476cm and 479cm depth (Figure 22). This site was only investigated for preliminary diatoms and no other proxies due to time constraints.

The mesohalobous *Tryblionella levidensis var salina* mesohalobous taxa represented approximately 4% of the assemblage suggesting that the sediment core has recorded some part of isolation. *Tryblionella levidensis var salina* prefers to live at the "fresher" end of the salinity spectrum for mesohalobous taxa as defined by Hustedt (1953) but is indicative of greater levels of salinity near the base. *Surirella brebbissonii* also constitutes ~4% of the basal assemblage and this species is considered fresh-brackish by Rundgren et al., (1997), despite being classified oligohalobous-indifferent. Oligohalobous-halophilous taxa constitute 20-50% throughout the section of core investigated. As with Hrishólsvatn the basal assemblage has been interpreted as representing a brackish environment when the lakes threshold was still close to sea-level.

Diatom preservation for the next 25cm above the base is poor, but where diatoms are observed they tend to be of the oligohalobous-indifferent and oligohalobous-halophilous. Diatom preservation improves by 488cm with the assemblage continuing to be dominated by the slightly salt tolerant oligohalobous-halophilous taxa, especially *Amphora ovalis var libyca*. Van der Werff (1958) considers these taxa to live in fresh-brackish lake environments which would support the earlier interpretation. The long continuation of oligohalobous-halophilous taxa suggest that this lake remained close to sea-level for some time after isolation. No mesohalobous taxa were observed other than at the very base of this core and it is not believed that the barren period without diatom fossil represents a marine environment, comparable to some of the interpretations in Rundgren et al (1997).

Diatom analysis of the sample cores from Hrishóls Bogs 2 and 3 revealed fresh diatoms to the base of both core. Hrishóls Bogs 2 has a slight count of the taxa *Amphora ovalis var libyca* at 289cm. This may indicate that the lake was close to sea-level at that time or exposed to sea-spray. The biostratigraphy from these basins has been interpreted as being above the marine limit.

5.2.5 Mýrahnúksvatn

Threshold altitude 57m +/- 1.3m a.s.l

Please refer to Figures 23 and 24 for lithology and Figure 20 for geographical location.

Diatom analysis

13 samples were taken across this core for diatom analysis and Figure 31 shows a summary diagram at >5% TDV. A summary diagram at 2% TDV can be viewed in Figure 17 in the Appendix. Excellent diatom preservation permitted diatom counts in excess of 300 valves to be made on all samples. Diatom analysis revealed a partially incomplete isolation sequence with the full marine phase missing. There is a distinct change between the brackish taxa of Zone A and freshwater taxa of Zone B across a marked lithological boundary (Figure 35 and Plate 9). Oligohalobous-indifferent and Halophobous taxa increase up through the core. Diatom counts were collected from within the Saksunarvatn Ash at 606cm.

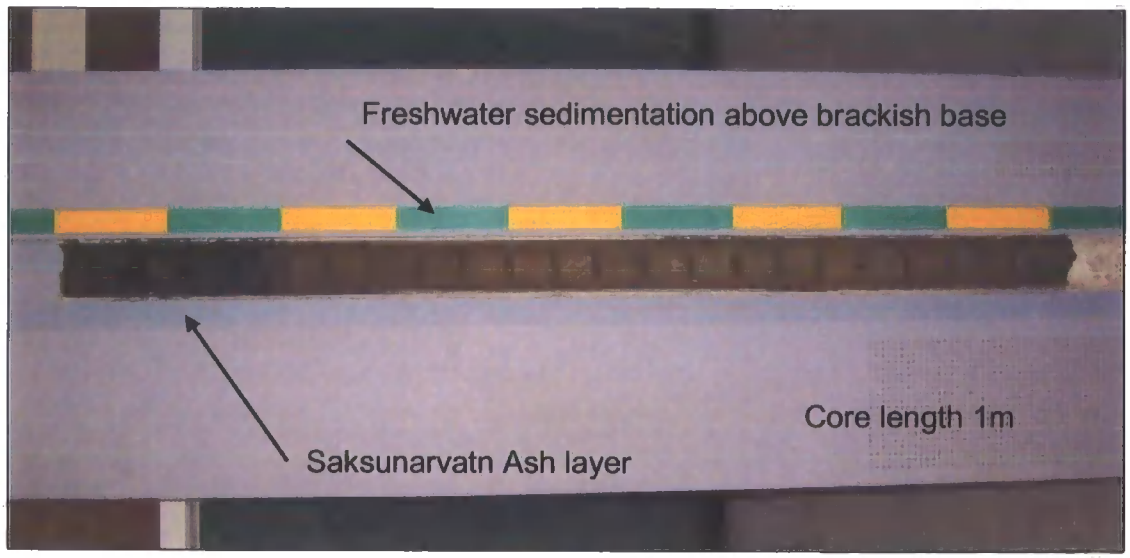

Plate 9 Sample core from Mýrahnúksvatn showing the Saksunarvatn Ash towards top.

Bio-stratigraphical Zone A (665-681.5cm)

The basal sediments from this core are blue-grey clay with some silt and organic matter plus gravel towards the base. This zone is dominated by mesohalobous and oligohalobous diatoms, particularly *Amphora ovalis var libyca*, *Cymbella ventricosa* and *Diploneis parma* (Figure 35). The lowest three samples from the basal 6cm contain significant amounts of *Tryblionella levidensis var salina*, a mesohalobous diatom that shows increasing abundance to the base where it constitutes almost 20% of the total diatom assemblage. Its presence at the base of this core is significant as it indicates a brackish lake environment during deposition. This distinct basal assemblage, lacking in polyhalobous taxa but still represents a transitional phase.

Bio-stratigraphical Zone B (665-651cm)

Dominated by small benthic oligohalobous-indifferent varieties of taxa with no other classifications of diatoms. Zone B is different from the freshwater assemblage Zone C (below) by the presence of *Pinnularia microstauron* and *Fragilaria construens var venter* and the lack of *Fragilaria brevistrata* and *Fragilaria virescens*.

Bio-stratigraphical Zone C (651-625cm)

Small, benthic oligohalobous-indifferent taxa especially *Fragilaria construens* and *Fragilaria pinnata* represent >70% of this assemblage (Figure 35). The persistent blooming of *Fragilaria spp.* is a common occurrence in recently emerged or deglaciated lake systems (e.g. Long et al., 2003; Stabell 1985; and Kjemperud 1981). It has been suggested that the reason for there dominance because they can compete ecologically

better in the rapidly changing chemical conditions of lake water during isolation (Bradshaw et al., 1994). It has been known since Stabel (1985) that high abundance of *Fragilaria spp.* can be indicative of lake isolation, although it has not been possible to determine the precise reasons for the bloom and its timing. This zone is therefore interpreted as typical of a recently isolated freshwater lake diatom assemblage.

The sediments of Zone C represent an early postglacial diatom flora with a poorly developed diatom community. There are no planktonic forms suggesting that deeper lake waters were still locked under ice for most of the year. Moreover, from the taxa identified we can assume that the areas of the lake that were ice-free with well oxygenated water.

Bio-stratigraphical Zone D (590-625cm)

Zone C contains an 8cm thick deposit of the Saksunarvatn Ash between 601-609cm (Figure 35 and Plate 10). Despite very low diatom abundances found within this layer, it was still possible to obtain diatom counts of over 300 valves. Taxonomically, the diatom assemblage observed from within the tephra unit was almost identical to those assemblages identified above and below. The magnitude of this eruption at 9.2 ^{14}C Ka BP was such that it is most unlikely that these diatoms represent living assemblages during its eruption. The fall-out from this eruption would have resulted in the cessation of almost all life within the lake and the prohibition of life-supporting processes. This is apparent from the diatom abundance and loss-on-ignition results for this layer which both provide minimums for biological productivity (Figures 36). The diatoms identified here were probably already a part of the diatom community before the eruption or/and the result of sediment disturbance and mixing.

Fragilaria virescens and *Achnanthes minutissima* increase in proportion within and above the Saksunarvatn Ash (Figure 31). It is possible that these increases are a response to the tephra fall-out, which would have nourished the lake with many important nutrients. The summary diagrams clearly show that at the same time that the Saksunarvatn Ash is deposited, the lake the numbers of both oligohalobous-halophobous and halophobous taxa begin to increase, particularly *Fragilaria virescens* (Figure 35).

Zone D has a diverse diatom assemblage indicating the "opening up" of a greater variety of habitats around and within the lake. There is also the first indication of a small planktonic diatom community highlighted by the presence of *Cyclotella antique* (Figure 35). This centric diatom indicates that deeper lake water is becoming increasingly available for habitation and nutrient cycling. *Cyclotella antiqua* is known to live in cold

environments and at this time local glaciers yet to waste away may still be influencing the lake. *Fragilaria* species are still present but in much less abundance than Zone B. Finally, there may be a response of some species to the deposition of the Saksunarvatn Ash.

Diatom Isolation Contact

There is a marked change in both bio- and lithostratigraphy in this core at 665cm depth. Here, the diatom assemblage undergoes a change from mesohalobous/Oligohalobous-halophilous taxa to Oligohalobous-indifferent diatoms. This corresponds with a change from brackish to freshwater depositional conditions within the basin. The DIC occurs at this point at this site.

Loss-on-ignition analysis

Mýrahnúksvatn was sampled for LOI at 4cm intervals and results can be viewed in Figure 36. This core is characterised by low percentages of organic content, minimum at the base with only 2% LOI and rises steadily to a peak at 614cm of just 11.6% organic content. Above 614cm the Saksunarvatn Ash was sampled and as expected contains absolutely no organic material.

Particle size analysis

Mýrahnúksvatn was sampled at 4cm intervals for particle size and the results illustrated in Figure 36. Clay falls steadily from a high of almost 40% at 675cm to around 10% at the top of the core, being at a minimum during the Saksunarvatn Ash. As with all the other particle analysis both silt and sand "mirror" each other's fluctuations suggesting coupling of process. Silt makes up the majority of the core remaining constant around 60-70% before falling sharply to a minimum of just 30% at the Saksunarvatn Ash. In comparison the sand fraction peaks at the ash layer with almost 70% of the core. Sand is stable in the middle section down to 650cm with levels between18-32% before dropping off significantly to values of 5% or lower at the core base.

Biogenic silica analysis

Samples at 4cm intervals were taken for BSi analysis of Mýrahnúksvatn and plotted in Figure 32. The BSi record shows considerable variability from a minimum of 7.5% at 602cm and a maximum of 12%BSi at 606cm. This variability may be a product of considerable problems that must be overcome during the preparation and analysis of BSi. There are three sections of this record: (1) There is an initial oscillation from

12.8%BSi at 680cm to 18.5%BSi at 674cm before a fall back to 9.8%BSi at 658cm; (2) BSi remains consistently high through the following 30cm of the middle section with values between 16.5 and 22%BSi; (3) A maximum occurs oddly within the bottom 3cm of the Saksunarvatn Ash, despite later experiments that will show that this method can distinguish between biogenic and inorganic silica. A minimum of 7.5%BSi occurs at the very top of the Saksunarvatn Ash and the variability across an otherwise homogenous sediment unit is unusual (Figure 36). There is a second oscillation but smaller than the one described at the very top of the core in a section of mixed tephra and lake gyttja.

Diatom abundance analysis

24 samples were prepared and analysed for diatom abundance across Mýrahnúksvatn at 4cm intervals. Diatom concentrations are initially very low (i.e. <1,000,000 valves per gram sediment sample) and increase steadily to a double peak at 656cm and 634cm (Figure 36). Thereafter, diatom concentrations fall to around 2,000,000 valves per gram sediment sample before falling to almost zero at the Saksunarvatn Ash.

Determination of the isolation contact

The analysis of changes in diatom communities throughout this core clearly shows that the base of this core reflects the brackish phase of the final period of isolation (Figure 31). The mesohalobous diatom *Tryblionella levidensis var salina* has been observed in other isolation basin and coastal lakes across the south coast of Vestfirðir (notably Berufjardenvatn) where the isolation sequence is far better constrained. In the bio-stratigraphical sequence of Berufjardenvatn, which contains an excellent and well-defined isolation sequence, *Tryblionella levidensis var salina* is present at the very top of the transitional phase, but only in small amounts. However, its position in the sediment sequence from Berufjardenvatn, at the top of the transitional sediments and surrounded by oligohalobous-indifferent taxa is consistent with Mýrahnúksvatn having isolated from the sea. *Tryblionella levidensis var salina* has also been observed in an assemblage in Hrishólsvatn with other mesohalobous taxa e.g. *Nitzschia sigma* (Figure 35), and these taxa have been found in abundance in other isolation basins on the south coast of Vestfiðir. Hence, there is evidence of *Tryblionella levidensis var salina* forming part a brackish water diatom community in the same region as Mýrahnúksvatn.

A gradual change in the lithology at 665cm from blue-grey clay with some silt and organic matter to a clastic brown-green gyttja (Figure 23 & 24). Lithological changes of this kind have been commonly observed in isolation basins and tend to represent the boundary between marine and brackish/fresh lake conditions (e.g. Corner et al., 2003). This boundary is also associated with a distinct change in the diatom flora from a

Fragilaria spp. dominated sediment unit above to one that is dominated by *Amphora ovalis var libyca*, *Cymbella ventricosa*, *Cymbella minutuns fo. latens*, *Diploneis parma*, as well as *Tryblionella levidensis var salina* below.

It is well known that *Fragilaria spp.* have a competition advantage over larger benthic taxa during the early stages of a lakes development after deglaciation (Stabell 1985) but, also that they respond readily to changes in lake water chemistry that are brought about by the isolation process (Grönlund and Kauppila 2002). However, it is far more likely that any bloom in *Fragilaria Spp.* is in response to meltwater given the proximity of the site to the wasting Icelandic ice sheet. Above 665cm *Fragilaria spp.* blooms dominate the assemblage to such a degree that it represents over 70% of the total diatom valves counted. This "blooming" of *Fragilaria Spp.* has been observed at Berufjardenvatn, Hrishólsvatn, and Mavatn sites occurring during and after the isolation of the basin.

Diatom analysis of Mýrahnúksvatn reveals a partial isolation sequence with the full marine phase missing. However, the basal sediments show evidence for a brackish depositional regime part of an isolation process. From the evidence available, isolation of this basin must have occurred well before 9.2 ^{14}C Ka BP and according to the age-depth model would have occurred before 11 ^{14}C Ka BP.

5.2.7 Age-depth model

In order to date the isolation contacts and the base of cores a simple age-depth model was constructed. Radiocarbon dating was unavailable for this pilot study and the model is therefore based on the position of known tephra deposits and a series of assumptions. Tephra layers are excellent chronological markers due to there almost instantaneous "blanket" deposition, their occurrence in many different environments facilitating correlations, as well as being well dated. It was assumed for the purpose of this study that sedimentation rates remained constant throughout the cores with minimal influence from sediment compaction. The author is well aware of the simplicity of this approach and limitations have been discussed in "Conclusions," however, it is believed that this model is "an as good as it gets" with the means and data available. With a conservative consideration of error margins this model will suffice for the purposes of this study.

Tephra deposits were analysed and identified by Anthony Newton, School of Geosciences, University of Edinburgh. The main stratigraphical marker observed in 5 of the 7 sites was the well dated and distributed Saksunarvatn Ash (ca. 9.2 ^{14}C Ka BP). Linear sedimentation rates were calculated between the known age of the base of in situ tephra deposits and the core top that was assumed to represent the present day focus of deposition. Once the time required for the deposition of 1cm of sediment was known

it was possible to calculate estimated radiocarbon ages for isolation contacts and core bases alike (Figure 41-43).

In the case of Mýrahnúksvatn, two tephras were observed within the full core stratigraphy providing two points to develop an age-depth model with. Unfortunately, both tephras were recorded in different investigative cores. To justify the combined use of both tephra I am assuming that this tephra is present in the main sample core, at a similar depth, where we have also the Saksunarvatn Ash. Furthermore, it is clear from the depths of the investigative cores that this basin has a concave bedrock profile (see Figure 47).

Figure 47 Basin morphology of Mýrahnúksvatn

Core	Distance from north bank (m)	Water depth (cm)	Core depth (cm)	Nature of core end
GJ03-01	20	95	608	Bedrock
GJ03-02	25	Not recorded	687	Bedrock
GJ03-03	45	98	588	Stopped in tephra
GJ03-04	65	95	303	Stopped in gravel
GJ03-05	85	55	118	Stopped in gravel

There is a tendency for the deeper parts of the basin to fill up with older sediments and as this process continues the concavity of the basin should reduce. This is supported by consistent water depths at around 1m deep indicating a modern day flat lake bottom, even if the bedrock is not. Hence, it can be assumed that the position of the Hekla tephra from core GJ03-04 would be approximately the same in core GJ03-02 as it is in GJ03-04.

Estimated radiocarbon ages were converted into calendar ages using Calib Rev4.4.2 (Stuiver & Reimer 1993) with an error range of 2 standard deviations. Means of these ranges were used to plot RSL curves in Figures 44-46.

Figure 21 Sample core lithology: South coast of Vestfirðir

Core	Altitude (m)	Depth (cm)	Troels-smith (1955)		Description
Mavatn	3.1m	0-59			Water
Ma03-06 (Livingstone)		59-78	Sh2 As1 Ld1 Gs+ Ag+	30210	Olive-green well humified organic material with traces of sand and silt. Tephra mixed in to the top 10 cm's
		78-80	Gg3 Gs1 Ld+	30202	Organic gravel layer
		80-97	As3 Gg1	20201	Blue-grey clay with gravel towards base
Hafrafellvatn	24.7m	350-372	Th2 Ld2	30200	Brown peaty-gyttja with abundant plant matter
Ha03-01 (Livingstone)		372-390	Ld2 Ag1 As1 Th+	20200	Pale green-brown clayey-silty gyttja with some plant fragments towards the top. Increasingly clayey to base
		390-450	Ag2 As2	20200	Blue-grey clayey silt
Hrisholsvatn	41.1m	0-130			Not recovered
Hr03-01 (Russian)		130-200	Ld3 Th1	20030	Greeny-brown limus with abundant plant fragments
		200-300	Ld2 Tb2	20030	Greeny-brown limus with abundant spagnum moss
		300-418	Ld4 Ag+	30210	Green-brown gyttja with black bands
		418-421	Ag4	40201	Black silt layer
		421-431	Ld4 As+ Th+	20212	Olive-green gyttja with some plant fragments and silt. Sharp upper contact
		431-436	As2 Ag1 Gmin1 Gmaj+	20201	Silty-clay with some sand and gravel

Sample core lithology: South coast of Vestfirðir (continued 1)

Core	Altitude (m)	Depth (cm)	Troels-smith (1955)		Description
Berufjardenvatn	51.1m	0-92			Water
Br03-03 (Livingstone)		92-310	Ld3 Th1	30020	Olive-green well humified limus with abundant rootlets. Dark grey silt band at 219cm-possible tephra
		310-325	Ld3 Ag1 Th+	20210	Olive-green clayey-gyttja with some plant remains
		325-326	Ag4	40201	Black silt (tephra)
		326-351-5	Ld3 As1 Gg+	30211	Pale olive-green/brown gyttja with course sand/gravel at base
		351.5-353.5	Ag4	40201	Homogenous black silt (tephra)
		353.5-410	As2 Ag2 Gg+	20202	Blue-green/grey silty-clay with some isolated course gravel (drop stones) Increasing clay content to base (As3 Ag1)
Berufjardenvatn	51.1m	360-401	Ld3 As1 Gg+ Th+	20220	Pale olive-grey gyttja with some course sand/gravel and plant remains near the top
Br03-03 (Russian)		401-450	Ag2 As1 Gmin+ Gmaj+	20201	Blue-grey clayey-silt with some sand and gravel

Sample core lithology: South coast of Vestfirðir (continued 2)

Core	Altitude (m)	Depth (cm)	Troels-smith (1955)		Description
Hrishols Bog I	79.1m	0-250	Th4	20210	Brown fibrous peat
(Russian)		250-450	Ld4 As+	20210	Light brown gyttja with flecks of black silt at 370cm and a pale
		450-476	Ld3 As1	20210	Olive-green-brown gyttja with some silt
		476-479	Ld2 As2	40201	Vertical stripes of black silt intercalated with green-brown gyttja
		479-513	Ld3 Ag1	20210	Olive-green-brown silty gyttja. Isolated Gg at 489cm
		513-525	Ld2 Ag2 As+ Gg+	20211	Pale brown organic gyttja with some clay and gravel
		525-540	Ld1 Ag3	20211	Greeny-blue organic silt
		540-550	Ag2 As1 Gmin1 Gg+	20201	Dark blue-grey clayey silt with some sand and gravel
Hrishols Bog 2	104.1m	245-249-5	As3 Ag1 Ld+	20300	Pale brown organic silty-clay
(Russian)		249.5-250	Ag4 Ld+	40301	Thin layer of black silt (tephra)
		250-275.5	As3 Ag1 Ld+	20300	Pale brown organic silty-clay
		275.5-278	Ag4	40301	Black silt (tephra)
		278-295	As3 Ag1	20301	Browny-grey clay with traces of sand and silt
Hrishols Bog 3	94.1m	240-280	As3 Ag1	20300	Light brown silty-clay
(Russian)		280-283	Ag4	40310	Black silt (tephra), sharp bottom contact
		283-290	As4 Ag+	20201	Light brown clay with some silt

Figure 22 Sample Core Lithology for sites along the south coast of Vestfirdir

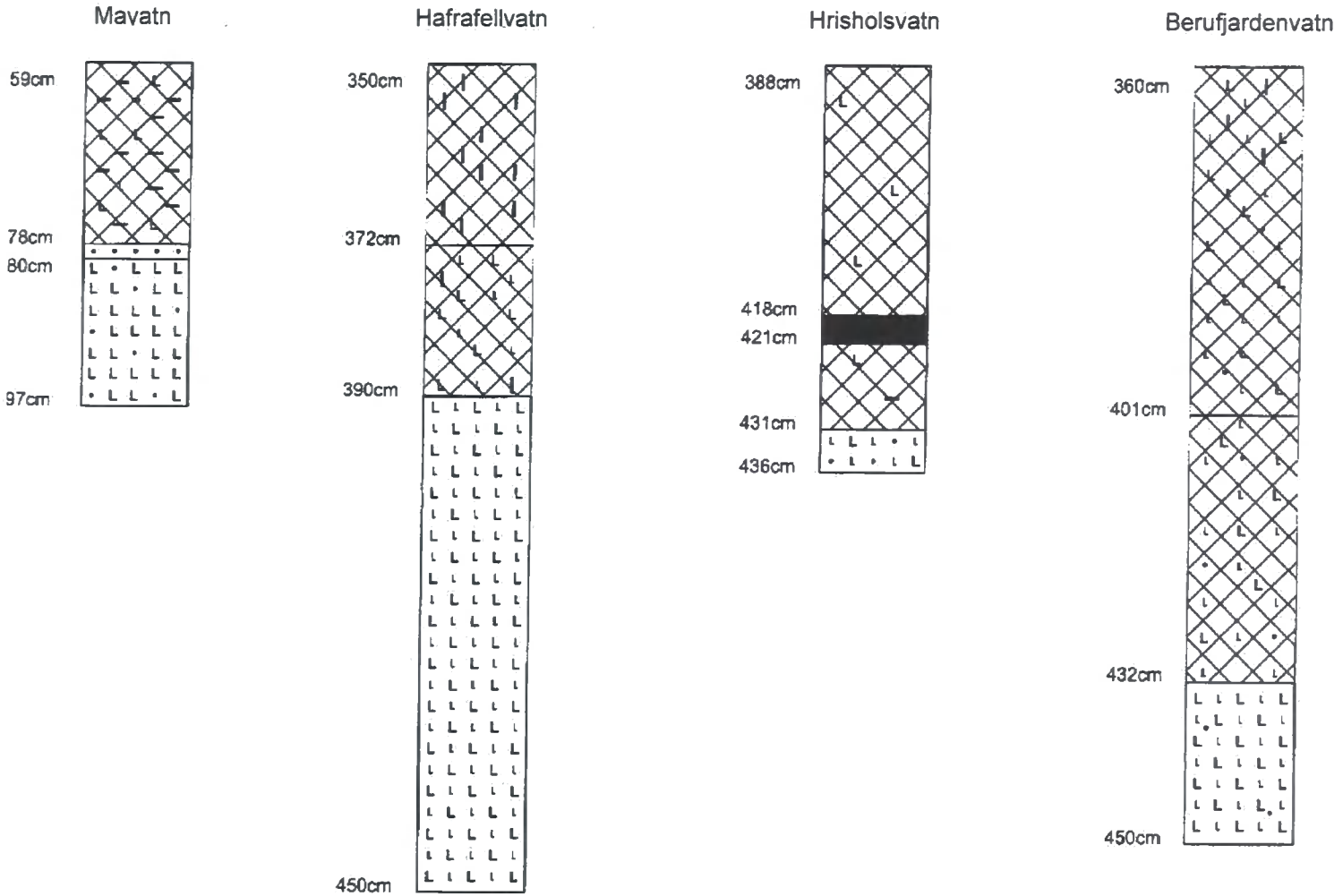

Figure 23 Lithology of tephra layers and identification

Source: Newton, A. (2004)

Location	Core	Depth (cm)	Description	Tephra relative to	Identification	Age	Ref.
Hrishólsvatn	HR03-01B	409-416	Fine black tephra	Tephra in band of greeny/brown limus	Saks	9000 ^{14}C BP	2
Berufjarðarvatn	BR03-03L	324.8-325.9	Tephra		mixed basaltic		
Berufjarðarvatn	BR03-03L	351.8-352.8	Tephra		Saks	9000 ^{14}C BP	2
Hrishóls Bog 1		387-389	Fine black tephra		Katla		
Hrishóls Bog 1		475-470	Disturbed 1cm fine black tephra, seems to have fallen into cracks		Saks	9000 ^{14}C BP	2
Hrishóls Bog 2		249.5-250	Fine black tephra		mixed basaltic		
Hrishóls Bog 2		276-278	Fine black tephra		Saks	9000 ^{14}C BP	2
Hrishóls Bog 3		280-282	Fine black tephra		Saks	9000 ^{14}C BP	2
Mýrahnúksvatn	GJ03-01	555	Fine black tephra	Tephra sits on limus with clay	Saks	9000 ^{14}C BP	2
Mýrahnúksvatn	GJ03-02	597-608.5	Fine black tephra		Saks	9000 ^{14}C BP	2
Mýrahnúksvatn	GJ03-03	575-588	Fine dark grey tephra				
Mýrahnúksvatn	GJ03-04	250	Tephra sampled in field		Hekla 4	3826±12 ^{14}C BP	1
Mýrahnúksvatn	GJ03-04	270	Tephra sampled in field		mixed/SILK	4400-4600 ^{14}C BP	
Mýrahnúksvatn	GJ03-04	280	Tephra sampled in field				
Djúpavik	DJ02-03-03	320	Bagged samples		Saks	9000 ^{14}C BP	2
Djúpavik	DJ02-04-03	520	7 mm dark tephra		mixed		

1: Dugmore, A. J., Shore, J. S., Cook, G. T., Newton, A. J., Edwards, K. J. and Larsen, G. (1995) The radiocarbon dating of Icelandic tephra layers in Britain and Ireland. Radiocarbon, 37, 2:286-295.

2: Andrews et al. (2002) Distribution, sediment magnetism and geochemistry of the Saksunarvatn (10 180 +/- 60 cal. yr BP) tephra in marine, lake, and terrestrial sediments, northwest Iceland, Journal of Quaternary Science, 17, Issue 8, pp.731-745

3: Ocean-transported pumice in the North Atlantic, Unpublished PhD thesis, University of Edinburgh, pp 394.

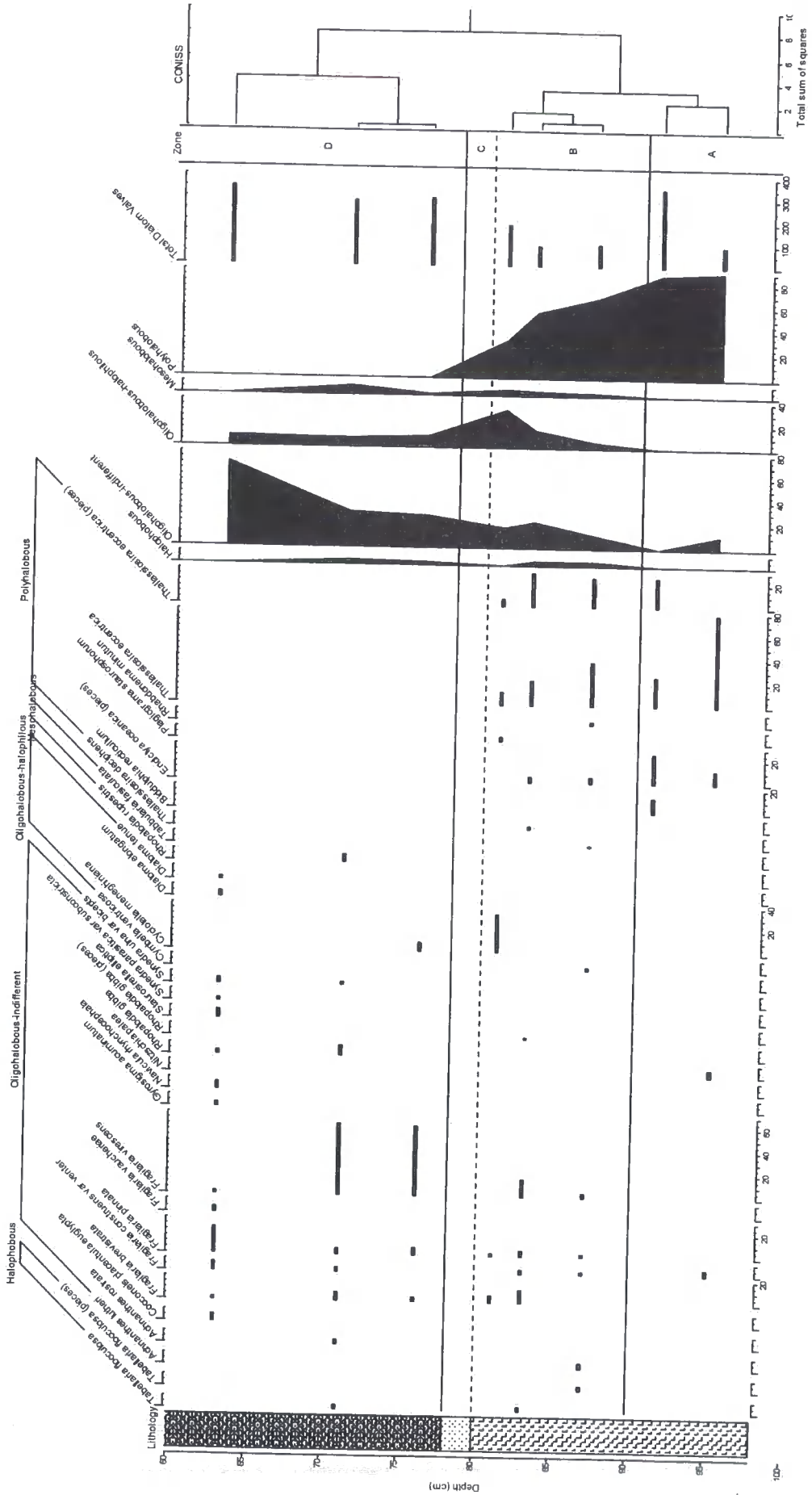

Figure 24 Mavath diatom assemblage

Figure 25 Mavatn results

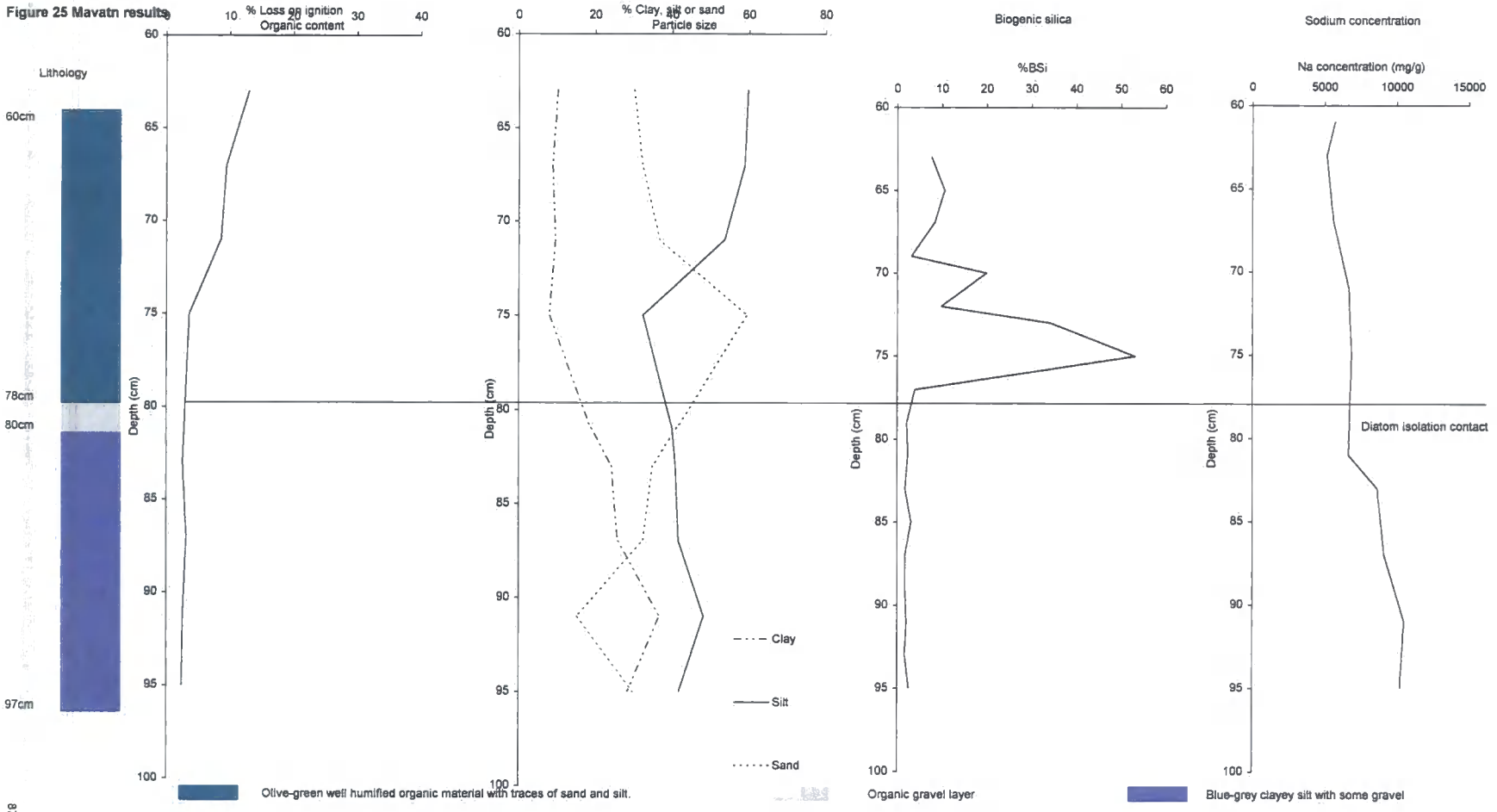

Figure 26 Hafrafellsvatn diatom assemblage

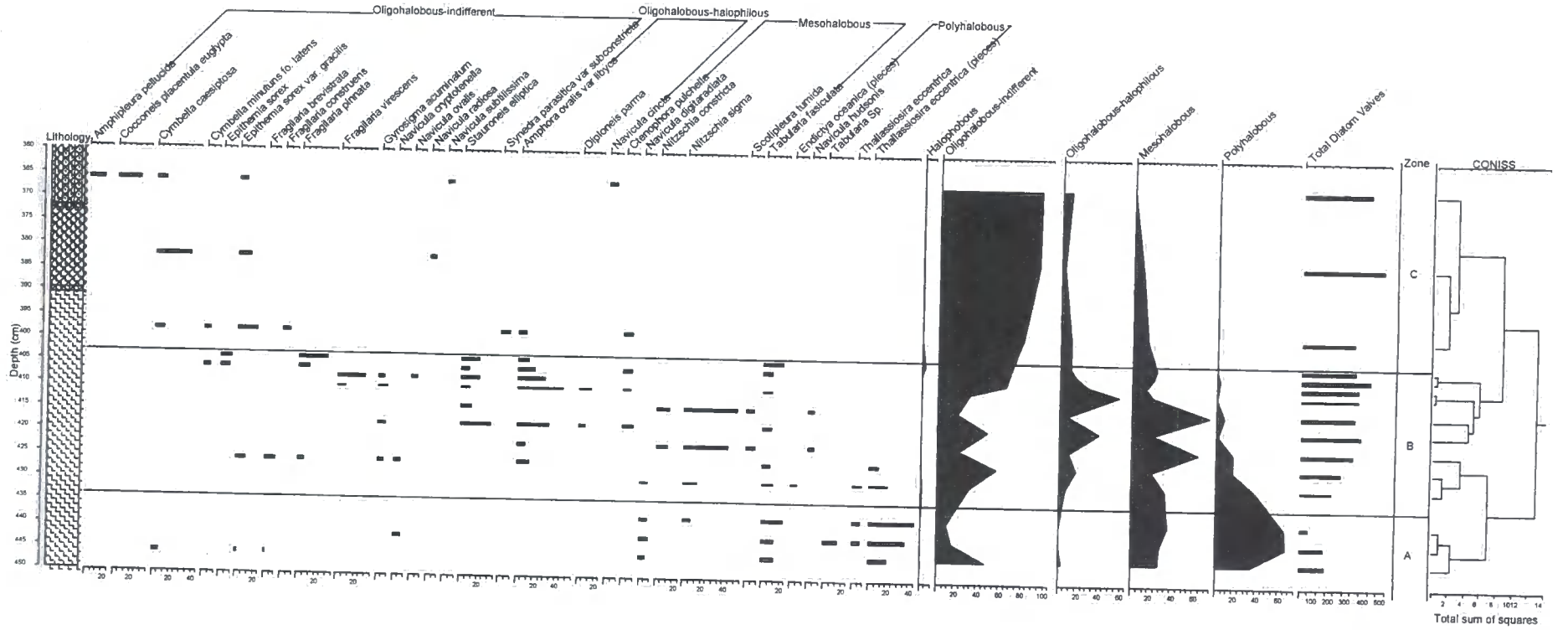

Figure 27 Hafrafellvatn results

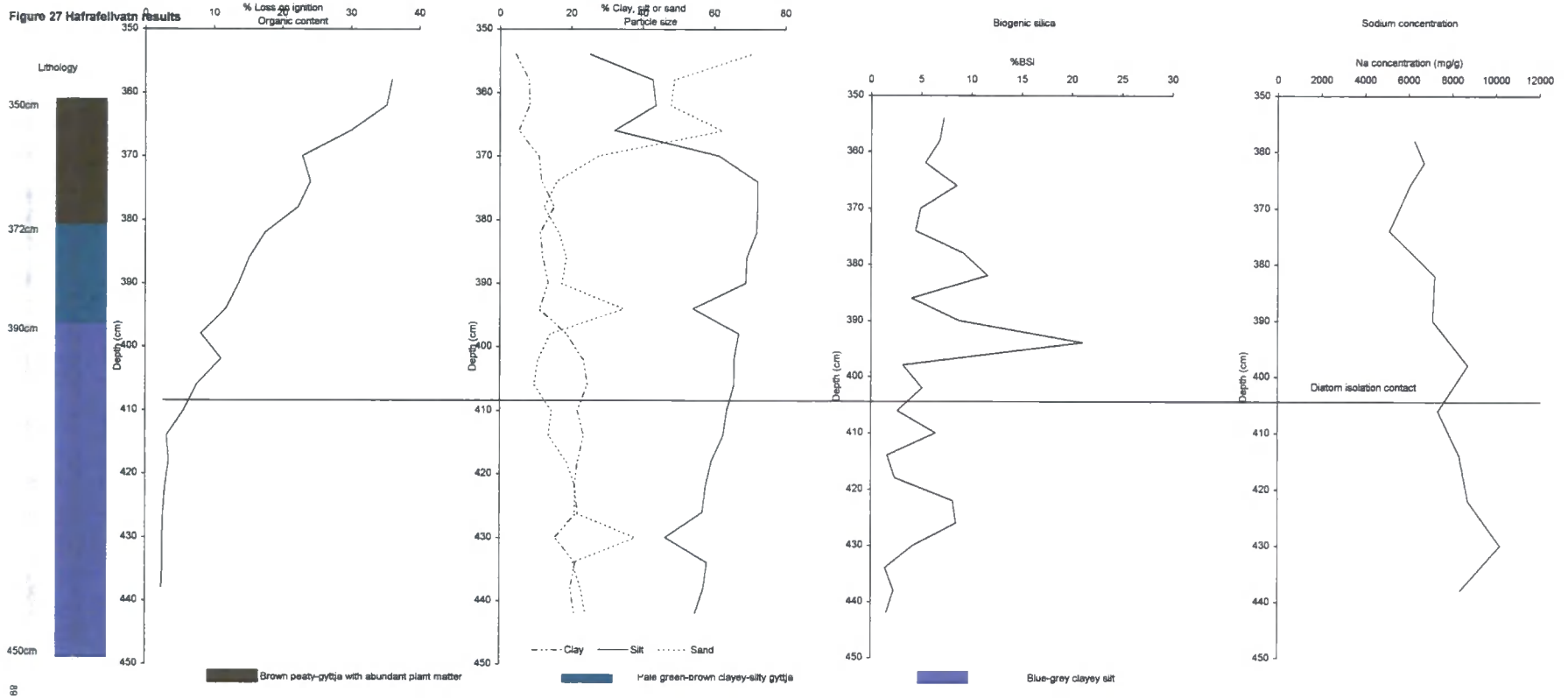

Figure 28 Hrisholsvatn diatom assemblage

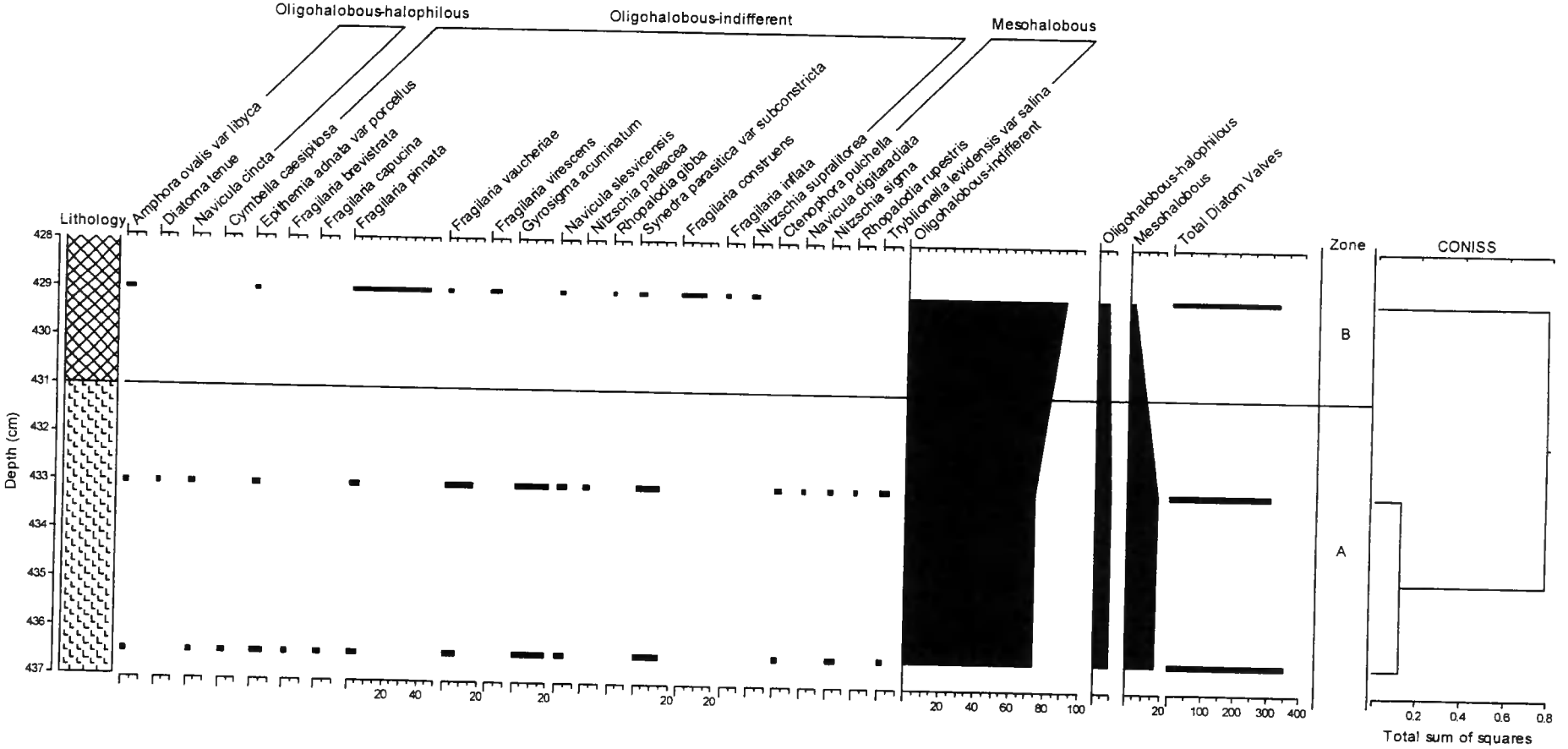

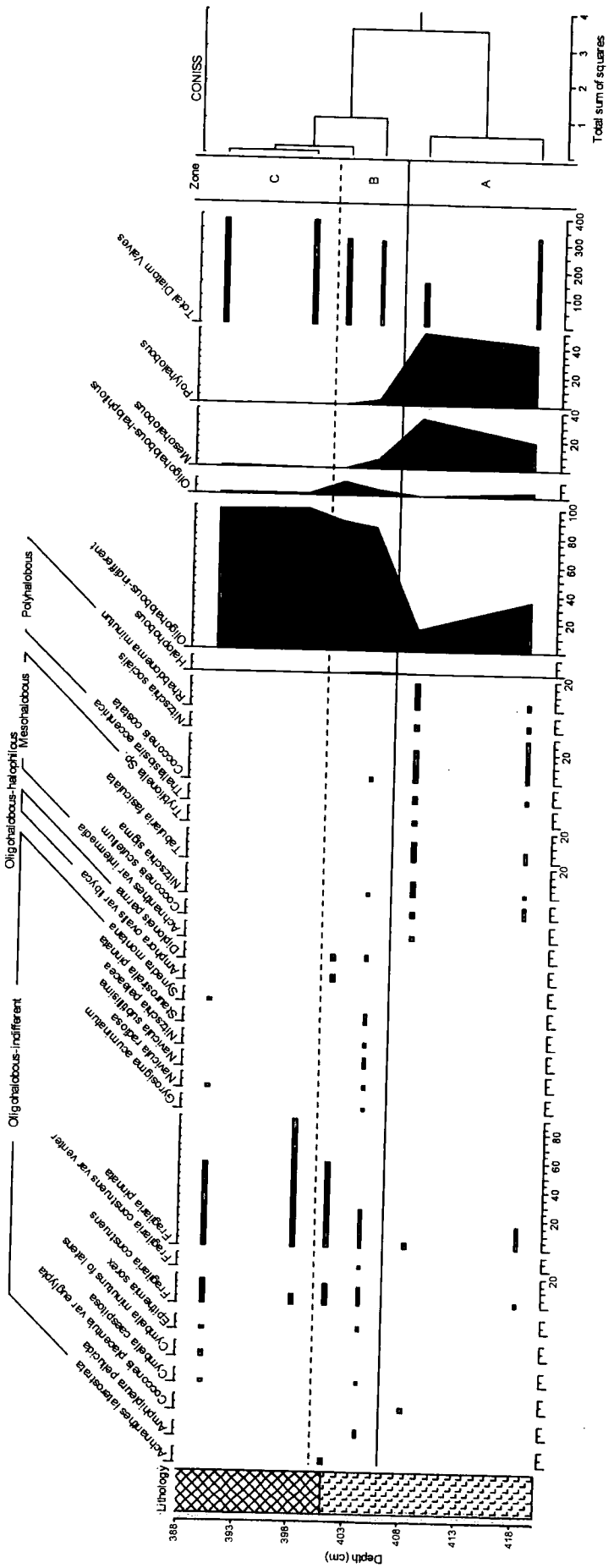

Figure 29 Berufjardenvatn diatom assemblage

Figure 30 Loss-on ignition analysis for Berufjardenvatn

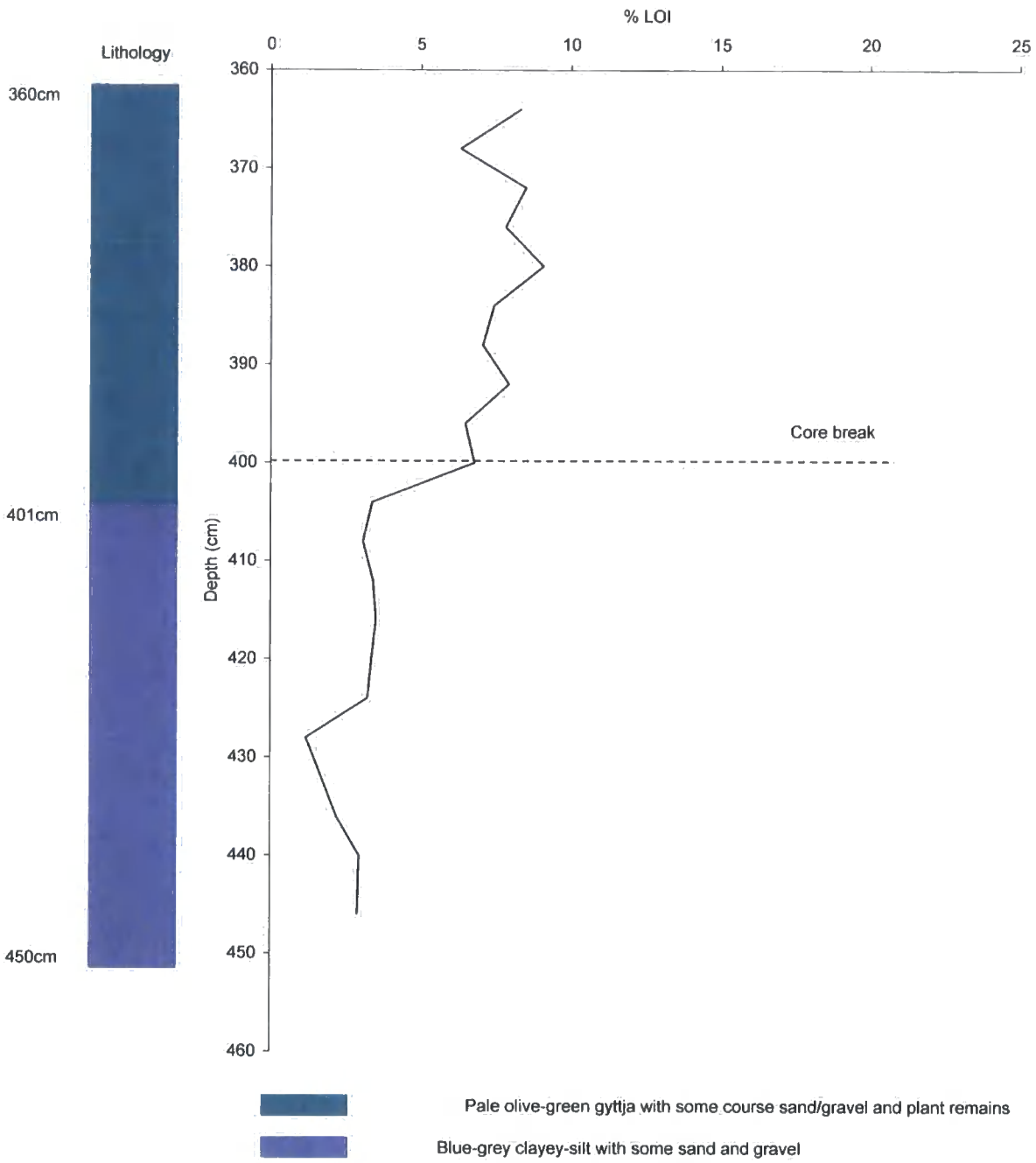

Figure 31 Hrishols Bog 1 diatom assemblage

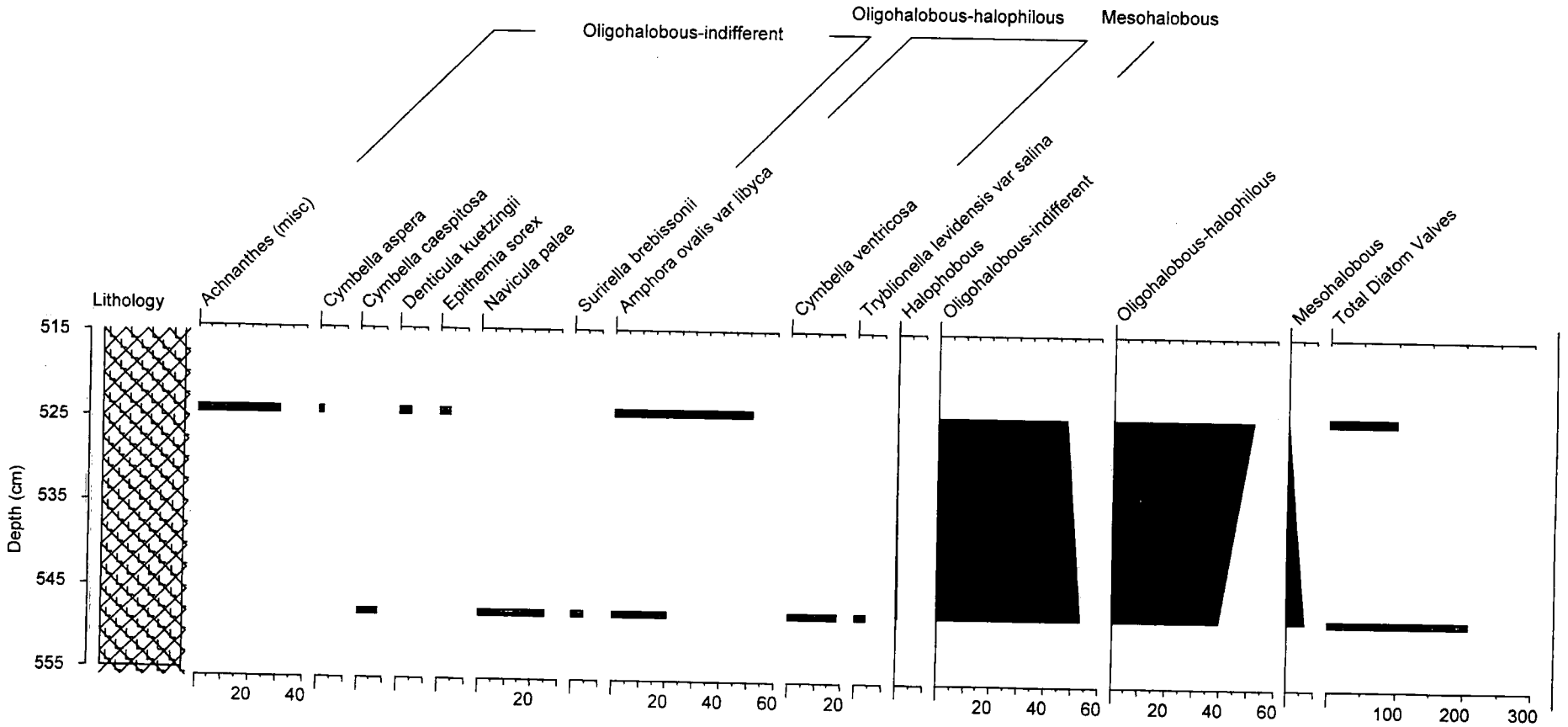

Figure 32 Hrishols Bog 2 diatom assemblage

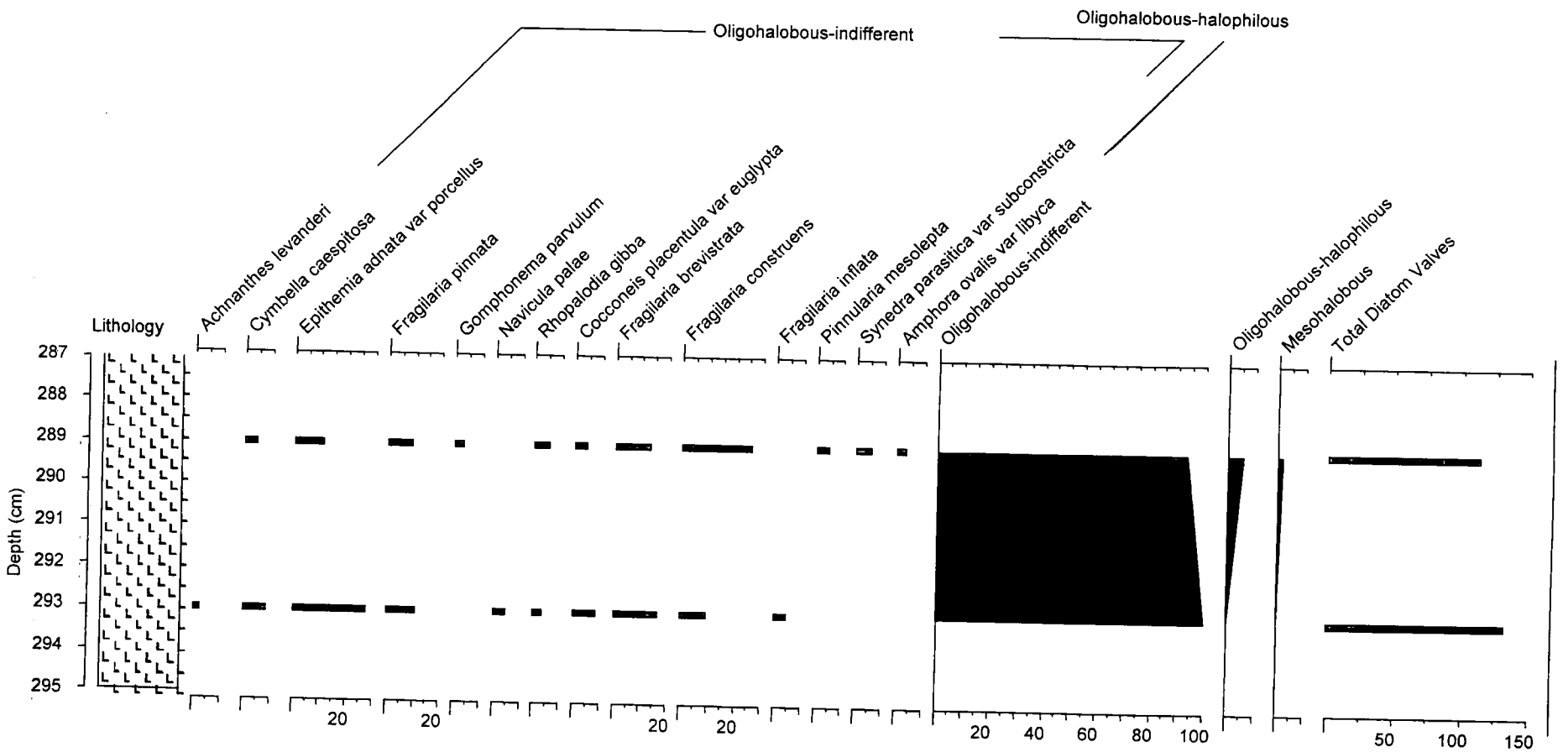

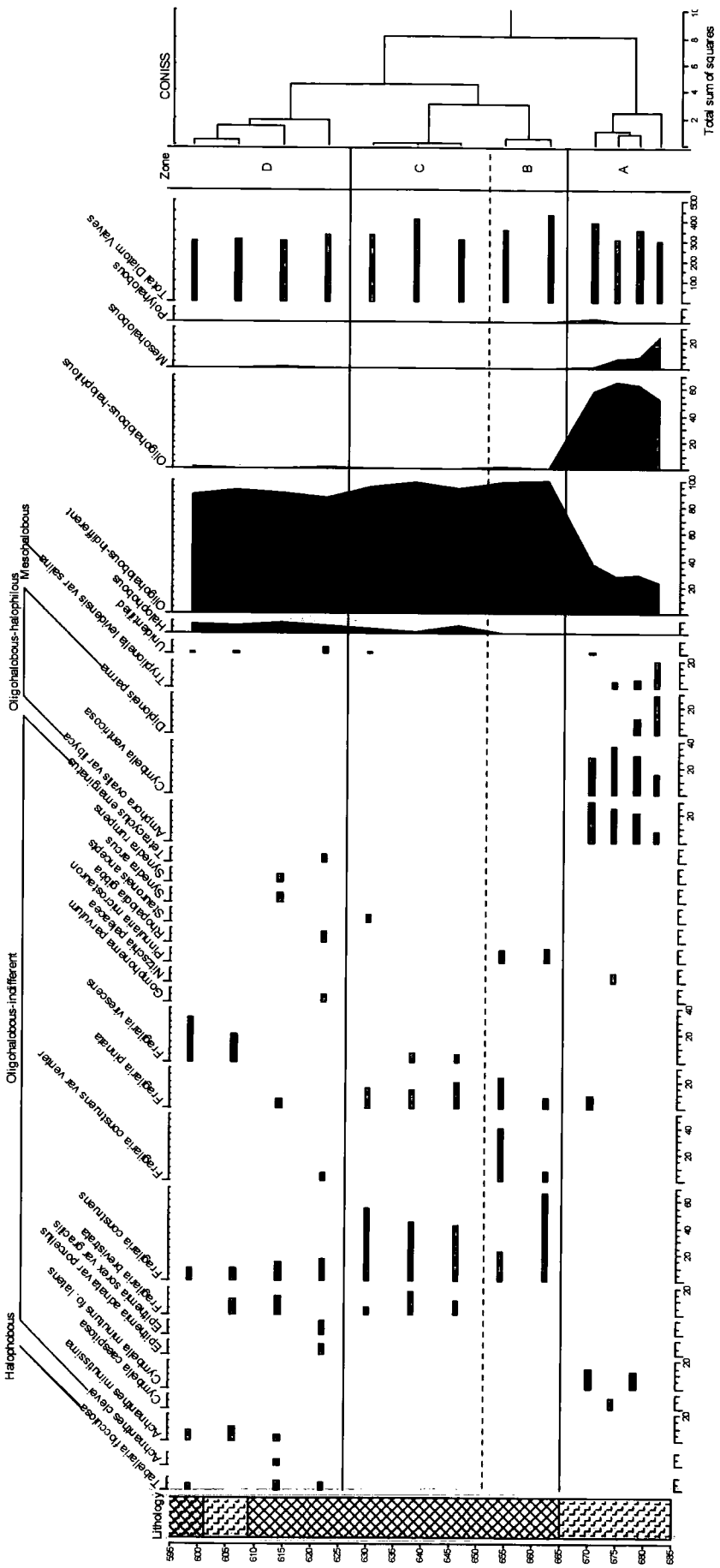

Figure 33 Myrahnuksvatn diatom assemblage

Figure 34 Mýrahnúksvatn results

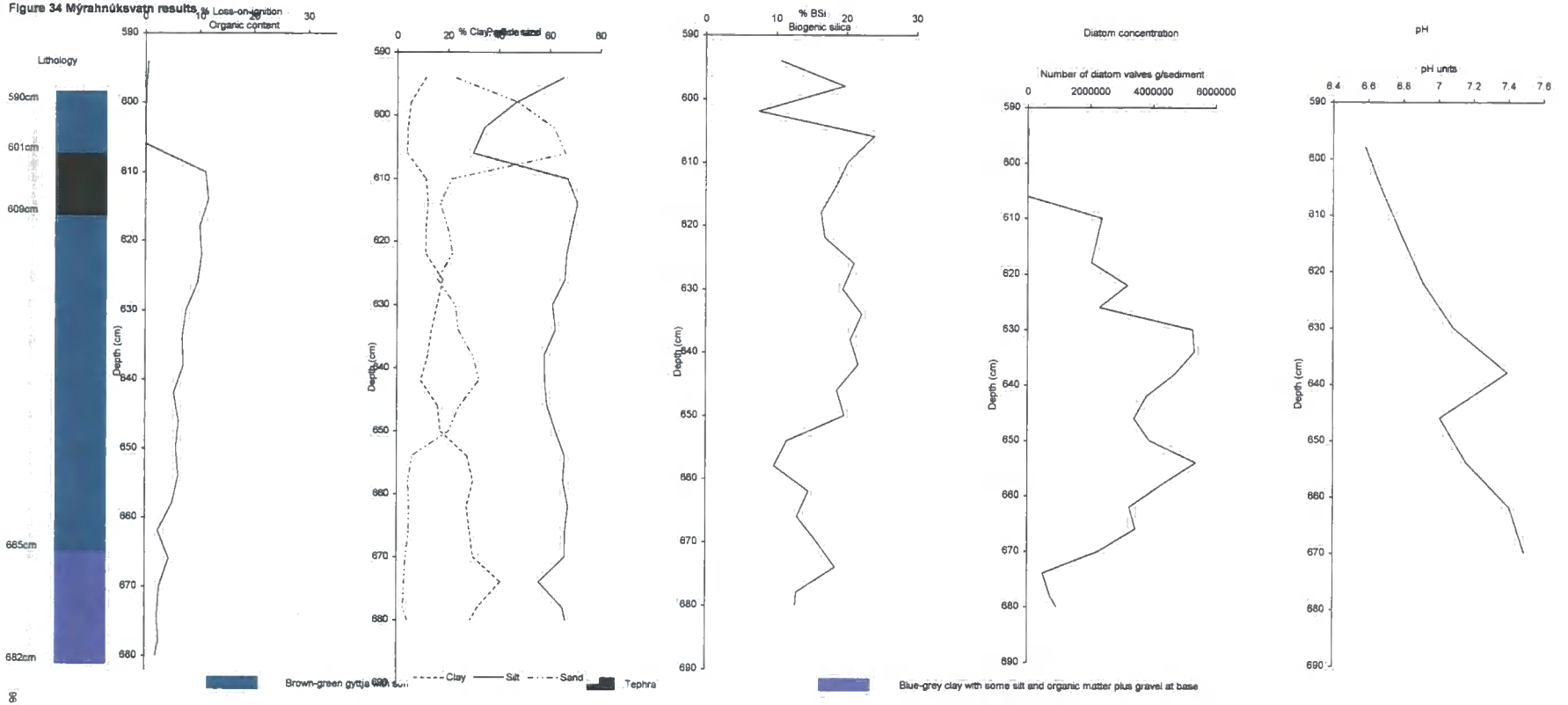

5.3 Evidence for environmental change in the early-middle Holocene NW Iceland

Proxies from Mýrahnúksvatn except pH were discussed earlier (See section 5.2.6) and so will not be repeated here. Here follows a discussion of the analysis conducted on Djúpavik (lower site). This core was bottomed out on the Saksunarvatn Ash (9.2 ^{14}C Ka BP) which we were only able to sampled by using a gouge corer. It was however, possible to core through the Saksunarvatn Ash at the Mýrahnúksvatn site and thus this stratigraphical marker has been used to correlate the cores and to construct an age-depth model. The combined record from these two basins covers the early to middle Holocene time period for Iceland, i.e. 10.5-4.5 ^{14}C Ka BP.

5.3.1 Djúpavik (lower site)

Lake altitude 14m +/- 0.25m a.s.l

Please refer to Figures 23 & 24 for lithology and Figure 20 for geographical location.

Diatom analysis

14 samples were taken and prepared for diatom analysis. Diatom preservation was good and counts in excess of 300 valves were made on all samples. 34 different taxa were identified and all but polyhalobous varieties were represented. Samples were taken to identify changes in fauna above and below lithological boundaries as well within homogenous sediment units. Summary information can be viewed in Figure 37 at 5% TDV and 2% TDV in Figure 18 in Appendix. Apart from an increase in silt and clay the green-brown gyttja is generally lithologically homogenous throughout this core. There are however, two occasions where the lithology differs from that described above (Figure 37). Between 520cm and 520.5cm there is a thin black silty layer of tephra that was unable to be identified. Secondly, between 419.5cm and 420.5cm there is a course gravely/sand layer.

The summary diagram in Figure 33 shows that the early to middle Holocene sediments of this lake system were dominated by oligohalobous-indifferent taxa (~70-80%) with the remainder being comprised of both oligohalobous-halophilous and halophobous taxa. A short period of mesohalobous taxa occurs from 375cm to the top of the core. Five taxa are significant in every sample: *Tabellaria flocculosa* (halophobe); *Fragilaria virescen, Fragilaria construens*, *Fragilaria pinnata*, and *Tabellaria fenestrata* (all oligohalobous-indifferent). This core has been subdivided into three zones and one sub-zone that will be described in turn.

Bio-stratigraphical Zone A (510-540)

Zone A is dominated by five main taxa: the halophobe *Tabellaria flocculosa*; alkaliphilous *Fragilaria virescens*; small benthic *Fragilaria construens and Fragilaria pinnata*; as well as *Tabellaria fenestrate* (Figure 37). There are small amounts of Nitzschia sociabilis, a mesohalobous taxa, but these extend throughout the core and unsupported by other like taxa, its occurrence is most likely a consequence of a combination of other favourable environmental conditions other than salinity. There are three main differences that Zone A has from the above sediments: (1) the frequency of *Fragilaria spp.* is much greater; (2) the diversity is lower with only 16 different species of diatom present; and (3) there are quite significant amounts of *Epithemia spp.* that although are present in the assemblages identified from sediments above, are not present in such large quantities.

At 520cm there is a slight layer of tephra 0.5cm thick (Figure 37). Telford et al., (2004) showed that diatoms can respond to changes directly or indirectly caused by the fall out of cold distal tephra. However, their results were somewhat inconclusive but did suggest a threshold of a >1cm thick deposit of tephra was required to induce a response by a diatom community. Diatoms were analysed above and below this thin layer of tephra. Four species showed increases in abundance i.e. *Fragilaria virescens*, *Fragilaria construens*, *Fragilaria pinnata*, *Tabellaria fenestrata*, and *Nitzschia sociabilis*; two diatom taxa had lower frequencies after deposition i.e. *Tabellaria flocculosa* and *Cymbella minutuns fo. latens*; and one species appeared for the first time i.e. the halophobe *Bracysira serians fo* (Figure 37). If this tephra is shown to be deposited in situ and not a facet of sediment reworking then there is some evidence for changes in the composition of the diatom community.

Bio-stratigraphical Zone B (380-510)

Zone B represents the middle 120cm of this sediment core and is dominated throughout by the five key taxa described in Zone A and summarised in Figure 37. There are however, some subtle differences that make this zone distinct. Firstly, the diversity of the assemblage has increased and 28 different taxa are present at >2% TDV. This increased diversity represents a greater number of larger benthic taxa including *Navicula radiosa*, *Pinnularia spp. Cymbella cistula*, and *Cocconeis placentula var euglypta*. The abundance of both *Fragilaria construens* and *Fragilaria pinnata* has decreased by almost half from Zone A suggesting that the factors that gave them increased advantage in competition has diminished. Planktonic taxa appear in this zone with *Cyclotella antiqua* at 465cm (Figure 37). However, the presence of *Cyclotella antiqua* is short lived and it does not appear significantly anywhere else within the core.

Sub-zone B(ii)

A 0.5cm thick layer of sand occurs at 420cm and some interesting changes in the diatom community can be observed at this lithological boundary (Figure 37). Four taxa can only be found at this level with the most significant being the aerophilic taxa *Hannaea arcus var amphioxys* and *Meridion circulare* that is known to prefer high oxygen levels in the lake water.

Bio-stratigraphic Zone C (310-380)

Zone C is the return to conditions similar to the base with lower assemblage diversity (only 14 species of diatom) and again dominated by the five key taxa identified earlier. Over 65% of this assemblage is composed of *Fragilaria spp* (Figure 37). There is no longer the mix of larger benthic taxa that was present in the middle section of this core although, the planktonic oligohalobous-halophilous diatom *Cyclotella meneghinian* is present throughout, especially at 374cm where it constitutes ~10% of the total diatom assemblage.

Loss-on-ignition analysis

The core from Djúpavik was sampled at 4cm intervals for loss-on-ignition analysis (Figure 34). There is much variability throughout the record despite the homogenous appearance of the sediment. Organic content peaks at 24% at 372cm and has a minimum of just 5.4% LOI at 420cm. From the base of the core the amount of organic material gradually increases from ~10% to >20% between 504cm and 494cm forming a broad peak in LOI. From here upwards the level of organic material in the sediment falls back to around 10% LOI before oscillating in a series of three peaks for the following 60cm of core with LOI values between 5 and 17% LOI (see Figure 38). After the minimum at 420cm LOI increases and remains between 15-20% LOI until it falls to ~10% once again at the very top of the core.

Particle size analysis

At first glance it is clear that there is a great deal of variability in the particle size analysis from Djúpavik (Figure 38). The oscillations in the clay record appear to become less frequent up through the sequence and values tend to remain between 10-20% clay. There does appear to be some periodicity in the record with lower than average values more frequent between 500-540cm, 425-460cm, 375-400cm, and at the very top of the core. Higher than average values occur between 460-500cm, 400-425cm, and 310-

350cm. The silt record is the most stable of the three with constant values at ~70% silt. Values appear slightly higher towards the base (~75-80%) with a single peak at 416cm representing the record minimum of 58% silt. The sand record demonstrates the most variability with oscillations throughout the sequence between 10-20% LOI (Figure 38). The minimum in sand content occurs at 420cm with just 10.3% of the sediment composed of sand, and this is just shortly before the sand maximum at 416cm of almost 28% LOI which, also correlates with the silt minimum and clay maximum.

The analysis of particle size for this core, despite indicating a great deal of variability (but low absolute amplitudes of change) does suggest a relatively stable sediment sequence dominated by silt (~70%) with continuously fluctuating amounts of clay and sand. The sand layer in the very centre of the core is nicely highlighted as the sand maximum at 416cm.

Biogenic silica analysis

The core from Djúpavik was sampled at 4cm intervals and the results plotted in Figure 34. Values for BSi range between 2 and 10% BSi and are consistently lower than Mýrahnúksvatn but in line with Mavatn and Hafrafellvatn. The record is characterised by three peaks evenly spaced at 525cm, 424cm, and 316cm. Between these peaks values for %BSi are lower and show slightly decreasing trends into minimums either side of the broad peak at 424cm. This "middle" peak may represent increased diatom productivity during the period 6.75 cal. Ka BP and 6.15 cal. Ka BP i.e. during the climatic optimum as inferred from Greenland ice cores (Dahl-Jensen et al., 1998). The record does appear to exhibit a weak cyclicity of the order of 1500 years matching the duration of Dansgaard-Oschegner Cycles.

Diatom abundance analysis

42 samples were analysed for diatom concentration as described in "Methodologies." Results have been illustrated in Figure 38. The mean average diatom concentration for this core is 3400000 (adjusted for generalisation) diatom valves per gram of dried sediment (frustules/g). Maximum diatom concentrations are found at the very base of the sample at >5000000 frustules/g and they remain above the average until 480cm. Between 480cm and 412cm a series of 5 oscillations occupy the middle section of the record (Figure 34). During this period values are on constantly below the average going above it briefly at 428cm. The minimum in the record occurs at 452cm with a concentration of ~1970000frustule/g. The depression in diatom concentration throughout the middle sequence is broken at 408cm with a prominent peak at 4317050

frustules/g and thereafter values oscillate about the mean, apart from a trough at 368cm of 2409592 frustules/g and a second fall at the very top of the record.

Figure 35 Sample core lithology: Northeast coast of Vestfirðir

Core	Altitude (m)	Depth (cm)	Troels-smith (1955)		Description
Myrahnuksvatn	61.1m	0-95			Water
GJ 03-02b (Livingstone)		95-590	Ld4 Th+	30020	Olive-green well humified gyttja with abundant rootlets
		590-601	Ld2 Ag2	30300	Brown-green gyttja with some silt (mixed in reworked tephra?)
		601-609	Ag4	40300	Thick black silt (tephra)
		609-665	Ld3 As1 Th+	30020	Brown-green gyttja with increasing amounts of clay and some plant fragments. At 653cm thin black laminae <2mm thick
		665-687	As2 Ag1 Ld1 Gg+	20020	Blue-grey clay with some silt and organic matter plus gravel at base
Djupavik	15.1m	0-250	Th4	30020	Dark brown turfa peat
DJ2-04-03 (Russian)		250-401	Ld4	20210	Brown gyttja
		401-419.5	Ld2 As2	20210	Green-brown clayey-gyttja
		419.5-420.5	Ld2 Gmaj2 As+	20201	Green-brown gyttja with gravel and traces of silt
		420.5-470	Ld2 As2	20210	Green-brown clayey-gyttja
		470-520	Ld3 Ag1 Th+	30220	Brown gyttja with some silt and plant fragments
		520-520.5	Ag4	40301	Black silt (tephra)
		520.5-541	Ld2 Ag1 As1	30222	Pale brown gyttja with some silt and clay

Figure 36 Sample Core Lithology for sites along the northeast coast of Vestfirdir

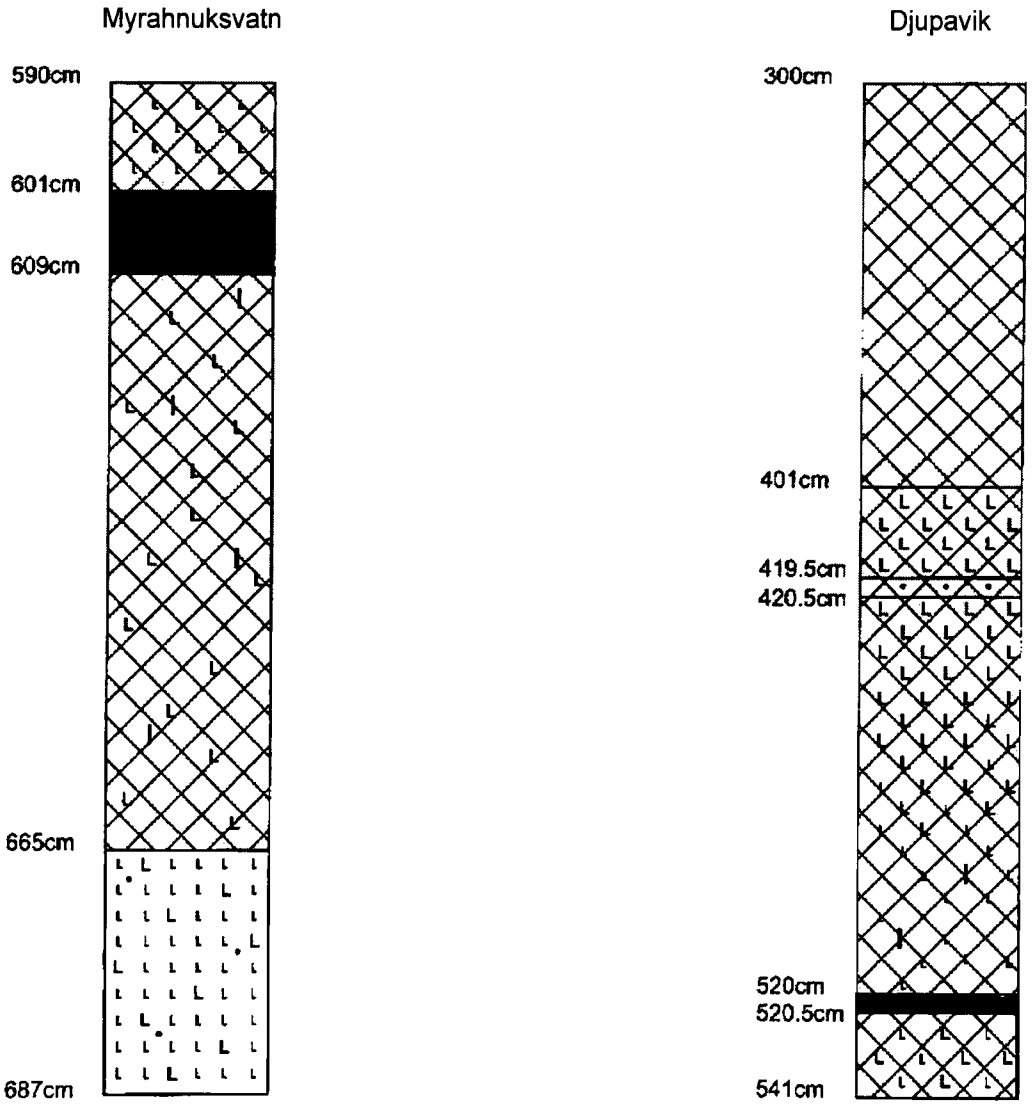

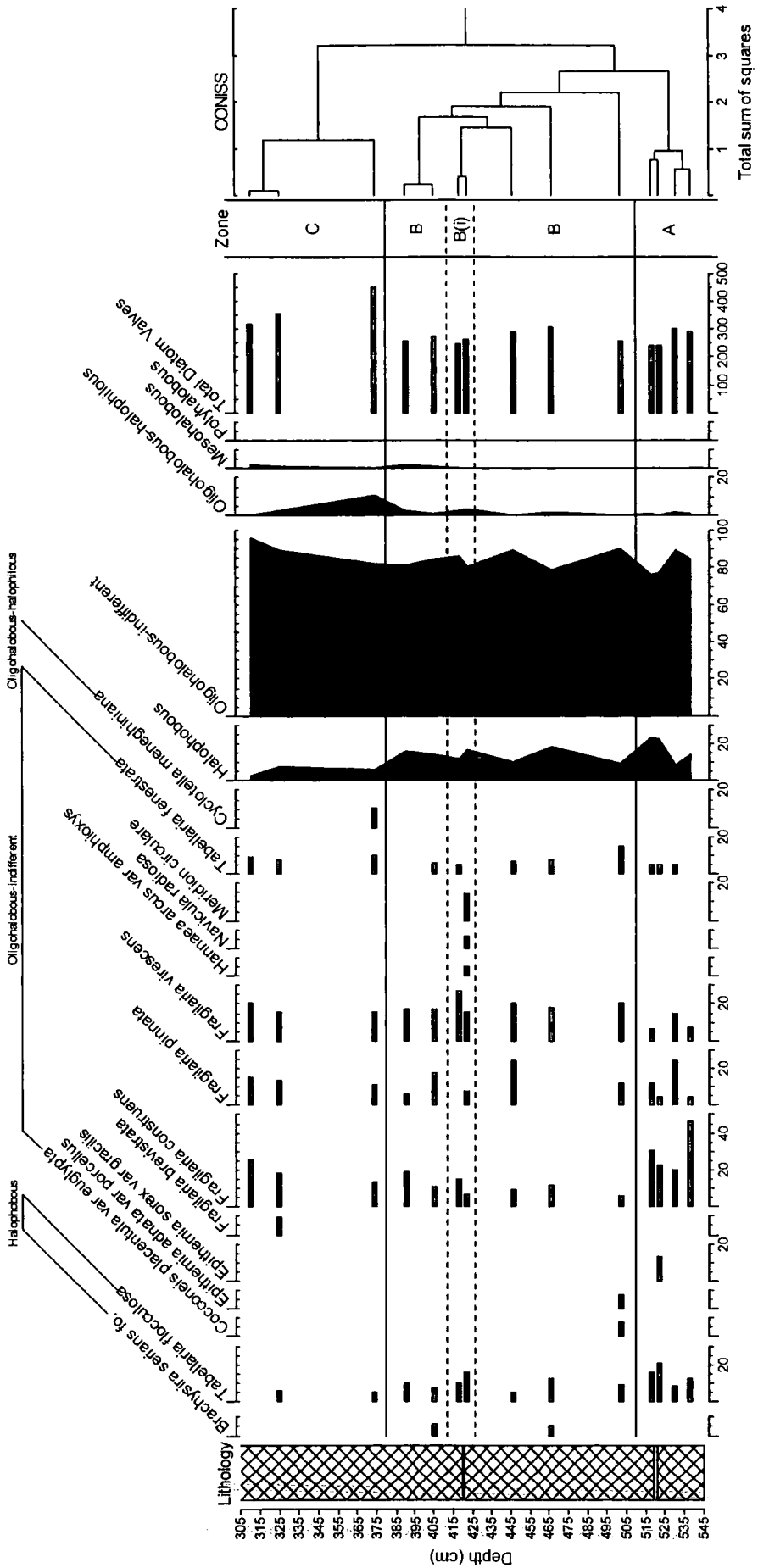

Figure 37 Djupavik diatom assemblage

Figure 38 Djúpavík results

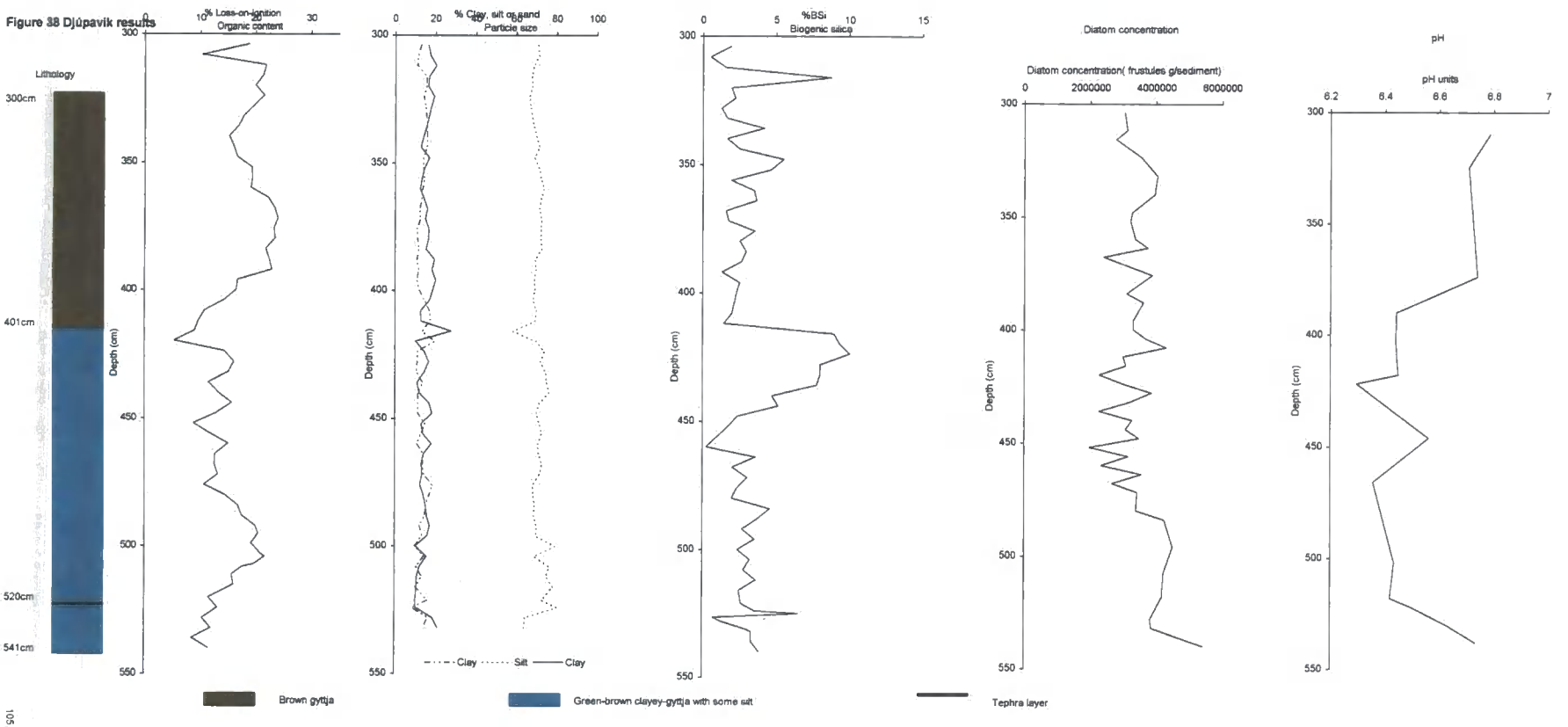

Figure 39 Time-dependent extraction of biogenic silica

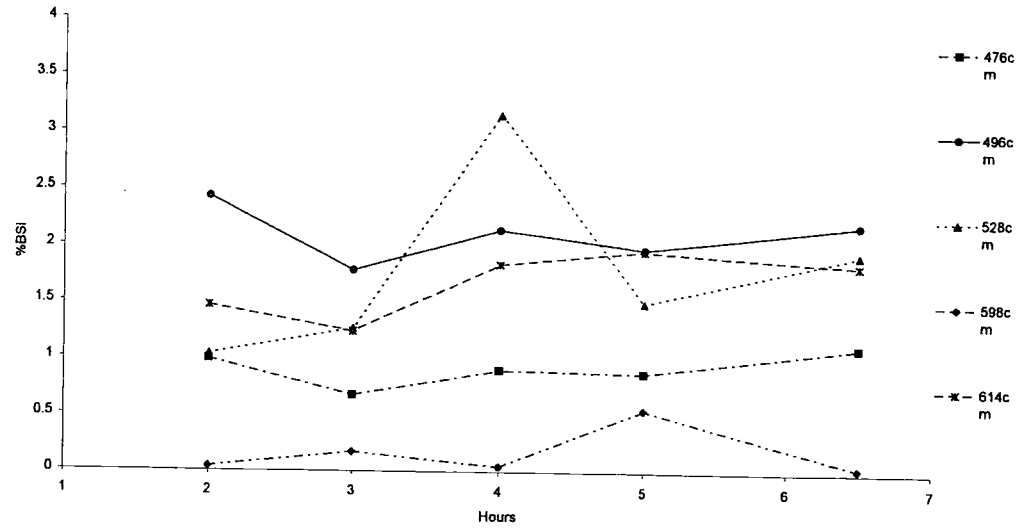

Figure 40 Increase in total silica with samples left over night

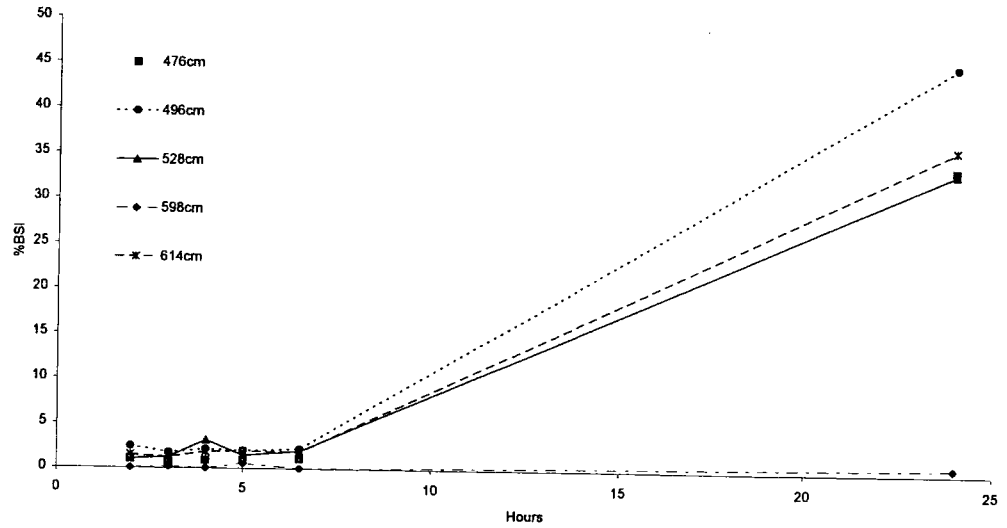

Figure 41 Age-depth model and calculation of date of isolation/basal sediments

Site	Threshold altitude (m)	Depth of Saksunarvatn Ash (cm)	Age-depth model	Depth of Isolation contact (cm)	Isolation/limiting radiocarbon age (^{14}C Ka BP)
Mavatn	1			78	#
Hafrafellvatn	22.7			406	#
Hrishólsvatn	38	409-416	1cm = 22.12yrs	>436	>9.64
Berufjardenvatn	47	351.8-352.8	1cm = 26.08yrs	400	10.43
Hrishóls Bog 1	75	470-475	1cm = 19.37yrs	>550	>10.76
Hrishóls Bog 3	90	280-282	1cm = 32.62yrs	above marine limit	9.46
Mýrahnúksvatn	57	597-608.5	1cm = 14.99yrs	>681.5	>10.3

Age-depth model for Mýrahnúksvatn

Core	Tephra	Tephra radiocarbon age	Tephra depth (cm)	Age-depth model
GJ03-02	Saksunarvatn	9.2 ^{14}C Ka BP	597-608.5	1cm = 15.3yrs between 0cm and 250cm
GJ03-04	Hekla 4	3826±12 ^{14}C Ka BP	250	1cm = 14.99yrs between 250cm and 608.5cm

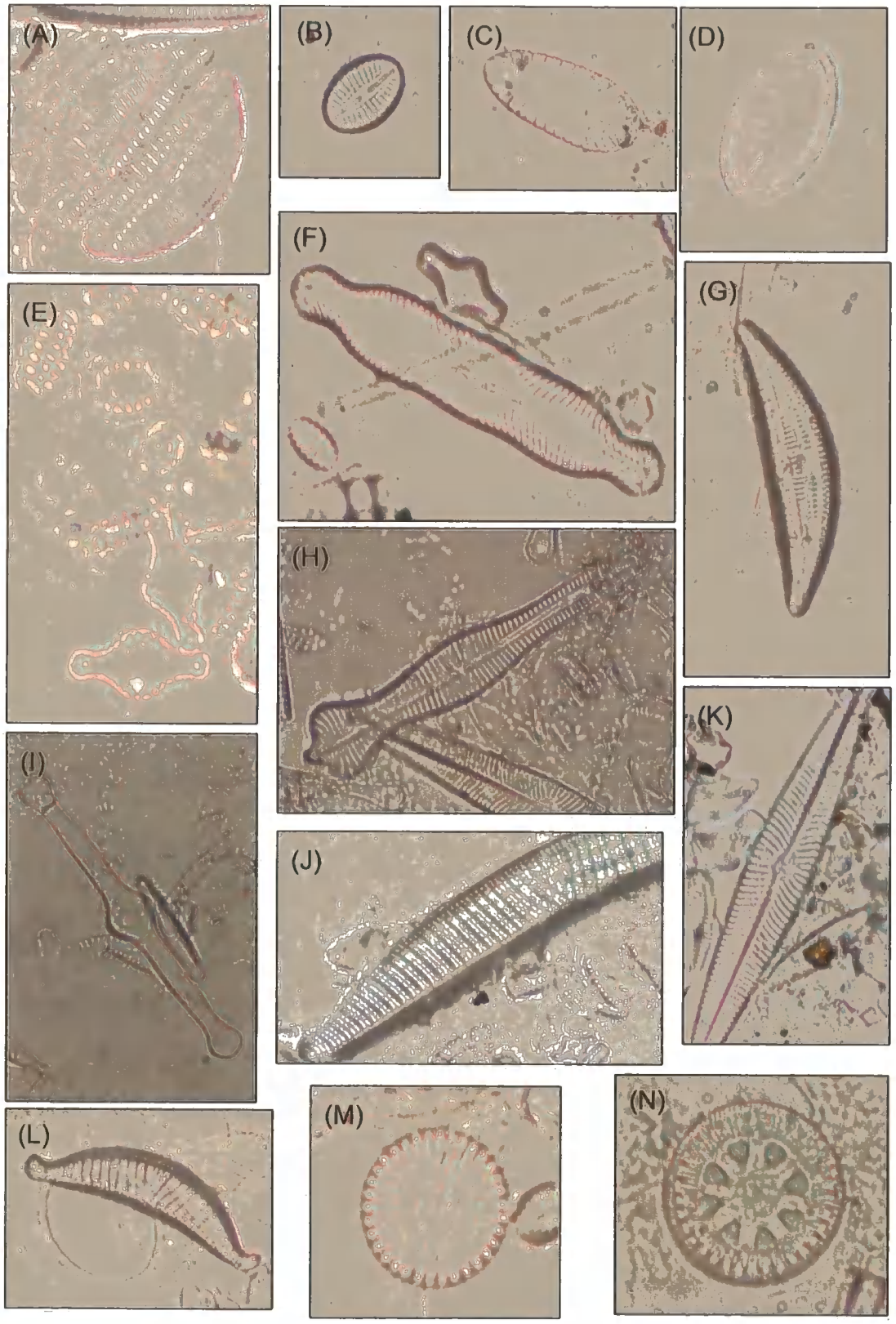

Plate 6 Fresh water diatoms (A) Cymbella caespitosa; (B) Diploneis parma; (C) Surirella brebbisonii; (D) Cocconeis placentula var euglypta; (E) Fragilaria spp; (F) Pinnularia mesolepta; (G) Amphora copulata; (H) Gomphonema acuminatum; (ITabellaria fenestrata; (J) Epithemia adnata var porcellus; (K) Navicula radiosa; (L) Epithemia sorex var gracilis;(M) Cyclotella meneghiniana; (N) Cyclotella antiqua.

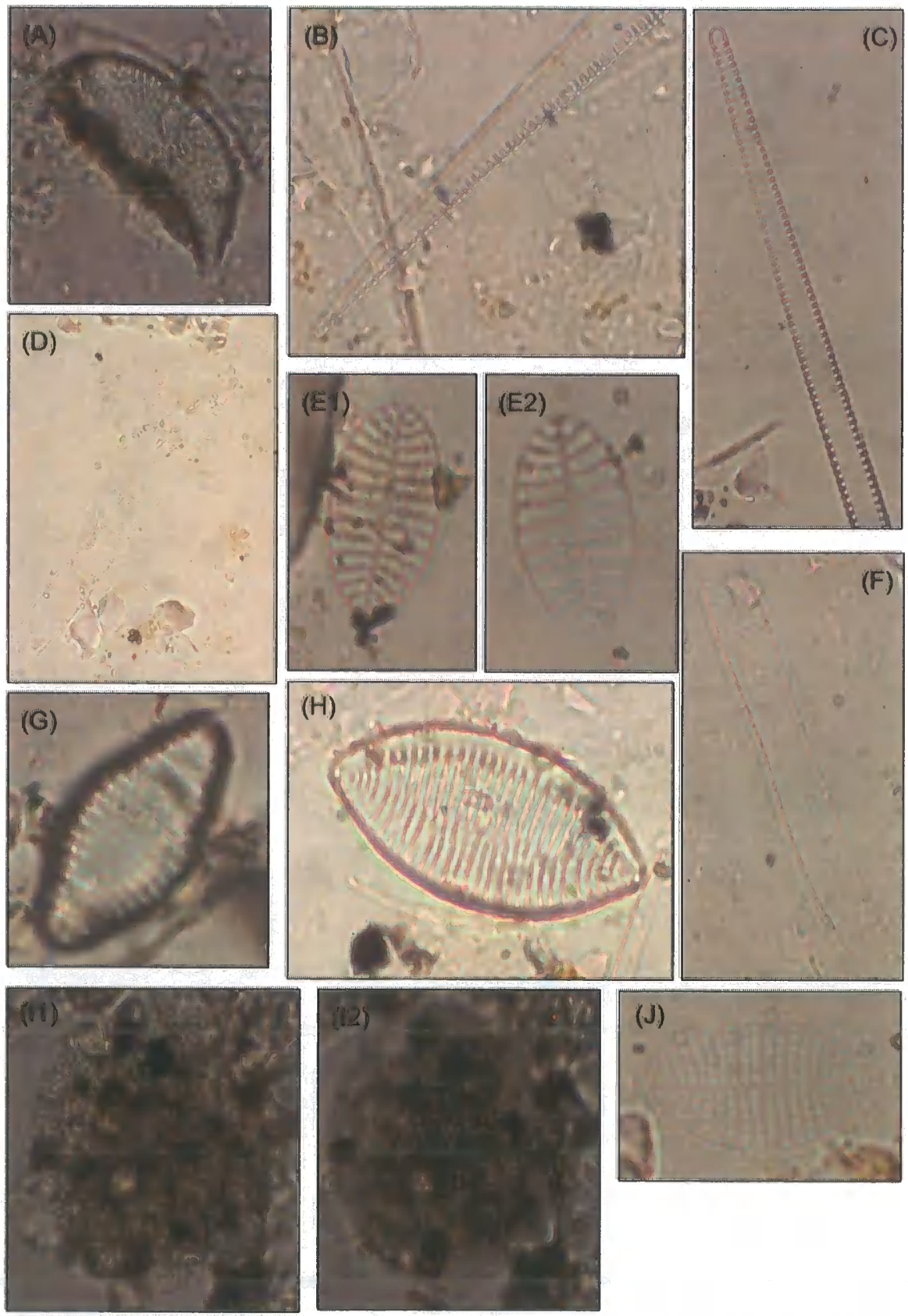

Plate 7 Brackish and Marine diatoms: (A) *Odontella aurita*; (B) *Nitzschia sigma*; (C) *Tabularia fasiculata*; (D) *Ctenophora pulchella*; (E1 & 2) *Cocconeis costata*; (F) *Nitzschia constricta*; (G) *Rhabdonema minutun*; (H) *Tryblionella var salina*; (I1 & 2) *Thallassiosira eccentrica*; (J) *Cocconeis scutellum*.

5.4 Residue Examination of biogenic silica samples from Mýrahnúksvatn

It has been recommended by Conley & Schelske (2001) that any remaining sediment residue left behind after filtering should be examined under a microscope to ensure complete dissolution of all amorphous silica components in the sediments. Six random samples spread across the entire core GJ03-02b were mounted on slides in the same way as described for diatom analysis.

A number of transects (minimum of 5) were completed on each sample and complete dissolution had been achieved on all samples. I am therefore confident that the wet chemical digestion technique and the way it has been applied has effectively removed all amorphous siliceous components of the sediment sample that were derived from diatoms as indicated by there absence. Despite this, the occasional diatom/diatom fragment was observed during residue examination and some features have been noted:

1. Whole diatoms of *Fragilaria brevistrata*, *Fragilariaforma virescen*, and *Tetracyclus emarginatus* were observed. Some small broken pieces of *Synedra ulna var bicepts* and *Tabularia fasiculata* were also present in some samples.

2. Most fragments and whole diatoms showed obvious signs of the affects of digestion by 2M $NaCO_3$ except for one larger, but unidentified diatom (possibly *Navicula radiosa* or a variety of *Nitzschia*) that appeared unaffected with valves still in place.

3. The most numerous diatom remains observed during the examination of BSi sample residues were of a small centric diatom of the *Cyclotella* or *Melosira* genera. The relatively good preservation of the outer wall implies that this is the most heavily silicified part of their anatomy and thus the hardest to remove. However, it was clear that the effects of chemical digestion had been acting on this species and it was impossible to make any firm identification given the removal of any definable features.

4. Finally, random samples 1 and 2 were originally sampled from a thick tephra band towards the top of core GJ03-02b where from previous analysis low diatom abundance was observed. It is therefore not surprising that these samples were found to be completely void of diatoms. Further to this, sample 3 had difficulty going into solution and this may have hampered attempts to examine diatom dissolution from this sample.

As a final remark, dissolution of all diatom derived amorphous silica is possible using the wet chemical digestion technique of (DeMaster 1979) and the way it has been implemented here (Dobbie 1988; after Eggiman et al., 1980). Furthermore, some of the difficulties with the methodology, i.e. the forced use of conical centrifuge tubes to digest samples, do not appear to significantly prevent the full dissolution of amorphous silica from diatom microfossils. Nevertheless, samples being digested in such apparatus should be thoroughly mixed frequently to ensure all sampled sediment is exposed to the digesting agent.

CHAPTER 6

DISCUSSION

6.1 Isolation basin litho-biostratigraphy from southern and northeastern Vestfirðir

6.1.1 Isolation characteristics for basins in NW Iceland

The main aim of this investigation was to apply the isolation basin method for relative sea-level reconstructions in NW Iceland. Currently, there has only been one investigation of this kind in Iceland (e.g. Rundgren et al., 1997) with the majority of RSL reconstructions based on morphological evidence. Isolation basin stratigraphy comprises intercalated clastic and organic sediments that record marine to fresh transitions via a brackish intermediate phase. Clear isolations were traced at three sites (Mavatn, Hafrafellvatn, and Berufjardenvatn) using diatoms and other proxies. Polyhalobous diatoms were systematically replaced by mesohalobous and oligohalobous-indifferent taxa up through the core. In three other basins (Hrishólsvatn, Hrishóls Bog 1, and Mýrahnúksvatn) the basal sediments contained brackish taxa which has been interpreted as the recovery of an incomplete isolation sequence. It is possible that marine sediments were earlier removed or not deposited in the basin or never formed due to influxes of melt water into the basin from wasting ice of the retreating former Icelandic ice sheet.

Isolation basin stratigraphy provides very accurate sea-level index points for the reconstruction of past RSL because the isolation is controlled by a bedrock sill. However, in order to retain this accuracy it is essential that the sample used for bulk or AMS radiocarbon dating is taken from the correct position in the sample core. This is only possible if the sediments contain sufficient organic material. It has been widely assumed that organic sediments begin to accumulate within the basin immediately after it has isolated (Kjemperud 1981). This assumption is based on some perceived changes in the sediment type and supply to a basin after isolation. After isolation marine clastic material is prevented from entering the basin and with a reduced sediment supply, deposition within the basin changes from mainly allochthonous minerogenic deposits to dominantly organic autochthonous sedimentation i.e. the sedimentary isolation contact (Kjemperud 1986). There is evidence that the biostratigraphy of isolation basins correlates with the lithology where the point of isolation does coincide with the onset of organic accumulation thus permitting radiocarbon dating (e.g. Long et al., 1999; Long & Roberts 2002). The data that I have presented here shows that the isolation may sometimes occur earlier than this, within the basal clastic material. Moreover, it will be shown that this problem is particularly acute in basins that isolated earlier indicating that the Pre-Boreal and early Holocene climate of Iceland may be the cause.

In the sample core from Berufjardenvatn diatom analysis records the total cessation of any marine influence within the basal blue-grey clayey-silt at 400cm (Figure 31). The isolation of Mavatn begins at 85cm and ends at 78cm below a gravely lag deposited above blue-grey clay and before 3-4cm before the onset of organic sedimentation (Figure 22). Mýrahnúksvatn isolated just before the core base as indicated by the presence of a brackish depositional environment below fresh sediments but no basal marine section. This isolation is within a blue-grey clay sediment unit, which continues to 665cm where it then gradually changes into a clastic-rich gyttja (Figure 35). Isolation of Hrishóls Bog1 occurred within basal clastic sediments 25cm before the onset of organic accumulation (Figure 33). The final isolation of Hrishólsvatn when mesohalobous diatoms disappear and oligohalobous-indifferent taxa coincides with a change from clastic sediment to organic sediment (Figure 30).

The relationship between isolation and the onset of organic accumulation is not so clear in the Hafrafellvatn sediment record, possibly due to its long isolation sequence. The isolation at 404cm occurs within the basal blue-grey clayey-silt. However, LOI analysis from Hafrafellvatn (Figure 28) clearly shows that the percentage organic content of the sediment begins to increase from 412cm and is approximately 10% LOI at the diatom isolation contact. An increase in LOI is caused by a decrease in minerogenic in wash, combined with increases in lake productivity and the in wash of terrestrial organic matter as vegetation and the catchment develop (Bradshaw et al., 2000). It is unclear what percentage of the total sediment mass is required to be organic to constitute the onset of organic accumulation. Nevertheless, the organic content of the sediments within the Hafrafellvatn sample core at the isolation contact is higher than all of the other cores analysed for LOI (Figures 27, 29, 32 and 36) where the percentage organic content is low for sometime after full isolation.

Mavatn, Berufjardenvatn, Hrishóls Bog1 and Mýrahnúksvatn clearly demonstrate full isolation from the sea occurring before the onset of organic accumulation. The evidence from Hrishólsvatn shows that this basin conforms to the assumption that isolation coincides with the onset of organic accumulation. The diatom isolation of Hafrafellvatn does occur within basal clastic sediments although the LOI profile from this lake begins to rise earlier than is seen from the other sites. This site was a large marsh-lake system and productivity may have been higher than at the other locations. Also, it may be that the LOI profile from Berufjardenvatn is compromised by a change in Russian cores, which coincides with the major stepwise change at 400cm.

Despite similarities with the climate of Greenland after isolation biostratigraphical changes do not appear to coincide with lithological changes in Iceland. Furthermore, this phenomenon is most pronounced in basins of higher altitude and earlier isolations.

Iceland's rapid early deglaciation may mean that when isolation occurred (especially for higher elevated basins) the climate regime in Iceland was cold and harsh. Cold waters have been observed around Iceland during the time period covered by the isolation of basins in this study by Eiríksson et al., 1997). Immature, early post-glacial diatom assemblages dominated by *Fragilaria* spp. are observed at the base of sample cores from Mýrahnúksvatn and Berufjardenvatn, but not Hrishóls Bog1 or Mavatn. It is unclear how accurate comparisons with Greenland may be here. Greenland lies at a higher latitude and experiences cooling generated by the large ice sheet. However, isolation basins from Greenland did not begin to isolate until ca. 10 cal. Ka BP (Long et al., 2003) when the warmth of the Holocene was beginning to be felt. Thus, it is not clear whether isolation of Greenland basins is an analogue for isolation of Icelandic basins during the Pre-Boreal. It may also be the case that the early isolation of Icelandic isolation basins allowed melt water still draining the wasting interior ice caps to have a much greater influence on the early lake sediments representing a new source of clastic material.

The assumption that full isolation coincides with the onset of organic accumulation is an unhelpful term. It poses the problem of at what point should sediments be described as organic and not clastic? And also why they have occurred in the clastic unit? Evidence from this study suggests that for NW Icelandic basins the threshold occurs when the sediments contain 10% organic material or more, although it is most likely that this value will be regional or even site specific. The stratigraphy from a series of isolation basins from NW Iceland indicate that biostratigraphical changes do not necessarily correspond to changes in lithology and dating the isolation should be identified through the analysis of microfossil. The onset of organic accumulation is a helpful marker for guidance for the field collection of sediments but should not be used as a basis for dating the isolation. Some authors prefer to date the base of transitional sediments to avoid the affect of meromictic stratification (e.g. Corner & haugane 1993; Snyder et al., 1997) and this may have reduced the error associated with locating the isolations by from the onset of organic sediment. Also, isolations occurring in clastic material may prove more difficult to radiocarbon date than organic gyttjas higher up the core. The presence of carbonaceous foraminifera may improve the potential for accurate radiocarbon dating. Finally, it is unclear the reasons why some isolations observed in NW Iceland have occurred in the clastic basal unit. They may be a product of a cold, harsh environment immediately after isolation, a result of Iceland being a small island in a cold Atlantic and having deglaciated relatively early, or a consequence of melt water draining into the lake and providing another source of minerogenic material.

Both Mavatn and Hafrafellvatn were sampled for particle size analysis (Figures 25 & 27). It is unusual to see the clay fraction decreasing up through the cores from both site, especially as you would expect slack water within the lake to have lower energy. It is

probable that at both sites the marine environment was the main source of clay into the lake basin and after isolation this source was disconnected. Furthermore, although the decrease in clay in the Hafrafellvatn core occurs shortly after isolation, the pattern within the Mavatn record is of a continually decreasing clay fraction, which levels out after isolation at 75cm. The silt and sand fractions "mirror" each other reflecting dilution of each fraction by the other and vice versa. However, it is also interesting to note that changes in the amount of silt and sand in Mavatn have been changing in opposite directions to corresponding point in the isolation in the Hafrafellvatn record. In the Mavatn core silt decreases up the core during the marine and brackish phase as sand increases. Shortly after isolation the pattern reverses and silt dominates the assemblage. The sand peak at 75cm reflects reworking from the gravely layer deposit at the end of isolation at 78cm. In comparison, the record from Hafrafellvatn indicates increasing silt and decreasing sand up through the core, as would be expected with a change from high to low energy conditions coinciding with isolation. However, the reverse of this pattern, with sand beginning to dominate above 370cm does not appear to have any connection to the isolation process.

The particle size data does not provide conclusive evidence of the isolation of either basin. Patterns between sediment fractions are consistent within cores but not between cores. An increase in silt reflects the post-isolation sediments in Mavatn, while a large increase in sand occurs 15cm after isolation in the Hafrafellvatn record. This is not the first time that high sand fractions have been recorded above isolations in the isolation basin stratigraphy. Tucker (2003) recorded very high levels of sand above the isolation contacts of two basins from western Greenland. This was interpreted as catchment in washing of loose sediment from a recently isolated landscape. In summary, the variation in the particle size data does not shed light on the onset of organic accumulation within the two basins nor do they reflect changes in energy levels within each basin.

6.1.2 Can *Fragilaria* spp. be used as isolation indicators for Icelandic isolation basins?

The isolation of a coastal lake from the sea is often associated with the mass occurrence of *Fragilaria* spp. within the diatom fossil assemblage (e.g. Long & Roberts 2002; Kjemperud 1986). Kjemperud (1981) demonstrated that for isolation basins in Scandinavia the greatest frequency of *Fragilaria* spp. was within those basins that isolated during deglaciation from the Younger Dryas. It is believed that this is in response to influx of melt water from wasting ice of the former Icelandic ice sheet. However, Stabell (1985) and Kjemperud (1986) both showed that the pre-dominance of *Fragilaria* spp. is also a distinctive characteristic of basins that isolated during the Holocene (e.g. Shennan et al., 1994; 1996). Hence, the mass occurrence of *Fragilaria*

spp. may occur in sediments of any chronozone (Stabell 1985). The pre-dominance of *Fragilaria* spp. may occur, after and during the isolation process and are therefore, not considered good isolation indicators (Stabell 1985). It is currently unknown why these small, benthic epipthytic taxa are such good colonizers, with greater competitive advantage over other diatom species during the early post-glacial.

The diatom populations of recently isolated basins, together with basal assemblages from recently deglaciated lakes are dominated by *Fragilaria* spp. to such an extent that it is not seen again within the sediment core. During this early period of a lakes evolution, 2-3 benthic taxa may represent more than 70% of the total diatom assemblage and in some cases more (e.g. Kjemperud 1986). *Fragilaria pinnata* is one of the most common varieties of *Fragilaria* spp. found in recently isolated lakes. *Fragilaria pinnata* is classified as oligohalobous-indifferent (Hustedt 1953); although it's actual salinity tolerance ranges between 32‰ to freshwater (Hargraves & Guillard 1974). Thus, it may be considered that this diatom belongs to the brackish phase of the isolation process (Stabell 1985). However, *Fragilaria pinnata* has also been observed in the early post-glacial lake sediments for sites above the marine limit (e.g. Kjemperud 1981) being abundant because of environmental changes brought about by deglaciation rather than salinity or even temperature (Stabell 1985).

Stabell (1985) proposed that the mass occurrence of *Fragilaria* spp. in both recently deglaciated/isolated lake sediments might be dependent on the nutrient supply into a lake. Stabell (1985) believes that *Fragilaria* spp. are responding to changes in water quality and chemistry brought about by high fluxes of nutrients into the lake system after deglaciation/isolation. Lake waters are known to gradually change from nutrient-rich (i.e. alkaline and eutrophic) to nutrient-poor (acid and oligotrophic) as lakes mature. A pH reconstruction for Mýrahnúksvatn clearly shows a trend from alkaline to more acidic lake waters up through the core (Figure 35). Stabell (1985) considers the main source of excess nutrient supply to be from washings of till and marine clays within the catchment. It would be interesting to see if isolation basins from NW Iceland contained any evidence of high concentrations of *Fragilaria* spp during isolation.

There was no evidence of large numbers of *Fragilaria* spp. occurring in Hrishöls Bog 2 and Hrishöls Bog 3 which are both located close to the local marine limit (Figures 34 and 7 and 8 Appendix). There was also no record of any mass occurrence of *Fragilaria* spp. from Hafrafellvatn (Figure 28). However, the maximum abundance of *Fragilaria pinnata* in this core does occur at the point of full isolation. *Fragilaria* spp. are preset in the sample core for Berufjardenvatn appearing at 406cm and increasing steadily throughout the brackish phase to a peak in the lower "fresh" clastic-rich olive-green gyttja (Figure 31). At this point (398cm) *Fragilaria pinnata* represents more than 90% TDV. The

Mavatn sample core contains abundant *Fragilaria virescens* (>60%) immediately above the isolation contact (Figure 26). However, this small and exposed oligotrophic lake is not productive as indicated by the loss-on-ignition analysis (Figure 27) and this coupled to the poor preservation observed during diatom analysis demonstrates that diatoms within this lake are not "blooming." The assemblage is dominated by *Fragilaria virescen,* but relative to other lakes they are low in numbers. However, *Fragilaria pinnata* does represent ~20% TDV in the uppermost sample, 12cm above the isolation contact (78cm). Hrishölsvatn contains brackish diatoms at its base with *Fragilaria pinnata* peaking at the base of the "fresh" unit and remaining abundant throughout the core (Figure 30). *Fragilaria pinnata* is represent at>40% TDV.

On the northeast coast the basal 30cm of core from Djúpavik record higher frequencies of *Fragilaria* spp. than are found anywhere else within the core. *Fragilaria construens* are most common representing more than 40% TDV and *Fragilaria pinnata* 25% TDV (Figure 33). However, despite *Fragilaria pinnata* being associated with the brackish phase of isolation (Stabell 1985), the presence of the halophobe *Tabellaria flocculosa* is evidence of a fully fresh diatom community by this point.

The pattern of *Fragilaria* spp. is more complicated for Mýrahnúksvatn. The brackish basal clastic unit is void of *Fragilaria* spp. suggesting that conditions in the basin were not favourable for *Fragilaria* spp. to survive. However, immediately above the basal sediments (from 665cm) *Fragilaria construens* consistently account for more than 40% TDV and *Fragilaria pinnata* up to 20% TDV in a clastic-rich fresh water lake gyttja. *Fragilaria* spp. continues to dominate the assemblage up and until 625cm. The base of the core has been estimated from its relation to the Saksunarvatn Ash near the top of the core by a simple age-depth model (Figures 41) giving a basal age of ca. 10.1 cal. Ka BP. Thus, isolation of this basin occurred shortly after the Younger Dryas chronozone. Kjemperud (1981) believed that the largest blooms in *Fragilaria* spp. occurred after deglaciation from the Younger Dryas. The evidence from Mýrahnúksvatn supports this observation.

In summary, significant mass occurrences of *Fragilaria spp.* have been identified in four isolation basins. *Fragilaria* spp. (especially *Fragilaria construens* and *pinnata*) are more abundant in those lakes that isolated earlier. This reflects melt water inputs into the lake due to deglaciation coinciding with isolation. This evidence also agrees with the Stabell (1985) hypothesis where catchment derived nutrients from surface tills and clays result in the pre-dominance of *Fragilaria* spp. during and after the isolation.

6.1.3 Preliminary results of the first use of biogenic silica as a proxy for tracing lake isolation from the sea

This thesis presents the first results of the first application of BSi as a potential proxy to trace basin isolation from the sea. Both Mavatn and Hafrafellvatn were analysed for BSi and, despite large differences in the productivity and length of the isolation sediment sequences from the two cores, there are some broad similarities to be highlighted from the records. It is believed that diatoms comprise the principal component of BSi (Conley 1988), although this depends on the application of the technique and the nature of the sediments being analysed. The point of full isolation in both lakes is immediately followed by large and broad peaks in BSi caused by subtle layers of reworked volcanic glass within both cores evident under examination of the cores.

As was discussed earlier the mass occurrence of *Fragilaria* spp. after isolation is a response to changes in water chemistry, especially an increased nutrient flux into the lake. However, it was shown that the fossil diatom records from Mavatn and Hafrafellvatn did not contain such a bloom in *Fragilaria* spp. The peak in BSi in the Mavatn core is >50% BSi, which is, more than double the peak recorded from Hafrafellvatn. This again is unusual as the small and exposed oligotrophic Lake Mavatn was not believed to be very productive, supported by low catchment productivity indicated by LOI values that do not rise above 15%. On the other hand, Hafrafellvatn is a large marsh-lake depository system with a much larger sedimentation rate inferred from the length of its transition based on the assumption that Iceland's isostatic rebound was very rapid with only small changes in rate. Yet, this basin does not contain significant mass occurrences of diatoms, but other species may contribute to the high levels of BSi.

Furthermore, the marine sediments from Mavatn are very low and consistently flat, which correlates with the sparsely populated basal clastic unit of diatoms observed when conducting diatom analysis. In contrast again, the basal sediments from Hafrafellvatn are low (~3% BSi) but show an increasing trend up to ~ 7% BSi by the top of the core. Both cores from Mavatn and Hafrafellvatn contain reworked tephra in the sediments around the position of the each peak, which can be a possible "contaminant" for the record. Thus, it appears that this reworked tephra is the most likely cause of these peaks given their position, size, and low lake diatom productivity.

6.2 Post-glacial RSL reconstruction for south coast of Vestfirðir

6.2.1 Identification of the marine limit

The marine limit (ML) is the maximum altitude that sea level has reached since the LGM and it forms at the edge of the LGM ice sheet. Observations of the ML in Iceland have so far relied heavily on the interpretation of morphological features e.g. raised beach ridges, and lithological deposits e.g. elevated marine sediments (e.g. Thors & Helgadöttir 1991), which are difficult to date. Hence, the ML is poorly defined spatially and the date of its formation is still unknown (Norðdahl 1990). Also, there is some doubt about the interpretations of some morphological evidence. Horizontal layered strata can produce features similar to raised beaches, thus some of the higher beach ridges may in fact be bedrock features (Lloyd 2004 per. comm.). The analysis of lacustrine sediments from isolation basins provides a means to accurately date the position of sea-level at a given time. Therefore, litho-biostratigraphical evidence from isolation basins can be effective in constraining the altitude and age of the marine limit. As part of this study, a series of coastal lakes were sampled along the south and northeast coast of Vestfirðir. The threshold altitudes of the highest basin containing marine sediments and the lowest basin without marine sediments would allow the altitude of the regional ML to be accurately defined. Furthermore, radiocarbon dating of lacustrine sediments from these lakes will allow the age of the ML to be constrained also.

Figure 43 provides a summary of the current evidence for the ML around Vestfirðir. The position of the estimated LGM ice position has also been annotated to aid discussion. Observations of the ML in Vestfirðir are concentrated into two main areas; to the south around the neck of land joining the peninsula to the mainland; and the West-fjörds, with the exception of Hornstrandir. The marine limit has been identified at varying altitudes around Vestfirðir.

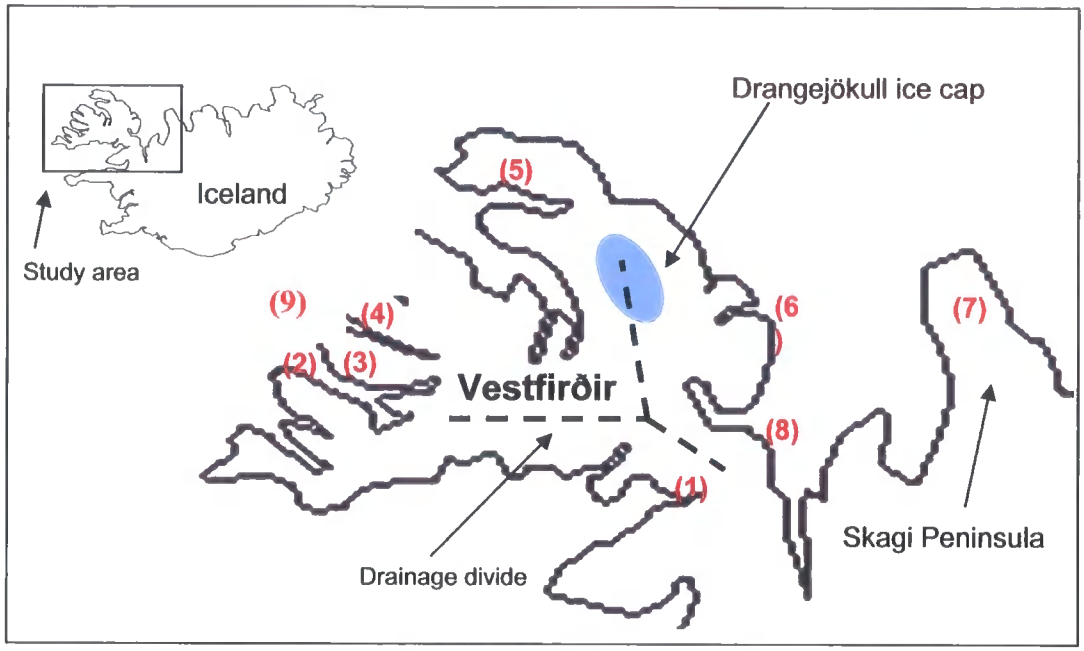

Figure 43 Current known positions of the marine limit in Vestfirðir and NW Iceland

Working anticlockwise Hjört et al., (1985) examined morphological features around Hornstrandir and interpreted the ML to have formed at ca. 26m a.s.l (5). This is the lowest altitude for the ML for the whole of Vestfirðir. In the west, John (1974) identified a marine terrace at ca. 135m a.s.l as the maximum altitude for the ML in Vestfirðir (9). Also in the west, Sigurvinsson (1982) placed the ML in Önundarfjördur at ca. 40-50m a.s.l (2); whereas the ML was interpreted as occurring at ca. 110m a.s.l in Dýrafjördur (3) and at ca. 85m a.s.l in Arnarfjördur (4) by Lárusson (1977). In the southeast, Hansom & Briggs (1991) recorded a ML of ca. 70m a.s.l based on a series of uninterrupted beach ridges at Smahámrar (8). Kjartansson (1968) identified the ML at ca. 80m a.s.l near Gilsfjördur (1). On the northeast coast, around Gjógur, Kjartansson (1968) found the ML to be ca. 70m a.s.l (6). Finally, to the east of Vestfirðir on the Skagi peninsula the ML is thought to be around ca. 65m (7) based on morphological evidence and constrained (to some extent) by isolation basin stratigraphy (Rundgren et al., 1997). The age of these marine limits is rather harder to identify and in some circumstance it has only been estimated speculatively.

Estimated altitudes for the ML in the south, and around the neck of land to the mainland, up to the northeast coast are consistently between 70-80m. These estimations also correlate well with the ML on the Skagi peninsula to the east. However, evidence from the West-fjörds is not so consistent ranging from ca. 40-50m a.s.l to ca, 110m a.s.l. over a relatively short distance. The altitude of the ML depends on the balance between glacio-hydro-isostacy and eustatic sea-level. Thus, a ML of over 100m a.s.l would require a considerably greater ice loading than a ML of just 50m a.s.l. Andrews et al., (2002a) identified the LGM ice position (of the former ice cap across Vestfirðir) at the

mouth of Ísafjardardjúp, and Norðdahl (1990) considered that a theoretical ice cap with an altitude of 400-500m would only extend a few ten's of Km off shore. The estimated ice position during the LGM correlates well with the low ML around Hornstrandir. It therefore, would seam unlikely that a ML of the order of >100m a.s.l would have been achieved in western Vestfirðir. Andrews & Helgadöttir (2003) recently presented evidence for the maximum ice position to the north of Iceland. They identified the LGM ice position to be close to the shelf break and suggested that it was fed by ice streams coalescing from the central west highlands flowing out through the Hunaflói trough between Vestfirðir and Skagi. The ML in the southeast and east of Vestfirðir would be affected by the ice load in Hunaflói, originated from the main Icelandic ice sheet.

The central south coast of Vestfirðir has yet to have its ML defined, either spatially or temporarily and so this thesis reports the first evidence for the ML in this area. Berufjardenvatn was the highest lake cored to contain basal marine sediments. The altitude of the controlling sill for this lake was 47m +/- 1.3m a.s.l. Thus, the ML must be above ca. 47m. To "top-out" the RSL curve and provide a "ceiling" to the local ML altitude, a series of smaller sites were cored near Hrishólsvatn. Three sites (Hrishóls Bog 1,2, and 3) had well defined rock sills at ca. 75m +/- 1.3m, 90m +/- 1.3m, and 100m +/- 1.3m a.s.l, respectively. The base of each site was sampled for diatom analysis and the results can be seen in Figures 33 and 34 and 6-8 in the Appendix. Hrishóls Bog's 2 and 3 contained only oligohalobous-indifferent diatoms at the base indicative of a fresh depositional environment and have never been inundated by the sea.

Hrishóls Bog 1 (ca. 75m +/- 1.3mm a.s.l) contained significant proportions of the mesohalobous taxa *Tryblionella levidensis var salina* in the basal sediment sample, a species that lives towards the "fresh-end" of the salinity spectrum for its classification. The diatom, *Surirella brebissonii* (fresh-brackish) was also abundant in significant amounts drawing correlations with Lake Torfadalsvatn (Skagi peninsula), which also contained this taxa. The presence of brackish taxa within Hrishóls Bog 1 implies that this basin was close to sea-level when organic sediments began to accumulate in the basin. The core was "bottomed-out" onto impenetrable substrate and thus, a full isolation sequence is not expected from this site. It is therefore possible that sea level must have been at or close to ca. 75m +/- 1.3m a.s.l, perhaps even slightly higher at the date of the base of this core, ca. 10.8 cal. Ka BP. This interpretation correlates well with the position of the local ML that was estimated to be ca. 80m a.s.l by Kjartansson (1968) for Gilsfjördur. However, it was not possible to trace changes in the composition of the diatom assemblage in the overlying 25cm of core, which were devoid of diatoms. This is not unexpected as "barren" zones void of diatoms were reported in many cores from the Skagi RSL record by Rundgren et al., (1997). Rundgren et al., (1997) interpreted barren periods above brackish zones as reflecting sea-level transgression where harsh marine

environmental conditions prevented the growth and preservation of diatoms. In the context of this record, a single sample containing brackish diatoms near the base of the core is sufficient evidence to imply proximity to local relative sea-level.

There is an argument that assumes a higher ML in the Reykholár area, which would explain the lack of a marine signal at the base of Hrishóls Bogs 2, & 3. There are a number of possibilities, but two main scenarios will be considered: (1) Marine sediments were removed by melt water, flushing through the fluvial system that networks the three sites, or that the basins were to poorly formed to act as depositories of sediment; and (2) That only Hrishóls Bog 1 was below the marine limit.

If these three sites were below the local ML then there may be alternative reasons why they have failed to accumulate marine sediments. The most obvious reason for this is that the basins were too shallow and poorly defined to act as depositories of marine sediments. Hrishóls Bog's 2 and 3 have core depths of just 290cm and 295cm each, respectively. Hrishóls Bog 1, on the other hand has a core depth of almost 5.5m and the argument that these basins were too shallow to accumulate marine sediments cannot be applied to this basin. An alternative reason why these three sites may not have been able to accumulate marine sediments may be that there relatively shallow depths (especially Hrishóls Bog's 2 and 3) meant that they were permanently frozen to the base or that ice from the surrounding area, and yet to melt, remained in these shallow basins when they were close to or slightly below sea-level.

Norðdahl (pers. Comm.) believes that the three sites are all part of the same fluvial network and although semi-isolated, they may well have been affected in the past by melt water draining down from the Hrishólsháls. All cores were "bottomed-out" onto impenetrable substrate which may represent a gravel lag left behind by the flushing of melt water and associated sediments through each site. Radiocarbon dating of the basal sediments would be able to determine whether these sites experienced melt water flushing and removal of *in situ* marine sediments during the early post-glacial period, or whether these basins were always above the local ML and never accumulated marine sediments.

The final scenario is that Hrishóls Bog's 2 and 3 were above the marine limit and never accumulated marine sediments. Both sites have fresh diatom assemblages to base, which fits well with the expectation of a local ML at ca. 70-80m a.s.l. It is most likely that Hrishóls Bog 1 began to accumulate organic sediments when sea-level was close to the altitude of its threshold, with some connection during the tidal cycle. Sea spray is an unlikely source of the brackish diatoms within this core since an assemblage affected directly by wind-blown diatoms would also contain polyhalobous taxa. It is also unlikely

that sea-spray would be sufficient to alter the lake water chemistry in any significant way given the volumes involved relative to precipitation, overland flows etc. The presence of brackish taxa usually indicates the circulation of marine water in and out of the lake for some period during the full tidal cycle with fresh water occupying the photic zone (Shennan et al., 1994). Since *Tryblionella levidensis var salina* prefers waters only weakly saline in nature any influence of the sea must have been limited.

In summary, the ML for the central south area of Vestfirðir lies above ca. 47m +/- 1.3m a.s.l, the height of the highest basin with basal marine sediments. There is no evidence from the diatom fossil records of Hrishóls Bog's 2 and 3 for any brackish or marine sediment above ca. 90m +/- 1.3m a.s.l. At ca. 75m +/- 1.3m a.s.l, Hrishóls Bog 1 contains a weak brackish signal near its base suggesting that this basin was close to sea-level when organic sediments began to accumulate around 12.8 cal. Ka BP. This basal date and limit on the timing of deglaciation/isolation correlate remarkably well with the 12.7 cal. Ka BP date given by Andrews & Helgadöttir (2003) for the deglaciation to the northeast Vestfirðir coast of the former Icelandic ice sheet. It has been shown that the origin of basal sediments of all three Hrishóls Bog's may have been disturbed during early isolation/deglaciation, which is supported by an (estimated) anomalously young date from Hrishóls Bog 3 of 10.7 cal. Ka BP. However, Hrishóls Bog 1 is least likely to have been affected by these problems and it is believed that the basal sediments were deposited in situ. Thus, the ML for central south Vestfirðir has been constrained between ca. 75m +/- 1.3m and ca. 90m +/- 1.3m a.s.l.

6.2.2 Relative sea-level reconstruction

It was possible to trace the isolation from the sea using a combination of litho-bio-chemostratigraphy of five basins on the south coast of Vestfirðir. At three sites polyhalobous diatoms were replaced by mesohalobous, oligohalobous-halophilous taxa and then oligohalobous-indifferent taxa in turn, reflecting the changing lake environment from marine to fresh water via a short brackish phase. Interestingly, transitions were completed within the basal clastic units, conflicting with the general assumption that the on set of organic accumulation represents the timing of deglaciation. Two other sites had mesohalobous and oligohalobous-halophilous diatom assemblages at the base. These have been interpreted earlier as indicative of a brackish depositional environment. The date of isolation will be determined from an age-depth model based on the analysis and identification of numerous tephra deposits found in cores from all but two of the sites listed above (Figure 41). A preliminary relative sea-level curve for the south coast of Vestfirðir will be reconstructed using this information and discussed in the context of other RSL data from southeast Vestfirðir and the nearby Skagi peninsula.

Isolation contacts were identified primarily through diatom analysis, but also supported by loss-on-ignition, sodium concentration, particle size, and for the first time biogenic silica. Clear isolations were found in sample cores from Mavatn, Hafrafellvatn, and Berufjardenvatn (Figures 26-29 & 31-32) providing an excellent range in altitudinal from 3m +/- 1.3m m, through 22.7m +/- 1.3m, to 47m +/- 1.3m a.s.l, respectively. The only other RSL reconstruction for Vestfirðir conducted by Hansom & Briggs (1991) lacked detail in the "earlier" sections of the record, being better constrained in the middle-late Holocene. Unfortunately, tephra deposits were not found in both Mavatn and Hafrafellvatn making dating of these sites difficult.

Three other lakes contained a weak brackish signal at the core base. Sample cores from Hrishólsvatn, Hrishóls Bog 1, and Mýrahnúksvatn all recorded a significant abundance of mesohalobous taxa in the basal sediments, which have been interpreted as representing the uppermost section of a brackish transitional unit. In the case of Hrishóls Bog 1 and Mýrahnúksvatn only a single mesohalobous taxa was identified i.e. *Tryblionella levidensis*. *Tryblionella levidensis* is a mesohalobous taxa but prefers to live towards the "fresher" end of the brackish spectrum (Zong pers. comm.) and thus would be expected to be present towards the top of transitional sediments (as it is in Hafrafellvatn where the isolation is well constrained biostratigraphically). Although, this mesohlaobous taxa was found in an assemblage that also contained significant numbers of salt-tolerant oligohalobous-halophilous taxa including *Amphora ovalis var libyca, Cymbella ventricosa* and *Diploneis parma*.A basal date from these basins would be limiting on the timing of isolation. Figure 41 summarise the inferred basal ages from all cores as determined from the age-depth model based on tephra deposits.

A summary of the RSL evidence from each basin and the presence of tephra layers used to infer core chronologies have been presented in Figures 42 and 43. Chronologies refer to the age-depth model discussed in "Results" and limitations of this method are found in "Conclusions." A preliminary sea-level curve has been reconstructed in Figure 45. Ages have been converted into calendar years (Stuiver & Reimer 1993) and threshold elevations relate to MHWST. Given the inaccuracy and unreliability method of dating those basins without the Saksunarvatn Ash it was felt appropriate to attach a sufficiently large age error range of +/- 1000 years

Hrishóls Bog 1 (ca. 75m +/- 1.3m a.s.l) gave a mean basal date to 2 standard deviations of 12.8 cal. Ka BP that is in good correlation with known patterns of deglaciation. Andrews & Helgadöttir (2003) presented evidence that the Icelandic ice sheet had retreated back to the Vestfirðir coastline by 12.7Ka BP. Unfortunately, the age of the ML in the central southern area of Vestfirðir remains uncertain since the basal date from Hrishóls Bog 3 was erroneously young at ca. 10.7 cal. Ka BP. It is not known whether

this relatively young date has been caused by a simple age-depth model coupled to very low sedimentation rates or a product of the removal of basal sediments by melt water.

The reconstruction of RSL falls rapidly from ca. 75m +/- 1.3m at 12.8 cal. Ka BP to below 22.7m +/- 1.3m after 10.4 cal. Ka BP. This section of the curve is well constrained by four points, two of which contain marine sediments, and all but the lowest site, the Saksunarvatn Ash from which chronology was calculated. There is evidence therefore, of a rapid regression of sea-level from ca. 75m +/- 1.3m to <22.7m +/- 1.3m a.s.l in 2.4 cal. Ka BP. Based on the assumption that the global eustatic sea-level curve produced by Fairbanks (1989) is accurate, southern Vestfirðir experienced a total of ~100.4m isostatic rebound between the start of deglaciation after the Younger Dryas and the early Pre-Boreal. This corresponds to an average rate of isostatic uplift of 4cm yr^{-1}. Ingolfsson et al., (1995) calculated a rate of isostatic uplift for southwestern Iceland of 6.9cm.^{14}C yr-1 for a RSL fall of at least 45m in the period 10.3-9.4 BP. Rundgren et al., (1997) recorded a total isostatic rebound of ca. 75m +/- 1.3m between 11.3 and 9.1 Ka BP for the Skagi peninsula. They recorded maximum uplift rates of ca. 11-12cm. cal. yr^{-1} between 9.7 and 9.1 cal Ka BP and mean absolute uplift rates of ca. 3cm. cal. yr^{-1}.

This reconstruction of RSL for southern Vestfirðir is limited by few sea-level points during the period between the Pre-Boreal and the Holocene. It is not possible to evaluate changes in sea-level during this period with the evidence generated from this study. I have assumed that the lowest lake in my series, Mavatn (ca. 3.1m a.s.l) must have isolated relatively recently i.e. last few thousand years. It has not been possible to identify whether sea-level regressed present sea-level at around 9.4 ^{14}C Ka BP as has been identified in southeast Vestfirðir (Hansom & Briggs 1991), at Seltjarnes, near Reykjavík (Ingólfsson et al., 1995) and by RSL data from Skagi (Rundgren et al., 1997). The resolution of our data is insufficient to corroborate reports of two transgressions of sea-level caused by a Younger Dryas and late Pre-Boreal readvances as inferred from the Skagi RSL reconstruction (Rundgren et al., 1997). In fact, the evidence at our disposal suggests that deglaciation occurred after the Younger Dryas with rapid marine regression below ca. 22.7m +/- 1.3m a.s.l before 10 000 cal. BP. Based on the data presented here these reversals seam unlikely, as we would have expected to see evidence in the cores for transgressions and regressions other than the basal regressions already mentioned.

The Hansom & Briggs RSL reconstruction for SE Vestfirðir has been reproduced in Figure 44. Figure 40 contains all RSL data for southern Vestfirðir. It is clear from our record that a much lesser rate of RSL change occurred throughout the early phase of isostatic rebound. Moreover, it is difficult to identify whether RSL ever fell below the position of present sea-level. There is evidence of submerged peat deposits off the

coast of western Iceland suggesting that sea-level fell below present around ca. 9.4 cal. Ka BP. There is also evidence of transgressions of sea-level to approximately -20 to -40m below present along the southeast and northeast coasts of Iceland (e.g.Thors & Boulton 1991; Thors & Helgadóttir 1991). However, these interpretations do not fit well with the evidence presented here, where RSL fell below 22.7m after 9.2 ^{14}C Ka BP (Sakaunarvatn Ash) and therefore unlikely to have continued to fall below present until after this. Rapid isostatic rebound at this rate implies a heavy glacial-isostatic loading coupled to a weak lithosphere. Since, lithological properties should be constant under the whole of Iceland, the slower rate of isostatic rebound suggested by our new RSL record for Vestfirðir implies much less glaciation over the Vestfirðir peninsula. This supports the hypothesis that a smaller and independent ice-cap persisted over Vestfirðir during the late Weichselian. Implications from this evidence are that much less melt water would be expected to have originated from Iceland during deglaciation that could have contributed to turning off the THC of the North Atlantic in the past.

Finally, Figure 40 shows the form of RSL curve for southern Vestfirðir after using all the note dated positions of sea-level. Both elevation of basin and age are well covered by the spread of sea-level index points. The forms of the curve requires more attention but it does appear that sea-level regressed rapidly at first before falling at a diminishing rate to present sea-level. There does not appear to be any regression below present sea-level or transgressions in the record.

Figure 42 Relative Sea-level data

Core	Age (Calendar Yr BP (1σ)		Age error (+/- Yr BP (1σ))	Min Sill Altitude (m)	Reference water level	Indicative Meaning	Altitude Error (+/- m)	Indicative Error (+/-m)	RSL (m a.s.l)	RSL error (+/-m)
	Range	Average								
Mavatn		Not applicable		3	MHWST-HAT	2	0.9	0.4	1	1.3
Hafrafellsvatn		Not applicable		24.7	MHWST-HAT	2	0.9	0.4	22.7	1.3
Hrisholsvatn	10750-10980	10865	105	40	MHWST-HAT	2	0.9	0.4	38	1.3
Berufjardenvatn	12060-12690	12375	315	49	MHWST-HAT	2	0.9	0.4	47	1.3
Hrishols Bog 1	12625-13000	12813	187	77	MHWST-HAT	2	0.9	0.4	75	1.3
Myrahnuksvatn	10440-9800	10120	320	59	MHWST-HAT	2	0.9	0.4	57	1.3

Blank Page

Figure 44 RSL reconstruction for southern Vestfirðir

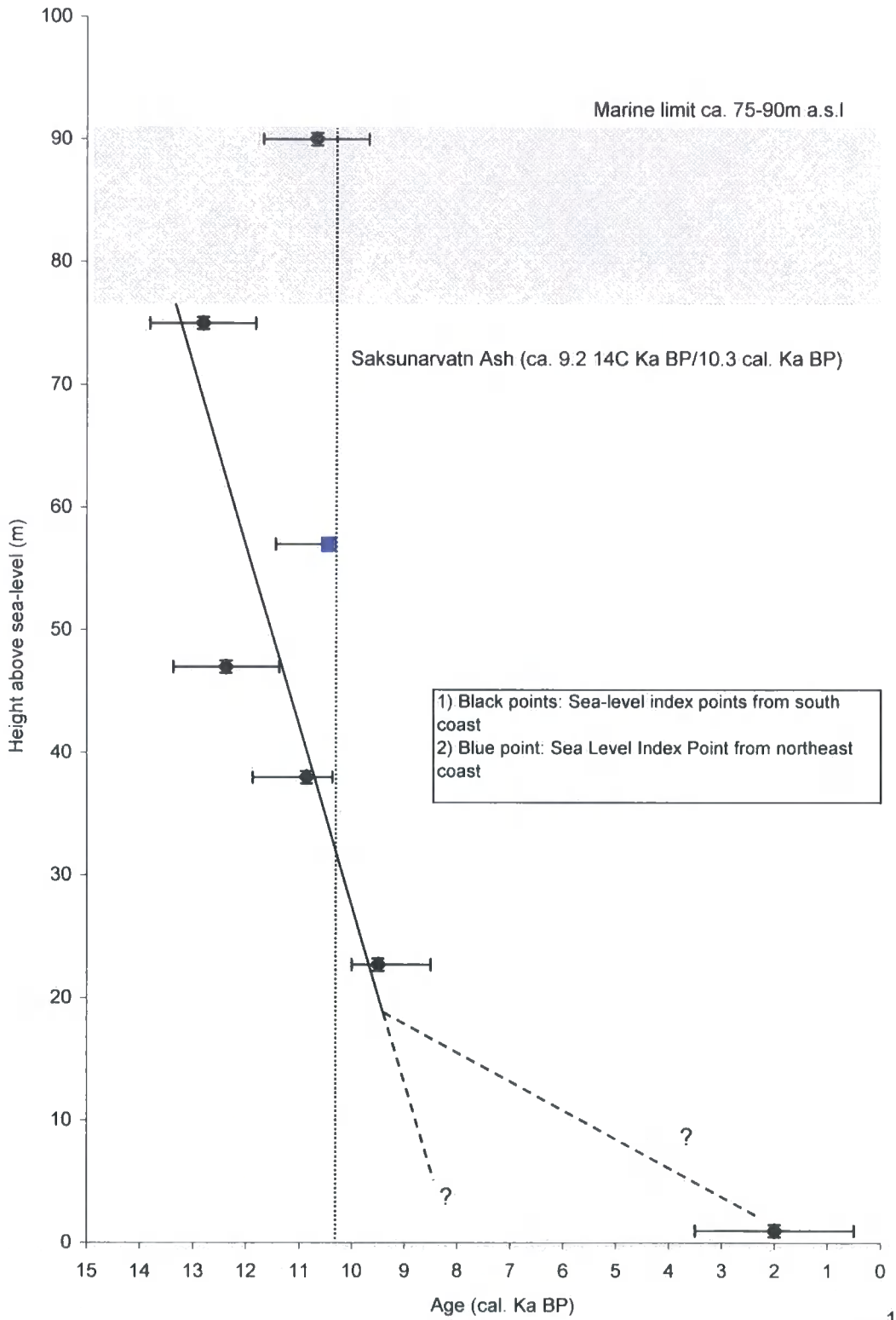

Figure 45 RSL reconstruction from SE Vestfirdir (Hanson & Briggs 1991)

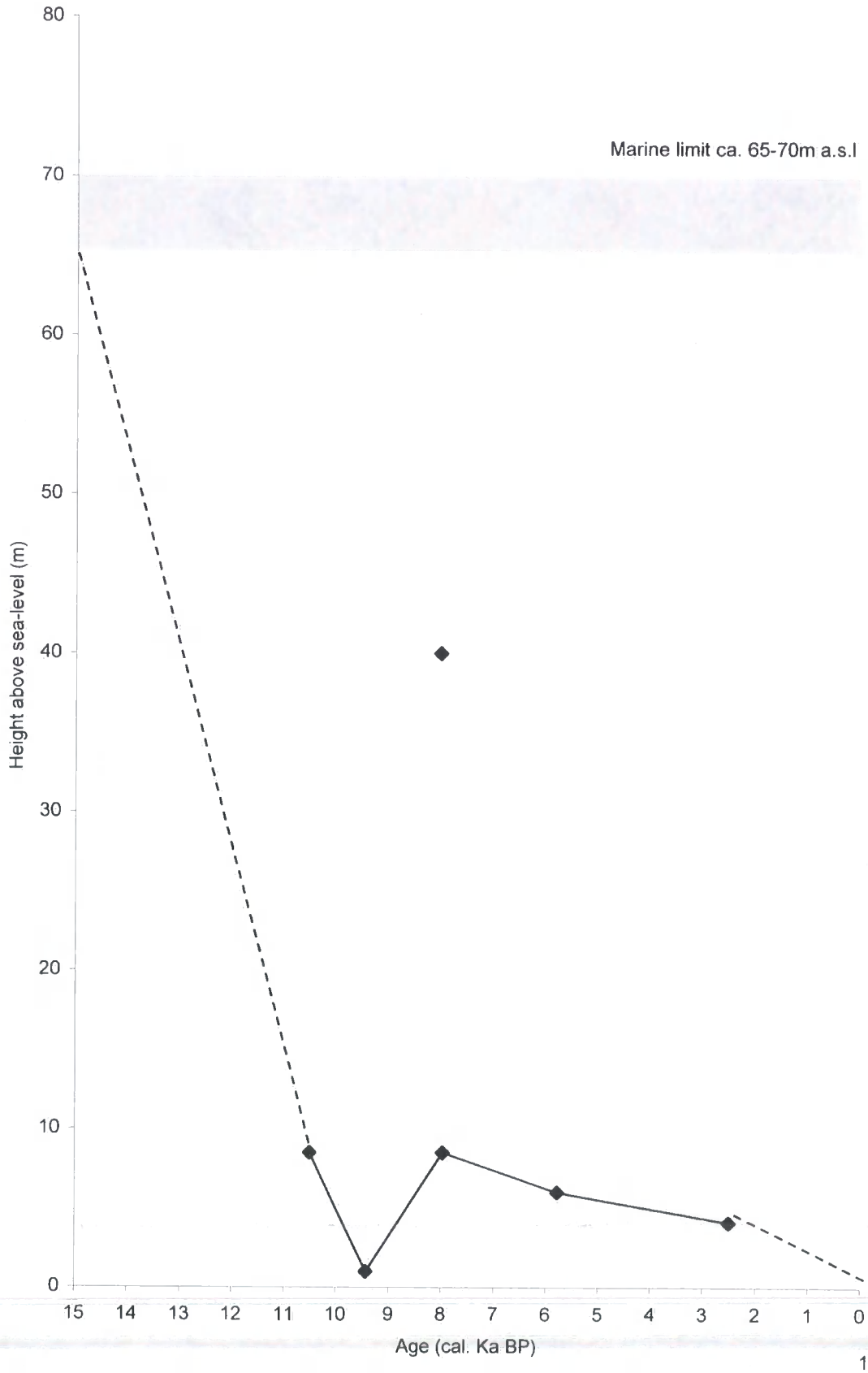

Figure 46 All sea-level index points for south and southeast Vestfirdir

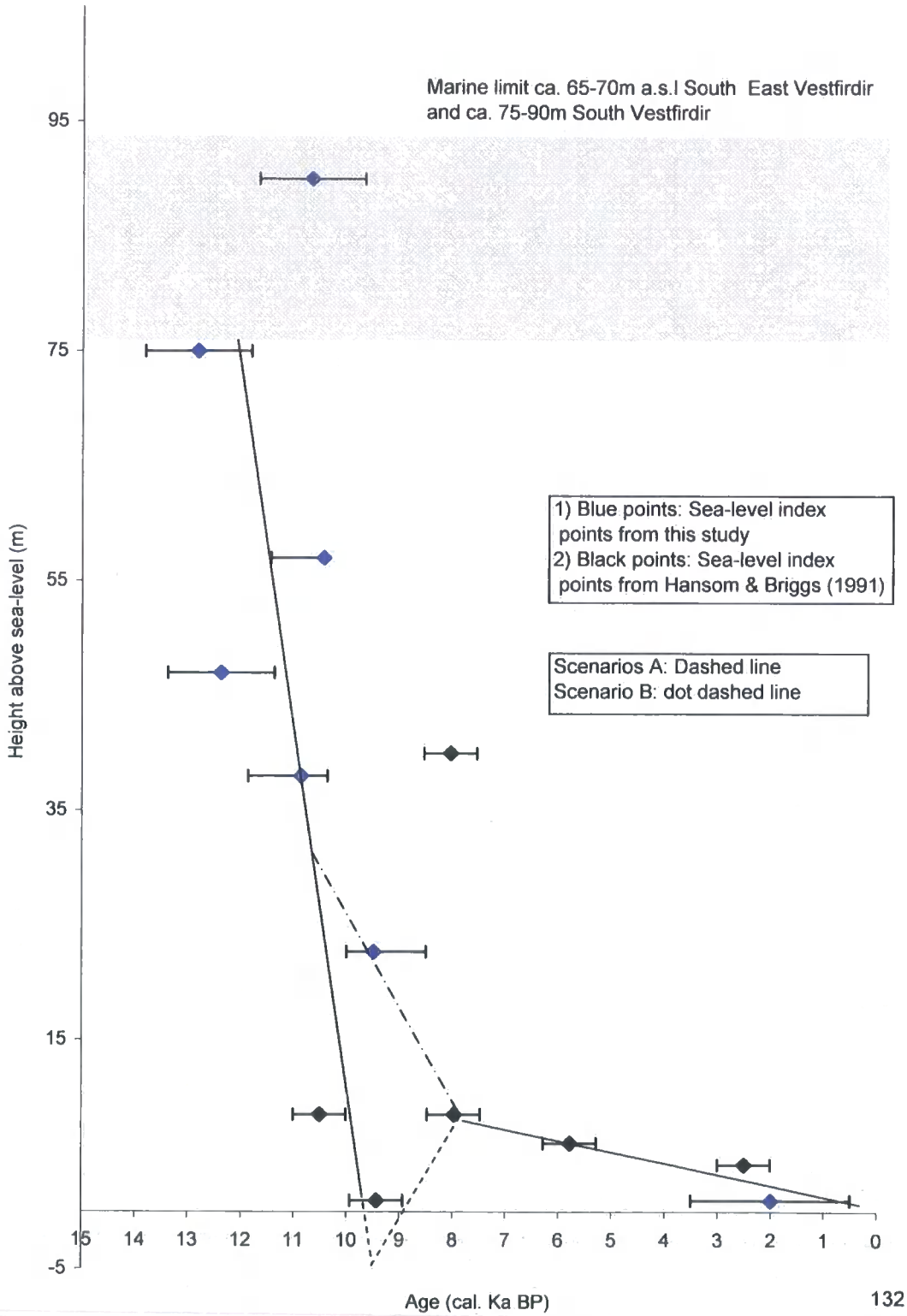

Environmental changes in Vestfirðir during the early-middle Holocene

6.3.1 Distribution of the Saksunarvatn Ash

The Saksunarvatn Ash was first observed by Mangerud et al., (1986) on the Faeroe Islands and dated to 9.2 ^{14}C Ka BP. This widely distributed chronological marker has also been observed in shelf cores off the northeast coast of Vestfirðir by Andrews et al., (2002). The Saksunarvatn Ash has been correlated with the Skógar tephra in Iceland by Norðdahl & Hafliðason (1992) as well as the Hælavik tephra identified by Hjört et al., (1985) in Hornstrandir.

The Saksunarvatn Ash has been observed in the lacustrine stratigraphy of 4 basins on the south Vestfirðir coast, and at one further site in the northeast. The ash deposit was also discovered in the lower Djúpavik site but it was only possible to sample using a gouge corer. The occurrence of this tephra at the base of the Djúpavik core, and again at the top of the sample core taken from Mýrahnúksvatn allows a much longer composite record of environmental change in Vestfirðir to be reconstructed. The thickest deposit of ~12cm was found at Mýrahnúksvatn. The distribution of this tephra from the northeast to the south coast of Vestfirðir within fresh water deposits indicates that these basins had isolated before 9.2 ^{14}C Ka BP. Furthermore, it shows that the former ice cap covering Vestfirðir during the late Weichselian had retreated back to the coast well before this date.

6.3.2 Evidence for the "8.2" event and climate change

Alley et al., (1997) presented evidence from the Greenland ice cores for a significant climate event that occurred in the North Atlantic between 8-8.4 cal. Ka BP. The magnitude of this event was approximately half the amplitude of the Younger Dryas and it had many similar characteristics. I have investigated the influence of the 8.2kyr event on Iceland based on a multiproxy study of sediments from a core taken from the lower basin near Djúpavik, on the northeast coast of Vestfirðir. It was expected that a cooling event of this kind may be reflected in the litho-bio-chemostratigraphy of lake sediments and high resolution records of diatoms, LOI, particle size, diatom abundance and BSi were conducted. The Saksunarvatn Ash provided an excellent reference chronological marker above which any signs of the "8.2" event would be expected. A summary of the results can be viewed in Figure 34.

There is no clear evidence of the "8.2" event in the diatom, diatom abundance, particle size, or pH reconstructions for Djúpavik. Thomas et al., (2004) presented high resolution chemical analysis of the 8.2 Kyr event from the GRIP ice core. It was

revealed that the most significant cooling was confined to a five year period with the entire event lasting just a few decades. It is possible that the 4cm resolution was insufficient to record this very short lived event. Alternatively, the climate of Iceland may have still been relatively cold during the late Pre-Boreal and early Holocene period and thus, the cooling caused by the "8.2" event may not have had as great an impact as it has been observed elsewhere. Perhaps any 8.2Kyr event is diluted by the influence of melt water and cold conditions experienced by NW Iceland at this time (e.g. Rundgren et al., 1995). Data from the LOI is not so straight forward. The percentage of organic sediment within the lake continues to increase up from the core base continuing the trend seen in the Mýrahnúksvatn core. However, shortly after 505cm depth (ca. 8.22 cal. Ka BP) LOI decreases rapidly to around 10% and continues to oscillate around that amount for the following 1.5 cal. Ka BP before increasing again. LOI is a measure of organic productivity within the lake and catchment. Organic deposition peaks around the timing of the "8.2" event before remaining low for a significant period after. It is possible that this pattern of changing LOI represents the washing into the lake of dead or dying organic matter from the catchment as climate deteriorated during the "8.2" event, followed by a period of low lake and catchment productivity brought on by the cooler climate. Further work is require to identify the "8.2" event in Iceland.

6.3.4 Evaluation of biogenic silica as an environmental proxy for Iceland

Biogenic silica (BSi) is the chemical determination of amorphous silica. It is believed that diatoms are the principal component of amorphous silica in lake environments and the measurement of BSi reflects diatom palaeo-productivity (Conley 1998). Productivity in this case is a measure of both the size and number of diatom taxa from a particularly diatom community. BSi has been used recently as part, of multiproxy studies as a method to identify regional climate change (e.g. Qui et al., 1993; Itkonen et al., 1999). A record of changes in BSi for the early Holocene was constructed and evaluated to find out whether it reflected known climatic changes for that period. Analysis was conducted following the wet alkaline digestion technique of Dobbie (1988), after Eggimann et al., (1980) and results can be seen in Figures 38, 39 & 40). Between 7.5 and 6.6 cal. Ka BP there is a wide isolated peak in BSi suggesting greater diatom productivity within this period (Figure 38). Interestingly, Itkonen (1999) also recorded high BSi values reflecting high diatom productivity between ca. 8-6 cal. Ka BP. However, the shape of this peak in BSi does not reflect the pattern of temperature change associated with the climatic optimum (Dahl-Jenson et al., 1998). A small peak in BSi towards the base correlates well with a thin layer of unidentified "mixed" tephra (Newton 2004 per. comm.) and following on from discussion made earlier, it is most likely that the concentration of background reworked tephra is more highly concentrated within the core at the time of the broad BSi peak.

Flower (1993) suggests that due to technique and natural uncertainties concerning the chemical determination of BSi, results should be calibrated against a second, alternative method. A duplicating run of a selection of samples was tested for BSi using the time-dependent method of DeMaster (1979) developed further by Conley & Schelske (2001). A summary of results can be seen in Figure 40. Values of BSi are consistent between the two methodologies suggesting that results are accurate. It was observed that leaving samples in the digestion solution after the digestion time had expired would result in an overestimation of BSi where the sample has been contaminated by non-organic silica. For all future BSi analysis, digestion and filtering must occur on the same day.

There are large differences between the amount of BSi recorded from Mýrahnúksvatn and Djúpavik implying that Mýrahnúksvatn has a much higher diatom productivity. Diatoms respond to many different environmental variables and it has been difficult to establish strong direct links with climate. Nevertheless, many of these variable that diatoms do respond to are controlled by climate e.g. Duration of the ice-pan, light availability, length of growing season, turbidity etc. Thus one would expect the BSi record to correlate well with that of diatom concentration if climate was the principal forcing mechanism for changes (Figure 38). It is therefore evident given the clear lack of any correlation between BSi and diatom concentration, as well as organic content, that this difference does not indicate that there has been any significant shift in climate. In fact, the lack of a clear pattern of BSi reflecting known changes in climate for the North Atlantic region implies that a climate signal may not be present within the BSi record. This may be because large errors associated with the technique (+/- 10%) are far greater than any potential climate induced changes in BSi, or that the diatom populations in these lakes are responding to changes in other non-climate related parameters e.g. nutrient availability, or contamination by volcanic glass (Conley & Schelske 1993).

Tephra was directly sampled from the Mýrahnúksvatn core and tested for BSi. The Saksunarvatn Ash is represented by a sharp trough followed by a peak in the BSi record. If this technique was able to differentiate between amorphous silica and inorganic forms minimal BSi was expected to be recorded here (this result was surprising for minimum values had been observed on the first round of BSi analysis which have not been used because the samples were left for too long before filtering and produced spurious results). However, this only would result in all silica being dissolved and under these conditions the tephra samples produced the lowest values). The values of BSi from this tephra are consistently above those values for BSi throughout the Djúpavik core where tephra was not present in significant deposits. Furthermore, it was discussed earlier that

mixed tephra layers within the cores from Mavatn and Hafrafellvatn coincided with peaks in BSi. It is therefore, concluded that amorphous silica derived from volcanic glass (otherwise known as deposits of tephra) can not be differentiated from actual BSi by the wet chemical digestion technique. With this in mind and the amount of background tephra within Icelandic lake systems, a climate record would be difficult to justify. Hence, BSi is not a practical environmental proxy for the investigation of climate change in Iceland where significant amounts of background tephra and frequent volcanic eruptions have contaminated the record.

CHAPTER 7

CONCLUSIONS AND EVALUATION

7.1 Conclusions

This thesis set out to rigorously test the application of isolation basin stratigraphy in NW Iceland as a means to reconstruct past RSL. RSL research in Iceland has been limited by a dependence on evidence from morphological features related to sea-level. There are concerns regarding the interpretation of many of these features (e.g. raised beach ridges) and they are often difficult to date accurately. If the methodology to reconstruct past RSL from the litho-biostratigraphic analysis of isolation basins can be successfully implemented in Iceland, there is the possibility to develop for the first time an accurate reconstruction of RSL that is well constrained in both time and space.

Only one other study using isolation basin stratigraphy and previously been conducted in Iceland. Rundgren et al., (1997) analysed the litho-biostratigraphy of a series of coastal rock basins on the Skagi peninsula. However, this investigation was hampered by poor marine diatom preservation and short transitional units coupled to very clastic sediments making identification of the isolation contact and radiocarbon dating difficult. It was from Lake Torfadalsvatn on the Skagi peninsula that Björck et al., (1992) presented the first biological record for Iceland dating from the end of the late Weichselian. The second intention of this thesis was exploit isolation basin sediments by a multi-proxy approach to record a high-resolution record of changes in climate and the environment for NW Iceland.

Full isolation sequences were traced principally by using diatoms microfossils, which was then supported by a number of other proxies (LOI, particle size, BSi, and sodium concentration) for three basins: Mavatn, Hafrafellvatn, and Berufjardenvatn. The basal sediments of three other basins (Hrishólsvatn, Hrishóls Bog 1, and Mýráhnuksvatn) were distinctly brackish in nature and have been interpreted as having been deposited during the latter stages of basin isolation. It is most likely that these three basins were connected to the sea in the past and the basal sediments record the end of isolation. The diatoms observed in these basins appear to show changes in assemblage brough about by changes in basin salinity. Furthermore, there are similarities with the biostratigraphy and chemostratigraphy of those other basins from this study where the isolation has been identified in greater detail.

Finally, diatom analysis was conducted across the basal sediments of sample cores from both Hrishóls Bog 2 and 3 and found that there bases were dominated by oligohalobous-indifferent taxa. These two basins have fresh diatoms to base and have been interpreted as having always been above the local marine limit.

Reports of the ML in Vestfirðir range from ca. 135m in the West-Fjörds (John 1974) to just ca. 26m a.s.l at Horstrandir in the very north (Hjort et al., 1985). The marine limit is

a key feature for the unresolved debate concerning the relative size of the former Icelandic ice sheet and whether Vestfirðir had an independent glaciation, since it is believed that the ML forms at the edge of the maximum ice sheet. To the east of my study location Kjartansson (1968) had observed the marine limit at ca. 80m a.s.l around Gilsfjördur (Figure 43). The highest lake cored that contained a full isolation sedimentary sequence was Berufjardenvatn at 47m +/- 1.7m a.s.l. At 75m +/- 1.3m a.s.l Hrishóls Bog 1 contain some brackish diatoms to base suggesting it was very close to sea-level when organic sediments began to accumulate. Above this basin at ca. 90m +/- 1.3m a.s.l and ca. 100m +/- 1.3m a.s.l the two other Hrishóls Bogs contained no evidence that they were ever inundated by the sea. Thus, there is strong biostratigraphical data supported by other chemical and physical proxies that the ML stood between ca. 47m +/- 1.3m a.s.l and ca. 90m +/- 1.3m a.s.l and was most likely very close to the altitude of the threshold from Hrishóls Bog 1 at ca. 75m +/- 1.3m a.s.l. This interpretation fits well with the known position of the ML for the study area. An estimated basal date of ca. 10.7 cal. Ka BP implies that the ML formed during the Younger Dryas chronozone.

Six sea-level index points were obtained from the stratigraphy of six isolation basins for the south coast and dated by reference to the Saksunarvatn Ash using a simple age-depth model (Figures 41). The reconstructed RSL is illustrated in Figure 45, as is the RSL from SE Vestfirðir constructed by Hansom & Briggs (1991) in Figure 46. Figure 47 shows all sea-level index points for southern Vestfirðir. The RSL curve reconstructed here must be considered an approximate of the actual form given the uncertainties encountered with the dating of isolation contacts (see Limitations). However, the form of the curve is constrained by the position of the Saksunarvatn Ash above the isolation in four cores. Also, where the Saksunarvatn Ash was not observed within the stratigraphy it has been assumed that it must have been deposited beneath the base of the core i.e. before isolation.

The pattern of RSL shows a rapid regression from approximately 75m +/- 1.3m a.s.l to below 22.7m +/- 1.3m a.s.l after 9.2 ^{14}C Ka BP (10.3 cal. Ka BP). The RSL reconstruction presented here is well constrained during the late Weichselian and Pre-Boreal chronozones but not during the early to middle Holocene period due to a lack of basins at these elevations. However, the form off the RSL curve in Figure 44 does not correlate well with the believed regression below present sea-level, which is thought to have occurred around 9.4 ^{14}C BP (e.g. Hansom & Briggs 1991; Ingólffson et al., 1995). Reconstructed RSL from central south Vestfirðir was at ca. 22.7m +/- 1.3m shortly after the eruption of the Saksunarvatn Ash, which contradicts earlier RSL reconstructions based on morphological evidence. There is also no evidence in the RSL record of the two minor transgressions of RSL reported by Rundgren et al., (1997) to have been

caused by glacier readvances during the Younger Dryas and Pre-Boreal. The greater productivity and diatom preservation of the lakes in this study compared to those on Skagi make it unlikely that these transgressions were simply not recorded. The cause of the occurrence of two minor transgressions on Skagi may not have occurred in Vestfirðir supporting an argument for independent glaciation and subsequent isostatic rebound in the area. It is also possible that they are mis-interpretations from the Skagi lake sediments.

RSL dropped at a rate of 4.6cm yr^{-1} between 12.8 cal. Ka BP and 10.3 cal. Ka BP assuming the position of eustatic sea-level from Fairbanks (1989). This isostatic uplift rate is lower than the maximum uplift rates of 11-12cm yr-1 described by Rundgren et al (1997) for the same period and the 6.9cm yr-1 reported for SW Iceland by Ingólffson et al., (1995) and correspond to a mean isostatic land uplift of ~98m.

At a number of site investigated here, especially those basins that isolated relatively early, the biostratigraphical and lithostratigraphical boundaries did not always coincide. The evidence presented here that the isolation contact can occur in the clastic basal sediments has implications for how we interpret the common assumption that the onset of organic accumulation represents the point of full basin isolation from the sea. Iceland deglaciated relatively early (there is evidence of ice retreat to the north coast of Vestfirðir by 12.7 cal. Ka BP (Andrew & Helgadöttir 2003)) and it may be that the cold and harsh climatic environment during the early Pre-Boreal (e.g. Rundgren 1995) prevented autochthonous productivity and organic deposition. It is possible that melt water from local wasting ice masses may have acted as the new source of clastic material when the basin finally isolated from the sea and the marine source was prohibited by the lake's sill.

The reasons for isolation within clastic sedimentation are yet to be resolved especially since it is not a common occurrence in Greenland where conditions are thought to have been similar during isolation. Nevertheless, Greenland deglaciated after 10 cal. Ka BP (e.g. Long et al 2003) and the Holocene climate may have encouraged organic sedimentation. LOI analysis has clearly illustrated the lag between isolation and onset of organic accumulation within some of the study sites. A low organic content of the sediment during the isolation contacts may pose problems for radiocarbon dating and thus may reduce the accuracy of the isolation basin methodology in Iceland. However, it may be possible to locate calcareous foraminifera in these sediments, which would improve the potential for radiocarbon dating.

The second part of this thesis was aimed at improving the records of climate and environmental change in NW Iceland. A multi-proxy approach was aimed at identifying any evidence of the 8.2Kyr event in Iceland as well as other known climate phenomenon

of the Holocene including the climatic optimum and the Neoglacial. Unfortunately, no record of these phenomena was found despite sampling at 4cm resolutions. With high-insight a more targeted approach rather than comprehensive sampling strategy may have been more appropriate. Recent evidence suggests that the duration of the 8.2Kyr event was of the order of a few decades (Dahl-Jenson et al., 1998) and sampling at 4cm provided a resolution for this study of only 60-80years.

In three cores, representing both the south and the northeast coast the mass occurrence of *Fragilaria* spp. was observed within the sedimentary record close to and during the isolation phase. This phenomenon was most pronounced in those isolation basins that isolated earlier i.e. Berufjardenvatn at ca. 47m +/- 1.3m a.s.l and ca. 12.4 cal. Ka BP and Mýrahnúksvatn ca. 57m +/- 1.3m a.s.l and ca. 10.1 cal. Ka BP. The development of *Fragilaria pinnata* in Berufjardenvatn (Figure 31) and Mýrahnúksvatn (Figure 35) reflects the effects of meltwater from the wasting former ice sheet draining into this basin early after isolation. Low productivity in the oligotrophic Mýrahnúksvatn lake emphasized by the immature diatom assemblage typical of early post-glacial environments, may also have been a factor. Therefore, there is evidence in the biostratigraphic record from this site of cold harsh environmental conditions around 10 cal. Ka BP. This interpretation fits well with the pH reconstruction which shows that the early Pre-Boreal was characterised by oligtrophic alkaline lakes which, gradually became more acidic into the early Holocene. This reflects the stabilisation of soils and the colonization by vegetation of a recently isolated landscape where humic acid production and the prevention by vegetation of base-cations from reaching the lake would result in the lake becoming increasingly acidic.

The Saksunarvatn Ash was observed in four cores from both the south and northeast coasts of Vestfirðir. On the northeast coast it has been used as a stratigraphical marker to correlate the Djúpavik and Mýráhnuksvatn cores in order to reveal a much longer environmental record. The presence of the Saksunarvatn Ash indicates that the study sites were deglaciated prior to 9.2 ^{14}C Ka BP (ca. 10.3 cal. Ka BP) and the occurrence of the ash in clastic-rich gyttja demonstrates that the Pre-Boreal in Iceland had a cool climate. This study has presented evidence of one of the major North Atlantic chronological markers in NW Iceland where chronologies of event can be correlated with marine, ice core and terrestrial sites from far a field.

Biogenic silica is a measure of amorphous silica derived principally from organic sources. It is believed that BSi represents palaeo-productivity primarily of diatoms (Conley 1998). This thesis presents the first use of BSi as a method for tracing the isolation of a basin from the sea. BSi was also used to record a climate record for the Pre-Boreal to early Holocene period in NW Iceland. Unfortunately, despite difficulties and significant error

margins with the methodology the large amounts of background tephra in Iceland appear to have contaminated the record. No evidence of any known climate phenomenon during the Holocene was observed in the record. The coincidence of layers of reworked tephra in Mavatn and Hafrafellvatn show that the wet chemical digestion technique cannot differentiate between organic biogenic silica and inorganic volcanic glass. There are a number of possibilities why BSi failed to act as an environmental proxy reflecting the changes in the more robust LOI results. Firstly, Iceland's frequent volcanism may have raised "background" levels of silica to a level that any climate signal was destroyed. Secondly, direct links between climate and diatom populations have been difficult to establish and the theory behind BSi assumes that there are links. It is possible that no links exist or that diatom populations have responded primarily to non-climate forcing variables. Finally, it is also possible, but most unlikely of the three, that Iceland did not experience the same climate phenomenon during the Holocene as the rest of the North Atlantic.

7.1 Limitations

7.2.1 Problems encountered in the field, and with diatom analysis

Attempts to core to contemporary isolation basins were prohibited by a course gravely lag immediately below the lakes sediment surface. Furthermore, thick tephra deposits and the highly clastic nature of the lake sediment made coring to depth difficult. On three occasions only the upper brackish phase of the isolation was recorded despite coring deep into blue-grey basal clays and silt. Longer cores from Mýráhnuksvatn, Hrishólsvatn and Hrishóls Bog 1 may reveal full isolation sediment sequences. The preservation of diatoms from marine sediments was particularly poor and lower diatom counts were often made. This feature of Icelandic isolation basins is also recorded by Rundgren et al (1997). Furthermore, the marine diatom assemblage from Mavatn is dominated by the polyhalobous and planktonic *Thallasiosira eccentrica*. *Thallassiosira eccentrica* does demonstrate a strong connection to the sea but is considered a "deep-water contaminant" containing no detailed knowledge of the littoral environment before isolation being established from this analysis.

7.2.2 Simplicity of chronology used to infer timing of lake isolations

The lack of accurate radiocarbon dating is possibly the largest limitation on this study. The age-depth model operates under the assumption that in each basin there has always been constant rates of sedimentation and that no compaction of the sediment has ever occurred. This of course, in reality, is most unlikely and is the biggest source of error on the RSL reconstruction. Spatially, the altitudes of each basin were accurately measured in the field and carefully related to mean sea-level. The age-depth model

may have been improved if more identifiable tephra layers other than the Saksunarvatn Ash had been observed in the cores. Other tephra layers tended to be unhelpful mixed deposits or one of the numerous and unidentifiable eruptions from the Katla volcanic complex. However, for the purposes of this study it has been possible to broadly constrain RSL in time and space. The major drawback here was the lack of any tephra deposit from two isolation basins, Mavatn and Hafrafellvatn. However, assuming that these two basins also accumulated the Saksunarvatn Ash, the lack of this tephra unit must mean that it pre-dates the basal sediments within each lake allowing us to draw boundaries for the RSL curve. Tephra layers can be very obvious within the core profiles but it is essential and good practice to follow the checks of Boygle (1999) in order to clarify whether the deposit has been deposited *in situ* or whether it represents a reworking of sediment.

7.2.3 Problems with the methodology for biogenic silica

It is assumed that BSi represents biological amorphous silica of which, diatoms are the principal component in mid-high latitudes. However, it is known that diatom communities may respond to non-climate related variables and not record a climate signal. It is also difficult to account for changes in diatom communities where species with larger frustules will contain a greater amount of silica. Furthermore, diatoms undergo large changes in size during the reproductive cycles, which is another consideration yet to be address appropriately. Another assumption made in the analysis of BSi is that diatoms dissolve into solution at a faster rate than more silicified organisms. Examination of the residues left behind after filtering from some samples did show that this process had successfully dissolved all the diatoms present. However, it is difficult to determine this until samples have been digested and duplications should be made when the parameters for digestion are better known.

It is advised that cornicle shaped centrifuge tubes are not used during the preparation of BSi samples because they concentrate sediment at the base prohibiting the digestion solution from acting on all the sample. This was unavoidable in this study, although attempts were made to continually mix the samples. It is also essential that very pure water is used throughout and that no glass wear or aluminium apparatus is used. BSi is a very labour intensive and time consuming method of analysis and the resolution conducted (4cm intervals) may not have been sufficient to identify the 8.2Kyr event.

7.3 Implications and future research

This project has clearly shown that isolation basin stratigraphy can be applied to Iceland to reconstruct past RSL. This study has presented evidence of the position of the

marine limit along the southern coast of Vestfirðir, as well as establishing that sea-level was close to ca. ~60m at 10 cal. Ka BP along the northeast coast. This information should help in the reconstruction of deglacial histories for NW Iceland. Probably the most significant implication of this investigation is that RSL in southern Vestfirðir did not fall beneath present any time before 9.2 ^{14}C Ka BP. Thus, it is apparent that the glacial loading on Vestfirðir during the LGM may not have been as extensive as previously believed. This research filters into the entire "small mainland ice sheet and separate Vestfirðir ice cap verses extensive continuous glaciation of Iceland to the shelf break" debate. It is important to estimate the size of the former Icelandic ice sheet in order to evaluate the likely impact that its deglaciation may or may not have had on the THC. Iceland lies in a critical location in the northern North Atlantic Ocean close to the positions of maximum NADW formation Greenland-Iceland-Norwegian Seas. It may not require as much melt water from such close proximity to have an effect on the operational mode of the THC.

It has also been established that isolations in NW Iceland may and do occur below the onset of organic sedimentation within basal clastic units. This may pose problems for conventional radiocarbon dating and stresses the importance to recover complete sediment sequences to improve age-depth models by tephrochronology. The Saksunarvatn Ash has been established within the sedimentary profiles of lakes on both the northeast and south Vestfirðir coast allowing future correlations to be made within the North Atlantic region.

List of references

Alexander, K. (2003) A detailed study of the transitional unit sediments of a series of isolation basins from the west-Fjords of Iceland using biostratigraphical and lithostratigraphical analysis techniques (unpublished B.S.c dissertation).

Alley et al., (1997) Holocene climate instability: A prominent, widespread event 8200 yr. ago, Geology 25 P. 483-486.

Anderson, N. J. (2000) Diatoms, temperature and climate change, European Journal of Phycology, 35 P. 307-314.

Andrews, J.T. & Helgadóttir, G. (2003) Late Quaternary ice cap extent and deglaciation, Húnaflóaál, NW Iceland: Evidence from marine cores, Arctic, Antarctic, Alpine Research 35 (2) P. 218-232.

Andrews, J.T; Á; Hardardöttir, J; Krisjánsdóttir, G.B; Gronvold, K; & Stoner, J. S. (2003) A high-resolution Holocene sediment record from Húnaflóaáll, N Iceland margin: Century- to Millennial-scale variability since the Vedde tephra, Holocene 13 (5) P. 625-638.

Andrews, J.T; Hardardöttir, J; Geirdóttir, Á; Helgadöttir, G. (2002a) Late Quaternary ice extent and glacial history from the Djupass trough, off Vestfirdir peninsula, north-west Iceland: A stacked 36 cal Ky environmental record, Polar Research 21 P. 2311-2326.

Andrews, J.T; Geirdóttir, Á; Hardardöttir, J; Principato, S; Gronvold, K; Krisjánsdóttir, G.B; Helgadöttir, G; Dexler, J; & Sveinbjörnsdóttir, A.E. (2002b) Distribution, sediment magnetism and geochemistry of the Saksunarvatn (10180+/-60 cal. Yr BP) tephra in marine, lake, and terrestrial sediments, northwest Iceland, Journal of Quaternary Science 17 P. 731-746.

Andrews, J.T; Hardardöttir, J; Helgadöttir, G; Jennings, A.E; Geirsdöttir; Sveinbjórnsdöttir, E; Krisjánsdóttir, G.B; Smith, L.M; & Syvitski, P.M. (2000a) The North and West Iceland Shelf: Insight into ice extent and deglaciation based on Acoustic stratigraphy and basal radiocarbon AMS dates, Quaternary Science Reviews 19 P. 619-631.

Battarbee. R.W. (1986) Diatom analysis, In: Berglund, B.E. (eds) Handbook of Holocene Paleoecology and Palaeohydrology, John Wiley.

Battarbee, R.W. (1973b) A new method for estimating absolute microfossil numbers with special reference to diatoms, Limnology and Oceanography 18 P. 647-653.

Bennett, K.D. (1986) Coherent slumping of early post-glacial lake sediments at Hall Lake, Ontario, Canada, Boreas 15 P. 209-215.

Bennike, O. (2000) Palaeoecological studies of Holocene lake sediments from West Greenland, Palaeogeography, Palaeoclimatology, Palaeoecology Vol. 155 P. 285-304.

Bennike, O. (1995) Palaeoecology of two lake basins from Disko, West Greenland, Journal of Quaternary Science Vol. 10 (2) P. 149-155.

Benninghoff, W.S. (1962) Calculation of pollen and spore density in sediments by addition of exotic pollen in known quantities, Pollen et Spores 4 P. 143-150

Birks, H.J.B; Line, J.M; Juggins, S; Stevenson, A.C; & Ter Braak, C.J.F. (1990) Diatoms and pH reconstruction, Philosophical Transactions of the Royal Society of London Series B 327 P. 263-278.

Björck, S; Ingólfsson, Ó; Haflidason, H; Hallsdóttir, M; & Anderson, J. (1992) Lake Torfadalsvatn: A high resolution record of the North Atlantic ash zone 1- the last glacial-interglacial environment changes in Iceland, Boreas 21 P.15-22.

Bond, G. & Lotti, R. (1995) Iceberg discharges into the North Atlantic on Milennial time-scales during the last glaciation, Science 267 P. 1005-1010.

Bond, G; Heinrich, H; Broeker, W; Labeyrie, L; McManus, J; Andrews, J; Huon, S; Jantschik, R; Clasen, S; Simet, C; Tedesco, K; Klas, M; Bonani, G, & Ivy, S. (1992) Evidence for massive discharges of icebergs into the North Atlantic ocean during the last glacial period, Nature 360 P.245-249.

Boygle, J. (1999) Variability of tephra in lake and catchment sediments, Svínavatn, Iceland, Global and Planetary Change 21 P. 129-149.

Brewster, N.A. (1983) The determination of biogenic opal in high latitude deep-sea sediments, In: Siliceous deposits of the Pacific region: developments in sedimentology Vol. 36 Iijima, A; Hein, J.R; & Siever, R. (eds.) Elsevier, New York, pp. 17-331.

Broecker, W.S. & Denton, D.H. (1989) What drives glacial cycles? Geochmica et Cosmochimica Acta 53 (10) P. 2465-2501.

Bradshaw, E.G; Jones, V.J; Birks, H.J.B; & Birks, H.H. (2000) Diatom response to lateglacial and early Holocene environmental changes at Kråkenes, Western Norway, Journal of Palaeolimnology 23 P. 21-34.

Brun, J (1965) Diatomées des Alpes et du jura, Asher & Co. Amsterdam.

Buckland, P. & Dugmore, A. (1991) "If this is a refugium, why are my feet so bloody cold?" The origins of the Icelandic biota in the light of recent research, In: Maizels, J.K. & Caseldine, C. (eds.) (1991) Environmental change in Iceland: Past and present, Kluwer Academic Publishers, P. 107-125.

Charles, D.F. (1985) Relationships between surface sediment diatom assemblages and lakewater characteristics in Adirondack Lakes, Ecology 66 (3) P. 994-1011.

Charles, D.F. (1982) Studies of the Adirondack Mountain (N.Y.) lakes: Limnological characteristics and sediment diatom-water chemical relationships, Dissertation, Indiana University, Bloomington, Indiana, USA.

Chester, R. & Elderfield, H. (1968) The infrared determination of opal in siliceous deep-sea sediments, Geochimica et Cosmochimica Acta 32 P. 1128-1140.

Colman, S.M; Peck, J.A; Karabanov, E.B; Carter, S.J; Bradbury, J.P; King, J.W; & Williams, D.F. (1995) Continental climate response to orbital forcing from biogenic silica records in Lake Baikal, Nature 378 P. 769-771.

Conley, D.J. (1998) An interlaboratory comparison for the measurement of biogenic silica in sediments, Marine Chemistry 63 P. 39-48.

Conley, D.J. (1988) Biogenic silica as an estimate of siliceous microfossil abundance in Great Lakes sediments, Biogeochemistry 6 P. 161-179.

Conley, D.J. & Schelske, C.L. (2001) Biogenic Silica, In: Smol, J.P; Birks, J.B; & Last, W.M. (eds.) (2001) Tracking environmental change using lake sediments, Volume 3: Terrestrial, algal, and siliceous indicators, *Kluwer Academic Publishers, Dordrecht, The Netherlands.*

Conley, D.J. & Schelske, C.L. (1993) Potential role of sponge spicules in influencing the silicon biogeochemistry of Florida Lakes, Canadian Journal of Fisheries and Aquatic Science 50 P. 296-302.

Conley, D.J; & Schelske, C.L; & Stoermer, E.F. (1993) Modification of the biogeochemical cycle of silica with eutrophication, Marine Ecological Progress Series 101 P. 179-192.

Corner, G.D; Kolka, V.V; Yevzerov V.Y; & Møller, J.J. (2001) Postglacial relative sea-level change and stratigraphy of raised coastal basins on Kola Penisula, Northwest Russia, Global Planetary Change 31 P.155-177.

Corner, G.D; Kolka, V.V; Yevzerov V.Y; & Møller, J.J. (1998) Isolation basin stratigraphy and Holocene relative sea-level change at the Norwegian-Russian boarder north of Nikel, North-west Russia, Boreas 28 P. 146-166.

Corner, G.D & Haugane, E. (1993) Marine-lacustrine stratigraphy of raised coastal basins and postglacial sea-level change at Lyngen and Vanna, Troms, Northern Norway, Norsk Geologisk Tidsskrift 73 P. 175-197.

Dahl-Jensen, D; Mosegaard, K; Gundestrup, N; Clow, G.D; Johnsen, S.J; Hansen, A.W; & Balling, N. (1998) Past temperatures directly from the Greenland ice sheet, Science 282 P. 268-271.

DeMaster, D.J. (1979) The marine budgets of silica and ^{32}Si, Ph.D Thesis, Yale University.

Dean, W.E; Bradbury, Y.P; Anderson, R.Y. (1984) The variability of Holocene climate change: Evidence from varved lake sediments, Science 226 P. 1191-1194.

Denys, L. (1991/2) A check-list of diatoms in the Holocene deposits of the western Belgian coastal plain with a survey of their apparent ecological requirements: 1. Introduction, ecological code and complete list, Service Geologique de belgique Proffesional paper No. 246.

Douglas, M.S.V. & Smol, J.P. (1999) Fresh water diatoms as indicators of environmental change in High Arctic, In: Stoermer, E.F. & Smol, J.P. (eds.) The diatoms: applications for the environmental earth sciences, Cambridge, Cambridge University Press, P.469.

Downing & Rath (1988) Spatial patchiness in lacustrine sedimentary environment, Limnology and Oceanography 33 P. 447-458.

Eggimann, D.W; Manheim, F.T; & Betzer, P.R. (1980) Dissolution and analysis of amorphous silica in marine sediments, Journal of Sedimentary Petrology 50 P. 215-225.

Einarsson, Th. (1978) Jarðfræði. Mál og Menning, Reykjavík.

Einarsson, Th. (1968) Jarðfræði. Saga bergs og lands, Mál og Menning, Reykjavík.

Einarsson, Th. (1967) Zu der Ausdehnung der weichselzeitlichen Vereisung Nordislands, Sönderöffententlichungen des Geologischen Institutes der Universität Köln 13 P. 167-173.

Einarsson, Th. & Albertsson, K.J. (1988) The glacial history of Iceland during the past three million years, Philosophical Transactions of the Royal Society of London 318, P. 637-644.

Eiríksson, J; Knudsen, K.L; Haflidason, H; & Henriksen, P. (2000a) Late-glacial and Holocene palaeoceanography of the North Icelandic Shelf, Journal of Quaternary Science 15 (1) P.23-42.

Eiríksson, J; Knudsen, K.L; Haflidason, H; Heinemeier, J. (2000b) Chronology of the late Holocene climatic events in the northern North Atlantic based on AMS 14C and tephra markers from the volcano Hekla, Iceland, Journal of Quaternary Science 15(6) P. 573-580.

Eiríksson, J; Simonarson, L.A; Knudsen, K.L; Krsitensen, P. (1997) Fluctuations of the Weichselian Ice sheet in SW Iceland: A glacio-marine sequence from Sudurnes, Seltjarnarnes, Quaternary Science Reviews 16 P. 221-240.

Ellis, B.B. & Moore, T.C. (1973) Calcium carbonate, opal and quartz in Holocene pelagic sediments and the calcite compensation level in the South Atlantic Ocean, Journal of Marine Research 31 P.210-227.

Eisma, D. & Van der Gaast, S.J. (1971) Determination of opal in marine sediments by X-ray diffraction, Netherlands Journal of Sea Research 5 P. 382-389.

Fairbanks, R.G. (1989) A 17,000 year glacio-eustatic sea-level record: influence of glacial melting rates on the Younger Dryas event and deep-ocean circulation, Nature 342 P.637-642.

Fleming, K., Johnston, P., Zwartz, D., Yoyoyama, Y., Lambeck, K., and Chapell, J., 1998. Refining the eustatic sea-level curve since the "Last Glacial Maximum" using far- and intermediate-field sites. Earth Planet. Sci. Lett., 163:327-342.

Flower, R.J. (1993) Diatom preservation: experiments and observations on dissolution and breakage in modern and fossil material, Hydrobiologia 269/270 P. 473-484.

Flower, R.J. & Nicholson, A.J. (1987) Relationships between bathymetry, water quality and diatoms in some Herbridean lochs, Freshwater Biology 18 P. 71-85.

Foged, N. (1977) The diatoms of four postglacial deposits at Godthåbsfjord, West Greenland, Meddelelser om Grønland 199 (4) P. 1-64.

Foged, N. (1973) Diatoms four southwest Greenland, Meddelelser om Grønland 194 (5) P.1-84.

Foged, N. (1972) The diatoms in four postglacial deposits in Greenland, Meddelelser om Grønland 194 (4) P.1-66.

Foged, N. (1964) Freshwater diatoms from Spitsbergen, Universilets Forlaget Tromsö/Oslo.

Fritz, S.C; Juggins, S; Battarbee, R.W; & Engstrom, D.R. (1991) Reconstruction in past changes in salinity and climate using a diatom based transfer function, Nature 352 P. 706-708.

Geirsdóttir, Á; & Eiríksson, J. (1994) Sedimentary facies and environmental history of the Late-glacial glacio-marine Fossvogur sediments in Reykjavik, Iceland, Boreas 23 P. 164-176.

Grönlund, T. & Kauppila, T. (2002) Holocene history of lake Soldatskoje (Kola Peninsula, Russia) inferred from sedimentary diatom assemblages, Boreas 31 P. 273-284.

Grönvold, K; Oskarsson, N; Johnsen, S.J; Clausen, H.B; Hammer, C.U; Bond, G; & Bard, E. (1995) Ash layers from Iceland in the Greenland GRIP ice core correlated with oceanic and land sediments, Earth and Planetary Science Letters 135, P. 149-155.

Grimm, E.C. (1990) TILIA and TILIA.GRAPH.PC spreadsheet and graphics software for pollen data, INQUA, Working Group on Data-Handling Methods, Newsletter 4 P.5-7.

Grimm, E.C. (1987) CONISS: A Fortran 77 program for stratigraphical constrained cluster analysis by the method of incremental sum of squares, Computers and Geosciences 13 P. 13-35.

Hall, R.I. & Smol, J.P. (1999) Diatoms as indicators of lake eutrophication, In: Stoermer, E.F. & Smol, J.P. (eds.) The Diatoms: Applications for the environmental and earth sciences, P.469pp Cambridge University Press, Cambridge.

Hafliðason, H; Eiríksson, J, & Kreveld, S.V. (2000) The tephrochronology of Iceland and the North Atlantic region during the Middle and Late Quaternary: A review, Journal of Quaternary Science 15(1) P. 3-22.

Hansen, H.H. (2001) Islandskort, Nordvesterlund Fjordungskort, 1:300 000, Mál og menning, Reykjavík.

Hansom, J.D. & Briggs, D.J. (1991) Sea-level change in Vestfirðir, NW Iceland, In: Maizels, J.K. & Caseldine, C. (eds.) (1991) Environmental change in Iceland: Past and present, Kluwer Academic Publishers, P. 79-91.

Hartley, B (eds.) (1996) An Atlas of British Diatoms, Biopress Limited.

Hecky, R.E. & Kilham, P. (1973) Diatoms in alkaline, saline lakes: Ecology and geochemical implications, Limnology and Oceanography 18 (1) P. 53-71.

Heiri, O; Lotter, A.F; & Lemcke, G. (2001) Loss on ignition as a method for estimating organic and carbonate content in sediments: reproducibility and comparability of results, Journal of Paleolimnology 25 P. 101-110.

Hjartarson, Á. (1991) A revised model of Weichselian deglaciation in south and southwest Iceland, In: Maizels, J.K. & Caseldine, C. (eds.) (1991) Environmental change in Iceland: Past and present, Kluwer Academic Publishers, P. 67-77.

Hjort, C.O; Ingolfsson, O; & Norddahl, H. (1985) Late Quaternary geology and glacial history of Hornstrandir, NW Iceland: A reconnaissance study, Jökull 35 P. 9-29.

Hoppe, G. (1982) The extent of the last inland ice sheet of Iceland, Jökull 32 P.3-11.

Hoppe, G. (1968) Grimsey and the maximum extent of the last glaciation of Iceland, Geografiska Annaler 50 P. 16-24.

Hu, F.S. & Shemesh, A. (2003) A biogenic silica oxygen isotope record of climatic change during the last glacial-interglacial transition in SW Alaska, In: Quaternary Record Vol. 59 P. 379-385.

Hurley, J.P; Armstrong, D.E; Kenoyer, G.L; & Bowser, C.J. (1985) Groundwater as a silica source for diatom production in a precipitation dominated lake, Science 227 P. 1576-1578.

Hustedt (1959) Die Kieslalgen, 2nd Edition, *Akademischeverlagsgesllschaft Geest & Portig K.-G.*

Hustedt, F. (1957) Diatoméenflora der Fluss-Systems der Weser im Gebeit der Hansestadt Bremen, Abh. Naturw. Ver. Bremen 34 P. 181-440.

Ingölfsson, O. (1991) A review of late Weichselian and early Holocene glacial and environmental history of Iceland, In: Maizels, J.K. & Caseldine, C. (eds.) (1991) Environmental change in Iceland: Past and present, Kluwer Academic Publishers, P. 13-48.

Ingölfsson, O. & Norddahl, H. (2001) High relative sea-level during the Bølling Interstadial in Western Iceland: a reflection of ice-sheet collapse and extremely rapid glacial unloading, Arctic, Antarctic, Alpine Research 33 (2) P. 231-243.

Ingölfsson, O & Norddahl, H. (1994) A review of the environmental history of Iceland, 13 000-9 000 yr BP, Journal of Quaternary Science 9 (2) P.147-150.

Ingolfsson, O; Norddahl, H; & Haflidason, H. (1995) Rapid isostatic rebound in southwestern Iceland at the end of the last glaciation, Boreas 24 P. 245-259.

Itkonen, A; Marttila, V; Meriläinen, J.J; & Salonen, V. (1999) 8000 year history of palaeoproductivity in a large Boreal lake, Journal of Paleolimnology 21 P. 271-294.

Jakobsson, S. (1979a) Petrology of recent basalts of the eastern volcanic zone, Iceland, Acta Naturalia Islandica 26 P. 1-103.

Jewson, D.H; Rippey, B.H; & Gilmore, W.K. (1981) Loss rates from sedimentation, parasitism, and grazing during the growth, nutrient limitation, and dormancy of a diatom crop, Limnology and Oceanography 26 (6) P. 1045-1056.

Jennings, A. E; Syvitski, P.M; Gerson, L; Gronvold, K; Geirsdóttir, Á; Hardardöttir, J; Andrews, J.T; & Hagen, S. (2000) Chronology and palaeoenvironments during the Late weichselian deglaciation of the southwest Iceland shelf, Boreas 29 P. 167-183.

Johns, B.S. (1975) Durham University Vestfiðir project, 1975, Department of Geography, Durham University Special Publication.

Johns, B.S. (1974) Northwest Iceland reconnaissance 1973 (Durham University Vestfiðir project), Department of Geography, Durham University Special Publication, 54pp.

Juillet Leclerc, A. & Labeyrie, L. (1987) Temperature dependence of oxygen isotope fractionation between diatom silica and water, Earth Planetary Science Letters 84 P. 69-74.

Kajartansson, G. (1968) Isaldarlok og eldfjöll á Kili, Náttúrufæðingurinn 34 P. 9-38.

Kershaw, A.P. (1997) A modification of the Troels-Smith system of sediment description and portrayal, At:
http://wwwrses.anu.edu.au/envgeo/AQUADATA/AQUA/QA/1997_15_2/15_2_p3.html

Kjartansson (1968) Geological map of Iceland, Sheet 1, NW Iceland, Menningarsjóður, Reykjavík.

Kjemperud, A (1986) Late Weichselian and Holocene shoreline displacement in Trondheimsfjord area, Central Norway, Boreas 15 P. 61-82.

Kjemperud, A. (1981) Diatom changes in sediments of basins processing marine/lacustrine transitions in Frosta, Nord-Trøndelag, Norway, Boreas 10 P. 27-38.

Lárusson, E. (1977) Um efstu fjörumörk í Dýrafirði og Arnarfirði, In: Dagshrá og ágrip, Abstract Vol. Jarðfæðafélag Ísland, Reykjavík, P. 9.

Leinen, M. (1977) A normative calculation technique for the determining opal in deep-sea sediments, Geochimica et Cosmochimica Acta 41 P.671-676.

Lindroth, C.H. (1931) Die Insektfauna Islands und iher Probleme, Zoologiska bidrag från Uppsala 13 P. 105-599.

Lisitsyn, A.P. (1971) Basic relationships in distribution of modern siliceous sediments and their connection with climate zonations, International Geology Review 9 P. 631-652, 842-865, 980-1004, 114-1130.

Lloyd, J.M; & Evans, J.R. (2002) Contemporary and fossil foraminifera from isolation basins in NW Scotland, Journal of Quaternary Science 17 (5-6) P. 431-443.

Lloyd, J.M. (2000) Combined foraminiferal and theocamoebrian environmental reconstruction from an isolation basin in Scotland, Journal of Foraminiferal Research 30 P.

Long, A.J; Roberts, D.H; & Rasch, M; (2003) New observations on the relative sea-level and deglacial history of Greenland from Innaarsuit, Disko Bugt, *Quaternary Research* (In press)

Long, A.J; Roberts, D.H; (2002) A revised chronology for the "Fjord Stage" moraine in Disko Bugt, West Greenland, Journal of Quaternary Science 17 P. 561-579.

Long, A.J; Roberts, D.H; Wright, M.R. (1999) Isolation basin stratigraphy and Holocene relative sea-level change on Arveprinsen Ejland, Disko Bugt, West Greenland, Journal of Quaternary Science 14 (4) P. 323-313.

Lotter, A.F. & Birks, H.J.B. (1993) The impact of the Laacher See tephra on terrestrial and aquatic ecosystems in the Black Forest, southern Germany, Journal of Quaternary Science 8(3) P. 263-276.

Maizels, J.K. & Caseldine, C. (eds.) (1991) Environmental change in Iceland: Past and present, Kluwer Academic Publishers.

Mangerud, J; Furnes, H; & Jóhansen, J. (1986) A 9000-year old ash bed on the Faroe Islands, Quaternary Research 26 P. 262-265.

Mortlock, R.A. & Froelich, P.N. (1989) A simple method for the rapid determination of biogenic opal in pelagic marine sediments, Deep-Sea Research 36 P. 1415-1426.

Moser, K.A; MacDonald, G.M; and Smol, J.P. (1996) Applications of freshwater diatoms to geographical research, Progress in Physical Geography 20 (1) P. 21-52

Newberry, T.L. & Schelske, C.L. (1986) Biogenic silica record in the sediments of Little Round Lake, Ontario, Hydrobiologia 143 P. 293-300.

Ng, S.L; & King, R.H. (1999) Development of a diatom-based specific conductivity model for the glacio-isostatic lake Truelove Lowland: Implications for palaeoconductivity and palaeoenvironmental reconstructions, Journal of Paleolimnology 22 P. 367-382.

Norddahl, H. (2003) pers. comm.

Norddahl, H. (1991) A review of the glaciation maximum concept and the deglaciation of Eyjafjördur, North Iceland, In: Maizels, J.K. & Caseldine, C. (eds.) (1991) Environmental change in Iceland: Past and present, Kluwer Academic Publishers, P. 31-49.

Norddahl, H. (1990) *Late Weichselian and early Holocene deglaciation history of Iceland*, Jökull 40, P. 27-47.

Norddahl, H. (1981) A prediction of minimum age for the Weichselian maximum glaciation in North Iceland, Boreas 10 P. 471-476.

Norddahl, H. (1978) Landmótun svæðisins Lágheiði-Ólafsfjöður, frum könnun á möguleikum til malartekju í Ólafsfirði, Eyjafjarðarsýslu, Mimeographed report, Icelandic Public Road Administration.

Norddahl, H. & Halflidsason, H. (1992) The Skogar tephra, a marker in N Iceland, Boreas 21 P. 23-41.

Nygaard, G. (1956) Ancient and recent flora of diatoms and chrysophyceae in Lake Gribso. In: Berg, I.B; & Petersen, C. (1956) Studies on the humid acid lake Gribso, Fol. Limnology Scandinavia 8 P. 32-94.

Palmer, A.J.M; & Abbot, W.H. (1986) Diatoms as indicators of sea-level change, In: O. Van de Plassche (eds) Sea-level research: A manual for the collection and evaluation of data, P. 457-488, Geobooks: Norwich.

Patrick (1971) The effects of increased light and temperature on the structure of diatom communities, Limnology and Oceanography 16 P. 405-421.

Peinerud, E.K. (2000) Interpretation of Si concentrations in lake sediments: Three case studies, Environmental Geology 40 (1-2) P. 64-72.

Perren, B; Bradley, R; & Francus, P. (2003) Rapid lacustrine response to recent high arctic warming: A diatom record from Sawtooth Lake, Ellesmere Island, Nunavut, Arctic, Antarctic, and Alpine Research 35 P. 271-278.

Pétursson, H.G. (1991) The Weichselian glacial history of west Melrakkaslétta, NE Iceland, In: Maizels, J.K. & Caseldine, C. (eds.) (1991) Environmental change in Iceland: Past and present, Kluwer Academic Publishers, P. 49-65.

Pienitz & Smol (1993) Diatom assemblages and their relation to environmental variables in the lakes from the boreal forest-tundra ecotone near Yellowknife, NW territories, Canada, Hydrobiologia 269/270 P. 391-404.

Pienitz et al: (1995) Assessment of fresh-water diatoms as quantitative indicators of past climate change in the Yukon and NW Territories, Canada, Journal of Paleolimnology 13 P. 21-49.

Pokeras, E. (1986) Preservation of fossil diatoms in Atlantic sediment cores-control by supply rate, Deep-sea Research 33 P. 893-902.

O. Van de Plassche (eds) Sea-level research: A manual for the collection and evaluation of data, Geobooks: Norwich,

Qiu, L; Williams, D.F; Gvorzdkov, A; Karabanov, E; & Shimaraeva, M. (1993) Biogenic silica accumulation and paleoproductivity in the northern basin of Lake Baikal during the Holocene, Geology 21 P. 25-28.

Renberg & Hellberg (1982) The pH history of lakes in SW Sweden, as calculated from the subfossil diatom flora of the sediments, Ambio 11 P.30-33.

Robbins, J.A; Edginton, D.N; and Parker, J.I. (1975) Distribution of amorphous, diatom frustule, and dissolved silica in a lead-210 dated core from southern Lake Michigan, In: Radiological and Environmental Research Division Annual Report, Ecology, Argonne National Laboratory, ANL-75-3.

Rosqvist, G.C; Rietti-Shati, M; & Shemesh, A. (1999) Late glacial to middle Holocene climatic records of lacustrine biogenic silica oxygen isotope from a Southern Ocean island, Geology 27 (11) P. 967-970.

Ruddiman, W.F. & McIntyre, A. (1981) The North Atlantic during the last glaciation, Palaeogeography, Palaeoclimatology, and Palaeoecology 35 P. 145-214.

Rundgren, M; Ingolfsson, O; Björck, S; Haflidason, H. (1997) Dynamic sea-level change during the last deglaciation of northern Iceland, Boreas 26 P. 201-215.

Rundgren (1995) Biostratigraphical evidence of the Allerød-Younger Dryas-Preboreal oscillation in northern Iceland, Quaternary Research 44 P. 405-416.

Schelske, C.L; Eadie, B.J; & Krausse, G.L. (1984) Measured and predicted fluxes of biogenic silica in Lake Michigan, Limnology and Oceanography 29 (1) P. 99-110.

Schelske, C.L; Stoermer, E.F; Conley, D.J; Robbins, J.A; Glover, R.M. (1983) Early eutrophication in the lower Great Lakes: new evidence from biogenic silica in sediments, Science 222 P. 320-322.

Seppa, H; Tikkanen, M; and Shemeikka, P. (2000) Late-Holocene shore displacement of the Finnish coast: diatom, litho- and chemostratigraphic evidence from three isolation basins, Boreas 29 P. 219-231.

Shennan, I; Lambeck, K; Horton, B; Innes, J; Lloyd, J; McArthur, J; Purcell, T; and Rutherford, M. (2000) Late devension and Holocene records of RSL change in NW Scotland and their implications for glacio-hydro-isostatic modelling, Quaternary Science Reviews 19 P.1103-1135.

Shennan, I; Green, F; Innes, J; Lloyd, J; Rutherford, M; and Walker. (1996) Evaluation of rapid relative sea-level change in Northwest Scotland during the last glacial-interglacial transition: Evidence from Ardtoe and other isolation basins, Journal of Quaternary Research 12 (4) P. 862-874.

Shennan, I; Innes, J.B; Long, A.J; and Y. Zong (1995) Holocene relative sea-level changes at Kentra Moss, Argyll, northwestern Scotland. Marine Geology 124 P. 43-60

Shennan, I; Innes, J.B; Long, A.J; & Zong, Y. (1994) Late Devension and Holocene relative sea-level changes at Loch nan Eala, vear Arisaig, Northwest Scotland, Journal of Quaternary Science 9 (3) P. 261-283.

Sigurvinsson, J.R. (1983) Weichselian glacial lake deposits in the highlands of NW Iceland, Jökull 33 P. 99-109.

Smith, G.M. (1950) Fresh-water algae of the United States, 2nd edition, McGraw-Hill.

Smol (1988) Paleoclimatie proxy data from freshwater arctic diatoms, Verhandlungen der internationallen veneinigung für theoretisch und angewandte limnologie 23 P. 837-844.

Smol, J.P; Birks, J.B; & Last, W.M. (eds.) (2001) Tracking environmental change using lake sediments, Volume 3: Terrestrial, algal, and siliceous indicators, Kluwer Academic Publishers, Dordrecht, The Netherlands.

Snyder, J.A; Forman, S.L; Mode, W.N; & Tarasov, G.A. (1997) Postglacial relative sea-level history: Sediment and diatom records of emerged coastal lakes, North-central Kola Peninsula, Russia, Boreas 26 P. 329-346.

Snyder, J.A; MacDonald, G.M; Forman, S.L; Tarasov, G.A; and Mode, W.N. (2000) Postgalcial climate and vegetation history, north-central Kola Peninsula, Russia: Pollen and diatom records from lake Yarnyshnoe-3, Boreas 29 P. 261-271.

Stabell, B. (1985) The development and succession of taxa within the diatom genus Fragilaria Lyngbye as a response to basin isolation from the sea, Boreas 14 P.273-286.

Stevenson, A.C; Birks, H.J.B; Flower, R.J; and Battarbee, R.W. (1989) Diatom-based pH reconstruction of Lake acidification using canonical correspondence analysis, Ambio 18 P. 228-233.

Stötter, C.R; Wastl, M; Caseldine, C; Haberle, T. (1999) Holocene palaeoclimatic reconstruction in northern Iceland: Approaches and results, Quaternary Science Reviews 18 P. 457-474.

Stuiver, M. & Reimer P.J., (1993) CALIB Rev4.4.2, Radiocarbon, 35, 215-230

Sveinbjörnsdóttir, Á.E; Eiríkson, J; Geirsdóttir, Á; Heinemeier, J; & Rud, N. (1993) The Fossvogur marine sediments in SW Iceland-confined to the Allerød/Younger Dryas transition by AMS ^{14}C dating, Boreas 22 P. 147-157.

Telford, R.J; Barker, P; Metcalfe, S; Newton, A (2004) Lacustrine responses to tephra deposition: examples from Mexico, (in press).

Thomas, R.E; Wolff, E.W; Mulvaney, R; Steffensen, J.P; & Johnsen, S.J. (2004) High-resolution analysis of the 8.2Kyr event from the Greenland Ice Core Project ice core, In: Symposium on Climate Change.

Thoroddsen, Th. (1905-1906) Island. Grundiß der geographie und geologie, Justus Perthes, Gotha, P.358pp

Thórarinsson, S. (1944) "Tephrokronologiska studier på Island," Geografiska Annaler 19, P. 1-217.

Thors, K. & Helgadóttir, G. (1991) Evidence from SW Iceland of low sea-level in early Flandrian times, In: Maizels, J.K. & Caseldine, C. (eds.) (1991) Environmental change in Iceland: Past and present, Kluwer Academic Publishers, P. 93-104.

Troels-Smith, J. (1955) Characterisation of unconsolidated sediments. Danm. geol. Unders. Ser.IV, 3(10), 73pp.

Tucker, O.E. (2003) Isolation basin stratigraphy with emphasis on marine-lacustrine transitions from Disko Bugt, West Greenland, unpublished B.S.c dissertation.

Van der Werff (1958)

Wastegard, S; Björck, J; and Risberg, J. (1998) Deglaciation, shore displacement and early-Holocene vegetation history in eastern middle Sweden, Holocene 8 (4) P. 433-441.

Weckström, J; Korhola, A; and Blom, T. (1997) Diatoms as quantitative indicators of pH and water temperature in sub-arctic Fennoscandinavian lakes, Hydrobiologia 347 P. 171-184.

Wolf, A. P. (2003) Diatom community responses to late-Holocene climatic variability, Baffin Island, Canada: a comparison of numerical approaches, Holocene 13 (1) P. 29-37.

Zong, Y. (2004) Pers. comm.

http://www.geo.arizona.edu/palynology/geos462/8200yrevent.html

APPENDIX

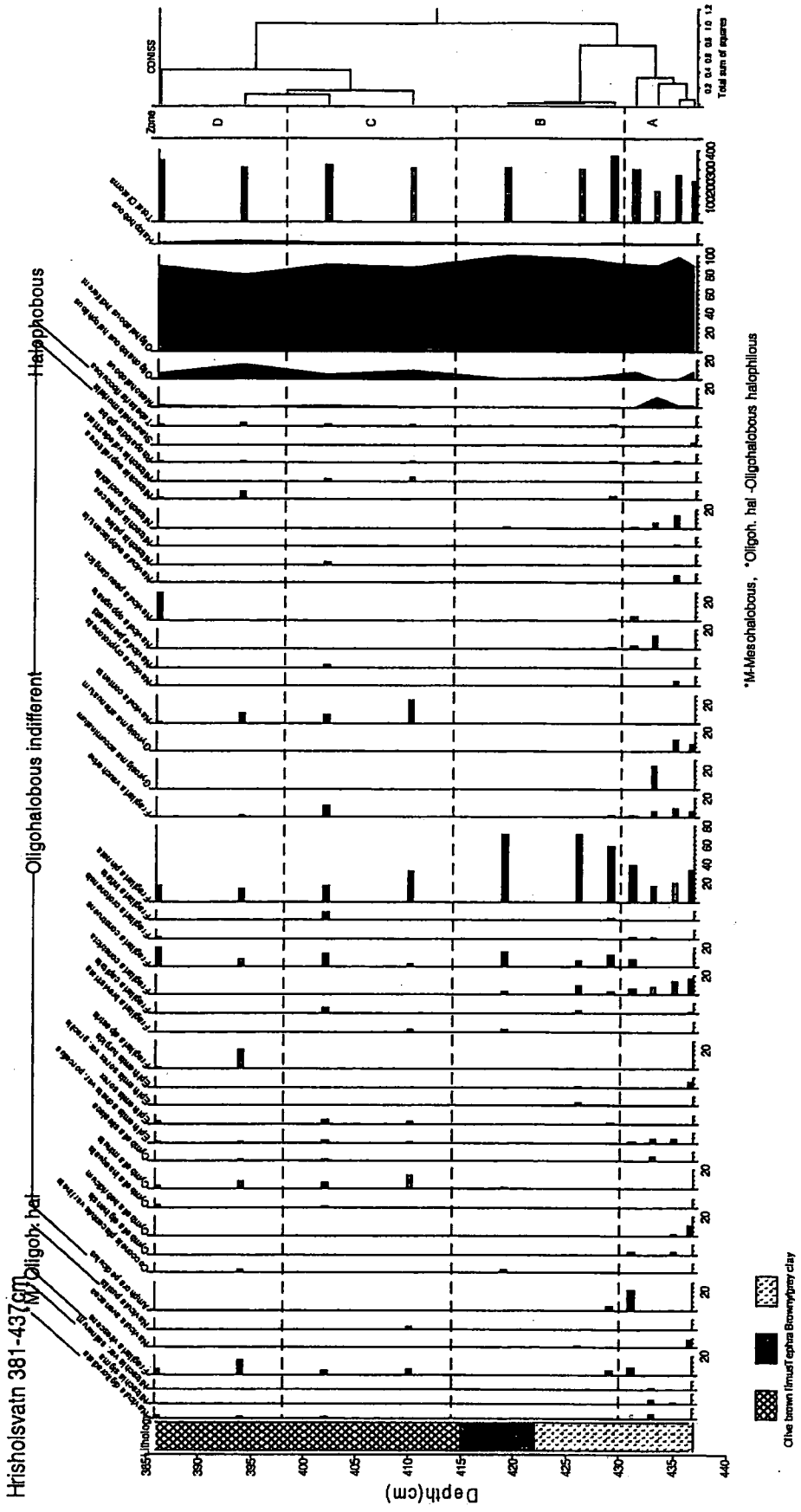
Hrisholsvatn 381-437 cm
Depth(cm)
Oligohalobous indifferent
Halophobous
M-Oligoh. hal
*M-Mesohalobous, *Oligoh. hal -Oligohalobous halophilous
Olive brown limus
Tephra
Brown/grey clay
CONISS
Zone
D
C
B
A

Fig. 4.2

Figure 2 Diatom assemblage information for Mavatn

Taxa name	Hustedt Classification (1953)	Sample depth (cm)					
		63	71	83	87	91	95
Ach. Hauckiana	Oligohalobous-indifferent	2					
Ach. Holstii??	Oligohalobous-indifferent	1					
Ach. Lanceolata	Oligohalobous-indifferent	2	1				
Ach. lutheri	Oligohalobous-indifferent				4		
Ach. Protracta	Oligohalobous-indifferent			1			
Ach. Rostrata	Oligohalobous-indifferent		7				
Amphora Commutata	Mesohalobous			2			
Amphora Copulata	Oligohalobous-indifferent	2	7				
Amphora Exigua	Oligohalobous-indifferent				2		
Biddulphia Recticullum (>2/3)	Polyhalobous					1	
Brachysira serians fo	Halophobous	1	2				
Bracyhsira brebissonii	Halophobous		3	2			
Cocconeis costata	Polyhalobous			1			
Cocconeis placentula euglypta	Oligohalobous-indifferent	17	1	1			
Ctenophora Pulchella	Mesohalobous	1					
Cyclotella menghiniana	Mesohalobous	5	5	1			
Cyclotella stelligera	Oligohalobous-indifferent			1			
Cyclotella stelligera	Oligohalobous-indifferent					1	
Cymatopleura librile	Oligohalobous-indifferent	6					
Cymbella Cistula	Oligohalobous-indifferent	2					
Cymbella Inaequalis	Oligohalobous-indifferent	2					
Cymbella Insigne	Oligohalobous-indifferent	1					
Cymbella minutuns fo latens	Oligohalobous-indifferent	2					
Denticula Kuetzingii	Oligohalobous-indifferent	2	3				
Diatoma elongatum	Oligohalobous-halophilous	12	1				
Diatoma tenue	Oligohalobous-halophilous	7	1				
E. adnata var porcellus	Oligohalobous-indifferent	2					
Eunotia Pectinalis	Halophobous	1					
E. Sorex	Oligohalobous-indifferent			2			
Endictya Oceanica	Polyhalobous				1		

Endictya Oceanica (pieces)	Polyhalobous			7	4	2	2
Eunotia (pieces)	Halophobous		4				
F. Brevistrata	Oligohalobous-indifferent	7	17	19			
F. construens	Oligohalobous-indifferent	1					
F. Construens var venter	Oligohalobous-indifferent	22	8	6	2		1
F. Inflata	Oligohalobous-indifferent	2		1			
F. Leptostauron	Oligohalobous-indifferent	1	2				
F. Pinnata	Oligohalobous-indifferent	64	10	7	2		
F. vaucheriae	Oligohalobous-indifferent	12	5	1			
F. Virescens	Oligohalobous-indifferent	7	16	24	4		
G. parvulum	Oligohalobous-indifferent	3	1				
Gomphoneis olivaceum	Oligohalobous-indifferent		1				
Gyrosigma acuminatum	Oligohalobous-indifferent	10			1		
Mastogloia Elliptica	Mesohalobous			1			
Meridion circulare	Oligohalobous-indifferent	1					
N. Cincta	Oligohalobous-halophilous			1			
N. Crypttotenella	Oligohalobous-indifferent	1					
N. Directa?	Polyhalobous				1		
N. Hudsonis	Polyhalobous						1
N. Plyinesis					1		
N. radiosa	Oligohalobous-indifferent	2					
N. Rhynchocephala	Oligohalobous-indifferent	17					
N. Subtllissima	Oligohalobous-indifferent		5				
Nitzschia Granulata (M)/Nitzschia gracilis (F)?					1		
Nitzschia socialis (piece)	Polyhalobous			1			
Nitzscia fasiculata	Mesohalobous		1				
Nitzscia Palea	Oligohalobous-indifferent		4	1			1
Nitzscia Sociabilis	Oligohalobous-indifferent		1				
P. Lapponica	Oligohalobous-indifferent	5					
P. mesolepta	Oligohalobous-indifferent		2				
P. microstauron	Oligohalobous-indifferent	1					
P. Viridis	Oligohalobous-indifferent	1					
P.parvua?	Oligohalobous-indifferent	1	2				
Pinnularia (medium sized)	Oligohalobous-indifferent	1					
Pinnularia appendiculata	Halophobous	1					
possibly N. Viridula?		1					

R. Gibba	Oligohalobous-indifferent	8	18				
R. Gibba (pieces)	Oligohalobous-indifferent			4			
R. Gibba var parrellela	Mesohalobous	3	3				
R. Rupestris	Mesohalobous		15				
Rhabdonema minutun	Polyhalobous				2		
See drawing (71cm A. Sp (m))			2				
See drawing (87cm) (cyclotella/melosira?)					8		
See drawing (A. Microphala/minutissima var. jockii/taeniata or Navicula lenzii)				1	1		
see drawing (pinnata)			113				
Fragilariaforma virescens	Oligohalobous-halophilous	46					
see drawing 1 (83cm)				1			
see drawing 1 (95cm)							
see drawing 2 (63cm)		2					
see drawing 2 (83cm)				2			
Stauroneis fo. Prominala	Oligohalobous-indifferent	1					
Staurosirella Elliptica	Oligohalobous-indifferent	21	3				
Staurosirella pinnata	Oligohalobous-indifferent	3					
Surirella brebbissonii	Oligohalobous-indifferent	1					
Surirella Linearis	Oligohalobous-indifferent		1				
Surirella?			3				
Synedra parasitica var subconstricta	Oligohalobous-indifferent	9					
Synedra rumpens (F. Sp.??)	Oligohalobous-indifferent		1				
Synedra ulna var bicepts	Oligohalobous-indifferent	16	7	2			
T. Fasiculata	Mesohalobous				2		
T. Fasiculata (piece)	Mesohalobous			1			
T. Fenestrata	Oligohalobous-indifferent	3	2				
T. Flocculosa	halaphobous	2	7	5			
T. Flocculosa (pieces)	halaphobous				3		
Thallassiosira Deciphens	Mesohalobous			5			
Thallassiosira Eccentrica (pieces)	Polyhalobous			47	22	2	
Thallassiosira Eccentrica (whole >1/3)	Polyhalobous			9			10
Thallassiosira Eccentrica (whole >2/3)/ or whole	Polyhalobous			26	34	2	5
			1				
		2					
		2					

Sample totals		352	290	185	95	8	20

Figure 3 Diatom assemblage information for Hafrafellvatn

Taxa name	Hustedt Class.	Sample depth (cm)													
	1953	366	382	398	404	406	410	414	418	422	426	430	438	442	446
Brachysira brebissonii					10										
Brachysira serians fo	Halophobous								2						
Denticula kuetzingii	Halophobous											2			
Tabellaria Flocculosa	halophobous	1													
Achnanthes lanceolata	oligo-ind		1				1	1						1	
Amphipleura pellucida	oligo-ind	56													
Amphora copulata	oligo-ind		8	22	30	61	133	15	103	21	26	8			
Amphora eximia	oligo-ind			13		2					3	3			
Amphora ovalis	oligo-ind					14		2		4					
Amphora pediculus	oligo-ind					2									
Cocconeis placentula euglypta	oligo-ind	81	7	2								1			2
Cyclotella stelligera	oligo-ind			10											
Cyclotella antiqua	oligo-ind	1													
Cymbell cistula var maculata	oligo-ind		1												
Cymbella caesiptosa	oligo-ind	36	146	27	2	8				2	7	6			9
Cymbella cistula	oligo-ind	5	15	3		1									1
Cymbella gracile	oligo-ind			1	1										
Cymbella Leptoceros	oligo-ind		1												
Cymbella microcephala	oligo-ind						1								
Cymbella minutuns fo latens	oligo-ind	14	13	18	9	20	2								
Cymbella silesiaca	oligo-ind			1											
Diploneis ovalis	oligo-ind			1											
Diploneis parma	oligo-ind						39								
Epithemia adnata	oligo-ind	2	6								1				2
Epithemia adnata var porcellus	oligo-ind		8		3		9		1			2			
Epithemia argus var porcellus	oligo-ind		15												
Epithemia sorex	oligo-ind	14	12		27	31		1		4	3	7			6
Epithemia Sorex var gracilis	oligo-ind	25	48	54		10		5		3	17	1			2
Epithemia Turgida	oligo-ind									1					
Fragilaria brevistrata	oligo-ind	6	11	2	3	2			2		21	1			1

Fragilaria construens	oligo-ind	2	16	21		17					4	3			1
Fragilaria construens var venter	oligo-ind		3			3					1		1		1
Fragilaria crotonensis	oligo-ind	13													
Fragilaria inflata	oligo-ind		2												
Fragilaria intermedia	oligo-ind										1				
Fragilaria pinnata	oligo-ind	2	5	2	78	38		1	2	4	12	3	1		3
Fragilaria pinnata var lancettula	oligo-ind														2
Fragilaria vaucheriae	oligo-ind	6	7	2	1	17	1		1						2
Gomphomema truncatum var capitata	oligo-ind			4											
Gomphonema acuminatum	oligo-ind											3			
Gomphonema parvulum	oligo-ind								1						
Gomphonema truncatum	oligo-ind					1									1
Gyrosigma acuminatum	oligo-ind		6	15	5	19	28	6	26	11	15	5	2	5	4
Mastogloia smithii var amphicephala	oligo-ind	9													
Melosira varians	oligo-ind											1			
Meridion circulare	oligo-ind											2		1	
Navicula creuzbergensis							2								
Navicula cryptocephala	oligo-ind		12												
Navicula cryptotenella	oligo-ind	7	18		4	3	13	6		4	12	8		9	2
Navicula declivis	oligo-ind								1						
Navicula ovalis	oligo-ind					19									
Navicula phyllepta	meso				3										
Navicula papula	oligo-ind		1												
Navicula radiosa	oligo-ind	12	24	1		1					1				6
Navicula recondita	oligo-ind			1											
Navicula rhynocephala	oligo-ind	1		13		6			11		5	5			2
Navicula stankovicii	oligo-ind								9						3
Navicula subtilissima	oligo-ind	22	2			15					8				2
Navicula tripunctata	oligo-ind					3									
Navicula tuscula	oligo-ind		4												
Navicula viridula	oligo-ind				3	6	1	2							
Navicula slesvicensis/137/meniscula					1		13								
Nitzschia ovalis	oligo-ind				6										2
Nitzschia dissipata	meso						1								
Nitzschia palea	oligo-ind						2	1	3	2	1				
Nitzschia paleacea	oligo-ind				5		1								1

Nitzschia sociabilis	oligo-ind	1		3		3			7	1	1			1	
Pinnularia (misc)	oligo-ind														1
Pinnularia microstauron	oligo-ind		1												
Pinnularia viridis	oligo-ind											2			
Rhopalodia Gibba	oligo-ind	2	6												3
Rhoiosigma abbreviatum	oligo-ind														1
Stauroneis elliptica	oligo-ind		6		50	23			93						
Stauroneis pinnata	oligo-ind		6	2				1			2				1
Staurosirella Sp.	oligo-ind											1			
Surirella brebbisonii	oligo-ind				2	4									
Surirella var kuetzigii	oligo-ind									1					
Synedra acus	oligo-ind	18	9												
Synedra parasitica var subconstricta	oligo-ind		4	21	2	3		2		1	1				2
Synedra tenera	oligo-ind	8													
Synedra ulna var bicepts	oligo-ind	3		3	3	3		1			1				
Synedra ulna var danica	oligo-ind									3					
Tabellaria fenestrata	oligo-ind		1											1	
Navicula decussis	oligo-hal										1				
Diatoma elongatum	oligo-hal	3							2		2				
Diatoma tenue	oligo-hal	5				1	2								1
Fragilariaforma virescens	oligo-hal	6	8	4			19		2		3				6
Navicula cincta	oligo-hal	28	4	9			1								2
Achnanthes gibberula	oligo-hal											1			1
Amphora commutata	meso								2		2				
Anomoeonis fo. Sphaeophora	meso		2	3		3					2				
Ctenophora pulchella	meso			24	6	32	22	4	30	5	10				
Cyclotella meneghiniana	meso		9												1
Diploneis interrupta	meso					4		1		2	1				
Diploneis psuedovalis	meso							7	21	3	6	1			
Navicula arenaria	meso													2	
Navicula digitaradiata	meso		12	8		1					3	12	4	11	9
Navicula peregrina	meso			10								1		1	1
Navicula peregrina (pieces)	meso										1			4	5
Navicula salinarum	meso		2				2	1			1				
Nitzschia acuminata	meso					2		6		*1*					
Nitzschia constricta	meso		1	2	2	2	8	35	1	31		2			

Nitzschia sigma	meso		3	8		2	4	146	2	115	3	14		2	5
Nitzschia sigma (pieces)	meso										3	8	3		
Nitzscia levidensis var salinarum	meso					1									
Pleurosigma strigosum	meso									1					
Rhopalodia Gibba var parellela	meso														
Rhopalodia Musculus	meso											1			
Rhopalodia Rupestris	meso				3	3	2		2						
Scolipleura tumida	meso							20	1	24					
Tabularia Fasiculata	meso				54	30	23		26		13	11	4	4	14
Tabularia Fasiculata (pieces)	meso										1	5	5	10	
Achnanthes danica	poly								2						
Cocconeis costata	poly										1				2
Cocconeis pinnata	poly												1		2
Cymatosia belgica	poly													1	
Endictya oceanica	poly													4	
Endictya oceanica (piece)	poly							1		2	3	9	2		6
licmophora hyalina	poly											2			
Navicula hudsonis	poly							16	1	17					
Navicula Sp.	poly														1
Nitzschia socialis	poly									2	3	1		4	
Nitzschia socialis (pieces)	poly													1	
Odontella (misc)	poly											1			
Odontella aurita	poly												2	3	2
Odontella obtusa	poly													1	
Rhabdonema arcuatum	poly											2	1	2	2
Tabularia Sp.	poly					9		3		10	2	2		6	
Tabularia Sp. (pieces)	poly							2		4		2	1	9	1
Thallassiosira eccentrica	poly									2	3	15	3	10	4
Thallassiosira eccentrica (pieces)	poly									8	17	28	20	44	24
Thallassiosira inerta	poly										4				1
Tryplionella levidensis	poly						1		1						
Tryplionella levidensis var salina							1								
Sample totals		389	466	310	313	425	332	286	355	289	228	182	50	137	153

Figure 4 Diatom assemblage information for Hrisholsvatn

Taxa name	Sample depth (cm)	
	433	436.5
Achnanthes levanderi		1
Amphora copulata	8	8
Ctenophora pulchella	9	4
Cymbella aspera		2
Cymbella caesipitosa	3	14
Cymbella minutuns fo. Latens		3
Cymbella microcephala		4
Diatoma ancepts		1
Diatom moniforme	1	
Diatoma tenue	7	4
Diploneis interrupter	3	1
Epithemia adnata		1
Epithemia adnata var porcellus	14	22
Fragilaria brevistrata	3	8
Fragilaria capucina		11
Fragilaria pinnata	16	13
Fragilaria vaucheriae	48	20
Fragilariafprma virescens	1	
Gyrosigma acuminatum	60	57
Hantzschia amphioxys	2	
Navicula cincta	11	9
Navicula digitaradiata var.	6	5
Navicula phylepta	2	6
Navicula radiosa	1	
Navicula rhynocephala	4	1
Navicula viridula (137)/slesvicensis	15	15
Nitzschia constricta	2	2
Nitzschia ovalis	2	
Nitzschia palae		2
Nitzschia palaceae	9	3
Nitzschia sigma/flexa/granulata/gracilis		14
Nitzschia sigma	8	3
Nitzschia sociabilis	1	3
Pinnularia krockii		4
Rhopalodia gibba	3	3
Rhopalodia rupestris	6	6
Stauroneis ancepts	1	
Surirella brebissonii	1	2
Synedra parasitica var subconstricta	40	41
Tabellaria fenestrata	1	1
Tryblionella levidensis var salinarum	16	9
Ttryblionella circumsuta	1	
Sample totals	305	303

Figure 5 Diatom assemblage information for Berufjardenvatn

Taxa name	Sample depths (cm)					
	390	398	401	404	408	418
Achnanthes frigida						
Achnanthes lanceolata		1	1	1		2
Achnanthes lanceolata var elliptica						
Achnanthes lemmermannii/laterostrata			13			4
Achnanthes levidensis				1		
Achnanthes minutissima			1	1		1
Achnanthes var intermedia (piece)					4	2
Amphipleura pellucida				19	1	3
Amphora copulata			15			
Amphora eximia						3
Brachysira brebissonii	2			2		
Brachysira brebissonii var thermalis				1		
Brachysira zellensis						
Cocconeis costata				7	33	93
Cocconeis placentula var euglypta					4	4
Cocconeis scutellum				3	7	28
Ctenophora pulchella				1	1	1
Cyclotella stelligera	6		4	3		1
Cymbella aspera						1
Cymbella caesipitosa	8	2	3	8		
Cymbella cistula	1					
Cymbella gracilis				1		
Cymbella microcephala			2	3		
Cymbella minutuns fo. Latens	15		1	4		
Cymbella navicularformis	2					
Denticula tenuis						1
Diatoma ancepts			1			
Diatoma tenue	1		3			
Diploneis parma (elliptica/smithii etc)	2	4	12	11		6
Epithemia adnata				1		

Epithemia adnata var porcellus				2		
Epithemia sorex				6	1	4
Epithemia sorex var gracilis	11		2	4		
Eunotia arcus				2		
Fragilaria brevistrata	1		2		1	4
Fragilaria construens	65	28	45	37	2	9
Fragilaria construens var venter				7		
Fragilaria pinnata	222	335	185	80	6	52
Fragilariaforma virescens						2
Gomphonema truncatum var capitata	2					
Gyrosigma acuminatum	3	6		7	2	6
Martyi martyi					1	2
Mastogloia smithii				2		
Navicula cincta						1
Navicula cryptotenella						
Navicula digitaradiata (B/F)	1			1		
Navicula digitaradiata (B/M)				1		
Navicula phyllepta	2			2		
Navicula pseudoscutiformis					1	
Navicula radiosa	9	2	1	8	2	7
Navicula rhynochephala						
Navicula Sp.						
Navicula subtillisima	4	1	6	22	3	4
Navicula viridula			2	1		
Nitzschia angusta (or?)						
Nitzschia dissipata						1
Nitzschia palaecea	3		2	8		3
Nitzschia sigma	6			7	17	8
Nitzschia sociabilis	4		4	3		
Nitzschia socialis				2	7	14
Pinnularia mesolepta				2		
Rhabdonema minutun					28	13
Rhopalodia gibba				5		
Rhopalodia gibba var parrallela				4		
see drawing (404 russian)				1		
Staurosirella pinnata				25		

Synedra montana	10		1			
Synedra parasitica var subconstricta	3		4			2
Synedra ulna var bicepts	1		2	3		
Synedra ulna var danica						
Tabularia fasiculata				3	21	23
Tabularia Sp.					2	2
Thallassiosira eccentrica (whole)						2
Thallassiosira eccentrica (piece)					7	6
Tryblionella levidensis			2			
Tryblionella Sp.					4	2
Odontella aurita						5
Sample totals	384	379	314	312	155	322

Figure 6 Diatom assemblage information for Hrishóls Bog

Taxa name	Sample depth (cm)					
	548cm	544cm	540cm	536cm	532cm	524cm
Achnanthes (misc.)						30
Achnanthes lanceolata	3					
Achnanthes levanderi	4					
Achnanthes minutissima	4					
Amphora copulata	42				1	50
Amphora eximia	38					
Brachysira brebissonii	1					
Cyclotella stelligera	2					
Cymbella amphicephala					1	
Cymbella aspera						2
Cymbella caespitosa	16					
Cymbella minutuns fo latens	4					
Denticula kuetzingii				1		4
Diploneis ovalis	2					1
Epithemia adnata var porcellus			2	4		1
Epithemia sorex						4
Fragilaria pinnata						1
Gomphonema parvulum					1	
Gomphonema truncatum var capitata				1		
Gyrosigma acuminatum						1
Meridion circulare	3					
Navicula palae	51					
Navicula phyllepta	4					
Navicula radiosa	4					1
Navicula subtillisima	1			1		
Nitzschia amphibia	2					
Nitzschia angustata	1					
Nitzschia fonticola	3					
Pinnularia abaujensis						1
Pinnularia microstauron	1					1
Rhopalodia gibba				1	3	7
Staurosirella pinnata	2					
Surirella brebissonii	9					
Synedra ulna var bicepts	2			1		
Tryblionella levidensis	8					
Sample totals	207		2	9	6	104

Figure 7 Diatom information for Hrishóls Bog 2

Taxa name	Sample depth (cm)	
	293cm	289cm
Achnanthes levanderi	3	
Amphora copulata		4
Amphora eximia		2
Cocconeis placentula var euglypta	11	5
Cymbella caespitosa	1	2
Epithemia adnata		5
Epithemia adnata var porcellus	36	7
Epithemia sorex		2
Eunotia tenella		1
Fragilaria brevistrata	22	15
Fragilaria construens	13	29
Fragilaria inflata	6	2
Fragilaria pinnata	14	10
Gomphonema parvulum		4
Gyrosigma acuminatum	2	
Navicu;a rhynocephala		1
Navicula radiosa	2	1
Nitzschia palea	6	2
Nitzschia sigma		1
Pinnularia abaujensis		1
Pinnularia mesolepta		5
Pinnularia microstauron	2	
Rhopalodia gibba	4	6
Stauroneis anceps		1
Synedra parasitica var subconstricta		6
Synedra ulna var bicepts	2	
Tryblionella levidensis		2
Sample totals	124	114

Figure 8 Diatom assemblage information for Hrishóls Bog 3

Taxa name	Sample depth (cm)	
	288cm	272cm
Achnanthes minutissima		1
Amphora copulata	3	
Cocconeis placentula var euglypta	20	4
Cyclotella antiqua	5	4
Cymbella aspera		1
Cymbella caespitosa	1	6
Cymbella minutuns fo latens	2	
Cymbella naviculartormis	5	1
Epithemia adnata	8	
Epithemia adnata var porcellus		9
Epithemia sorex		2
Fragilaria construens	12	35
Fragilaria construens var venter		5
Fragilaria pinnata	43	35
Fragilariaforma virescens		19
Gomphonema parvulum		2
Navicula radiosa	1	5
Navicula sociabilis		2
Navicula subtilissima		4
Nitzschia angustata		1
Nitzschia constricta		2
Pinnularia abaujensis	1	1
Pinnularia mesolepta	1	
Rhopalodia gibba	3	3
Rhopalodia rupestris		2
Stauroneis anceps	1	
Staurosirella lapponica		2
Synedra parsitica var subconstricta	1	
Synedra ulna var bicepts	2	
Tabellaria flocculosa		7
Sample totals	109	153

Figure 9 Diatom assemblage information for Mýrahnúksvatn

Taxa name	Hustedt Class. 1953	Sample depth (cm)												
		598	606	614	622	630	638	646	654	662	670	674	678	681.5
Brachysira serians fo	halophous	2												
Cymbella gracilis	halophous		1					1						
Eunotia pectinalis	halophous	3	2	3										
Eunotia subtilissima	halophous	3												
Eunotia spp	halophous	1	1											
Navicula laevissima	halophous						2	9						
Pinnularia nobilis	halophous					8	4	8						
Tabellaria flocculosa	halophous	15	14	21	22	3		1						
Achnanthes gibberula	oligo-hal		1											
Diatoma elongatum	oligo-hal	3												
Fragilariaforma virescens	oligo-hal	98	62	13	13	11	27	16			6	1		4
Achnanthes clevei	oligo-ind			17										
Achnanthes lanceolata	oligo-ind		5				6	3				1		7
Achnanthes levanderi	oligo-ind	7	12	11	1		4				2	1		5
Achnanthes minutissima	oligo-ind	26	32	15			3			1		5		
Achnanthes montana	oligo-ind		3											
Achnanthes oestrupii	oligo-ind	1	9		5		2	1						
Achnanthes rostrata	oligo-ind	1									3			
Amphipleura pellucida	oligo-ind	2												
Amphora copulata	oligo-ind	1			5		2	1	2	1	116	77	78	23
Amphora eximia	oligo-ind			2					4		108	113	102	45
Amphora ovalis	oligo-ind											10		1
Brachysira brebbissonii fo. themalis	oligo-ind	1												
Cocconeis placentula euglypta	oligo-ind	9	4	9	10	1	4							
Cyclotella antiqua	oligo-ind		11	8	8									
Cyclotella comta	oligo-ind	2												
Cymbella amphicephala	oligo-ind		1					2						
Cymbella caesiptosa	oligo-ind		1	2			1	1	2			24		1
Cymbella cistula	oligo-ind		1	1		1								
Cymbella cornuta	oligo-ind				9									

Cymbella lanceolata	oligo-ind				1									
Cymbella minutuns fo latens	oligo-ind													
Cymbella silesiaca	oligo-ind													
Cymbella casipitosa/minutuns	oligo-ind						2	1			58		45	
Diploneis ovalis	oligo-ind										5		4	3
Diplonies parma	oligo-ind											1	42	87
Epithemia adnata	oligo-ind													
Epithemia adnata var porcellus	oligo-ind	11	7	4	28									
Epithemia argus var porcellus	oligo-ind	3												
Epithemia sorex	oligo-ind			5	5									
Epithemia Sorex var gracilis	oligo-ind	8	7	3	28	2								
Fragilaria brevistrata	oligo-ind	7	35	43	4	19	69	32		2	1	3		3
Fragilaria construens	oligo-ind	29	31	42	55	182	182	128	78	286	7		2	
Fragilaria construens (barrelled)	oligo-ind	7	4	1										
Fragilaria construens var venter	oligo-ind	1		2	21	7	6	13	141	33				
Fragilaria crotonensis	oligo-ind	4	6	2										
Fragilaria inflata	oligo-ind		2	3										
Fragilaria leptostauron	oligo-ind		2							3				
Fragilaria pinnata	oligo-ind	6	8	21	15	51	55	60	79	33	33			
Fragilaria vaucheriae	oligo-ind	2	1				5							
Gomphomema truncatum var capitata	oligo-ind		2			1	1							
Gomphonema acuminatum	oligo-ind	1	1	1	4	2								
Gomphonema parvulum	oligo-ind	2		5	19	2								
Gomphonema truncatum	oligo-ind													
Hanaea var amphioxys	oligo-ind									1				
Mastogloia elliptica														2
Melosira varians	oligo-ind	1	4	5	3									
Meridion circulare	oligo-ind							2					1	1
Navicula cincta												1		
Navicula cryptotenella	oligo-ind	3								9				
Navicula novasiberica							1				2			
Navicula papula	oligo-ind		1											
Navicula pseudoscutiformis	oligo-ind				3	1								
Navicula radiosa	oligo-ind	3	1	4	1	9	9	9	4	4	7	6	17	4
Navicula rhynocephala	oligo-ind	1	1		6		2	3	4	16				
Navicula Sp	oligo-ind													4

Navicula subtiissima	oligo-ind			1										
Nitzschia amphibia	oligo-ind						2						8	
Nitzschia archibaldii	oligo-ind												3	
Nitzschia angustata/see drawing	oligo-ind	2				3	4	1				7		16
Nitzschia capitellata														2
Nitzschia dissipata	oligo-ind												4	
Nitzschia fonticola	oligo-ind											1		10
Nitzschia ovalis	oligo-ind	3									2	5		
Nitzschia palea	oligo-ind	3	3	1		1								5
Nitzschia paleacea	oligo-ind	6						1			3	21	3	7
Nitzschia sociabilis	oligo-ind			1							1			
Nitzschia supralittorea														1
Pinnularia microstauron	oligo-ind		1				7		32	42		3		
Pinnularia mesolepta	oligo-ind	2	1		3			2						
Rhopalodia gibba	oligo-ind	9	8	2	24									
Stauroneis ancepts	oligo-ind	2				17	4	2			1			
Stauroneis ancepts fo. gracilis	oligo-ind								1					
Surirella angusta	oligo-ind										6		6	
Surirella linearis	oligo-ind				1									
Surirella brebbisonii	oligo-ind	2									3	10	7	5
Synedra acus	oligo-ind			19		1	2							
Synedra parasitica var subconstricta	oligo-ind	1	1		7									
Synedra rumpens	oligo-ind			15										
Synedra ulna var bicepts	oligo-ind			1	2	1	2	4			6		2	
Tabellaria fenestrata	oligo-ind	2	9	5	4									
Tetracyclus emarginatus	oligo-ind	4	13	13	18	1		1			1			
Amphora proteus	meso												3	
Navicula phyllepta/simplex	meso											3	8	12
Rhopalodia gibba var parellela	meso			1										
Rhopalodia rupestris	meso			2										
Tryplionella levidensis	meso										7		22	
Tryplionella levidensis var salinarum	meso											15		57
Opephora marina	poly				7									
Cocconeis costata	poly										7		1	
Unidentified		5	3			4					6			
					2									

					13									
					2									
Sample totals		305	312	304	349	328	408	302	347	431	391	308	358	305

Figure 10 Diatom assemblage information for Djúpavik

Taxa name	Hustedt Class.	Sample depth (cm)													
	1953	310	325	374	390	405	418	422	446	466	502	518	522	530	538
Achnanthes (lanceolata) var. Elliptica	olig-indiff							5				2			
Achnanthes Delicatula	meso								1						
Achnanthes Gracillima		3													
Achnanthes Lanceolata (could be N. Schmassmanii	olig-indiff	4			1			4	2	1	1				
Achnanthes Ploenensis	olig-indiff							2							
Amphipleum pellucida	olig-indiff	3													
Amphora Copulata	olig-indiff			1	1	1	5	7				1		4	2
Amphora Eximia	olig-indiff							1							
Anomoeoneis Sphaerophora fo.				1											
Brachysira (serians fo.?)	halophobous		2	3	9	16			3	17		9	4		
Brachysira Sp./Anomoeoneis vitrea		10													
Cocconeis Costata	poly			1											
Cocconeis Placentula var. Euglypta	olig-indiff				2		2	3		1	20	3	1		1
Construen (barrelled)	olig-indiff	5	2				3						1		1
Cyclotella Antiqua	olig-indiff	1		2		1	1		1	8		1	2		4
Cyclotella Menghiniana	meso		9	46	2					5					
Cymbella Amphicephala	olig-indiff						1								
Cymbella Caespitosa	olig-indiff			2	2				2	3	6			3	
Cymbella Cesati/descripta	olig-indiff											3			
Cymbella Cistula	olig-indiff	8	2	7	3	1	2	1	3	9		1	2	3	3
Cymbella Cornuta	olig-indiff										1				
Cymbella minutuns	olig-indiff			3											
Cymbella minutuns fo. Latens	olig-indiff	3	2	2	2		3	2			1	5	11	1	3
Cymbella Gracile	halophobous				1	2			10				1		3
Cymbella Naviculaformis	olig-indiff		1			2							1		
Cymbella Similis/Descriptor?	olig-indiff						2								
Denticula Kuetzingii	oligo-halophil									1					
Diatoma (hymale) var. Quadratum							1	5				1			
Meridion Circulare	oligo-indiff	3	1		3	4	9	38	2	3	3	4	2		
Diatoma Tenue	oligo-halophil							1							

Epithemia Adnata	olig-indiff														
Epithemia (adnata) var. Porcellus	olig-indiff	1	8	6	5	5	4		4	4	19	3	8	12	
Epithemia (argus) var. Porcellus	olig-indiff													9	3
Epithemia (sorex) var. Gracilis	olig-indiff		3	15	4	7	2		8	4	8	2	31	9	5
Epithemia Sorex	olig-indiff		5	2											1
Eunotia?		1													
Eunotia (pectinalis) fo. Intermedia	halophobous							1							1
Eunotia (Veneris?)														1	
Eunotia Arcus	halophobous									1					
Eunotia Curvata	halophobous														1
Eunotia Exiqua	halophobous						1								
Eunotia Glacilis	halophobous							1							
Eunotia Pectinalis	halophobous		2	1	4			1	2			4			
Eunotia Tenella	halophobous											4			
Eunotians Lunans (Forged)/ E. Sp (H218)	halophobous						4								
F. Alpestris	olig-indiff							7							
F. Brevistrata	olig-indiff	8	34	18	6	6	8	1	3	5		4	1	8	13
F. Construens	olig-indiff	81	65	58	50	30	37	18	27	36	15	73	53	61	135
F. Construens var. Binodis	olig-indiff	12											1		1
F. Construens var. Venter	olig-indiff		7	20	10	7	1	4	5	13	3		5	10	4
F. Crotonensis	olig-indiff	3	6	1	3			2					1		2
F. Inflata	olig-indiff		3				3		1	3	2	4		3	3
F. lapponica	olig-indiff								1						
F. Leptostauron	olig-indiff	10	10	11	5	5	7	3	13	8	2		1	1	
F. Pinnata	olig-indiff	47	48	50	15	47	11	19	70	7	30	29	11	73	14
F. Vauchariae	olig-indiff						3	7	1			3			
Fragilariaforma Virescens	oligo-halophil	64	55	68	44	46	65	40	58	55	51	16	9	44	21
Fragilariaforma (constricta) fo. Stricta								1							
Fragilariaforma Bicapitata	olig-indiff						2								
Gomphonema (truncatum) var. Capitata	olig-indiff	2		9	4	5	1				2		1		2
Gomphonema Acuminatum	olig-indiff	2	4	12	1	7	5	2	5	13	7	3	10	3	9
Gomphonema Parvulum	olig-indiff	1	3	3			3			3			4	3	4
Hannaea Arcus var. Amphioxys	olig-indiff							13							
Hantschia Amphioxys	olig-indiff							3							
Melosira Varians	olig-indiff									1					
N. Angusta	halophobous							1							

N. Cincta	oligo-halophil				2											
N. Laevissima	halophobous	1								1						
N. Papula							1									
N. Pseudoscutiformis			1			1	3	2	1	2		5				
N. Radiosa	oligo-indiff	5	6	13	9	4	7	17	7	9	5	3		2	1	
N. Subtilissima		2	1	1	3	6	2	2	1	7		3	2		1	
Neidium Alpina							2									
Nitzschia Dissipata	oligo-indiff						1								1	
Nitzschia Gracilis								4								
Nitzschia palaea				2												
Nitzschia Paleacea	oligo-indiff														1	
Nitzschia Sigma	meso				1											
Nitzschia Aciculans									1							
Nitzschia Angustata	meso	4			1	2			1	7	1	2	2	1	10	
Nitzschia Sociabilis	oligo-indiff	4	1	1	5	8		4	3	5	3	11	7	2		
Nitzschia Socialis	poly								1							
Orthoseira Epidendron fo. (Planktonic)	olig-indiff										1					
Pinnularia Abaujensis (var. linearis-small version)	olig-indiff														2	
Pinnularia Mesolepta	olig-indiff		1	1			5	5	1			2			1	
Pinnularia Microstauron	olig-indiff		1		1	1	2	1							1	
Pinnularia Rupestris	meso						3								1	
Pinnularia subsolaris	olig-indiff			2												
Pinnularia Sp. (250-300um long/40um wide)	olig-indiff		3	4												
Pinnularia Viridis	olig-indiff	4				2		3	1	6	3					
Pinnularia Viridis (sudentica?)	olig-indiff															
Pinnularia (misc pieces/large type)	olig-indiff													1		
Rhopalodia (gibba) var. Parellela	meso	5	2	3	2	2								1		
Rhopalodia Gibba	olig-indiff		1	3	3	12	1	1	10	5	1		8	2		
Rhopalodia Rupestris	meso		1							2						
Stauroneis (Ancepts) fo. Gracilis	oligo-indiff							1								
Stauroneis Ancepts??	oligo-indiff							3			1					
Stauroneis Ancepts fo linearlis	oligo-indiff	2	3	2												
Stauroneis Phoenicenteron	oligo-indiff								1							
Staurosira Elliptica	oligo-indiff	1	7	6	7	1	2	1	1	4	6					
Staurosirella Pinnata	oligo-indiff	1	6	5	8	2	5	3	3					2		
Synedra Arcus	oligo-indiff	5	1	3	2	8	3		5	7	1	1	1	1	1	

Synedra Parasitica var subconstricta	oligo-indiff	1	4			1							1	1	1
Synedra Ulna var. Bicepts	oligo-indiff	3	6	4	2	2	3	2	2	4	3			1	
Synedra Ulna var. Danica	oligo-indiff				2										
Tabellaria Fenestrata	oligo-indiff	28	26	44	11	17	13	7	19	23	38	13	12	15	11
Tabellaria Flocculosa	halophobous	8	22	24	26	21	24	40	14	38	24	38	49	26	37
Tetracyclus Emarginatus	oligo-indiff		1				3	7		2		1		1	
Achnanthes minutissima	oligo-indiff	1	2	3	23	4		7	8	23	16	54	43	2	9
Achnanthes minutissima	oligo-indiff		1		6	22	10	6	1	6	2	10	9	3	6
Martyi martyi	oligo-indiff	8	11	8	9	6	11	8	14	13	20	7			
Sample totals		355	380	471	300	314	287	317	317	365	296	325	295	316	320

Figure 11 Loss on ignition analysis

Sample	Core	Depth (cm)	Crucible weight (g)	Sample dry weight (g)	Ignited weight (g)	Dry-ignited	Dry-crucible	%LOI
1	Mavatn	95	19.3212	20.3933	20.3673	0.026	1.0721	2.425146908
2	Mavatn	91	17.175	18.2583	18.2299	0.0284	1.0833	2.621619127
3	Mavatn	87	19.5516	20.8148	20.7749	0.0399	1.2632	3.158644712
4	Mavatn	83	19.3394	20.5631	20.5313	0.0318	1.2237	2.598676146
5	Mavatn	75	18.2915	19.4473	19.4051	0.0422	1.1558	3.651150718
6	Mavatn	71	19.5677	20.2169	20.161	0.0559	0.6492	8.610597659
7	Mavatn	67	19.4307	20.0159	19.9606	0.0553	0.5852	9.449760766
8	Mavatn	63		19.5952	19.5481	0.0471	0.3621	13.0074565
9	Hafrafellvatn	358	19.1864	19.5170	19.3979	0.1191	0.3306	36.02540835
10	Hafrafellvatn	362	19.4802	19.8961	19.7495	0.1466	0.4159	35.2488579
11	Hafrafellvatn	366	19.3663	19.7132	19.6089	0.1043	0.3469	30.06630153
12	Hafrafellvatn	370	17.8745	18.3066	18.2073	0.0993	0.4321	22.98079148
13	Hafrafellvatn	374	19.1437	19.5453	19.4484	0.0969	0.4016	24.12848606
14	Hafrafellvatn	378	20.0094	20.4467	20.349	0.0977	0.4373	22.34164189
15	Hafrafellvatn	382	19.7588	20.2746	20.1842	0.0904	0.5158	17.52617294
16	Hafrafellvatn	386	19.4104	20.0311	19.9366	0.0945	0.6207	15.22474625
17	Hafrafellvatn	390	19.4586	20.1314	20.0391	0.0923	0.6728	13.71878716
18	Hafrafellvatn	394	19.8075	20.6361	20.5382	0.0979	0.8286	11.81510982
19	Hafrafellvatn	398	17.5807	18.5038	18.4284	0.0754	0.9231	8.16812913
20	Hafrafellvatn	402	19.2731	20.0022	19.921	0.0812	0.7291	11.13701824
21	Hafrafellvatn	406	17.4425	18.3698	18.2998	0.0700	0.9273	7.548797584
22	Hafrafellvatn	410	17.1590	17.9836	17.9367	0.0469	0.8246	5.687606112
23	Hafrafellvatn	414	*19.3705*	20.8341	20.7877	0.0464	1.4636	3.1702651
24	Hafrafellvatn	418	*19.3000*	20.4647	20.4243	0.0404	1.1647	3.468704387
25	Hafrafellvatn	422	*19.4569*	20.8493	20.8085	0.0408	1.3924	2.930192473
26	Hafrafellvatn	426	17.5968	18.8980	18.8635	0.0345	1.3012	2.651398709
27	Hafrafellvatn	430	19.9513	21.2138	21.1814	0.0324	1.2625	2.566336634
28	Hafrafellvatn	434	16.9818	18.3281	18.2934	0.0347	1.3463	2.57743445
29	Hafrafellvatn	438	19.3422	21.0117	20.9711	0.0406	1.6695	2.431865828

30	Berufjardenvatn	364	19.4605	19.7751	19.7489	0.0262	0.3146	8.328035601
31	Berufjardenvatn	368	19.2811	19.5622	19.5444	0.0178	0.2811	6.332266097
32	Berufjardenvatn	372	19.2352	19.5672	19.539	0.0282	0.332	8.493975904
33	Berufjardenvatn	376	19.5238	19.8203	19.7971	0.0232	0.2965	7.824620573
34	Berufjardenvatn	380	19.3932	19.6704	19.6452	0.0252	0.2772	9.090909091
35	Berufjardenvatn	384	17.9028	18.2132	18.1901	0.0231	0.3104	7.442010309
36	Berufjardenvatn	388	19.1677	19.5734	19.5447	0.0287	0.4057	7.074192753
37	Berufjardenvatn	392	20.0327	20.3462	20.3213	0.0249	0.3135	7.942583732
38	Berufjardenvatn	396	19.783	20.1306	20.108	0.0226	0.3476	6.501726122
39	Berufjardenvatn	400	19.4329	19.8061	19.7807	0.0254	0.3732	6.806002144
40	Berufjardenvatn	404	19.4787	20.1722	20.1474	0.0248	0.6935	3.576063446
41	Berufjardenvatn	408	19.8268	20.5916	20.5679	0.0237	0.7648	3.098849372
42	Berufjardenvatn	404	17.5959	18.528	18.4977	0.0303	0.9321	3.250724171
43	Berufjardenvatn	408	19.2871	19.9098	19.8905	0.0193	0.6227	3.099405813
44	Berufjardenvatn	412	17.4529	18.0396	18.0194	0.0202	0.5867	3.442986194
45	Berufjardenvatn	416	17.167	17.8153	17.7924	0.0229	0.6483	3.532315286
46	Berufjardenvatn	420	19.3721	20.0296	20.0073	0.0223	0.6575	3.391634981
47	Berufjardenvatn	424	19.299	19.8754	19.8566	0.0188	0.5764	3.261623872
48	Berufjardenvatn	428	17.598	20.5152	20.4806	0.0346	2.9172	1.186068833
49	Berufjardenvatn	432	19.9518	18.5755	18.5452	0.0303		
50	Berufjardenvatn	436	19.4593	20.6676	20.6408	0.0268	1.2083	2.21799222
51	Berufjardenvatn	440	16.9825	17.7122	17.6904	0.0218	0.7297	2.987529122
52	Berufjardenvatn	446	16.8253	17.6922	17.6668	0.0254	0.8669	2.92998039
53	Mýrahnúksvatn	594	17.235	18.3373	18.331	0.0063	1.1023	0.571532251
54	Mýrahnúksvatn	598	19.6638	21.0292	21.0274	0.0018	1.3654	0.131829501
55	Mýrahnúksvatn	602	19.3979	20.9428	20.9414	0.0014	1.5449	0.090620752
56	Mýrahnúksvatn	606	18.3484	19.8489	19.8484	0.0005	1.5005	0.033322226
57	Mýrahnúksvatn	610	19.6251	20.0805	20.0301	0.0504	0.4554	11.06719368
58	Mýrahnúksvatn	614	19.4078	19.8292	19.7803	0.0489	0.4214	11.60417655
59	Mýrahnúksvatn	618	19.4591	19.9295	19.8823	0.0472	0.4704	10.03401361
60	Mýrahnúksvatn	622	19.2787	19.719	19.6733	0.0457	0.4403	10.37928685
61	Mýrahnúksvatn	626	19.2333	19.6696	19.6274	0.0422	0.4363	9.672243869
62	Mýrahnúksvatn	630	19.5213	19.9525	19.92	0.0325	0.4312	7.537105751
63	Mýrahnúksvatn	634	19.3918	19.8391	19.8083	0.0308	0.4473	6.885758998

64	Mýrahnúksvatn	638	17.9018	18.4147	18.3784	0.0363	0.5129	7.077403003
65	Mýrahnúksvatn	642	19.1668	19.7084	19.6796	0.0288	0.5416	5.317577548
66	Mýrahnúksvatn	646	20.0309	20.5299	20.4989	0.031	0.499	6.21242485
67	Mýrahnúksvatn	650	19.7807	20.2622	20.2346	0.0276	0.4815	5.732087227
68	Mýrahnúksvatn	654	19.4311	19.9378	19.9066	0.0312	0.5067	6.157489639
69	Mýrahnúksvatn	658	19.4767	20.0146	19.9878	0.0268	0.5379	4.982338725
70	Mýrahnúksvatn	662	19.8243	20.751	20.7287	0.0223	0.9267	2.406388259
71	Mýrahnúksvatn	666	17.5941	18.1057	18.083	0.0227	0.5116	4.437060203
72	Mýrahnúksvatn	670	19.2848	20.3168	20.2889	0.0279	1.032	2.703488372
73	Mýrahnúksvatn	674	17.4502	18.6787	18.6502	0.0285	1.2285	2.31990232
74	Mýrahnúksvatn	678	17.1646	18.1732	18.1477	0.0255	1.0086	2.52825699
75	Mýrahnúksvatn	680	19.3691	20.5889	20.5646	0.0243	1.2198	1.992129857
76	Djúpavik	304	19.2972	19.5456	19.499	0.0466	0.2484	18.76006441
77	Djúpavik	308	19.4563	19.854	19.8125	0.0415	0.3977	10.43500126
78	Djúpavik	312	17.5965	17.7353	17.705	0.0303	0.1388	21.82997118
79	Djúpavik	316	19.9506	20.1829	20.1333	0.0496	0.2323	21.35170039
80	Djúpavik	320	16.9812	17.2202	17.1725	0.0477	0.239	19.958159
81	Djúpavik	324	19.3422	19.5627	19.5152	0.0475	0.2205	21.54195011
82	Djúpavik	328	17.0745	17.3189	17.2706	0.0483	0.2444	19.76268412
83	Djúpavik	332	19.5416	19.8141	19.7654	0.0487	0.2725	17.87155963
84	Djúpavik	336	19.7945	20.0545	20.0104	0.0441	0.26	16.96153846
85	Djúpavik	340	19.8152	20.1015	20.0577	0.0438	0.2863	15.29863779
86	Djúpavik	344	18.9349	19.252	19.2041	0.0479	0.3171	15.10564491
87	Djúpavik	348	17.1271	17.3847	17.3361	0.0486	0.2576	18.86645963
88	Djúpavik	344	17.3652	17.6561	17.6066	0.0495	0.2909	17.01615675
89	Djúpavik	348	18.939	19.2587	19.2122	0.0465	0.3197	14.54488583
90	Djúpavik	352	20.1464	20.4289	20.3742	0.0547	0.2825	19.36283186
91	Djúpavik	356	16.8255	17.0795	17.0302	0.0493	0.254	19.40944882
92	Djúpavik	360	16.2903	16.5352	16.4883	0.0469	0.2449	19.15067374
93	Djúpavik	364	17.2456	17.4765	17.4249	0.0516	0.2309	22.34733651
94	Djúpavik	368	17.1493	17.3739	17.3212	0.0527	0.2246	23.46393589
95	Djúpavik	372	16.8564	17.0824	17.0281	0.0543	0.226	24.02654867
96	Djúpavik	376	17.3008	17.5411	17.4851	0.056	0.2403	23.30420308
97	Djúpavik	380	16.359	16.6283	16.565	0.0633	0.2693	23.50538433
98	Djúpavik	384	16.0587	16.3192	16.2613	0.0579	0.2605	22.22648752

99	Djúpavik	388	17.5264	17.7753	17.722	0.0533	0.2489	21.41422258
100	Djúpavik	384	17.4257	17.7077	17.6472	0.0605	0.282	21.45390071
101	Djúpavik	388	17.1697	17.4161	17.3579	0.0582	0.2464	23.62012987
102	Djúpavik	392	16.4044	16.6738	16.6121	0.0617	0.2694	22.90274684
103	Djúpavik	396	16.1816	16.4965	16.4436	0.0529	0.3149	16.7989838
104	Djúpavik	400	17.339	17.6865	17.6291	0.0574	0.3475	16.51798561
105	Djúpavik	404	15.2047	15.5363	15.4886	0.0477	0.3316	14.38480097
106	Djúpavik	408	21.0306	21.586	21.5255	0.0605	0.5554	10.89305005
107	Djúpavik	412	20.6892	21.3025	21.2425	0.06	0.6133	9.783140388
108	Djúpavik	416	20.479	21.2154	21.1487	0.0667	0.7364	9.057577404
109	Djúpavik	420	20.3271	21.4733	21.4115	0.0618	1.1462	5.391729192
110	Djúpavik	424	20.6254	21.0544	21.0003	0.0541	0.429	12.61072261
111	Djúpavik	428	37.0244	37.4491	37.3794	0.0697	0.4247	16.41158465
112	Djúpavik	424	30.826	31.1167	31.0695	0.0472	0.2907	16.23667011
113	Djúpavik	428	33.326	33.5984	33.5553	0.0431	0.2724	15.82232012
114	Djúpavik	432	33.684	33.9818	33.9366	0.0452	0.2978	15.17797179
115	Djúpavik	436	17.9432	18.3078	18.2655	0.0423	0.3646	11.60175535
116	Djúpavik	440	18.3895	18.6806	18.6417	0.0389	0.2911	13.36310546
117	Djúpavik	444	17.9872	18.2773	18.2315	0.0458	0.2901	15.78765943
118	Djúpavik	448	38.6331	38.9523	38.911	0.0413	0.3192	12.93859649
119	Djúpavik	452	43.4522	43.9071	43.8668	0.0403	0.4549	8.85908991
120	Djúpavik	456	40.5194	40.8989	40.8538	0.0451	0.3795	11.88405797
121	Djúpavik	460	39.8573	40.1377	40.0953	0.0424	0.2804	15.12125535
122	Djúpavik	464	44.3172	44.7285	44.6839	0.0446	0.4113	10.84366642
123	Djúpavik	468	40.3371	40.7221	40.6772	0.0449	0.385	11.66233766
124	Djúpavik	464	43.0548	43.3883	43.3396	0.0487	0.3335	14.60269865
125	Djúpavik	468	38.2634	38.5884	38.544	0.0444	0.325	13.66153846
126	Djúpavik	472	40.2471	40.6102	40.562	0.0482	0.3631	13.27458001
127	Djúpavik	476	38.9972	39.393	39.3503	0.0427	0.3958	10.78827691
128	Djúpavik	480	38.5202	38.8514	38.8031	0.0483	0.3312	14.58333333
129	Djúpavik	484	39.4514	39.7457	39.696	0.0497	0.2943	16.88752973
130	Djúpavik	488	38.7303	39.0329	38.9797	0.0532	0.3026	17.58096497
131	Djúpavik	492	17.235	17.5146	17.4586	0.056	0.2796	20.0286123
132	Djúpavik	496	19.6636	19.9406	19.8844	0.0562	0.277	20.28880866
133	Djúpavik	500	19.3984	19.6837	19.6273	0.0564	0.2853	19.76866456
134	Djúpavik	504	18.3482	18.6263	18.5658	0.0605	0.2781	21.75476447

135	Djúpavik	508	19.6254	19.932	19.8778	0.0542	0.3066	17.67775603
136	Djúpavik	495	19.4083	19.6864	19.6293	0.0571	0.2781	20.53218267
137	Djúpavik	499	19.46	19.7529	19.6964	0.0565	0.2929	19.28986002
138	Djúpavik	503	19.281	19.5749	19.513	0.0619	0.2939	21.06158557
139	Djúpavik	507	19.2347	19.4957	19.4442	0.0515	0.261	19.73180077
140	Djúpavik	511	19.5228	19.8542	19.8017	0.0525	0.3314	15.84188292
141	Djúpavik	515	19.3932	19.708	19.6574	0.0506	0.3148	16.07369759
142	Djúpavik	520	17.9016	18.2841	18.2397	0.0444	0.3825	11.60784314
143	Djúpavik	524	19.1675	19.4759	19.4352	0.0407	0.3084	13.19714656
144	Djúpavik	528	20.0309	20.4442	20.4009	0.0433	0.4133	10.47665134
145	Djúpavik	532	19.7811	20.1503	20.1059	0.0444	0.3692	12.02600217
146	Djúpavik	536	37.0237	37.4884	37.4485	0.0399	0.4647	8.586184635
147	Djúpavik	540	34.8081	35.1939	35.1492	0.0447	0.3858	11.58631415

Figure 12 Diatom abundance analysis

Core	Depth (cm)	Wet weight (g)	Diatom count	Slide count	% Organics	%non-organics	LOI controlled	1-weightloi*count	Diatoms per gram
Djúpavik	304	0.52	11704	1287440	18.7600644	81.23993559	0.422447665	2.367157124	3047572.768
Djúpavik	312	0.46	10208	1122880	21.8299712	78.17002882	0.359582133	2.78100581	3122735.804
Djúpavik	316	0.52	10384	1142240	21.3517004	78.64829961	0.408971158	2.445160204	2792959.791
Djúpavik	324	0.45	11418	1255980	21.5419501	78.45804989	0.353061224	2.832369942	3557400
Djúpavik	332	0.45	13574	1493140	17.8715596	82.12844037	0.369577982	2.705788899	4040121.636
Djúpavik	340	0.47	14344	1577840	15.2986378	84.70136221	0.398096402	2.511954376	3963462.093
Djúpavik	348	0.47	11671	1283810	16.7056727	83.29432727	0.391483338	2.554387128	3279347.739
Djúpavik	352	0.5	11825	1300750	19.3628319	80.63716814	0.403185841	2.48024583	3226179.763
Djúpavik	360	0.44	10912	1200320	19.1506737	80.84932626	0.355737036	2.811065197	3374177.778
Djúpavik	364	0.54	14322	1575420	22.3473365	77.65266349	0.419324383	2.384788581	3757043.626
Djúpavik	368	0.58	9724	1069640	23.4639359	76.53606411	0.443909172	2.252713085	2409592.024
Djúpavik	376	0.47	12727	1399970	23.3042031	76.69579692	0.360470246	2.774154073	3883732.478
Djúpavik	384	0.46	10197	1121670	21.8401941	78.15980589	0.359535107	2.781369553	3119778.786
Djúpavik	388	0.48	12243	1346730	22.5171762	77.48282378	0.371917554	2.688767951	3621044.463
Djúpavik	396	0.57	14278	1570580	16.7989838	83.2010162	0.474245792	2.108611223	3311742.614
Djúpavik	400	0.47	11825	1300750	16.5179856	83.48201439	0.392365468	2.548644268	3315149.032
Djúpavik	404	0.46	13222	1454420	14.384801	85.61519903	0.393829916	2.53916719	3693015.544
Djúpavik	408	0.48	16786	1846460	10.8930501	89.10694995	0.42771336	2.338014414	4317050.094
Djúpavik	412	0.47	11583	1274130	9.78314039	90.21685961	0.42401924	2.358383548	3004887.23
Djúpavik	416	0.46	11736	1290960	9.0575774	90.9424226	0.418335144	2.390427901	3085946.803
Djúpavik	420	0.45	8800	968000	5.39172919	94.60827081	0.425737219	2.348866757	2273703.021
Djúpavik	424	0.52	12144	1335840	14.4236964	85.57630364	0.444996779	2.247207277	3001909.369
Djúpavik	428	0.48	14168	1558480	16.1169524	83.88304762	0.402638629	2.483616646	3870666.87
Djúpavik	432	0.53	13156	1447160	15.1779718	84.82202821	0.449556749	2.224413272	3219081.91
Djúpavik	436	0.57	10428	1147080	11.6017554	88.39824465	0.503869995	1.984638917	2276539.608
Djúpavik	440	0.6	15499	1704890	13.3631055	86.63689454	0.519821367	1.923737774	3279761.294
Djúpavik	444	0.56	13211	1453210	15.7876594	84.21234057	0.471589107	2.12049003	3081517.316
Djúpavik	448	0.58	15994	1759340	12.9385965	87.06140351	0.50495614	1.980370017	3484144.185
Djúpavik	452	0.59	9647	1061170	8.85908991	91.14091009	0.53773137	1.859664614	1973420.299
Djúpavik	456	0.52	13167	1448370	11.884058	88.11594203	0.458202899	2.182439271	3160979.567
Djúpavik	460	0.46	8316	914760	15.1212554	84.87874465	0.390442225	2.561198392	2342881.841

Djúpavik	464	0.46	13024	1432640	12.7231825	87.27681747	0.40147336	2.490825292	3568455.946
Djúpavik	468	0.48	10164	1118040	12.6619381	87.33806194	0.419222697	2.385367029	2666935.753
Djúpavik	472	0.42	11407	1254770	13.27458	86.72541999	0.364246764	2.745391583	3444834.997
Djúpavik	480	0.48	12708	1397880	14.5833333	85.41666667	0.41	2.43902439	3409463.415
Djúpavik	484	0.49	15774	1735140	16.8875297	83.11247027	0.407251104	2.45548751	4260614.598
Djúpavik	496	0.48	15730	1730300	20.2888087	79.71119134	0.382613718	2.613602053	4522315.633
Djúpavik	508	0.47	14916	1640760	17.677756	82.32224397	0.386914547	2.584550022	4240626.294
Djúpavik	518	0.47	15345	1687950	14.0315306	85.46305488	0.401676358	2.489566489	4202263.754
Djúpavik	528	0.46	14388	1582680	10.4766513	89.52334866	0.411807404	2.428319624	3843252.902
Djúpavik	532	0.46	14278	1570580	12.0260022	87.97399783	0.40468039	2.471085886	3881038.07
Djúpavik	540	0.42	18359	2019490	11.5863142	88.41368585	0.371337481	2.692968128	5438422.205
Mýrahnúksvatn	594	0.4864	110	12100	0.57153225	99.42846775	0.483620067	2.067738847	25019.64005
Mýrahnúksvatn	598	0.468	24	2640	0.1318295	99.8681705	0.467383038	2.139572725	5648.471993
Mýrahnúksvatn	602	0.537	26	2860	0.09062075	99.90937925	0.536513367	1.863886461	5330.715278
Mýrahnúksvatn	606	0.4866	59	6490	0.03332223	99.96667777	0.486437854	2.055761063	13341.8893
Mýrahnúksvatn	610	0.4831	9273	1020030	11.0671937	88.93280632	0.429634387	2.327560431	2374181.467
Mýrahnúksvatn	614	0.4693	8338	917180	11.6041766	88.39582345	0.414841599	2.410558636	2210916.17
Mýrahnúksvatn	618	0.4521	7557	831270	10.0340136	89.96598639	0.406736224	2.458595866	2043756.985
Mýrahnúksvatn	622	0.5055	13167	1448370	10.3792869	89.62071315	0.453032705	2.207346156	3197053.952
Mýrahnúksvatn	626	0.5339	10087	1109570	9.67224387	90.32775613	0.48225989	2.073570746	2300771.893
Mýrahnúksvatn	630	0.5275	23419	2576090	7.53710575	92.46289425	0.487741767	2.050265258	5281667.828
Mýrahnúksvatn	634	0.4742	21450	2359500	6.885759	93.114241	0.441547731	2.264760818	5343703.15
Mýrahnúksvatn	638	0.5364	21373	2351030	7.077403	92.922597	0.49843681	2.006272369	4716806.527
Mýrahnúksvatn	642	0.4667	15312	1684320	5.31757755	94.68242245	0.441882866	2.263043168	3811688.869
Mýrahnúksvatn	646	0.4288	12474	1372140	6.21242485	93.78757515	0.402161122	2.48656557	3411916.081
Mýrahnúksvatn	650	0.4291	14355	1579050	5.73208723	94.26791277	0.404503614	2.472165801	3903673.407
Mýrahnúksvatn	654	0.4775	21945	2413950	6.15748964	93.84251036	0.448097987	2.231654748	5387102.978
Mýrahnúksvatn	658	0.4547	16929	1862190	4.98233873	95.01766128	0.432045306	2.314572075	4310172.972
Mýrahnúksvatn	662	0.4902	14223	1564530	2.40638826	97.59361174	0.478403885	2.09028403	3270312.073
Mýrahnúksvatn	666	0.4451	13387	1472570	4.4370602	95.5629398	0.425350645	2.351001489	3462014.263
Mýrahnúksvatn	670	0.4918	9966	1096260	2.70348837	97.29651163	0.478504244	2.089845622	2291014.162
Mýrahnúksvatn	674	0.5386	2453	269830	2.31990232	97.68009768	0.526105006	1.900761233	512882.4035
Mýrahnúksvatn	678	0.4811	3135	344850	2.52825699	97.47174301	0.468936556	2.132484636	735387.3266
Mýrahnúksvatn	680	0.4603	3872	425920	1.99212986	98.00787014	0.451130226	2.216654841	944117.6299

Figure 13 Biogenic silica analysis

Sample	Core	Depth (cm)	Silica (ppm)	Alluminium (ppm)	%Bsi
1	Mavatn	63	76885448.68	17131.831	7.685118502
2	Mavatn	65	105781398	32027.43	10.57173432
3	Mavatn	67	83275479.53	15282.596	8.324491434
4	Mavatn	69	31853636.5	9529.248	3.1834578
5	Mavatn	70	200229768.1	227292.646	19.97751828
6	Mavatn	71	150366279.6	351487.124	14.96633053
7	Mavatn	72	99386661.84	373937.209	9.863878742
8	Mavatn	73	341347754.9	112679.466	34.11223959
9	Mavatn	75	533139703.2	794767.036	53.15501691
10	Mavatn	77	39495485.1	55154.671	3.938517576
11	Mavatn	79	21845940.25	40871.902	2.176419645
12	Mavatn	81	23935696.68	69724.723	2.379624723
13	Mavatn	83	17911830.18	53685.38	1.780445942
14	Mavatn	85	31617739.61	67207.226	3.148332515
15	Mavatn	87	17832969.89	68189.024	1.769659184
16	Mavatn	89	18273428.99	60715.474	1.815199804
17	Mavatn	91	21284520.36	75263.307	2.113399375
18	Mavatn	93	17355733.88	39806.868	1.727612014
19	Mavatn	95	25892424.31	83918.252	2.572458781
20	Hafrafellvatn	354	72429362.11	37137.451	7.23550872
21	Hafrafellvatn	358	68493876.53	27028.11	6.843982031
22	Hafrafellvatn	362	54433265.47	30086.04	5.437309339
23	Hafrafellvatn	366	85736544.01	26862.978	8.568281805
24	Hafrafellvatn	370	49580092.45	16174.62	4.954774321
25	Hafrafellvatn	374	44371935.86	15858.009	4.434021984
26	Hafrafellvatn	378	91754821.27	26652.477	9.170151632
27	Hafrafellvatn	382	116507381	49842.218	11.64076966
28	Hafrafellvatn	386	40560258.76	41725.536	4.047680769
29	Hafrafellvatn	390	88220736.74	87540.377	8.804565598
30	Hafrafellvatn	394	211787605.9	432535.682	21.09225346
31	Hafrafellvatn	398	31950228.66	86632.275	3.177696411
32	Hafrafellvatn	402	51475043.11	144871.699	5.118529971
33	Hafrafellvatn	406	26815355.67	82532.334	2.6650291
34	Hafrafellvatn	410	65302213.57	398945.856	6.450432186
35	Hafrafellvatn	414	16735943.56	70292.709	1.659535814
36	Hafrafellvatn	418	24314687.99	125952.16	2.406278367
37	Hafrafellvatn	422	82632176.59	400795.807	8.183058497
38	Hafrafellvatn	426	86038279.59	459489.585	8.511930042
39	Hafrafellvatn	430	43056843.56	340233.548	4.237637647
40	Hafrafellvatn	434	14779024.25	65457.763	1.464810873
41	Hafrafellvatn	438	23252771.29	114190.748	2.30243898
42	Hafrafellvatn	442	16076972.59	101755.338	1.587346191
43	Mýrahnúksvatn	594	109413145.668	1301601.39	10.68099429
44	Mýrahnúksvatn	598	203859277.996	3167607.516	19.7524063
45	Mýrahnúksvatn	602	81772791.577	3231129.368	7.531053284
46	Mýrahnúksvatn	606	245129216.607	2724590.908	23.96800348
47	Mýrahnúksvatn	610	202223426.796	98752.688	20.20259214
48	Mýrahnúksvatn	614	184480929.733	198976.451	18.40829768
49	Mýrahnúksvatn	618	163928476.380	132800.108	16.36628762

50	Mýrahnúksvatn	622	169730029.884	168533.682	16.93929625
51	Mýrahnúksvatn	626	211881771.738	307894.413	21.12659829
52	Mýrahnúksvatn	630	195264827.163	87606.741	19.50896137
53	Mýrahnúksvatn	634	222611531.315	134808.918	22.23419135
54	Mýrahnúksvatn	638	206656431.973	373130.468	20.5910171
55	Mýrahnúksvatn	642	217897252.357	395303.224	21.71066459
56	Mýrahnúksvatn	646	187196966.694	368605.738	18.64597552
57	Mýrahnúksvatn	650	198228085.736	290801.584	19.76464826
58	Mýrahnúksvatn	654	115922640.911	121340.168	11.56799606
59	Mýrahnúksvatn	658	98005600.747	121734.842	9.776213106
60	Mýrahnúksvatn	662	147231470.003	329402.266	14.65726655
61	Mýrahnúksvatn	666	131007555.903	210887.094	13.05857817
62	Mýrahnúksvatn	670	158940261.227	216114.043	15.85080331
63	Mýrahnúksvatn	674	185580436.993	429885.757	18.47206655
64	Mýrahnúksvatn	678	130491084.357	455719.035	12.95796463
65	Mýrahnúksvatn	680	129233153.523	502659.875	12.82278338
66	Djúpavik	304	192158557.9	12315.78947	1.921339263
67	Djúpavik	308	54481247.9	11306.72269	0.544586345
68	Djúpavik	312	158797701.7	19003.04414	1.587596956
69	Djúpavik	316	875498668.8	73375.09789	8.753519186
70	Djúpavik	320	198060896.8	12571.42857	1.98035754
71	Djúpavik	324	223437957.3	19401.7094	2.233991538
72	Djúpavik	328	128518357.1	8906.25	1.285005446
73	Djúpavik	332	167030891.1	14869.48695	1.670011521
74	Djúpavik	336	419542807.5	25975.93583	4.194908556
75	Djúpavik	340	167373421.1	17709.96641	1.673380011
76	Djúpavik	344	237792458.1	28414.80447	2.538685514
77	Djúpavik	348	612271530.6	46545.1895	5.529901641
78	Djúpavik	352			4.655052122
79	Djúpavik	356			1.97788216
80	Djúpavik	360			3.534754822
81	Djúpavik	364			3.683069378
82	Djúpavik	368			1.609670611
83	Djúpavik	372			1.792779227
84	Djúpavik	376			3.578708672
85	Djúpavik	380			2.552911803
86	Djúpavik	384			2.972533263
87	Djúpavik	388			2.673212863
88	Djúpavik	392			1.32673655
89	Djúpavik	396			2.534902414
90	Djúpavik	400			2.33599741
91	Djúpavik	404			2.178112968
92	Djúpavik	408			2.011326709
93	Djúpavik	412			1.468360367
94	Djúpavik	416			8.972401389
95	Djúpavik	420			9.360543746
96	Djúpavik	424			10.05809695
97	Djúpavik	428			8.046634431
98	Djúpavik	432			8.031443791
99	Djúpavik	436			7.791386019
100	Djúpavik	440			4.758647972
101	Djúpavik	444			5.169388466
102	Djúpavik	448			2.408073439
103	Djúpavik	452			1.778767181
104	Djúpavik	456			1.025388674

105	Djúpavik	460	0.267386436
106	Djúpavik	464	3.638721335
107	Djúpavik	468	2.059974861
108	Djúpavik	472	3.075242927
109	Djúpavik	476	2.384748234
110	Djúpavik	480	2.013575832
111	Djúpavik	484	4.618830038
112	Djúpavik	488	3.766420993
113	Djúpavik	492	2.725223626
114	Djúpavik	496	3.591946072
115	Djúpavik	500	2.418552639
116	Djúpavik	504	3.277654674
117	Djúpavik	508	2.817834745
118	Djúpavik	512	3.668040403
119	Djúpavik	516	2.50999696
120	Djúpavik	521	2.671765499
121	Djúpavik	524	3.599168973
122	Djúpavik	525	6.568569385
123	Djúpavik	526.5	0.747142805
124	Djúpavik	528	1.286203937
125	Djúpavik	531	2.990400351
126	Djúpavik	532	3.353452308
127	Djúpavik	536	3.359752863
128	Djúpavik	540	3.876907335

Figure 13 Biogenic silica analysis

Sample	Core	Depth (cm)	Silica (ppm)	Alluminium (ppm)	%Bsi
1	Mavatn	63	76885448.68	17131.831	7.685118502
2	Mavatn	65	105781398	32027.43	10.57173432
3	Mavatn	67	83275479.53	15282.596	8.324491434
4	Mavatn	69	31853636.5	9529.248	3.1834578
5	Mavatn	70	200229768.1	227292.646	19.97751828
6	Mavatn	71	150366279.6	351487.124	14.96633053
7	Mavatn	72	99386661.84	373937.209	9.863878742
8	Mavatn	73	341347754.9	112679.466	34.11223959
9	Mavatn	75	533139703.2	794767.036	53.15501691
10	Mavatn	77	39495485.1	55154.671	3.938517576
11	Mavatn	79	21845940.25	40871.902	2.176419645
12	Mavatn	81	23935696.68	69724.723	2.379624723
13	Mavatn	83	17911830.18	53685.38	1.780445942
14	Mavatn	85	31617739.61	67207.226	3.148332515
15	Mavatn	87	17832969.89	68189.024	1.769659184
16	Mavatn	89	18273428.99	60715.474	1.815199804
17	Mavatn	91	21284520.36	75263.307	2.113399375
18	Mavatn	93	17355733.88	39806.868	1.727612014
19	Mavatn	95	25892424.31	83918.252	2.572458781
20	Hafrafellvatn	354	72429362.11	37137.451	7.23550872
21	Hafrafellvatn	358	68493876.53	27028.11	6.843982031
22	Hafrafellvatn	362	54433265.47	30086.04	5.437309339
23	Hafrafellvatn	366	85736544.01	26862.978	8.568281805
24	Hafrafellvatn	370	49580092.45	16174.62	4.954774321
25	Hafrafellvatn	374	44371935.86	15858.009	4.434021984
26	Hafrafellvatn	378	91754821.27	26652.477	9.170151632
27	Hafrafellvatn	382	116507381	49842.218	11.64076966
28	Hafrafellvatn	386	40560258.76	41725.536	4.047680769
29	Hafrafellvatn	390	88220736.74	87540.377	8.804565598
30	Hafrafellvatn	394	211787605.9	432535.682	21.09225346
31	Hafrafellvatn	398	31950228.66	86632.275	3.177696411
32	Hafrafellvatn	402	51475043.11	144871.699	5.118529971
33	Hafrafellvatn	406	26815355.67	82532.334	2.6650291
34	Hafrafellvatn	410	65302213.57	398945.856	6.450432186
35	Hafrafellvatn	414	16735943.56	70292.709	1.659535814
36	Hafrafellvatn	418	24314687.99	125952.16	2.406278367
37	Hafrafellvatn	422	82632176.59	400795.807	8.183058497
38	Hafrafellvatn	426	86038279.59	459489.585	8.511930042
39	Hafrafellvatn	430	43056843.56	340233.548	4.237637647
40	Hafrafellvatn	434	14779024.25	65457.763	1.464810873
41	Hafrafellvatn	438	23252771.29	114190.748	2.30243898
42	Hafrafellvatn	442	16076972.59	101755.338	1.587346191
43	Mýrahnúksvatn	594	109413145.668	1301601.39	10.68099429
44	Mýrahnúksvatn	598	203859277.996	3167607.516	19.7524063
45	Mýrahnúksvatn	602	81772791.577	3231129.368	7.531053284
46	Mýrahnúksvatn	606	245129216.607	2724590.908	23.96800348
47	Mýrahnúksvatn	610	202223426.796	98752.688	20.20259214
48	Mýrahnúksvatn	614	184480929.733	198976.451	18.40829768
49	Mýrahnúksvatn	618	163928476.380	132800.108	16.36628762

50	Mýrahnúksvatn	622	169730029.884	168533.682	16.93929625
51	Mýrahnúksvatn	626	211881771.738	307894.413	21.12659829
52	Mýrahnúksvatn	630	195264827.163	87606.741	19.50896137
53	Mýrahnúksvatn	634	222611531.315	134808.918	22.23419135
54	Mýrahnúksvatn	638	206656431.973	373130.468	20.5910171
55	Mýrahnúksvatn	642	217897252.357	395303.224	21.71066459
56	Mýrahnúksvatn	646	187196966.694	368605.738	18.64597552
57	Mýrahnúksvatn	650	198228085.736	290801.584	19.76464826
58	Mýrahnúksvatn	654	115922640.911	121340.168	11.56799606
59	Mýrahnúksvatn	658	98005600.747	121734.842	9.776213106
60	Mýrahnúksvatn	662	147231470.003	329402.266	14.65726655
61	Mýrahnúksvatn	666	131007555.903	210887.094	13.05857817
62	Mýrahnúksvatn	670	158940261.227	216114.043	15.85080331
63	Mýrahnúksvatn	674	185580436.993	429885.757	18.47206655
64	Mýrahnúksvatn	678	130491084.357	455719.035	12.95796463
65	Mýrahnúksvatn	680	129233153.523	502659.875	12.82278338
66	Djúpavik	304	192158557.9	12315.78947	1.921339263
67	Djúpavik	308	54481247.9	11306.72269	0.544586345
68	Djúpavik	312	158797701.7	19003.04414	1.587596956
69	Djúpavik	316	875498668.8	73375.09789	8.753519186
70	Djúpavik	320	198060896.8	12571.42857	1.98035754
71	Djúpavik	324	223437957.3	19401.7094	2.233991538
72	Djúpavik	328	128518357.1	8906.25	1.285005446
73	Djúpavik	332	167030891.1	14869.48695	1.670011521
74	Djúpavik	336	419542807.5	25975.93583	4.194908556
75	Djúpavik	340	167373421.1	17709.96641	1.673380011
76	Djúpavik	344	237792458.1	28414.80447	2.538685514
77	Djúpavik	348	612271530.6	46545.1895	5.529901641
78	Djúpavik	352			4.655052122
79	Djúpavik	356			1.97788216
80	Djúpavik	360			3.534754822
81	Djúpavik	364			3.683069378
82	Djúpavik	368			1.609670611
83	Djúpavik	372			1.792779227
84	Djúpavik	376			3.578708672
85	Djúpavik	380			2.552911803
86	Djúpavik	384			2.972533263
87	Djúpavik	388			2.673212863
88	Djúpavik	392			1.32673655
89	Djúpavik	396			2.534902414
90	Djúpavik	400			2.33599741
91	Djúpavik	404			2.178112968
92	Djúpavik	408			2.011326709
93	Djúpavik	412			1.468360367
94	Djúpavik	416			8.972401389
95	Djúpavik	420			9.360543746
96	Djúpavik	424			10.05809695
97	Djúpavik	428			8.046634431
98	Djúpavik	432			8.031443791
99	Djúpavik	436			7.791386019
100	Djúpavik	440			4.758647972
101	Djúpavik	444			5.169388466
102	Djúpavik	448			2.408073439
103	Djúpavik	452			1.778767181
104	Djúpavik	456			1.025388674

105	Djúpavik	460	0.267386436
106	Djúpavik	464	3.638721335
107	Djúpavik	468	2.059974861
108	Djúpavik	472	3.075242927
109	Djúpavik	476	2.384748234
110	Djúpavik	480	2.013575832
111	Djúpavik	484	4.618830038
112	Djúpavik	488	3.766420993
113	Djúpavik	492	2.725223626
114	Djúpavik	496	3.591946072
115	Djúpavik	500	2.418552639
116	Djúpavik	504	3.277654674
117	Djúpavik	508	2.817834745
118	Djúpavik	512	3.668040403
119	Djúpavik	516	2.50999696
120	Djúpavik	521	2.671765499
121	Djúpavik	524	3.599168973
122	Djúpavik	525	6.568569385
123	Djúpavik	526.5	0.747142805
124	Djúpavik	528	1.286203937
125	Djúpavik	531	2.990400351
126	Djúpavik	532	3.353452308
127	Djúpavik	536	3.359752863
128	Djúpavik	540	3.876907335

Figure 14 Time-dependant biogenic silica analysis for Djúpavik

Depth (cm)	Time-interval (hrs)	Silica (ppm)	Aluminium (ppm)	%Bsi
476	2	11018315.35	540720.429	0.993687449
496	2	25072203.26	388371.085	2.429546109
528	2	11144467.75	389256.208	1.036595534
598	2	552261.493	97839.61	0.035658227
614	2	15617477.57	453937.854	1.470960186
476	3	7303136.844	265768.98	0.677159888
496	3	18361667.26	262064.367	1.783753853
528	3	13066256.73	199639.692	1.266697735
598	3	1834226.95	57023.996	0.172017896
614	3	14903696.49	1236395.897	1.24309047
476	4	9394232.271	194918.904	0.900439446
496	4	22913732.92	733837.314	2.144605829
528	4	32058677.14	257149.361	3.154437842
598	4	651042.53	94074.678	0.046289317
614	4	18946912.42	277353.364	1.83922057
476	5	9233475.123	220259.43	0.879295626
496	5	20222707.38	228716.942	1.976527349
528	5	15470864.49	227725.959	1.501541257
598	5	5737552.941	97932.12	0.55416887
614	5	19922305.96	153598.743	1.961510847
476	6.5	11636735.31	256740.746	1.112325382
496	6.5	24228290.06	1146649.322	2.193499142
528	6.5	19498039.82	87136.199	1.932376742
598	6.5	554083.785	61264.727	0.043155433
614	6.5	18832755.41	235241.092	1.836227323
476	overnight	343543790.5	3137913.326	33.72679639
496	overnight	457237583.4	2816122.882	45.16053377
528	overnight	335221132.3	585045.997	33.40510403
598	overnight	8069087.192	418168.427	0.723275034
614	overnight	362776427.2	1408973.589	35.99584801

Figure 15 Sodium concentration analysis

Sample number	Core	Depth (cm)	Wet weight (g)	Dry weight for Na	Na conc. (mg.g)
1	Mavatn	61	1	0.2033	5702.164289
2	Mavatn	63	1	0.21	5145.619048
3	Mavatn	67	1	0.2186	5620.082342
4	Mavatn	71	1	0.2333	6671.067295
5	Mavatn	75	1	0.2628	6870.167428
6	Mavatn	81	1	0.24	6688.416667
7	Mavatn	83	1	0.3158	8660.60798
8	Mavatn	87	1	0.3102	9148.065764
9	Mavatn	91	1.01	0.227	10527.40088
10	Mavatn	95	1.01	0.2982	10263.38028
11	Hafrafellvatn	358	1.02	0.12931	6271.750058
12	Hafrafellvatn	362	1	0.12371	6717.322771
13	Hafrafellvatn	366	1.07	0.15011	6055.559257
14	Hafrafellvatn	374	1.02	0.18595	5125.033611
15	Hafrafellvatn	382	1.03	0.20568	7195.643718
16	Hafrafellvatn	390	1	0.21661	7109.551729
17	Hafrafellvatn	398	1.05	0.2105	8726.840855
18	Hafrafellvatn	406	1.01	0.20039	7370.627277
19	Hafrafellvatn	414	1.04	0.22476	8342.231714
20	Hafrafellvatn	422	1.02	0.20823	8740.335206
21	Hafrafellvatn	430	1.04	0.24618	10203.91583
22	Hafrafellvatn	438	1.05	0.21346	8385.646023

Figure 16 pH reconstruction for northeast coast of Vestfirðir

Sample	Core	Depth (cm)	pH Index B (Nygaard (1956)	pH
1	Djúpavik	310	0.3516	6.786
2	Djúpavik	325	0.433	6.709
3	Djúpavik	374	0.3979	6.74
4	Djúpavik	390	0.8905	6.443
5	Djúpavik	405	0.8926	6.442
6	Djúpavik	418	0.8731	6.45
7	Djúpavik	422	1.3204	6.297
8	Djúpavik	446	0.6453	6.562
9	Djúpavik	466	1.122	6.358
10	Djúpavik	502	0.9106	6.435
11	Djúpavik	518	0.9457	6.421
12	Djúpavik	522	0.7692	6.497
13	Djúpavik	530	0.5394	6.628
14	Djúpavik	538	0.4036	6.735
15	Mýrahnúksvatn	598	0.60727	6.584
16	Mýrahnúksvatn	606	0.46153	6.685
17	Mýrahnúksvatn	614	0.3422	6.796
18	Mýrahnúksvatn	622	0.2498	6.912
19	Mýrahnúksvatn	630	0.1559	7.086
20	Mýrahnúksvatn	638	0.0676	7.395
21	Mýrahnúksvatn	646	0.1914	7.01
22	Mýrahnúksvatn	654	0.1265	7.163
23	Mýrahnúksvatn	662	0.0654	7.407
24	Mýrahnúksvatn	670	0.052	7.491
25	Mýrahnúksvatn	678	Not enough data	

RADIOCARBON CALIBRATION PROGRAM*
CALIB REV4.4.2

*To be used in conjunction with:
Stuiver, M., and Reimer, P.J., 1993, Radiocarbon, 35, 215-230.
Annotated results (text) - c14res.doc
Export file - c14res.csv

Gjogur
Lab Code
Sample Description (80 chars max)
Radiocarbon Age BP 10300 +/- 55
Calibration data set: intcal98.14c (Stuiver et al., 1998a)

% area enclosed	cal AD age ranges	relative area under probability distribution
68.3 (1 sigma)	cal BC 10376- 10255	0.326
	10244- 9994	0.628
	9845- 9827	0.046
95.4 (2 sigma)	cal BC 10787- 10781	0.001
	10718- 10521	0.097
	10438- 9802	0.901
	9756- 9755	0.000

References for calibration datasets:
Stuiver, M., and Braziunas, T.F., (1993), The Holocene 3:289-305.
Stuiver, M., Reimer, P.J., and Braziunas, T.F., (1998b) Radiocarbon 40:1127-1151. (revised dataset)
Stuiver, M., Reimer, P.J., Bard, E., Beck, J.W., Burr, G.S., Hughen, K.A., Kromer, B., McCormac, F.G., v.d. Plicht, J., and Spurk, M. (1998a), Radiocarbon 40:1041-1083.
McCormac, F.G., Reimer, P.J., Hogg, A.G., Higham, T.F.G., Baillie, M.G.L., Palmer, J., Stuiver, M., (2002), Radiocarbon 44: 641-651.

Comments:
* This standard deviation (error) includes a lab error multiplier.
** 1 sigma = square root of (sample std. dev.^2 + curve std. dev.^2)
** 2 sigma = 2 x square root of (sample std. dev.^2 + curve std. dev.^2)
where ^2 = quantity squared.
[ ] = calibrated with an uncertain region or a linear extension to the calibration curve
0* represents a "negative" age BP
1955* or 1960* denote influence of nuclear testing C-14

NOTE: Cal ages and ranges are rounded to the nearest year which may be too precise in many instances. Users are advised to round results to the nearest 10 yr for samples with standard deviation in the radiocarbon age greater than 50 yr.

RADIOCARBON CALIBRATION PROGRAM*
CALIB REV4.4.2

*To be used in conjunction with:
Stuiver, M., and Reimer, P.J., 1993, Radiocarbon, 35, 215-230.
Annotated results (text) - c14res.doc
Export file - c14res.csv

Reykholar
Lab Code
Sample Description (80 chars max)
Radiocarbon Age BP 10460 +/- 55
Calibration data set: intcal98.14c (Stuiver et al., 1998a)

% area enclosed	cal BP age ranges	relative area under probability distribution
68.3 (1 sigma)	cal BP 12177 - 12205	0.047
	12316 - 12638	0.876
	12747 - 12787	0.077
95.4 (2 sigma)	cal BP 11968 - 12010	0.021
	12080 - 12827	0.979

Asmundarne
Lab Code
Sample Description (80 chars max)
Radiocarbon Age BP 9936 +/- 55
Calibration data set: intcal98.14c (Stuiver et al., 1998a)

% area enclosed	cal BP age ranges	relative area under probability distribution
68.3 (1 sigma)	cal BP 11228 - 11342	0.747
	11390 - 11404	0.064
	11509 - 11546	0.189
95.4 (2 sigma)	cal BP 11198 - 11565	0.994
	11618 - 11629	0.006

Hvitahlid
Lab Code
Sample Description (80 chars max)
Radiocarbon Age BP 8830 +/- 60
Calibration data set: intcal98.14c (Stuiver et al., 1998a)

% area enclosed	cal BP age ranges	relative area under probability distribution
68.3 (1 sigma)	cal BP 9748 - 9922	0.612
	9931 - 9957	0.070
	9993 - 10011	0.057
	10017 - 10031	0.046
	10056 - 10069	0.042
	10077 - 10112	0.139
	10135 - 10147	0.033

95.4 (2 sigma)	cal BP	9633 - 9637	0.003
		9683 - 10159	0.997

Hvitahlid
Lab Code
Sample Description (80 chars max)
Radiocarbon Age BP 6910 +/- 100
Calibration data set: intcal98.14c (Stuiver et al., 1998a)

% area enclosed	cal BP age ranges	relative area under probability distribution
68.3 (1 sigma)	cal BP 7620 - 7628	0.029
	7659 - 7838	0.971
95.4 (2 sigma)	cal BP 7582 - 7878	0.918
	7889 - 7937	0.082

Baer brodd
Lab Code
Sample Description (80 chars max)
Radiocarbon Age BP 4000 +/- 55
Calibration data set: intcal98.14c (Stuiver et al., 1998a)

% area enclosed	cal BP age ranges	relative area under probability distribution
68.3 (1 sigma)	cal BP 4411 - 4529	0.981
	4562 - 4566	0.019
95.4 (2 sigma)	cal BP 4261 - 4267	0.003
	4287 - 4615	0.978
	4766 - 4789	0.019

References for calibration datasets:
Stuiver, M., and Braziunas, T.F., (1993), The Holocene 3:289-305.
Stuiver, M., Reimer, P.J., and Braziunas, T.F., (1998b) Radiocarbon 40:1127-1151. (revised dataset)
Stuiver, M., Reimer, P.J., Bard, E., Beck, J.W., Burr, G.S., Hughen, K.A., Kromer, B., McCormac, F.G., v.d. Plicht, J., and Spurk, M. (1998a), Radiocarbon 40:1041-1083.
McCormac, F.G., Reimer, P.J., Hogg, A.G., Higham, T.F.G., Baillie, M.G.L., Palmer, J., Stuiver, M., (2002), Radiocarbon 44: 641-651.

Comments:
* This standard deviation (error) includes a lab error multiplier.
** 1 sigma = square root of (sample std. dev.^2 + curve std. dev.^2)
** 2 sigma = 2 x square root of (sample std. dev.^2 + curve std. dev.^2)
where ^2 = quantity squared.
[ ] = calibrated with an uncertain region or a linear extension to the calibration curve
0* represents a "negative" age BP
1955* or 1960* denote influence of nuclear testing C-14

NOTE: Cal ages and ranges are rounded to the nearest year which may be too precise in many instances. Users are advised to round results to the nearest 10 yr for samples with standard deviation in the radiocarbon age greater than 50 yr.

Sample ID
Lab Code
Sample Description (80 chars max)
Radiocarbon Age BP 9200 +/- 55
Calibration data set: intcal98.14c (Stuiver et al., 1998a)

% area enclosed	cal BP age ranges	relative area under probability distribution
68.3 (1 sigma)	cal BP 10242 - 10352	0.684
	10355 - 10403	0.300
	10463 - 10466	0.016
95.4 (2 sigma)	cal BP 10224 - 10229	0.004
	10234 - 10502	0.996

Hrisholsva
Lab Code
Sample Description (80 chars max)
Radiocarbon Age BP 9640 +/- 55
Calibration data set: intcal98.14c (Stuiver et al., 1998a)

% area enclosed	cal BP age ranges	relative area under probability distribution
68.3 (1 sigma)	cal BP 10791 - 10800	0.032
	10806 - 10826	0.076
	10855 - 10941	0.409
	11066 - 11164	0.483
95.4 (2 sigma)	cal BP 10751 - 10971	0.548
	10978 - 11022	0.056
	11039 - 11174	0.396

Berufjarde
Lab Code
Sample Description (80 chars max)
Radiocarbon Age BP 10430 +/- 55
Calibration data set: intcal98.14c (Stuiver et al., 1998a)

% area enclosed	cal BP age ranges	relative area under probability distribution
68.3 (1 sigma)	cal BP 12134 - 12226	0.161
	12297 - 12432	0.275
	12452 - 12631	0.551
	12760 - 12770	0.014
95.4 (2 sigma)	cal BP 11958 - 12028	0.044
	12062 - 12686	0.873
	12699 - 12809	0.082

Hrishols B
Lab Code
Sample Description (80 chars max)
Radiocarbon Age BP 10764 +/- 55
Calibration data set: intcal98.14c (Stuiver et al., 1998a)

% area enclosed	cal BP age ranges	relative area under probability distribution
68.3 (1 sigma)	cal BP 12664 - 12722	0.226
	12807 - 12953	0.774
95.4 (2 sigma)	cal BP 12434 - 12460	0.013
	12625 - 13000	0.978
	13065 - 13085	0.008

Hrishols B
Lab Code
Sample Description (80 chars max)
Radiocarbon Age BP 9460 +/- 55
Calibration data set: intcal98.14c (Stuiver et al., 1998a)

% area enclosed	cal BP age ranges	relative area under probability distribution
68.3 (1 sigma)	cal BP 10579 - 10617	0.181
	10636 - 10752	0.652
	10966 - 10993	0.094
	11022 - 11040	0.074
95.4 (2 sigma)	cal BP 10510 - 10518	0.005
	10554 - 10792	0.716
	10796 - 10809	0.009
	10825 - 10858	0.028
	10940 - 11069	0.242

Mavatn
Lab Code
Sample Description (80 chars max)
Radiocarbon Age BP 2000 +/- 55
Calibration data set: intcal98.14c (Stuiver et al., 1998a)

% area enclosed	cal BP age ranges	relative area under probability distribution
68.3 (1 sigma)	cal BP 1879 - 2000	1.000
95.4 (2 sigma)	cal BP 1824 - 1852	0.044
	1859 - 2068	0.916
	2079 - 2110	0.039

Hafrafellv
Lab Code
Sample Description (80 chars max)
Radiocarbon Age BP 8500 +/- 55
Calibration data set: intcal98.14c (Stuiver et al., 1998a)

% area enclosed	cal BP age ranges	relative area under probability distribution
68.3 (1 sigma)	cal BP 9473 - 9481	0.104
	9484 - 9533	0.896
95.4 (2 sigma)	cal BP 9331 - 9336	0.007

9427 - 9550 0.993

References for calibration datasets:

Stuiver, M., and Braziunas, T.F., (1993), The Holocene 3:289-305.
Stuiver, M., Reimer, P.J., and Braziunas, T.F., (1998b) Radiocarbon 40:1127-1151. (revised dataset)
Stuiver, M., Reimer, P.J., Bard, E., Beck, J.W., Burr, G.S., Hughen, K.A., Kromer, B., McCormac, F.G., v.d. Plicht, J., and Spurk, M. (1998a), Radiocarbon 40:1041-1083.
McCormac, F.G., Reimer, P.J., Hogg, A.G., Higham, T.F.G., Baillie, M.G.L., Palmer, J., Stuiver, M., (2002), Radiocarbon 44: 641-651.

Comments:

* This standard deviation (error) includes a lab error multiplier.
** 1 sigma = square root of (sample std. dev.^2 + curve std. dev.^2)
** 2 sigma = 2 x square root of (sample std. dev.^2 + curve std. dev.^2)
where ^2 = quantity squared.
[ ] = calibrated with an uncertain region or a linear extension to the calibration curve
0* represents a "negative" age BP
1955* or 1960* denote influence of nuclear testing C-14

NOTE: Cal ages and ranges are rounded to the nearest year which may be too precise in many instances. Users are advised to round results to the nearest 10 yr for samples with standard deviation in the radiocarbon age greater than 50 yr.

Figure 33 Myrahnuksvatn diatom assemblage

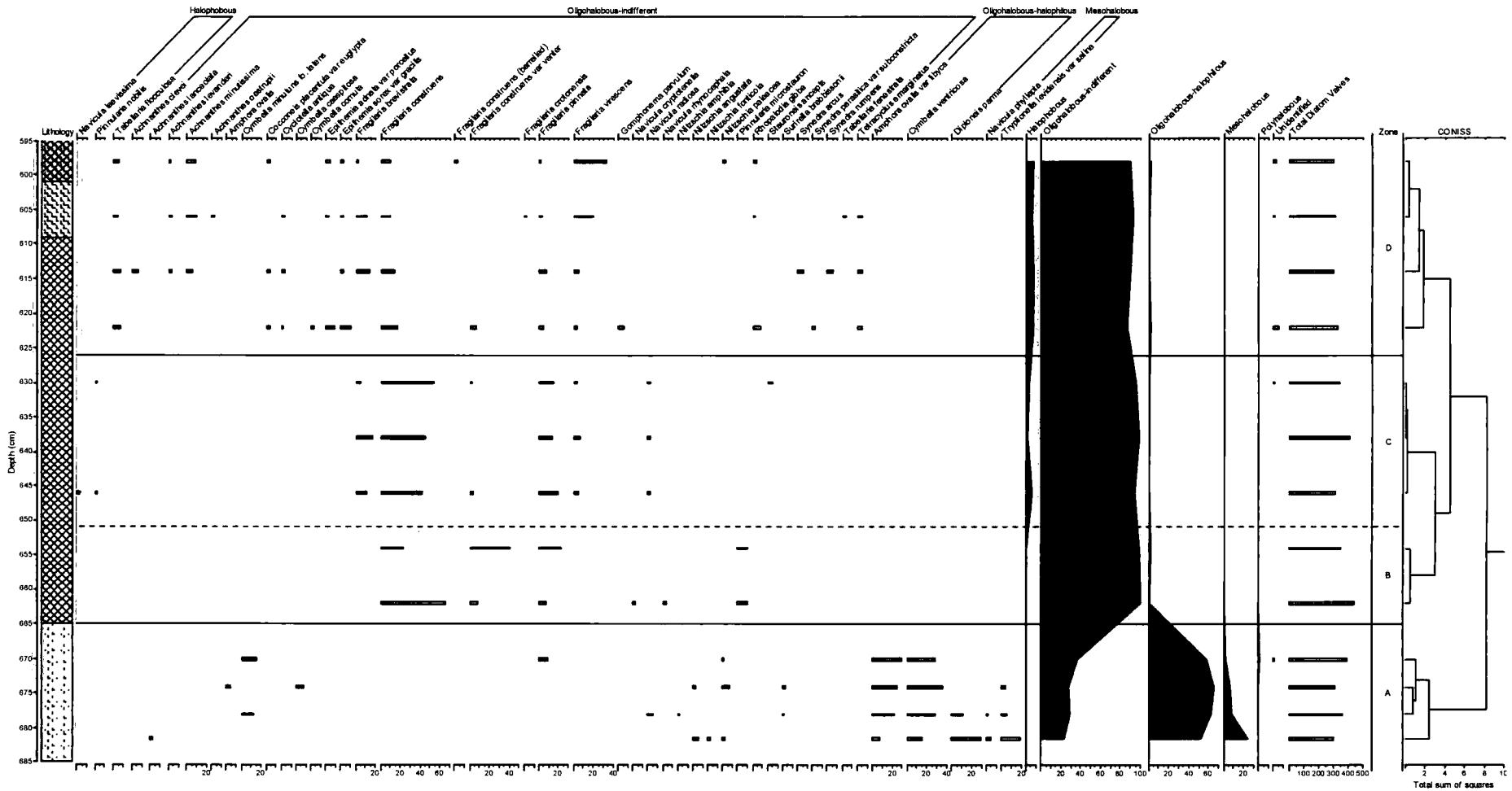

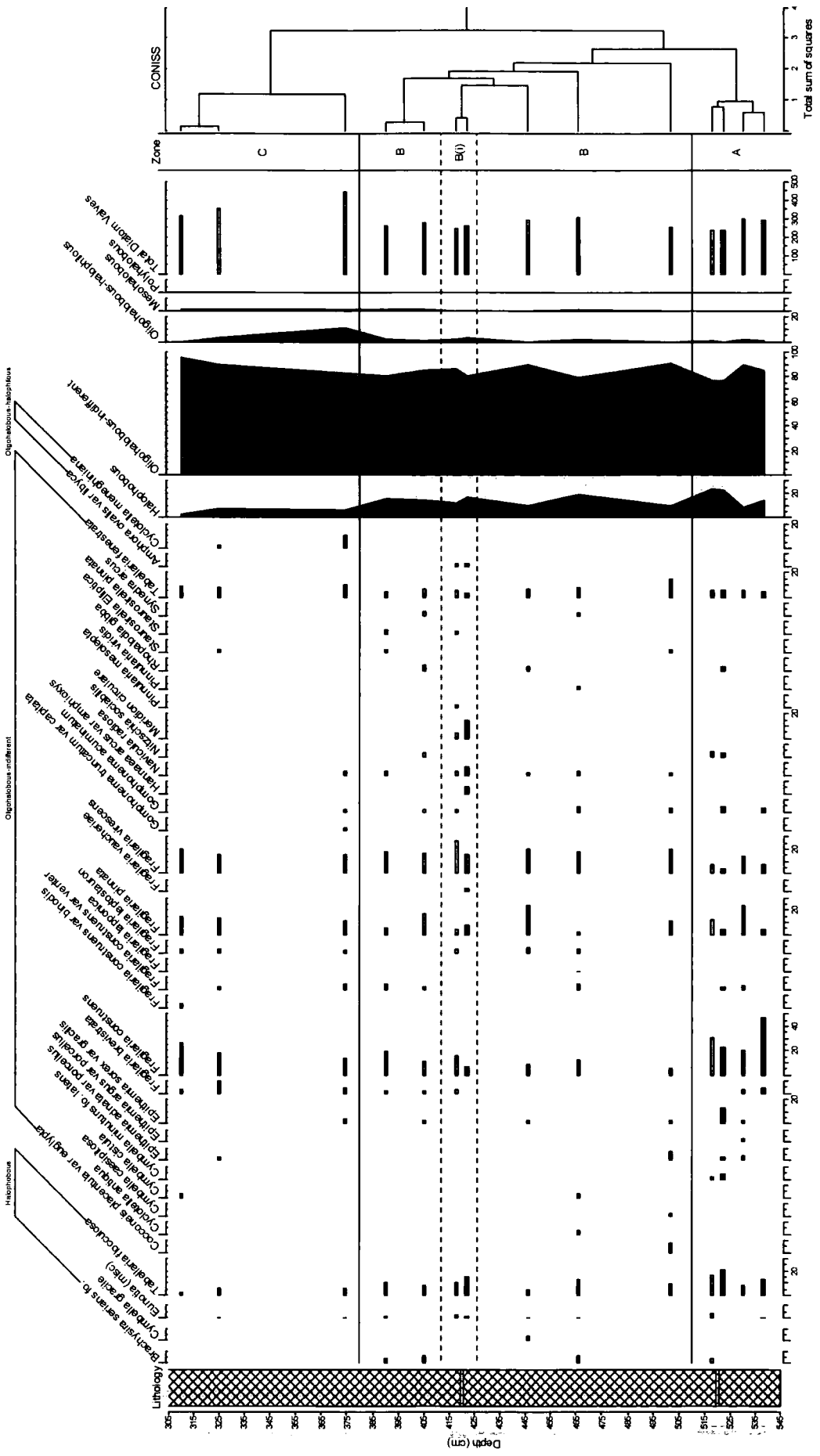

Figure 37 Djupavik diatom assemblage